Role of DYRK1A in the development of the cerebral cortex. Implication in Down Syndrome

Sònia Najas Sales

TESI DOCTORAL UPF / 2014

DIRECTOR DE LA TESI

Dra. Mariona Arbonés de Rafael,

Institut de Biologia Molecular de Barcelona (IBMB-CSIC)

DEPARTAMENT CEXS UPF-PHD PROGRAMME IN BIOMEDICINE

Universitat Pompeu Fabra Barcelona

ACKNOWLEDGMENTS

La tesis ja està escrita! Sembla mentida després de tants anys però ha arribat el dia! Com un gran music de Sant Antoni deia (Buira quin gran poeta estàs fet!)...hay personas que dejan huella sin pisar...i jo li vull agrair i dedicar la meva tesis a totes aquelles persones que d'una manera o un altre m'han acompanyat durant aquest llarg viatge.

Primer de tot agrair a la **Mariona** el haver-me donat la possibilitat de fer la tesis al seu laboratori. Mariona moltes gràcies per ensenyar-me a pensar críticament, a fer-me preguntes i a intentar anar sempre una mica més enllà. Sense tu aquesta tesis no s'hauria pogut fer.

Als meus companys de labo...ufff tantes coses a agrair!! **Maria José** tu has fet que m'encanti la neurociència! Des del primer dia m'has transmès la teva passió per la ciència i les teves ganes de descobrir. Me'n recordo perfectament de les primeres immunos que vaig mirar amb tu...Que bonitas que son estas neuronas! Mira que bonito! Has sigut un pilar al laboratori durant tot aquest temps, m'encanta la teva energia i la manera que tens d'afrontar els problemes. Ets tot un exemple a seguir a la vida en general! **Juan**, sinceramente en estos dos años te has convertido en un gran amigo! Quien te lo iba a decir eh! Con lo seca que era yo al principio! Gracias por todas las risas, el buen humor y las "terapias" que hemos compartido. Muchas gracias también por estar siempre dispuesto a ayudar en todo. Eres un sol! **Mari**, gràcies per cuidar dels nostres ratolinets i per les xerrades al metro. La nova incorporació....**Isa**! La veritat és que amb tu no he pogut compartir gaires moments...m'has enganxat tota estressada escrivint la tesis... però igualment m'alegro de tenir-te al laboratori, sempre tranquil·la i somrient! Y sobre los ex compis de labo... como no hablar de **Baldu**! Ai baldu! Se te echa mucho de menos! Gracias por enseñarme el fantástico mundo del RNA, por animarme a seguir cuando las cosas se ponían negras y sobretodo por tu vitalidad contagiosa. Hablando de miembros pasados, **Erikita!** Tantas cosas a agradecer también! La super técnico! Muchísimas gracias por todo lo que me has enseñado, hasta a coger un ratón! Gracias también por estar allí siempre dispuesta a ayudar a cualquier hora. **Ariadna**, jo arribava que tu ja marxaves casi! Tot i així tots els consells de "supervivència"

que em vas donar m'han sigut molt útils aquest anys, moltes gràcies! **Uli**, gracias por acompañarme durante mi primer año de tesis y tratarme siempre como un igual aunque yo fuera un pollito que acababa de llegar!

Al començar la tesis al CRG i acabar-la al IBMB al llarg d'aquests 4 anys he conegut molta gent que ha anat posant el seu granet de sorra. Del CRG m'agradaria agrair especialment als nois de la **Susana de la Luna**. Durant els dos primers anys de tesis vam compartir laboratori i es va crear una gran amistat amb tots vosaltres. Muchas gracias **Susana** por enseñarme tanto, por estar siempre encantada de ver mis westerns y por esas últimas copas tan entretenidas. Muchas gracias **Alicia** por las charlas con el café, **Kriszti** por siempre sonreír y descubrirme la danza tribal, **Esteban** por tu amabilidad, **Julia** por esos partidos de volley y **Chiara** por aguantarme en el labo y en casa durante dos años!
Als nois de la Mara, especialment a la **Carla** per les hores i hores compartides al CAST; a l'**Ignasi** per ser la persona que m'arrenca un somriure més ràpid del món; a la **Meritxell**, per anar sempre en paral·lel amb mi; **Susana**: per ser tant energètica i positiva; a la **Maria** i el **Davide**, pel seu bon rollo; i a la **Monica** per ser una teacher fantàstica y super estilosa!
A la gent de la Cristina Fillat: a l' Anabel (tu vas més endavant), al **Xevi,** per treure conversa de sota les pedres; a la **Núria**, per tenir tanta paciència; a la **Vicky** per la seva energia; y al Luciano, pels seus consells.
A més a més agrair a altra gent del PRBB amb qui he compartit grans moments i grans converses com el **Cedrik,** l'**Alexis,** la **Marina** i segur que me'n deixo molts! A tots els ex companys de Uni que corrien pel PRBB i sobretot a **l'Alba Mas** i al **Davide Rubbini** per ser una grans amics dins i fora del laboratori.

Quan vam arribar al IBMB la veritat és que ens vam posar tots una mica tristos... no teníem la platja al davant....no hi havia terrassa per dinar...totes les maquines importants estaven dos pisos per sota del laboratori... però sobretot NO coneixíem a ningú! Ràpidament per això aquesta tristesa va passar i jo personalment estic molt contenta de les grans persones i científics que he conegut en aquest centre. Chicos de Elisa Martí! Muchas gracias por acogernos tan bien, por los lab meetings y congresos compartidos, por las cañas y copazos que caen de vez en cuando, por la batucada....**Irene, Murielle, Susana, Ángeles, Thiago, Elena, Rene, Lucia** y como no

Gwen. Gwen muchas gracias especialmente a ti por enseñarme a electroporar pollos, por ser el otro obseso de la corteza cerebral y sobretodo por nuestras conversaciones del futuro y tu humor francés que me hace tanta gracia!

A otros estudiantes del IBMB que son compañeros de micro y mil aventurillas más: **Susana, Ofelia, Toni, Eva, David Moreno**....

Y finalmente como no a mis Swing kids! Mi último año de doctorado no habría sido lo mismo sin el Swing terapéutico de los jueves! **Raquel** eres la persona más friki de la ciencia que conozco! Muchas gracias por solventarme dudas de la real-time i el misterioso mundo de la epigenética. Muchas gracias por haberte convertido en una amiga con quien contar en cualquier momento y muchas gracias por "liarme" a hacer jazz steps :p
Raúl sé que ho estaves esperant...ara et toca a tu. Tot i que el nostre primer contacte no va ser el més idoni...mira que adormir-te al meu seminari....ara no m'imagino l'últim any sense tu. Gràcies per les converses que feien que les hores de confocal passessin volant, gràcies per les bromes tontes, per punxar-me per anar al gimnàs, per les curses, pels kit kats...i sí! Per la super triatló que farem en breu.

Clarament, també vull agrair-li a la meva **família** el recolzament que m'ha donat durant tot aquest temps. Per animar-me a seguir, per escoltar-me amb els problemes del labo tot i no entendre massa de que els hi parlava i per una infinitat més de coses. Ells sempre estan i estaran allà! Així que moltes gràcies i sí per fi la vostre filla / germana / neta serà doctora!

Moltes gràcies als superhullahops! Ja fa molts anys que ens coneixem i seguim tots allà per quan faci falta. No sabria ni per on començar a agrair....**Heleia, Nina, Cutando, Martina, Lucia, Veiga, Uri, Lahuerta i Solde** sou genials i us estimo un munt! Espero que ens fem vellets seguint fent soparets amb la guitarrilla com si els anys no passessin! I seguint parlant de persones especials... **Eli**, tu ho ets! Ets una de les persones que més d'aprop ha viscut tota la tesis! Moltes gràcies per acompanyar-me els caps de setmana a mirar plugs, per preparar-me sopars boníssims, per treure'm fora de Barcelona quan estava agobiada, pels estius que em passat juntes, per escoltar-me sempre encara que no entenguessis res... ets el meu cuquet preferit i la meva persona! **Anabel**, gran pilar durant aquest temps... moltes gràcies per tot. Que dir-te que no

sàpigues... sempre m'has ajudat tant en la feina com en lo personal. M'alegro molt d'haver-te conegut, ets una d'aquelles persones que quan entren a la teva vida no vols que en surtin mai!

Finalment, dir que els meus anys de tesis sempre estaran lligats al rugby, esport que vaig conèixer per casualitat però que m'ha fet créixer com a persona i m'ha permès conèixer gent excepcional. M'heu ensenyat què és l'esforç i la superació i que els límits estan on els poses tu, i tot això m'ha servit pel camp de rugby i també al llarg de la tesis i de la vida. El rugby i sobretot el Gòtics sempre formarà part de mi. Així que moltíssimes gracies a les entrenadores Eva, Moli, Cati i Belén i a totes les companyes d'equip actuals i passades: Carmina, Tortu, Diana, Èlia, Anna Gràcia (super compi de pis ara, gràcies a tu també per les xerrades nocturnes!), Sere, Botey, Roser, Cris, Lidia, Mar, Anita, Lara, Aina, Catia, Paulin, Bàrbara, Adriana, Sonajero, Bibi, Ruth, Anamar, Lois, Marina (tu ara també entres en aquest apartat!), Marta, Laia, Arantza, Andina...i òbviament menció especial a la Nena i la Mire Lleida! Nena i Mire sou uns solets!
Gràcies a tots i a cadascun de vosaltres. Aquesta tesis porta una mica de tots.

Per a la realització d'aquesta Tesis Doctoral he gaudit de la beca FI d'ajuda per la contractació de personal en centres d'investigació de la Generalitat de Catalunya, entre els anys 2010 i 2011, i de la beca FPU de "Ayuda de posgrado para la formación de profesorado universitario" del Ministeri d'enocomia i competitivitat, entre els anys 2012 i 2013.

ABSTRACT

In this work we have assessed the possible contribution of the human chromosome-21 gene *DYRK1A* in the developmental cortical alterations associated with Down syndrome using the mBACTg*Dyrk1a* mouse, which carries 3 copies of *Dyrk1a*, and a trisomic model of the syndrome, the Ts65Dn mouse. We show that trisomy of *Dyrk1a* changes the cell cycle parameters of dorsal telencephalic radial glial (RG) progenitors and the division mode of these progenitors leading to a deficit in glutamatergic neurons that persist until the adulthood. We demonstrate that *Dyrk1a* is the triplicated gene that causes the deficit in early-born cortical glutamatergic neurons in Ts65Dn mice. Moreover, we provide evidences indicating that DYRK1A-mediated degradation of Cyclin D1 is the underlying mechanism of the cell cycle defects in both, mBACTg*Dyrk1a* and Ts65Dn dorsal RG progenitors. Finally, we show that early neurogenesis is enhanced in the medial ganglionic eminence of mBACTg*Dyrk1a* embryos resulting in an altered proportion of particular cortical GABAergic neuron types. These results indicate that the overexpression of DYRK1A contributes significantly to the formation of the cortical circuitry in Down syndrome.

RESUM

En aquest treball s'ha avaluat la possible contribució del gen *DYRK1A*, localitzat en el cromosoma humà 21, en les alteracions del desenvolupament de l'escorça cerebral associades a la Síndrome de Down (SD) mitjançant l'estudi de dos models murins: el ratolí mBACTg*Dyrk1a*, el qual conté 3 còpies de *Dyrk1a*, i el ratolí Ts65Dn, un dels models trisòmics de la SD més ben caracteritzats. Els nostres resultats mostren que la trisomia de *Dyrk1A* altera alguns paràmetres del cicle cel·lular i el tipus de divisió dels progenitors neurals del telencèfal dorsal, donant lloc a un dèficit de neurones glutamatèrgiques que persisteix fins l'edat adulta. Hem demostrat que *Dyrk1a* és el gen triplicat responsable del dèficit inicial en la generació de neurones glutamatèrgiques corticals observat en el ratolí Ts65Dn. A més a més, hem proporcionat evidències de que la degradació de Ciclina D1 induïda per DYRK1A és el mecanisme molecular subjacent a les alteracions de cicle cel·lular observades en els progenitors neuronals dels embrions mBACTg*Dyrk1a* i Ts65Dn. Per altra banda, hem demostrat que la neurogènesis inicial està incrementada en l'eminència ganglionar medial dels embrions mBACTg*Dyrk1a*, fet que altera la proporció de subtipus específics d'interneurones GABAèrgiques en l'escorça cerebral adulta. En conclusió, els nostres resultats indiquen que la sobreexpressió de DYRK1A contribueix significativament a la formació dels circuits cortical en la SD.

PRESENTATION

Intellectual disability is the most invalidating hallmark in Down syndrome (DS), which is caused by an extra copy of human chromosome (HSA) 21. The analysis of brain tissue from foetuses and children with DS and from trisomic mice that model the syndrome indicated that intellectual disability in DS is caused, at least in part, by alterations in the cytoarchitecture of the cerebral cortex that arise during prenatal and postnatal development. The Ts65Dn mouse, a well studied trisomic mouse model that recapitulates some DS phenotypes including learning and memory defects, shows abnormal embryonic neurogenesis in the dorsal and ventral telencephalon, that results in a deficit in glutamatergic neurons and an excess in GABAergic interneurons in the adult cerebral cortex of this mouse.

One of the important questions to solve in DS research is which are the gen or group or genes in HSA21 that are responsible to the different DS phenotypes. At the beginning of this Doctoral Thesis none of the triplicated gene/s that are causing the structural brain alterations in DS were identified.

Among the different HSA21 genes, *DYRK1A* was a good candidate to explain some of the developmental brain alterations in DS because: 1) *DYRK1A* lies on the " DS critical region"; 2) the phenotype of *DYRK1A* loss-of-function mutations in humans and mice indicates that it is a crucial dosage-dependent gene for brain development; and 3) all transgenic mice studied that overexpress *Dyrk1a* show defects in learning and memory.

To provide new insights into the role of DYRK1A in brain development and to determine the possible implications of *DYRK1A* trisomy in the cortical alterations associated with DS, I have analysed the gross morphology of the brain and the development of the cerebral cortex of a new mouse model, the mBACtg*Dyrk1a* mouse, that contains and extra copy of the entire *Dyrk1a* gene, mimicking the situation in DS. The results of this analysis indicated that trisomy of *Dyrk1a* alters neurogenesis in both the dorsal and the ventral telencephalon leading to defects in the number of cortical glutamatergic and GABAergic neurons that persist until the adulthood. Similar to what has been previously described in the Ts65Dn model, the defect in dorsal neurogenesis in the mBACtg*Dyrk1a* model was associated to defects in cell cycle parameters. By performing genetic rescue experiments, I was able to demonstrate that *Dyrk1a* is the triplicated gene that is causing the neurogenic defects in the dorsal telencephalon of Ts65Dn embryos. I have also studied the possible molecular mechanisms underlying the neurogenic defects in *Dyrk1a* trisomic embryos. This has led to the identification of DYRK1A-mediated regulation of Cyclin D1 degradation as an important mechanism to couple cell cycle progression and neurogenesis in dorsal telencephalic radial glial progenitors.

Finally, some of the morphological brain alterations observed in the mBACtg*Dyrk1a* model suggest that trisomy of *DYRK1A* might also affect the development of other regions besides the cerebral cortex in DS brains.

ABBREVIATIONS

AD: Alzheimer's disease

BAC: Bacterial artificial chromosome

BDNF: Brain-derived neurotrophic factor

BMP: Bone morphogenetic protein

BrdU: 5-bromo-2'-deoxyuridine

BS: Bloquing solution

CDK: Cyclin-dependent kinase

CGE: Caudal ganglionic eminence

CNS: Central nervous system

CP: Cortical plate

CR: Calretinin

Delta1: Delta-like1

DM: Dissociating media

DS: Down syndrome

DSCR: Down syndrome critical region

DYRK1A: Dual-specificity tyrosine-(Y)-phosphorylation Regulated Kinase 1A

E: Embryonic day

EDU: 5-ethynyl-2'-deoxyuridine

EGCG: Epigallocatechin gallate

FBS: Fetal bovine serum

FGF: Fibroblast growth factor

FGFR: Fibroblast growth factor receptor

GF: Growth factor

GFAP: Glial fibrillary acidic protein

GFP: Green fluorescent protein

GLAST: Glutamate aspartate transporter

HSA: Human chromosome

IF: Immunofluorescence

IHC: Immunohistochemistry

IP: Intermediate progenitor

iPSCs: Induced pluripotent stem cells

IS: Incubating solution

IZ: Intermediate zone

LGE: Lateral ganglionic eminence

LTD: Long term depression

LTP: Long term potentiation

MGE: Medial ganglionic eminence

MMU: *Mus musculus* chromosome

MZ: Mantel zone

NECs: Neuroepithelial cells

NES: Nuclear export signal

miRNA: microRNA

NFAT: Nuclear factor of activated T-cells

NgN: Neurogenin

NLS: Nuclear localization signal

NPC: Neural precursor cells

NPY: Neuropeptide Y

NT4: Neurotrophin-4

ON: Overnight

OPCs: Oligodendrocytes precursors cells

oRG: outer Radial Glial

P: Postnatal day

PBS: Phosphate Buffered Saline

PCD: Programmed cell death

PCR: Polymerase chain reaction

PFA: Paraformaldehyde

pH3: Phosphohistone 3

POA: Preoptic area

Ppia: Peptidyl-prolyl isomerase a

PV: Parvalbumin

RA: Retinoic acid

Rb: Retinoblastoma

REST: RE1 silencing transcription factor

RG: Radial glial

RT: Room temperature

RT-PCR: real time PCR

SBC: Somatosensory barrel cortex

Ser: Serine

SEM: Standard error of the mean

Shh: Sonic hedgehog

SNPs: Short neural precursors

SP: Subplate

SST: Somatostatin

SVZ: Subventricular zone

Tc: Cell cycle duration

Thr: Threonine

TrkB: Tropomyosin kinase receptor B

Ts: S phase duration

Tyr: Tyrosine

VIP: Vasoactive intestinal peptide

VZ: Ventricular zone

WT: Wild-type

YAC: Yeast artificial chromosome

TABLE OF CONTENTS

Results

Discussion

INTRODUCTION

1. The cerebral cortex

1.1 Cellular composition and functionality

The mammalian cerebral cortex is the brain region responsible for high order functions, such as cognition, sensory perception, control of motor functions and consciousness. It contains hundreds of different neuronal and glial cell types organized in six histological distinct layers (Jones et al., 1984). Around 70-80% of cortical neurons are glutamatergic projection neurons that extend axons to distant intracortical, subcortical or subcerebellar targets, while the remaining ones are GABAergic inhibitory interneurons that make local connections within the cortex (Parnavelas et al., 2000; Molyneaux et al., 2007).

Cortical excitatory and inhibitory neurons can be grouped in different subclasses based on their morphology, electrophysiological properties and pattern of expression. **Glutamatergic neurons** are classified according to their radial position within the six cortical layers because neurons with similar connectivity and gene expression profile tend to occupy the same cortical layer (see Figure I-1). Briefly, neurons from layers II-III project to intracortical regions of the same hemisphere or to the contralateral hemisphere; neurons from layer IV project locally within a neocortical column; neurons from layer V project mainly to subcerebral regions such as the basal ganglia, midbrain, hindbrain and the spinal cord; while most of the neurons in layer VI project to the thalamus (Molyneaux et al., 2007). Importantly, specific transcription factors are differentially expressed across layers. For instance layer VI neurons express

Tbr1, layer V neurons express Ctip2, while neurons of the external cortical layers (layers II-IV) express Cux1 and Cux2 (Molyneaux et al., 2007; see schemes in Figure I-1).

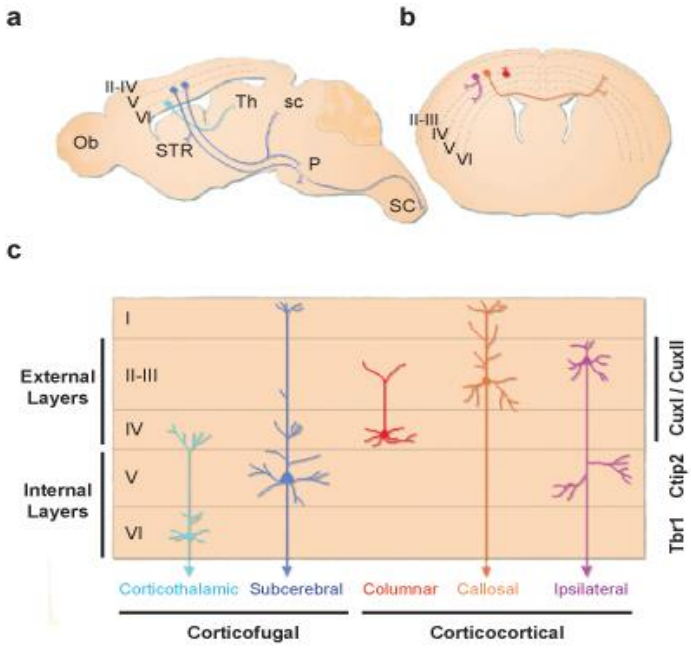

Figure I-1: Major subtypes of cortical glutamatergic neurons in the mouse adult brain. (a) A sagittal view of the adult brain showing the cortical layer origin and the projection destinies of the two types of corticofugal neurons: corticothalamic (faith blue) and subcerebral (dark blue). **(b)** A coronal view of the adult brain showing the cortical layer origin and the projection destinies of the three types of cortico-cortical neurons: ipsilateral (purple), callosal (orange) and columnar (red). Ob: olfactory bulb; Th: thalamus; STR: striatum; sc: superior coliculus (in the brain); P: pons; SC: spinal cord. **(c)** Magnified view of the glutamatergic neuron subtypes depicted in **a** and **b** detailing their laminar position, morphology and expression of layer-specific transcription factors (right column). Adapted from Franco and Muller (2013).

GABAergic interneurons are extremely heterogenic and at least 20 distinct subtypes of interneurons have been described in the neocortex (Gelman and Marin, 2010). The most common system to classify inhibitory neurons is using protein markers,

such as calcium binding proteins, neuropeptides and glycoproteins, which are expressed in specific interneuron subtypes that differ in their morphology, expression and distribution of ions channels, firing characteristics, and the domains of the post-synaptic projection neurons that they innervate (see Figure I-2). For example, GABAergic basket cells and chandelier cells, which represent 40% of GABAergic interneurons, express the calcium binding protein parvalbumin (PV), innervate the soma and proximal dendrites of excitatory projection neurons, and show a fast-spiking pattern of firing. Cells expressing somatostatin (SST) account for 30% of the neocortical interneurons, are morphologically heterogeneous (one type are the Martinotti cells), innervate distal dendrites of excitatory projection neurons and typically exhibit non- fast-spiking or intrinsic burst firing pattern of firing (Markram et al., 2004; DeFelipe et al., 2013). SST-expressing interneurons can be subdivided based on the expression of the calcium binding protein calretinin (CR). Interneurons expressing both SST and CR are localized in external cortical layers and show a bipolar morphology, while those that do not express CR are localized in internal cortical layers and show a stalled morphology (Miyoshi et al., 2007). The remaining 30% of neocortical interneurons are comprised by interneurons expressing the vasointestinal peptide (VIP) and/or CR with bipolar or double-bouquet morphologies and fast adapting firing patterns, and by interneurons expressing Reelin, with a neuro-glia morphology and late-spiking firing patterns. Additionally, a small population of cortical interneurons consists of multipolar cells that contain the neuropeptide Y (NPY) and display irregular or fast adapting AD firing properties (Sultan et al., 2013) (Figure I-2).

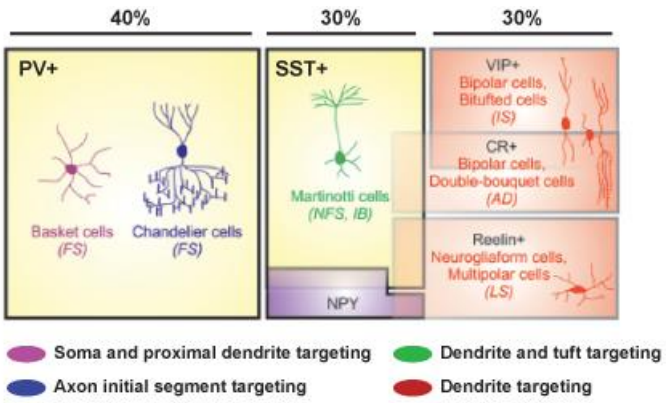

Figure I-2: Major subtypes of GABAergic interneurons in the mouse cerebral cortex. Representation of the different types of GABAergic interneurons classified by the expression of the molecular markers parvalbumin (PV), somatostatin (SST), neuropeptide Y (NPY), vasointestinal peptide (VIP), calretinin (CR) and Reelin. The size of the rectangles is proportional to their proportion with respect to the total GABAergic interneurons in the cerebral cortex. Electrophysiological profiles are indicated bellow the name of each interneuron subtype: fast-spiking (FS); non-fast-spiking (NFS); intrinsic burst firing (IB); irregular-spiking (IS); fast adapting firing (AD); and late-spiking (LS). The subcellular synaptic targeting specificity of each type of GABAergic interneuron is indicated below the rectangles. Adapted from Sultan et al., (2013).

The precise execution of the functions of the mammalian neocortex depends on the correct generation and integration into neural circuits of glutamatergic neurons and GABAergic interneurons. Glutamatergic neurons are the main players in cortical functionality by receiving afferent inputs and responding to them. In contrast, interneurons play a crucial role in controlling and synchronizing the activity of projection neurons by preventing excessive excitation and controlling synaptic integration and spike timing (Isaacson et al., 2011). The influence of interneurons on pyramidal cells is largely dependent on the subcellular location of their inputs, which varies among different interneuron

subtypes (see Figure I-2). There is evidence that an imbalance in the proportion of excitatory/inhibitory neurons in the neocortex leads to an abnormal cortical functionality. Indeed, it has been proposed that an imbalance between excitatory and inhibitory inputs in cortical neurons is a common pathogenic mechanism in diverse neurological and psychiatric disorders such as epilepsy, autism spectrum disorder, schizophrenia and intellectual disability (Marin et al., 2012; Bozzi et al., 2012). Furthermore, oligodendrocytes and astrocytes, which are the two major types of macroglial cells in the central nervous system (CNS), also contribute to neocortical function by myelinating axons and by providing regulatory functions within the neuronal networks, respectively. Alterations in the number of these cells or in their functionality have also been reported in neurological disorders (Seifert et al., 2006).

1.2 Development

1.2.1 General aspects

The genesis of the different cell populations of the neocortex is temporally and spatially segregated. In the mouse, neurons are generated from embryonic day 11 (E11) to E17, astrocytes appear around E18, with their numbers peaking in the neonatal period, while differentiated oligodendrocytes are first seen postnatally (Kriegstein and Alvarez-Buylla, 2009). Multiple progenitor zones contribute to the rich variety of cell types observed in the neocortex. Projection neurons and astrocytes are generated from progenitors of the dorsal telencephalon (pallium) (Kriegstein and Alvarez-Buylla, 2009), while interneurons are

generated from progenitors of the ventral telencephalon (subpallium) (Welagen and Anderson, 2011). In contrast, oligodendrocytes are generated from progenitors of the dorsal and ventral telencephalon at three different developmental stages: at E12.5, at E15.2 and around birth (Kessaris et al., 2006) (see scheme in Figure I-3).

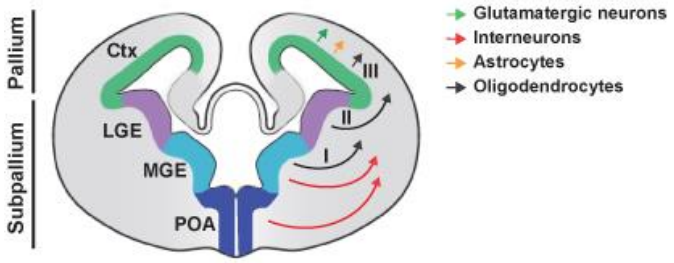

Figure I-3: Domains of generation of cortical cells. In the left half of the picture are represented the ventricular zone domains were different cortical cells are generated (Ctx: cortex; LGE: lateral ganglionic eminence; MGE: medial ganglionic eminence; POA: preoptic area). The right half of the figure depicts the cell type generated in each domain and their migratory routes (indicated by arrows). Glutamatergic neurons (green arrow), astrocytes (orange arrow) and some oligodendrocytes (black arrows) are generated in the pallium, while interneurons (red arrows) and part of oligodendrocytes (black arrows) are generated in the subpallium. Roman numbers represent the three waves of oligodendrocytes generation. Adapted from Kriegstein and Alvarez-Buylla (2009).

Like in other regions of the CNS the development of the neocortex can be divided in three sequential phases: a proliferative phase, a neurogenic phase and a gliogenic phase (see Figure I-4). During the **proliferative phase** neuroepithelial cells (NECs) of the ventricular zone (VZ) undergo symmetric divisions to expand their pool (Cai et al., 2002; Noctor et al., 2004). By the end of this phase, between E9 to E10 in the mouse, NECs transform to a distinct type of progenitor, named radial glial

(RG) progenitor. This progenitor is pluripotent, thus is capable to generate all differentiated cells of the mature brain (Temple et al., 2001). Similar to NECs, RG progenitors show apico-basal polarity through two long processes radially oriented: one that extends apically and contacts the ventricle and the other that extends basally and contacts the basal lamina and the blood vessels of the meninges (Bentivoglio and Mazzarello, 1999; Gotz et al., 2002). However, RG progenitors lose some of the epithelial properties of the NECs, like the presence of tight junctions (Aaku-Saraste et al., 1996), and express proteins that are characteristic of astroglial cells, such as glial fibrillary acidic protein (GFAP) and the glutamate aspartate transporter (GLAST). Another characteristic of these progenitors is that they undergo interkinetic nuclear migration, which means that their nuclei migrate between the apical surface and the basal part of the VZ in synchrony with the cell cycle. After mitosis at the apical surface (M phase), the nuclei migrate basally during G1 phase and subsequently stay at the basal region of the VZ during S phase. In G2 phase, the nuclei migrate apically, entering M phase upon reaching the apical surface (Taverna and Huttner, 2010). During the **neurogenic phase**, RG progenitors switch their mode of division and start to generate neurons directly or indirectly via a more restricted progenitor named intermediate progenitor (IP). The **gliogenic phase** in the dorsal telencephalon starts at late embryonic period, when RG progenitors detach from the ventricle and convert into astrocytes (Choi and Lapham, 1978; Schmechel and Rakic, 1979). These astrocytes migrate radially towards the basal surface were they divide, expanding the number of astrocytes that are produced postnatally (Ge et al., 2012). Oligodendrocyte precursor cells (OPCs) are generated from RG

progenitors of the ventral (first and second waves) or the dorsal (third wave) telencephalon. Then OPCs migrate during embryogenesis, in a way that by the time of birth they are evenly distributed throughout the brain (Richardson et al., 2006; Kessaris et al., 2006). OPCs generate mature oligodendrocytes mainly during the first two postnatal weeks. However, proliferating OPCs continue to exist in the adult brain as a relative stable population (Rivers et al., 2008; Dawson et al., 2003).

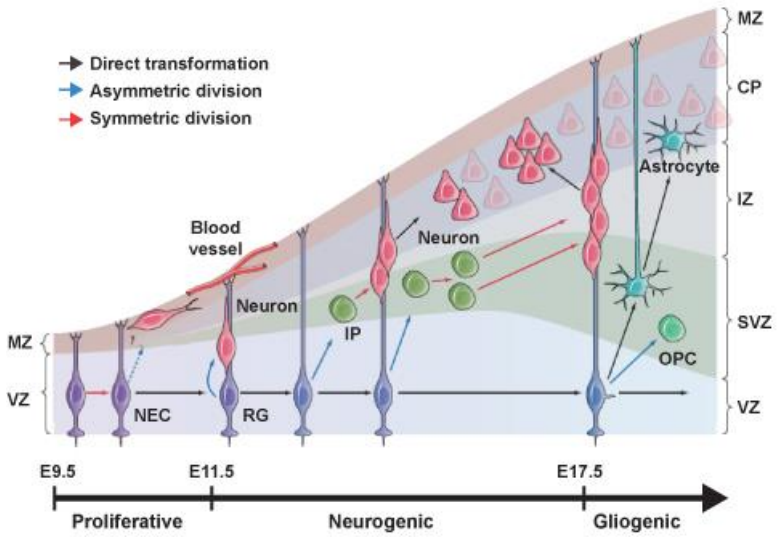

Figure I-4: Development of the cerebral cortex. Representation of the three phases of cortical development, the main types of cortical progenitors and how different cortical cell types are generated during embryonic development. Solid arrows are supported by experimental evidences; dashed arrows are hypothetical. Mouse developmental stages corresponding to each phase are indicated. NEC: neuroepithelial cells; RG: radial glia progenitor; IP: intermediate progenitor; OPC: oligodendrocyte precursor cell; VZ: ventricular zone; SVZ: subventricular zone; IZ: intermediate zone; CP: cortical plate, MZ: marginal zone. Adapted from Kriegstein and Alvarez-Buylla (2009).

The final number of neurons in the adult cerebral cortex depends on the combination of two developmental processes:

neurogenesis and programmed cell death. In the following sections I describe the contribution of these two processes in the formation of the cortical circuitry.

1.2.2 Neurogenesis of glutamatergic neurons

- General description

Cortical glutamatergic neurons are generated from **RG progenitors** localized in the VZ of the dorsal telencephalon, which are characterised by the expression of the transcription factor Pax6 (Englund et al., 2005).

Time-lapse imagining studies revealed that during the neurogenic phase RG progenitors undergo self-expanding asymmetric divisions that produced another RG progenitor and one neuron (neurogenic division) or one IP (proliferative division) (Attardo et al., 2008; Noctor et al., 2004; see scheme in Figure I-4). Importantly, the histological analysis of a Tis21-GFP knock-in mouse, which only expresses GFP in cells undergoing neurogenic divisions, demonstrates that around 10-20% of asymmetrically dividing RG progenitors generate neurons directly (Attardo et al., 2008; Kowalczyk et al., 2009). **IPs** are neurogenic restricted progenitors that differ from RG progenitors for its morphology and mode of division. IPs show a multipolar shape and do not contact with either the apical or basal cortical surface and always divide symmetrically to self-expand or terminally differentiate into neurons (Kowalczyk et al., 2009; Noctor et al., 2004). IPs can be further distinguished by the expression of the transcription factor Tbr2 (also named Eomes) and the down-regulation of Pax6 (Englund et al., 2005). Once they are

generated from a RG progenitor in the VZ they move basally and form the subventricular zone (SVZ) where they divide (Noctor et al., 2004; Kowalczyk et al., 2009; see scheme in Figure I-4).

Recently, a third type of neuronal progenitor has been identified in the mouse dorsal telencephalon: the **short neural precursors (SNPs),** which are also generated from asymmetric divisions of RG progenitors. SNPs are localized in the VZ and express Pax6. However, unlike RG progenitors SNPs do not contact the pial surface and do not express GLAST (Stancik et al., 2010). Another important difference between these types of progenitors is their mode of division, since SNPs divide symmetrically to generate neurons (Tyler and Haydar, 2013). These progenitors were identified at midcorticogenesis in embryos coelectroporated with GLAST and Tubulinα1 reporters. Thus it remains unknown when RG progenitors start to produce SNPs and which is their contribution to the total neuron production. In addition, it is controversial if these cells are a real distinct type of progenitor or are newborn IPs that have not yet lost their ventricular contact (Lui et al., 2011).

Newly generated neurons radially migrate out of the proliferative zone using RG processes as migratory scaffold (Rakic et al., 1978) and give rise to the cortical plate (CP), which will become the multilayered neocortex at postnatal stages (Figure I-1). The generation of the different subtypes of projection neurons is tightly regulated in time. The earliest born neurons form a layered structure named the preplate, which later splits into the more superficial marginal zone (MZ) and the deeply located subplate (SP). The CP develops between these two layers (Marin-Padilla et al., 1978). *In vivo* birth-dating studies using thymidine

analogues showed that the different subtypes of projection neurons are generated in sequential waves and that they settle in the CP following and inside-outside model, in which the early born neurons populate deeper neocortical layers (layer VI and layer V), then late-born neurons pass through these layers and progressively populate more superficial layers (layer IV and layer II-III) (Molyneaux et al., 2007; Greig et al., 2013; see scheme in Figure I-5).

During the last decade, several studies have been done in order to define how this neuronal diversity is established. Two main models that are not mutually excluded have been proposed. In the first one, neurons arise from a unique type of progenitor that progressively reduces its neurogenic competence over the course of development. In the second model there are linage-restricted progenitors since the beginning of neurogenesis. Despite there are evidences supporting both models, nowadays the most accepted model is the first one (Franco and Muller, 2013). It is important to highlight that since the mouse SVZ starts to be visible at E13.5 and expands significantly during late corticogenesis (Englund et al., 2005), it has been proposed that as neocortical development progresses IPs become the major source of projection neurons and, therefore, generate most neurons of the external layers (Breunig et al., 2011; Kowalczyk et al., 2009; Haubensak et al., 2004; Nieto et al., 2004). This model implies that internal layer neurons are generated from RG asymmetric divisions. Consistent with these ideas, some RG progenitors express markers of internal layer neurons, including Fezf2 and Otx1 (Frantz et al., 1994; Chen et al., 2005), while genes specific for external layer neurons such as Cux1 and Cux2

are highly expressed in IPs of the SVZ during middle and late corticogenesis (Nieto et al., 2004; Zimmer et al., 2004).

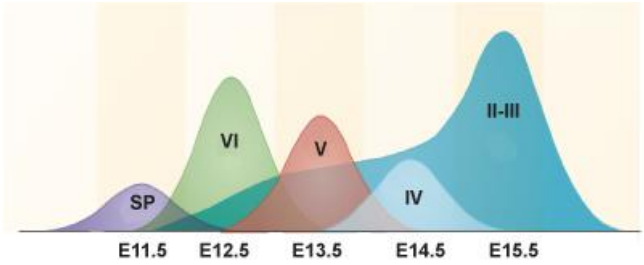

Figure I-5: Neurogenic waves of cortical glutamatergic neurons. Representation of the waves of generation of the distinct glutamatergic neuron subtypes. Note that it follows an inside-outside model. Peak sizes are proportional to the approximate number of neurons of each subtype. The developmental stages indicated correspond to the mouse. Adapted from Greig et al. (2013).

The model of neocortical development explained above is largely based on cellular and molecular studies of the mouse and rat cortex, which exhibit many key features of the mammalian neocortex such as the six-layered organization. However, they differ from human and other primate's cerebral cortex in the size and shape. The human cerebral cortex is large and highly folded (gyrencephalic), while rodents cortex is significantly smaller and non-folded (lisencephalic) (Lui et al., 2011). Recent observations of the developing neocortex of humans and other primates led to the hypothesis that the large neocortical volume and surface in these species is related to the expansion of the SVZ and the formation of a third germinal region named outer subventricular zone (OSVZ) (Smart et al., 2002; Zecevic et al., 2005). This proliferative region is formed by **outer radial glial (oRG) progenitors,** which are likely originated from asymmetric divisions of VZ RG progenitors and can be distinguished from these progenitors because oRGs lack the apical process and are

located more basally (Fietz et al., 2010; Hansen et al., 2010). oRGs divide asymmetrically to generate neurons or outer intermediate progenitors, which express Tbr2 and function as an amplifying cell (Hansen et al., 2010). Importantly, thymidine-labelling studies in primates indicate that proliferation of OSVZ progenitors coincides with the major wave of cortical neurogenesis, suggesting that these progenitors are the major contributors to cortical neurons in primates (Betizeau et al., 2013; Lukaszewicz et al., 2005). A detailed analysis of the mouse cerebral cortex revealed the presence of oRGs, but in rodents they represent a very small proportion of all cortical progenitors, around 5% (Shitamukai et al., 2011; Wang et al., 2011). These observations strongly suggest that, although the presence of oRG is not sufficient to drive gyrencephaly, their abundance impact on the expansion and folding of the cerebral cortex. In agreement, increasing the abundance of oRG via targeted genetic manipulation in the mouse leads to cortical expansion and folding (Stahl et al., 2013). In addition, the observation that an increment in the abundance of IPs in the gyrencephalic ferret drives the formation of additional folds and fissures indicates that IPs also contribute to the cortical folding (Nonaka-Kinoshita et al., 2013).

- Regulation of neuron production

The cerebral cortex is functionally organized in radial columns (Mountcastle et al., 1997). According to the previously explained model of neurogenesis, the number and proportion of projection neuron subtypes generated in a cortical radial column depends on the duration of the neurogenic phase and the rate of neurogenesis.

The **duration of the neurogenic phase** is determined by its initiation, when NECs transform into RG progenitors that undergo asymmetric neurogenic divisions, and its end, when the neurogenic-gliogenic switch occurs and gliogenesis begins. Different growth factors and cell signalling pathways regulate the transformation of NECs into asymmetric dividing RG progenitors. Among them the most relevant are Fibroblast growth factor (FGF), Notch and Retinoic acid (RA).

Among the different members of the **FGF** family of growth factors, FGF10 plays a crucial role in the regulation of NEC to RG transition in the rostral neocortex. FGF10 is expressed in the cortical proliferative region when the NEC-RG transition starts and its rapidly downregulated when this conversion is completed (Sahara and O'Leary, 2009). Its disruption results in a prolonged duration of the proliferative phase that leads to delayed RG emergence and initial decrease of neuronal production followed by increased number of neurons at later stages (Sahara and O'Leary, 2009). Similarly, the observations that the expression of the **Notch** ligand Delta-like 1 (Delta1) roughly coincides with the onset of neurogenesis (Kawaguchi et al., 2008; Hatakeyama et al., 2004) and that forced activation of Notch signalling increases the expression of RG progenitor markers, while its inactivation reduces them, leads to the conclusion that Notch signalling is involved in the transition from NECs to RG progenitors and promotes RG identity (Gaiano et al., 2000; Anthony et al., 2005). In addition, **RA**, which is produced by the meninges, is essential for the initiation of neurogenesis in the dorsal telencephalon. In fact, the emergence of RA-producing meningeal cells correlates with the onset of neurogenesis and mutations that decrease

meningeal formation lead to an impaired production of RG-derived neurons (Siegenthaler et al., 2009). Importantly, this impairment in neuron generation is reverted by *in utero* treatment with RA (Siegenthaler et al., 2009). Although the cellular mechanisms by which RA regulates the production of RG-derived neurons remain elusive, a recent study shows that this RA function requires the expression of the orphan nuclear hormone receptor CoupTFI (Harrison-Uy et al., 2013).

As already mentioned, the neurogenic-gliogenic switch occurs at late embryonic stages. During the neurogenic phase the expression of glial genes is repressed in neural progenitor cells (NPCs) via two mechanism: 1) Neurogenin 1 (Ngn1) sequestrates the transcriptional co-activator p300 required for the janus kinase (JAK)-signal transducer and activator of transcription (STAT) astroglial signaling pathway (Sun et al., 2001; Bonni et al., 1997) and 2) Dnmt1 methylates glial promoters impeding the STAT-dependent activation of glial genes (He et al., 2005; Takizawa et al., 2001; Namihira et al., 2004). The neurogenic-gliogenic switch requires the PcG-mediated accumulation of H3K27me3 inhibitory mark at the *Ngn1* loci, which leads to its down-regulation and the release of the co-activator p300 (Hirabayashi et al., 2009). In addition newly generated neurons induce the astroglial fate through two complementary mechanisms. First they release Cardiotropin1, that together with the leukemia inhibitory factor and the ciliary neurotrophic factor cytokines activate the astrogliogenic JAK-STAT pathway (Barnabe-Heider et al., 2005). Second, they express Jag1 and Dll ligands that activate Notch signalling in the neighbouring NPCs and induce the expression of Nuclear Factor-

Ia (Namihira et al., 2009). This transcription factor is a key activator of astrogliogenesis (Deneen et al., 2006) and induces Dnmt1 dissociation from glial genes promoters, thus allowing their demethylation and STAT binding (Namihira et al., 2009). External signals such as Notch and Bone morphogenetic protein (BMP) 2 at late embryonic stages promotes the neurogenic-gliogenic switch. Notch signalling promotes astrogliogenesis by driving the expression of *Gfap* and other astroglial genes via direct binding of its effector CBF1 to their promoters (Ge et al., 2002); by repressing pro-neural genes via Hes1 (Kato et al., 1997); and by recruiting JAK2 kinase and thus promoting STAT3 phosphorilation and activation (Kamakura et al., 2004). On the other hand, the BMP2 signalling acts synergistically with the JAK/STAT pathway by recruiting p300 to the astrocytic promoters, via Smad1 activation (Gross et al., 1996; Nakashima et al., 1999; Nakashima and Taga 2002).

The **rate of neurogenesis** is determined by the initial pool of RG progenitors, the type of division of cortical progenitors (proliferative vs neurogenic) and by the duration of the cell cycle.

The pool of RG progenitors is determined by the number of symmetric divisions underwent by NECs and RG progenitors, and establishes the number of radial columns and therefore the surface of the cerebral cortex (Rakic et al., 1995). Different growth factors regulate the expansion of cortical progenitors; the most relevant among them are Wnt and FGF. Activation of canonical **Wnt signalling** positively regulates proliferative symmetric divisions of RG progenitors at the onset of neurogenesis. In the absence of Wnt, cytosolic β-catenin is recruited into a complex with adenomatous polyposis coli and

axin. This association facilitates its N-terminal phosphorylation by glycogen synthase kinase 3β and its consequent ubiquitination and degradation by the proteosome. Wnt activation of Frizzled-LRP co-receptors increases the stable pool of β-catenin by disrupting this complex. Then free β-catenin enters to the nucleus where it associates with TCF/LEF family members to direct transcription of Wnt target genes (Logan and Nusse, 2004; Clevers et al., 2006). It has been shown that expression of a stabilised form of β-catenin, which can not be degraded, in cortical progenitors induces RG progenitors amplification, leading to striking enlargement of the cerebral cortical surface and the generation of convoluted folds resembling the gyri and sulci of the neocortex in higher mammals (Chenn and Walsh, 2002; 2003). Conversely, targeted inhibition of β-catenin signalling causes cortical precursor cells to prematurely exit the cell cycle and differentiate into neurons, which leads to an earlier exhaustion of the pool of progenitors and therefore a thinner cerebral cortex (Woodhead et al., 2006). The dorsal VZ also expresses FGF2, which is required for the expansion of NECs because it favours the maintenance of NEC proliferative divisions (Raballo et al., 2000) and prevents neurogenesis (Vaccarino et al., 1999). In agreement with this anti-neurogenic role of FGF2, the disruption of FGF2 receptors, FGFRs 1, 2 and 3 during the proliferative phase induces precocious neurogenesis, leading to an early depletion of the progenitor pool and a drastic reduction of the cortical size (Rash et al., 2011). Importantly, FGF signalling maintains Notch activity in the dorsal telencephalon in a cell autonomous manner (Rash et al., 2011), which as it would be explained later is crucial for progenitor maintenances.

Asymmetric division of RG progenitors during the neurogenic phase, involve the asymmetric inheritance of fate determinants (Siller and Doe, 2009; Morin and Bellaiche, 2011). Different events and processes have been proposed as regulators of asymmetric divisions. One is the axis of RG progenitor division, which is determined by the orientation of the mitotic spindle. The orientation of the mitotic spindle is regulated by polarity cues that are used to position cortical forces generators that pull on astral microtubules to orient the mitotic spindle along a specific axis (Morin and Bellaiche, 2011). These cues are the apical complex, which as its name indicates is apically located and it is composed by Par3, Par6 and aPKC. The apical complex recruits inscuteable during the division and interacts with the LGN complex, which is enriched in the lateral membrane of neural progenitors and interacts with microtubules and the dynein complex through the GDP-bound Gαi subunit and NuMa (Peyre and Morin, 2012). Oblique and vertical (parallel to the apico-basal axis) divisions tend to give rise to asymmetric fate outcomes (Chenn and McConnell, 1995; Zhong and Chia, 2008) while planar divisions (parallel to the ventricle) give rise to symmetric divisions (Konno et al., 2008). These observations led to a model in which the unequal segregation of the apical complex directs cell fate (Zhong and Chia, 2008). Consistent with this, mitotic spindles with horizontal orientations that give rise to vertical divisions are only found during the neurogenic phases of brain development (Haydar et al., 2003), while during the early expansion phase, keeping precise vertical spindle orientation is crucial to maintain the neural progenitor pool (Fish et al., 2006; Yingling et al., 2008). In agreement, disruption of these orientations alters neural production (Lancaster and Knoblich

2012). For example, the overexpression of the mouse inscuteable in RG progenitors increases the fraction of oblique divisions at the expense of planar divisions leading to increase IP production and indirect neurogenesis (Postiglione et al., 2011).

An unequal inheritance of the apical complex in cortical progenitors is associated to an unequal inheritance of Notch activity (Chenn and McConnell, 1995). One of the principle functions of Notch is to maintain the pool of neural progenitor by lateral inhibition (Kawaguchi et al., 2008). Daughter cells with greater Notch activity remain as RG progenitors, while those with lesser Notch activity become neurons or IPs (Kageyama et al., 2008). The cells undergoing neuronal differentiation up-regulate Notch ligands that in turn activate Notch receptors in the neighbouring cells and induce the repression of neurogenic programs, *via* its effectors Hes1 and Hes5 (Kageyama et al., 2007). It was observed that the apical complex component Par3 sequesters the Notch inhibitor Numb and inhibits its activity (Bultje et al., 2009). Hence, daughter cells that inherit high levels of Par3 show increased Notch activity and maintain the RG fate, while daughter cells that inherit low levels of Par3 have high Numb activity, low Notch signalling and differentiate (Bultje et al., 2009). In addition, it has been revealed that *Hes* genes show an oscillatory expression in neural progenitors, which controls the timing of neurogenic waves and maintain the equilibrium between neural progenitors and committed neurons (Shimojo et al., 2008). *Hes* oscillations are generated by an auto-regulatory feedback loop (Hirata et al., 2002), and are likely to be influenced by external signals, like the morphogen Sonic hedgehog (Shh) (Ingram et al., 2008; Wall et al., 2009). One of the transcription

factors that are repressed by Hes1 and Hes5 is the proneural basic helix-loop-helix transcription factor Ngn2, which induces the expression of neurogenic genes such as *NeuroD* (Lee et al., 1997; Seo et al., 2007), therefore promoting neuronal differentiation. Another direct target of Ngn2 is the IP transcription factor Tbr2, suggesting that Ngn2 could also promote the specification of IP (Ochiai et al., 2009). Importantly, Ngn2 increases the expression of the Notch ligand Delta, which in turn favours progenitor maintenances in the surrounding cells.

Asymmetric divisions of cortical progenitors are also characterised by the asymmetric inheritance of specific cell structures such as the basal process and the centrosomes (Wang et al., 2009; Lancaster and Knoblich, 2012; Paridaen et al., 2013). Time-lapse imaging of dividing RG progenitors shows that the daughter cell that does not inherit the basal process mostly differentiate into a neuron or an IP (Miyata et al., 2004; Shitamukai et al., 2011). It has been proposed that the basal process could provide to the progenitor an increased exposure to the Delta ligand expressed by neural committed cells that migrate along the fiber towards the CP, thus favouring Notch signalling in progenitors that inherit this process (Peyre and Morin, 2012). Other signals originated from the pial surface, where the basal process is attached, could also influence cell fate, such as the RA (Siegenthaler et al., 2009). In addition, Cyclin D2, which is localised at the endfoot of RG progenitors, is co-inherited with the basal process and it has been proposed to be involved in the maintenance of RG fate (Tsunekawa et al., 2012). The centrosomes are composed by two centrioles, which replicates in a semi-conservative fashion during interphase, leading to the

existence of a “young” and an “old” centrosome in each spindle pole (Nigg and Stearns, 2011). *In vivo* fluorescent analysis of the behaviour of both centrosomes in the mouse neocortex led to the conclusion that the older centrosome is preferentially inherited by the daughter cell that will remain as a progenitor (Wang et al., 2009). The mechanism that allows old centrosome to grant progenitor identity is still unknown, however it has been proposed that it could be related to the quicker regrowth of the primary cilia in these cells (Anderson and Stearns, 2009). Primary cilium is a small sensor localized in the apical region of RG progenitors that sense external signals such as Shh (Louvi and Grove, 2011). It is dismantled during cell division and regrowth after cytokinesis, hence cells that regrowth faster the primary cillium after mitosis could respond to external signals while the other daughter cell could not, generating an asymmetry of the activity of these signalling and influencing cell fate (Paridaen et al., 2013).

Regarding cell cycle regulation, it has been shown that premature cell cycle exit of cortical progenitors leads to earlier exhaustion of progenitors which give rise to a dramatic decrease in the final neuronal cellularity of the neocortex (Dehay and Kennedy, 2007). The cell division cycle is controlled by different Cyclins that bind to specific Cycling-dependent kinases (CDKs) allowing the progression through the different cell cycle phases. The activity of the different Cyclins/CDK complexes is regulated by CDK inhibitors of the INK and KIP/CIP families (see Figure I-6).

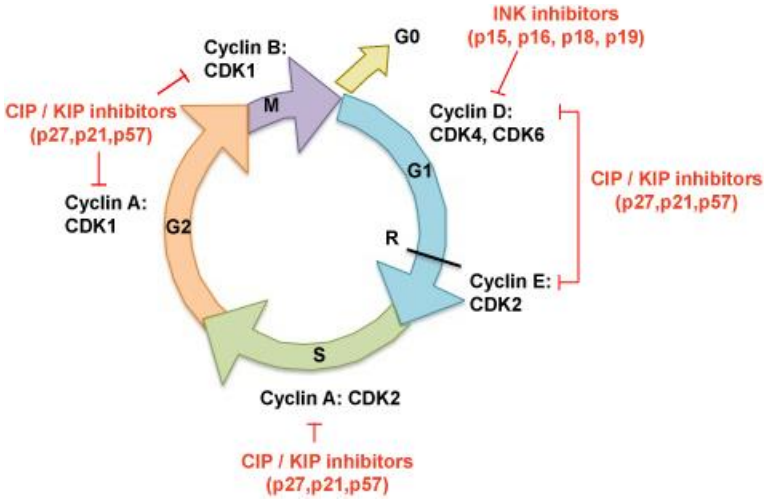

Figure I-6: Cell cycle regulation. Scheme showing the successive phases of the cell cycle: M phase, in which the nucleus and the cytoplasm divide; S phase, in which the DNA in the nucleus replicates, and two gap phases, gap1 (G1) and gap2 (G2). The G1 phase is a critical stage, allowing responses to extracellular cues that induce either commitment to a further round of cell division or withdrawal from the cell cycle (G0) to initiate the differentiation pathway. The G1 phase is also involved in the control of DNA integrity before the onset of DNA replication. During G2 phase the cell checks the completion of DNA replication and the genomic integrity before cell division starts. Cell cycle progression is positively regulated by distinct Cyclins and CDK complexes (in black) and negatively regulated by distinct inhibitors (in red).

Pioneer cumulative S phase labelling experiments performed in the mouse embryo showed that as neurogenesis progresses cell cycle duration of neocortical progenitors increases due to a progressive lengthening of the G1 phase (Takahashi et al.,, 1995). These studies also show that neural production increases in parallel to the increase in cell cycle duration (Caviness et al., 2003). These and other evidences showing a correlation between cell cycle length and neurogenesis led to the cell cycle length hypothesis (Gotz and Huttner, 2005). According to this hypothesis the time that a progenitor spends in G1 determines

the final effect of a particular cell fate determinant, which could be equal (symmetric divisions) or unequal (asymmetric divisions) in the two daughter cells (Gotz and Huttner, 2005; Dehay and Kennedy, 2007; Salomoni and Calegari, 2010). In agreement with this hypothesis, it has been described that protein levels of the neurogenic fate determinant Ngn2 are regulated by CDK phosphorylation. According to this hypothesis, a short G1 phase is accompanied with increased CDK activity and therefore rapid degradation of Ngn2, which prevents the expression of neurogenic genes and promotes progenitor maintenance. Contrary, internal CDK activity will lead to longer G1 phases and sufficient Ngn2 protein to induce neuronal differentiation (Ali et al., 2011; Hindley et al., 2012). In addition, during G1 progenitors integrate external signals that could induce either commitment to a further round of cell division or withdrawal from the cell cycle allowing entry into a differentiation pathway (Zetterberg et al., 1995; Cunningham and Roussel, 2001; Dehay and Kennedy, 2007; Salomoni and Calegari, 2010). For example, morphogens, such as Shh induce proliferation in cortical progenitors, while others such the Transforming growth factor beta promote cell cycle exit (Komada et al., 2012; Komada et al., 2008; Dave et al., 2011; Siegenthaler and Miller, 2005). Importantly, there is evidence that cell cycle regulators can influence cell fate and, inversely, that fate determinants can influence cell cycle progression (Salomoni and Calegari, 2010). For example, the cell cycle inhibitor $p27^{KIP1}$ induces neuronal differentiation by stabilizing Ngn2, and neuronal migration by inhibiting RhoA activity (Nguyen et al., 2006). Moreover, in the spinal cord Cyclin D1 promotes neurogenesis in a cell cycle independent manner by regulating the expression of Notch effectors (Lukaszewicz and

Anderson, 2011), and in retinal progenitors it promotes the transcription of important cell fate determinants (Bienvenu et al., 2010). On the other hand, Ngn2 induces cell cycle exit by repressing the expression of Cyclins involved in G1 and S phases (Lacomme et al., 2012).

The identification of specific genes expressed in neurogenic divisions, such as the antiproliferative gene *Tis21*, has been fundamental to the field allowing the estimation of cell cycle parameters in neural progenitors that undergo proliferative divisions (do not express Tis21) and those that undergo neurogenic divisions (express Tis21) (Haubensak et al., 2004). A comparative analysis of the cell cycle parameters in $Tis21^{+}$ and $Tis21^{-}$ RG progenitors and IPs at mid-corticogenesis revealed that in both progenitor types the length of the S phase is longer in proliferative divisions than in neurogenic divisions (Arai et al., 2011). If the duration of S phase is what dictates the type of division or this accommodates to the type of division remains unknown. Another important finding in this work is that IPs have longer G1 phases than RG progenitors (Arai et al., 2011). Given that IPs have a more restricted potential than RG progenitors and can only differentiate into neurons, the fact that they show a longer G1 suggest that the length of this phase correlates with the neurogenic capacity of cortical progenitors. In fact, the artificial manipulation of G1 phase duration in progenitors of the pallium via electroporation of a CyclinD1/CDK4 or a CyclinD1 expression construct alters the generation of IPs and neurons (Lange et al., 2009; Pilaz et al., 2009; Nonaka-Kinoshita et al., 2013). These observations demonstrate that the length of the G1

phase does not change as a consequence of neurogenesis but rather it changes to regulate neuron production.

It is important to highlight that the molecular mechanisms that regulate the proliferation and mode of division of RG progenitors and IPs are not completely understood. The few studies that try to address these questions show that the transcription factor APγ induces the generation of IPs specifically in the caudal cerebral cortex (Pinto et al., 2009) and that upregulation of Wnt signalling increases IPs terminal divisions (Munji et al., 2011), a phenotype that is also observed in Cyclin D2 loss of function embryos (Glickstein et al., 2009). Given that a high percentage of neocortical neurons are produced by IPs, alterations in the division mode of either RG progenitors or IPs are expected to have a dramatic impact on the expansion of the neocortex.

1.2.3 Neurogenesis of GABAergic interneurons

- General description

The knowledge about the mechanisms that regulate neurogenesis in the ventral telencephalon is more limited than for the dorsal telencephalon.

Two recent studies in which individual ventral progenitors were labelled using retrovirus-mediated gene transfer, together with mouse genetic studies demonstrate that these progenitors are in fact RG progenitors. They show morphological characteristics of RG progenitors, including a short process reaching the ventricle and a large process with an endfoot in contact with the pial surface (Brown et al., 2011; Ciceri et al., 2013). Moreover they express the RG marker GLAST and the neural progenitor marker

Nestin (Brown et al., 2011). Time-lapse imaging in organotypic cultures revealed that RG progenitors of the ventral telencephalon undergo interkinetic nuclei migration and perform asymmetric divisions that generate either a neuron or an IP. Similar than in the dorsal telencephalon, ventral IPs divide symmetrically and generate two neurons, however it seems that these IPs undergo more rounds of symmetric proliferative divisions than in the pallium (Brown et al., 2011). Unfortunately, the lack of a specific marker for ventral IPs hinders the study of these progenitors population.

Next, I summarize what is known about the mechanisms that generate neuron diversity in the ventral telencephalon.

- Regional specification

Cortical interneurons are produced in three regions of the ventral telencephalon: the medial ganglionic eminence (MGE), the caudal ganglionic eminence (CGE) and the preoptic area (POA) (see Figure I-7). This suggests that interneuron diversity is achieved at least in part by regional restriction of neurogenic potential. In fact, these regions show differential expression of specific transcription factors, which gives specific identity to the VZ neuroepithelium (Flames et al., 2007) (Figure I-7).

Neural progenitors of the **MGE** express the transcription factor Nkx2.1. The analysis of Nkx2.1 mutant mice revealed that Nkx2.1 expression is necessary for the specification of this region and that the MGE gives rise to around 50-60% of all cortical interneurons (Sussel et al., 1999; Butt et al., 2008).

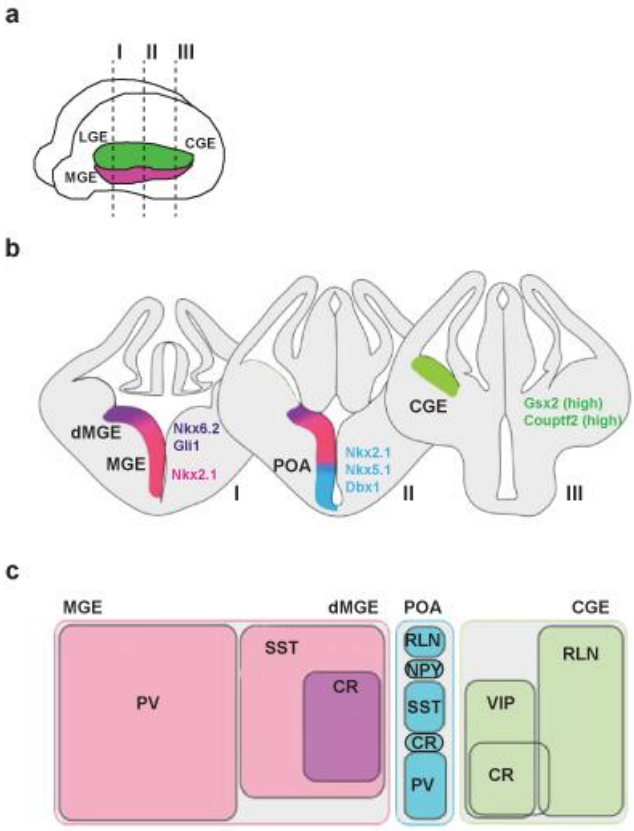

Figure I-7: Developmental origin of cortical interneuron diversity. **(a)** Scheme of a mouse embryo brain showing the three ganglionic eminences. Dash lines indicate the rostro-caudal level of pictures in b. **(b)** Representation of coronal sections showing the subpallial domains that generate cortical interneurons. Note that each domain is characterised by the expression of specific transcription factors. **(c)** The major classes of interneurons grouped by the domain were they are generated. CGE: caudal ganglionic eminence; MGE: medial ganglionic eminence; dMGE: dorsal MGE; POA: preoptic area; PV: parvalbumin; SST: somatostatin; CR: calretinin; RLN: reelin; NPY: neuropeptide Y; VIP: vasointestinal peptide. Adapted from Kessaris et al., (2014).

In vivo transplantation studies and genetic-fate mapping have shown that the majority of interneurons derived from the MGE express PV or SST (Xu et al., 2004; Xu et al., 2008; Wonders et al., 2008; Flames et al., 2007; Fogarty et al., 2007; Butt et al., 2008; see Figure I-7). The VZ of the MGE can be subdivided in 5

distinct progenitor domains (Flames et al., 2007). Several lines of evidences suggest that dorsal domains preferentially generate SST-expressing interneurons, while most PV interneurons are generated in ventral domains (Wonders et al., 2008; Flames et al., 2007; Fogarty et al., 2007). The dorsal MGE domain is characterized by the expression of the transcription factor Nkx6.2 and generates SST interneurons that also express the neuronal marker CR (Fogarty et al., 2007; Sousa et al., 2009). In contrast, in addition to PV interneurons the medial domains of the MGE generate SST interneurons that do not express CR (Fogarty et al., 2007; Inan et al., 2012; see Figure I-7). This raises the question of whether these two populations of interneurons (PV^+ and SST^+ CR^-) come from the same progenitor or from different progenitors. *In vivo* clonal analyses of single MGE progenitors revealed that individual subpallial progenitors generate clusters of interneurons that in some cases are formed exclusively by one subtype of interneuron (preferentially PV), while the vast majority contains both types of interneurons (Ciceri et al., 2013; Brown et al., 2011). These observations strongly suggest that these SST and PV interneurons may be generated from the same progenitor.

The migration of MGE-derived interneurons from the ventral to the dorsal cerebral cortex requires the downregulation of Nkx2.1 and the expression of the transcription factor Lhx6 (Nobrega-Pereira et al., 2008; Du et al., 2008), which is important for the differentiation of these neurons (Liodis et al., 2007; Zhao et al., 2008). In addition, Lhx6 induces the expression of the transcription factor Sox6, which is important for the correct laminar position and maturation of these interneurons (Batista-Brito et al., 2009).

The **CGE** is the second largest contributor to cortical interneurons generating around 30-40% of the total population in the adult cortex (Kessaris et al., 2014; see Figure I-7). Usually this region is defined anatomically due to the lack of specific CGE molecular markers. For example, CGE progenitors express the transcription factors Gsx2 and Couptf2, which are also expressed in the lateral ganglionic eminence and the MGE and POA, respectively (Wonders and Anderson, 2006; Kanatani et al., 2008; Cai et al., 2013). Therefore, the mechanisms underlying the specification of CGE-derived interneurons are poorly understood. Nonetheless, *in vitro* and *in vivo* studies revealed that the CGE produces interneurons that can be classified in two large groups: bipolar interneurons that express VIP and/or CR (but not SST) (Xu et al., 2004; Butt et al., 2005), and multipolar interneurons that contain NPY or Reelin (Miyoshi et al., 2010; see Figure I-7).

The **POA** generates different interneuron subtypes that represent around 10% of the total interneurons in the adult cortex (Kessaris et al., 2014). Like in the MGE, progenitors of the POA express Nkx2.1. but the interneurons derived from this region do not express Lhx6, which is specific for MGE-derived interneurons (Flames et al., 2007). In addition, these progenitors express Nkx5.1 and Dbx1 in different domains (Figure I-7). Fate-mapping analysis of both Nkx5.1 and Dbx1 domains showed that the POA generate NPY and/or Reelin expressing interneurons (Gelman et al., 2009), as well as a small subset of PV and SST expressing interneurons (Gelman et al., 2011; see Figure I-7).

- Temporal specification

The combination of genetic fate mapping and birthdating analysis with thymidine analogues have shown that distinct interneuron subtypes are generated at different developmental time points (Miyoshi et al., 2007; Inan et al., 2012; Taniguchi et al., 2013). As indicated in Figure I-8a, in the mouse, the neurogenic phases of SST and PV interneurons partially overlaps and the first one (the SST phase) peaks at the beginning of neurogensis, around E11, while the second one (the PV phase) peaks around E13. In contrast, most of the CR and VIP interneurons are generated at later embryonic stages (Miyoshi et al., 2007; Xu et al., 2008; Miyoshi et al., 2010). Interestingly, this temporal organization correlates with the laminar distribution of these interneuron subtypes within the cerebral cortex (Figure I-8). This observation indicates that, like in the pallium, neurogenesis in the subpallium also follows an inside-outside model in which early born neurons tend to locate in deeper layers and late-born neurons in the external layers (Valcanis and Tan, 2003; Pla et al., 2006). This has been partially contradicted by more recent *in vivo* clonal analysis of MGE progenitors showing that clusters of interneurons derived from single progenitors localize either in internal or external cortical layers, although the proportion of late-born clusters in external layers is higher than in internal layers and vice versa (Ciceri et al., 2013).

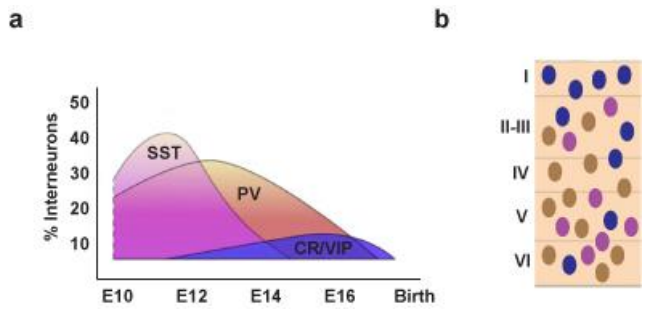

Figure I-8: Sequential generation and laminar organization of cortical interneurons. (a) Graph showing the waves of generation of the main interneuron subtypes during mouse development. **(b)** Distribution of these interneuron subtypes within the different layers of the adult neocortex. Note that early born interneurons tend to occupy internal layers, while late born neurons mostly occupied external layers. Adapted from Bartolini et al., (2013).

Finally, it is important to mention that factors others besides the region and time of generation also influence the laminar organization of interneurons, such as the position of pyramidal cells (Hevner et al., 2004; Lodato et al., 2011).

- External cues

Different studies, most of them performed in the MGE, demonstrate that external cues can influence the regionalization of VZ domains and the proliferation and specification of neuron precursors in the subpallium.

Shh is one of the principle morphogens that regulate the development of the MGE. Initially, Shh is required for the correct patterning of this region, the first ganglionic eminence that is formed during development around E9 (Smart et al., 1976). At this stage, Shh is expressed in all the territory that will become the MGE and represses the expression of the transcription factor that gives identity to the progenitors of the pallium, Pax6 (Echelard et al., 1993; Nery et al., 2001; Sousa and Fishell

2010). In addition, Shh is required to inhibit the expression of Gsx2 in MGE progenitors, therefore preventing an expansion of the CGE (Xu et al., 2010). During the neurogenic phase, postmitotic neurons of the MGE mantel zone became the principle source of Shh, since the transcription factors Lhx6 and Lhx7 induce its expression (Flandin et al., 2011).

Reduction of Shh signalling during the neurogenic phase leads to decreased number of Nkx2.1 progenitors and consequently reduced number of PV and SST interneurons (Xu et al., 2005). Interestingly, the proliferation rate of the progenitors is mantained upon Shh reduction (Xu et al., 2005). This result indicates that the proliferation of MGE progenitors is independent of Shh signalling but it is required to maintain their identity. In fact, Nkx2.1 expression is stimulated by Shh signalling (Xu et al., 2005; Fuccillo et al., 2004; Gulacsi and Anderson, 2006; Sousa and Fishell, 2010), and vice versa, Nkx2.1 induces Shh expression (Sussel et al., 1999; Jeong et al., 2006).

The analysis of the expression of the Shh signalling effectors Gli1 and Ptch1 revealed that the germinal zone of the MGE shows a gradient in Shh signalling activity, which is high in the dorsal MGE and very low or inactive in the ventral MGE (Wonders et al., 2008; Xu et al., 2010). Conditional mosaic inactivation of the Shh receptor smoothened in the MGE results in a cell non-autonomous upregulation of Shh signalling in neighbouring progenitors, which leads to the ectopic expression of Gli1, Ptch1 and Nkx6.2 and the conversion of middle MGE progenitors to dorsal MGE. As a consequence, the number of SST interneurons increases and the number of PV interneurons decreases. Accordingly, the exposition of ventral MGE progenitors to

exogenous Shh increases the production of SST cells at the expense of PV cells (Xu et al., 2010).

Another morphogen that can alter the proportion of PV and SST interneurons is BMP4. Both, the treatment of cultured progenitors with BMP4 and the overexpression of BMP4 *in vivo* increase the number of PV interneurons and reduce the number of SST interneurons. BMP4 is also necessary postnatally to ensure proper differentiation of PV interneurons (Mukhopadhyay et al., 2009).

In addition, different *in vitro* and *in vivo* studies have shown that FGF and Wnt signalling pathways induce proliferation of MGE progenitors (Gulacsi and Anderson 2008; Gutin et al., 2006) and that this effect of FGF is downstream of Shh signalling (Gutin et al., 2006).

Finally, external signals are also involved in the maturation of interneurons. For example, it has been shown that electrical activity induces the expression of the maturation-promoting factor SATB1 in SST interneurons (Denaxa et al., 2012; Close et al., 2012).

- Migration

Newborn interneurons migrate from the subpallium to the cerebral cortex following three phases: first, they tangentially migrate to reach the pallium; second, they spread out tangentially to occupy the entire cerebral cortex mainly following two migratory streams, the MZ and the SVZ; and third, they radially migrate to invade the CP and integrate into specific layers of the cortex (Marin, 2013). During these phases, interneuron migration is controlled by the presence of particular chemoattractive and

chemorepulsive guidance factors (Marin, 2013). Different classes of interneurons specifically respond to particular guidance factors based on the complement of receptors that they express, a process that is controlled by region-specific transcriptional programs (Nobrega-Pereira and Marin, 2009). Hence, for example MGE- and POA-derived interneurons reach the cortex *via* a route superficially to the striatum (Marin et al., 2001; Gelman et al., 2009; Zimmer et al., 2011), while CGE-derived interneurons colonize the cortex through its caudal pole (Yozu et al., 2005). With respect to MGE-derived interneurons, it is well established that brain-derived neurotrophic factor (BDNF) and neurotrophin-4 (NT4), which bind to the Tropomyosin kinase receptor B (TrkB) expressed by migrating interneurons, promote the tangential migration of these interneurons (Polleux et al., 2002). In addition, they actively avoid the striatum through a mechanism that involves the expression of the chemorepulsive factors semaphorin 3A and Ephrin A in the striatum and the expression of neuropilin receptors, Robo1 and the EphrA receptor in interneurons (Marin et al., 2001; Hernandez-Miranda et al., 2011; Rudolph et al., 2010). In addition, Neuroregulin-1, which is expressed in the pallium, acts as a chemoattractive cue and binds to the receptor Erbb4 expressed by interneurons (Yau et al., 2003; Flames et al., 2004).

There is evidence that postmitotic levels of Nkx2.1 also controls MGE-derived interneurons migration. In addition to cortical GABAergic interneurons, Nkx2.1 progenitors generate striatal cholinergic interneurons (Fragkouli et al., 2009). It has been shown that deletion of the transcription factor Sip1 in postmitotic interneurons prevents the downregulation of Nkx2.1 in cortical committed interneurons and induces their migration to the

striatum and the acquisition of a partial cholinergic fate (van den Berghe et al., 2013; McKinsey et al., 2013).

1.2.4 Programmed cell death

Programmed cell death (PCD) in the cerebral cortex occurs in two consecutive waves that lead to around 50% reduction in the number of neurons (Ferrer et al., 1992; Blaschke et al., 1996). The first wave occurs during the embryonic period and mainly affects neural progenitors, while the second wave occurs postnatally and affects differentiated neurons.

Embryonic PCD has been extensively characterised in the dorsal telencephalon. Apoptotic PCD is widespread in the germinal layers of the dorsal telencephalon and is evident in the VZ and SVZ at E14.5 during the peak of neurogenesis (Blaschke et al., 1996; Thomaidou et al., 1997; Haydar et al., 1999). In fact, mathematical modelling of neuronal production within the neocortex revealed that PCD in dorsal progenitors is necessary to achieve the final number of cortical glutamatergic neurons (McConnell et al., 2009). In addition, there is evidence that increased apoptosis of neural progenitors is linked to decreased number of neurons and therefore decreased cortical size. For example, constitutive activation of Notch1 or Pax6 in neural progenitors induces apoptosis and reduces the size of the progenitor pool (Berger et al., 2007; Yang et al., 2004). Alterations in the DNA damage sensors or repair mechanisms, such as the breast cancer 1, also lead to increased apoptosis and decreased neuronal production (Pulvers and Huttner 2009). Furthermore, ectopic expression of Ephrin A5 in early cortical progenitors also gives rise to increased apoptosis and thinner

cortices (Depaepe et al., 2005). Conversely, decreased apoptosis has been linked to the opposite phenotype, an expansion of the cerebral cortex. In fact, both caspase-3 and caspase-9 knockout mice display markedly enlarged and malformed cortices (Kuida et al., 1996, 1998).

Postnatal cell death in the mouse and rat cerebral cortex occurs from birth to around postnatal (P) day 15, peaking around P7 (Ferrer et al., 1992). It was estimated that around 20% of glutamatergic neurons and 50% GABAergic interneurons of the cerebral cortex die during this period (Miller et al., 1995). The observation that a reduction in the number of cortical neurons by late embryonic treatment with X-rays leads to a reduction in the naturally occurring cortical cell death at postnatal stages, led to the hypothesis that postnatal cell death controls the final cell number of this structure (Ferrer et al., 1992). Molecules that provide trophic support to the cortical neurons are also of particularly importance in the control of the survival of postmitotic neurons (Catapano et al., 2001). Genetic studies showed that inactivation of the BDNF and NT-4 receptor TrkB substantially increased cell death in the cerebral cortex (Alcantara et al., 1997). A role of glutamatergic and GABAergic neurotransmission in the control of PCD in the cerebral cortex has also been described. For instance, the inhibition of the NMDA receptors or excessive activation of the $GABA_A$ receptors greatly enhanced cell death in the cerebral cortex, particularly in layers II and V (Ikonomidou et al., 1999; Pohl et al., 1999; Ikonomidou et al., 2001). Interestingly, this effect was observed only during a limited period of development, during the first postnatal week. However, a recent study shows that postnatal PCD of cortical interneurons is

controlled by intrinsic factors instead of by a competition for extrinsically derived trophic signals (Southwell et al., 2012). In this study, the authors characterised PCD in postnatal interneurons *in vivo* and they showed that these neurons are eliminated through Bcl-2-asociated X-dependent apoptosis. They also observed that many cortical interneurons undergo PCD *in vivo* between P7 and P11, however when embryonic interneurons are transplanted into older cortices (P3), they undergo PCD later than normal, around P15. The authors proposed that cortical interneurons should have an intrinsic clock that determines when they have to die independently of the environment. In fact, the death of transplanted cells was not affected by the cell-autonomous disruption of the main neurotrophin receptor TrkB (Southwell et al., 2012).

2. Down syndrome

2.1 General description

Down syndrome (DS), affecting 1 in 800 live births, is the most frequent genetic cause of intellectual disability, a cognitive disorder with hard impact on pubic health (Epstein, 2002). DS is caused by the presence of a complete or partial additional copy of human chromosome 21 (HSA21), which in most cases is due to a chromosomal non-disjunction during maternal meiosis.

Individuals with DS present a wide range of phenotypic abnormalities with variable penetrance that include: cardiac malformations (Ferencz et al., 1989), gastrointestinal abnormalities (Levy et al., 1991), craniofacial and skeletal

anomalies (Frostad et al., 1971), motor alterations (Latash and Corcos, 1991) and contrasting cancer phenotypes: increased frequency of childhood leukaemia, which is linked to macrocytosis and thrombocytosis, but reduced prevalence of many cancers in adults (Wechsler et al., 2002; Yang et al., 2002). Despite this variability, intellectual disability is one of the invariable hallmarks of the disorder and the most invalidating aspect of this syndrome (Chapman and Hesketh, 2000). DS cognitive impairments are associated to abnormal brain development (see Chapter 2.4 in Introduction section). Other constant alterations in DS individuals include hypotonia and the development of early-onset Alzheimer's disease (AD) (Sabbagh et al., 2011; Mann et al., 1985).

2.2 Genetics

Different hypothesis have been proposed to explain how the presence of an extra copy of the genes on HSA21 give rise to the many abnormal features that define DS. The first one is the **gene dosage effect hypothesis**, which proposes that dosage imbalance of specific HSA21 genes or chromosomal regions causes specific DS phenotypes (Epstein et al., 1990; Antonarakis et al., 2004). The second one is the **amplified developmental instability hypothesis**, which claims that dosage imbalance of genes on HSA21 determines a non-specific disturbance of the genomic regulation and expression that alters normal development and leads to most manifestations of DS (Pritchard and Kola, 1999). In agreement with the last hypothesis, a meta-analysis of heterogeneous DS data sets identified 324 genes with consistent gene expression deregulation in DS, among them 77

were HSA21 genes but the others 247 were localised in non-HSA21 regions (Vilardell et al., 2011). It is important to highlight, that these two hypotheses are not mutually exclusive. It is possible that single genes or specific subset of HSA21 genes are involved in specific DS phenotypes, while some other phenotypes result from a more general disturbance in gene-dosage of both, HSA21 genes and genes in other chromosomes (Antonarakis et al., 2004).

The analysis of rare cases of partial trisomy of HSA21 has been able to define a minimal chromosomic region, named DS critical region (DSCR), which in trisomy leads to the manifestation of most of DS features, including intellectual disability (Rahmani et al., 1990; Ronan et al., 2007; Delabar et al., 1993). DSCR is localized in the long arm of HSA21 and contains around 33 genes (red rectangle in Figure I-9). According to the above stated hypotheses, the over-dosage of genes located in this region, directly or indirectly, might impact on cellular processes that are crucial for brain development and functionality contributing to the intellectual disability associated with the syndrome (Rachidi and Lopes, 2007). The analysis of DS mouse models (see chapter 2.3 in the Introduction section) supports the causative role of this region in some DS brain features.

Interestingly, new findings suggest that some DS phenotypes may also result from the effects of copy number alteration of functional, non-traditional genomic elements such as microRNAs (miRNAs) or non-coding RNAs. These observations led to a third hypothesis, the **genome instability hypothesis,** in which the additive effect of multiple HSA21 and non-HSA21 genes that are affected by the dosage imbalance is combined with changes in

functional regulation of miRNAs or other non-coding and epigenetic elements. In fact, HSA21 contains at least five miRNA genes (miR-99a, let-7c, miR-125b-s, miR-155 and miR-802). miRNA expression profiling, miRNA RT-PCR, and miRNA *in situ* hybridization experiments have demonstrated that HSA21-derived miRNAs are over-expressed in both DS foetal and adult brains. This could result in a decreased expression of specific target proteins that could contribute to disease phenotypes (Elton et al., 2010). Importantly, miRNAs are dynamically regulated during brain development and are involved in critical steps of neurogenesis (Volvert et al., 2012). For example, miR125-b is a positive regulator of astrogliosis and glial cell proliferation (Pogue et al., 2010) and, therefore, its overexpression could participate in the increased number of astrocytes observed in DS brains (Mito and Becker, 1993).

Epigenetic modifications involving DNA methylation and histone modifications should also be taken into consideration. Indeed, a recent analysis of the transcriptome of fibroblast from monozygotic twins discordant for trisomy 21 highlighted the existence of chromosomal domains of gene expression deregulation with an altered DNA methylation profile (Letourneau et al., 2014). The authors of this work propose that the overexpression of one or more HSA21 genes modifies the chromatin environment of nuclear compartments in trisomic cells causing general perturbations of the transcriptome in these compartments.

2.3 Mouse models

The conserved synteny between the genomic segments on HSA21 and mouse chromosome 16 (MMU16), MMU10 and MMU17 (Sturgeon and Gardiner 2011; Pletcher et al., 2001) (see Figure I-9) has led to the generation of many trisomic and single-gene overexpressing transgenic mice to elucidate the role of particular chromosomal regions or specific genes in the pathogenesis of DS (Rachidi and Lopes, 2007; Salehi et al., 2007; Antonarakis et al., 2004; Liu et al., 2011; Dierssen, 2012). Trisomic models reproduce most of the clinical phenotypes observed in DS individuals, but their genetic complexity makes impossible to analyze single gene effect in DS pathogenesis. In contrast, transgenic mouse models overexpressing one or few genes, allow a direct genotype-phenotype correlation, but their limitation is the loss of interactions with other HAS-21 triplicated genes contributing to the complexity of the phenotypes.

The different trisomic DS mouse models are summarized below and schematically represented in Figure I-9. These models contain different HSA21 regions or their mouse orthologous regions in trisomy. Regarding the transgenic mouse models that overexpress single genes, I describe only those overexpressing DYRK1A (see chapter 3.1 in the Introduction section).

The **Ts16** mouse was the first DS mouse model generated and contains and extra copy of the entire MMU16, which comprises around 713 genes (Gropp et al., 1975; Figure I-9). Although this mouse model shows alterations that resemble those observed in DS, such as craniofacial abnormalities, immunological defects, congenital heart defects and brain morphological alterations (Gearhart et al., 1986; see Chapter 2.4 in the Introduction

section), its usage has been limited because of the lethality of the trisomy that occurs during late embryogenesis or at early postnatal stages probably due to severe cardiovascular malformations and to a hypoplasia of placental vasculature (Miyabara et al., 1982). Another disadvantage of this model is that it contains genes in trisomy that are not HSA21, since MMU16 also present syntenies with regions of HSA3, HSA8 and HSA16 (Mural et al., 2002).

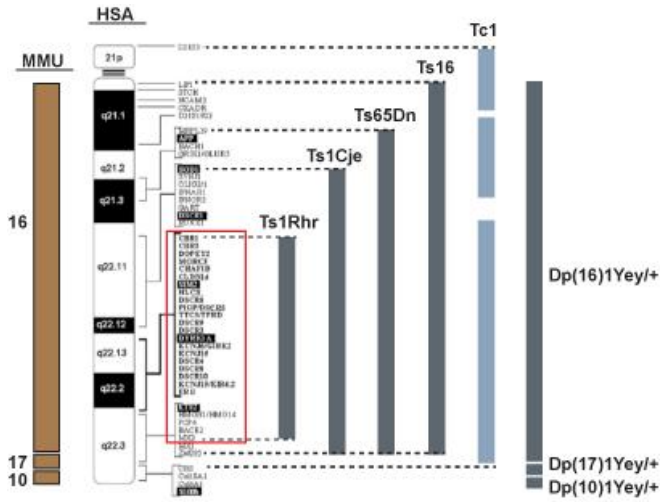

Figure I-9: Genetics of segmental trisomic mouse models for Down syndrome. Scheme of human chromosome 21 (HSA21) and the syntenic regions in mouse chromosomes (MMU) 16, 17 and 10 (brown). The genes in the Down syndrome critical region are within the red rectangle. Trisomic regions of HSA21 (blue) or MMU16, MMU17 and MMU10 (grey) in each mouse model are indicated. Adapted from Rachidi and Lopes (2007).

The **Ts65Dn** is the segmental trisomic DS mouse model best characterized. This model was generated from the translocation of the distal region of MMU16 onto the centromere of MMU17 and contains in trisomy approximately 100 genes that are orthologous to HSA21 genes, including those present in the DSCR (Davisson et al., 1990; see Figure I-9). Importantly,

Ts65Dn mice survive to adulthood and recapitulate some of the phenotypic features in DS. These animals show: 1) significant learning deficits in specific behavioural tasks; 2) craniofacial dysmorphogenesis; 3) motor dysfunction; 4) age-dependent loss of cholinergic neurons in basal forebrain, which has been associated to the early-onset AD; 5) hematopoietic alterations such as macrocytosis and thrombocytosis; and 6) congenital vascular and intracardiac defects (Costa et al., 1999; Patterson and Costa 2005; Seregaza et al., 2006; Kirsammer et al., 2008; Williams et al., 2008; Richtsmeier et al., 2002).

Two more segmental MMU16 trisomic mice have been generated, the **Ts1Cje** mouse and the **Ts1Rhr** mouse (Sago et al., 1998; Olson et al., 2004a). These mice have smaller regions in trisomy than the Ts65Dn mouse; the Ts1Cje mouse contains in trisomy around 70 genes, including those of the DSCR, while the Ts1Rhr mouse contains only the 33 genes comprised within the DSCR (Sago et al., 1998; Olson et al., 2004a) (see scheme in Figure I-9). The **Ts1Cje** mouse shows learning and behavioural deficits, although less severe than those displayed by the Ts65Dn model (Sago et al., 1998, 2000), morphological brain alterations (see chapter 2.4 in the Introduction section) and hematopoietic abnormalities similar to those observed in Ts65Dn mice (Carmichael et al., 2009). This mouse model does not present in trisomy the *APP* gene, which has been associated to the early-onset of AD observed in DS (Wisniewski et al., 1985). Nonetheless, Ts1Cje mice show tau hyperphosphorylation, an early sign of AD (Shukkur et al., 2006), suggesting HSA21 genes other than *APP* may contribute to this phenotype. On the other hand, **Ts1Rhr** mice show craniofacial abnormalities (Olson et al.,

2004a) and cognitive and behavioural abnormalities (Belichenko et al., 2009a).

As an attempt to completely reproduce all DS phenotypes the mouse model **Tc1** has been generated. This mouse carries an almost intact freely segregating HSA21, which comprises 150 genes (O'Doherty et al., 2005; see scheme in Figure I-9). Unfortunately, the Tc1 phenotypic characterization showed only a limited number of DS phenotypes, including learning and memory impairment, cardiac defects, craniofacial abnormalities, motor impairments and decreased tumour angiogenesis, and these phenotypes were not as severe as they were in the mouse trisomies (O'Doherty et al., 2005; Galante et al., 2009; Reynolds et al., 2010). This milder phenotype was attributed to the mosaicism and the internal deletions in HSA21 present in this model (Gardiner et al., 2003; O'Doherty et al., 2005). However, it should also be noted that human genes often have different spatial and temporal gene expression patterns compared with mouse genes, and time-dependent developmental or functional processes may significantly differ between the two species. Therefore, to overcome these potential species-specific differences and analyse the effect of the simultaneous presence of the three segmental trisomies on the DS relevant phenotypes a new model, the Dp(10)1Yey/+;Dp(16)1Yey/+;Dp(17)1Yey/+ mouse has been generated by Cre–loxP-mediated chromosome engineering (Li et al., 2007). This mouse model has in trisomy the three HSA21 syntenic mouse chromosomal regions (Figure I-9). This model exhibits Down syndrome-related neurological defects, including impaired cognitive behaviours (Yu et al., 2010),

but unexpectedly, it does not present striking phenotypic differences with respect to previous models.

On the other hand, in order to study the contribution of specific set of genes to DS features a library of mouse models containing small segmental regions in trisomy of approximately 2 Mb of HSA21 in a YAC (Yeast Artificial Chromosome) were created (Smith et al., 1995, 1997). One of these YAC transgenic mice, the TgYAC152F7 mouse carrying a YAC with 5 HSA21 genes including *DYRK1A* (Branchi et al., 2004), has a special importance in this Thesis and its phenotype is described here in chapter 3.1.

2.4 Developmental brain alterations

The severe cognitive impairments in DS individuals and trisomic mouse models for DS are associated to altered brain morphology. Post-mortem **macroscopic** observations and magnetic resonance analysis of the brain of adult DS individuals revealed brachycephaly, reduced brain volumes with disproportionately smaller hippocampus, prefrontal cortex and cerebellum, and ventricle enlargement (Aylward et al., 1999; Pearlson GD, 1998; Pinter et al., 2001b). Similarly, the brain of adult Ts65Dn shows a brachycephalic morphology, but its size is maintained (Aldridge et al., 2007; Richtsmeier et al., 2002). However, the volume of specific brain regions such as the cerebellum is reduced in this mouse model (Baxter et al., 2000; Olson et al., 2004b). Ts1Cje mice also show normal brain and enlargement of the ventricles (Ishihara et al., 2010). The Ts1Rhr mouse shows brachycephaly but in contrast to DS its brain has increased brain volume (Aldridge et al., 2007). Finally, the

Dp(10)1Yey/+;Dp(16)1Yey/+;Dp(17)1Yey/+ mouse shows hydrocephaly (Yu et al., 2010), which give rise to enlarged ventricles.

The fact that brachycephaly and reduced brain volume can already be observed in DS foetuses from gestation week 15 (Pinter et al., 2001a; Winter et al., 2000; Schmidt-Sidor et al., 1990; Guihard-Costa et al., 2006; Stempfle et al., 1999), suggests that morphological brain alterations in DS are caused by abnormal development of this structure. In agreement, the brain of Ts16 foetuses show reduced brain size (Haydar et al., 1996).

The **Histological** examination of post-mortem adult brain tissue revealed changes in the number and distribution of different cellular populations together with dendritic abnormalities in brain regions such as the hippocampus, the cerebellum and the cerebral cortex (Haydar and Reeves, 2012). Abnormalities in this last region of the brain include a 20 to 50% reduction in the number of neurons (Wisniewski, 1990), a significant alteration in both the number and the morphology of dendrites and synapses (Takashima et al., 1989), and astrogliosis (Mito and Becker, 1993). Again, these alterations may be originated during development since they are already observed in DS foetuses and children (Becker et al., 1991; Golden and Hyman 1994; Zdaniuk et al., 2011).

Some DS mouse models also show alterations in the cellularity of the adult cerebral cortex and the hippocampus (see Chapter 2.5 in the introduction section) and abnormal dendritic morphology in cortical and hippocampal glutamatergic neurons. Both, Ts65Dn and Ts1Rhr mice, show enlargement of dendritic spines and a

reduction in the density of spines in the hippocampus (Belichenko et al., 2009b; Belichenko et al., 2004; Kurt et al., 2000).

2.5 Excitatory/inhibitory imbalance in the cerebral cortex

Alterations in the proportion of cortical glutamatergic and GABAergic neurons may cause intellectual disability (see chapter 1.1 in the Introduction section). Indeed, the cerebral cortex of foetuses, infants and adults with DS show hypocellularity and disorganized lamination (Wisniewski 1990; Golden and Hyman 1994; Larsen et al., 2008; Schmidt-Sidor, 1990).

The cerebral cortex of adult Ts65Dn mice shows decreased number of excitatory neurons, while specific subtypes of inhibitory neurons are increased (Chakrabarti et al., 2010; Perez-Cremades et al., 2010; Hernandez et al., 2012). These phenotypes are also observed in the hippocampus. In both brain structures, the altered neuronal cellularity results from an abnormal prenatal development (Insausti et al., 1998; Chakrabarti et al., 2007; Chakrabarti et al., 2010). The imbalance in the number of excitatory and inhibitory neurons in the hippocampus is accompanied by an excess of inhibitory synapses (Belichenko et al., 2009b). The number of excitatory synapses in the cerebral cortex of Ts65Dn mice is decreased, at least in the temporal cortex (Kurt et al., 2000), and although there is not information about the number of inhibitory synapses in this region, the increased expression of GABAergic signalling molecules such as GAD65, GAD67 and the vesicular GABA

transporter in cortical extracts suggest that inhibition is also increased in this region (Souchet et al., 2014; Perez-Cremades et al., 2010). Altered number of excitatory and inhibitory cells and synapses in the hippocampus leads to increased long term depression (LTD) and decreased long term potentiation (LTP), processes that have been involved in synaptic plasticity and learning and memory (Kleschevnikov et al., 2004; Belichenko et al., 2009a; Siarey et al., 1999). Decreased hippocampal LTP has also been described in other DS mouse models, such as the Ts1Rhr and the Dp(10)1Yey/+;Dp(16)1Yey/+;Dp(17)1Yey/+ mice (Belichenko et al., 2009a; Yu et al., 2010). Importantly, chronic systemic treatment of adult Ts65Dn mice with $GABA_A$ receptor antagonists at non-epileptic doses causes a persistent post-drug recovery of cognition and LTP (Fernandez et al., 2007).

Different developmental alterations may contribute to the cerebral cortex alterations associated with DS. These include reduced proliferation, altered neuronal and glial differentiation and increased apoptosis (Table I-1). Recent studies performed with induced pluripotent stem cells (iPSCs) derived from monozygotic twins discordant for trisomy 21 revealed that DS iPSCs differentiate less efficiently into NPCs than euploid iPSCs both *in vivo* and *in vitro,* and that NPCs derived from trisomic iPSCs have proliferation defects, increased apoptosis, reduced capacity to differentiate into neurons and augmented capacity to differentiate into glial cells (Hibaoui et al., 2013). This study extends previous findings and confirms that trisomy of HSA21 affects the survival and the proliferative and differentiation capacities of neural stem cells.

Table I-1: Embryonic neurogenic deficits in DS foetuses or derived neural progenitor cells

Age (W)	Study	Phenotype
8-18	*In vitro* (1)	Impaired neurogenesis
17-21	*In vivo* (2)	Impaired proliferation and altered numbers of cells in S, G2 and M phases
17-21	*In vivo* (3)	Impaired proliferation, neuronal and glial differentiation, and apoptosis
19-21	*In vitro* (4)	Impaired neurogenesis and increased gliogenesis
13-18	*In vitro* (5)	Impaired GABAergic neuron production

w: weeks of gestation; (1) (Bahn et al., 2002); (2) (Contestabile et al., 2007); (3) (Guidi et al., 2008); (4) (Lu et al., 2011); (5) (Bhattacharyya et al., 2009).

The histological analysis of the **dorsal telencephalon** in Ts65Dn embryos revealed that although the pool of RG progenitors is well established the production of neurons is significantly impaired during early corticogenesis. Concomitant with the decreased neurogenesis, Ts65Dn progenitors show longer cell cycles due to an increased duration of the cell cycle phases G1 and S (Chakrabarti et al., 2007). At midcorticogenesis, Ts65Dn embryos exhibit a compensatory expansion of IPs in the SVZ and, as a result, the cortical thickness at the end of the neurogenic phase is normal. However, postnatal Ts65Dn mice show a deficit of neurons in the layer VI of the neocortex (Chakrabarti et al., 2007; 2010), which contains the projection neurons that are generated during early neurogenesis (Molyneaux et al., 2007; see Figure I-5). A recent genetic fate mapping of cortical progenitors at midcorticogenesis revealed

that the generation of SNP is severely reduced in Ts65Dn embryos (Tyler and Haydar, 2013), which indicate that cortical progenitor specification is also altered in this trisomic model. In agreement with the results obtained in Chakrabarti et al., 2007, neurospheres generated from NPCs derived from Ts65Dn newborn mice display defective proliferation, increased cell cycle duration, decreased neuronal differentiation and increased production of astrocytes (Trazzi et al., 2011).

Similar neurogenic alterations have been observed in other trisomic DS models. For instance, Ts16 embryos also show a transient delay in the radial expansion of the cortical wall (Haydar et al., 1996), decreased neuronal production and an enlargement of the cell cycle duration (Haydar et al., 2000). As a consequence of this delay in neurogenesis, the SP of Ts16 embryos have less neurons and, consequently, the thalamocortical innervations are decreased (Cheng et al., 2004). One important difference between these two trisomic models is that in Ts16 embryos the pool of progenitors at the onset of neurogenesis is reduced by 26%, while in Ts65Dn embryos the number of progenitors seems normal (Chakrabarti et al., 2007; Haydar et al., 2000). The Ts1Cje model also shows impaired corticogenesis *in vivo* and *in vitro*. By E13.5, Ts1Cje embryos exhibit reduced thickness of the cortical wall, being the CP the most affected layer, and reduced proportion of cells exiting cell cycle, which suggests that neuronal production is also impaired in this model (Ishihara et al., 2010). In agreement, proliferation rates of neurospheres derived from Ts1Cje embryos are significantly reduced due to a longer cell cycle duration. These cells also show a biased differentiation to astrocytes (Moldrich et al., 2009).

Given that cortical neurogenic defects have been observed in three different trisomic mouse models, it is plausible that the gene or the set of genes responsible for this alteration are localized in the overlapping trisomic region in these models.

The excess of GABAergic interneurons in the cerebral cortex and hippocampus of adult Ts65Dn mice is due to a specific increase PV and SST interneurons. The histological analysis of the **ventral telencephalon** of Ts65Dn embryos revealed that this increase in interneurons results from the combination of an excess of Olig2 progenitors and an increased neurogenesis in the MGE. Importantly, cell cycle length is not affected in ventral progenitors (Chakrabarti et al., 2010). Performing an *in vivo* genetic rescue experiment, the authors of this work were able to narrow down the HSA21 locus responsible of the phenotype to *Olig1/2* genes (Chakrabarti et al., 2010).

It is worthy to point out that the defects on proliferation observed in dorsal and ventral cortical progenitors in the Ts65Dn model are opposite; decreased in dorsal progenitors and increased in ventral progenitors. This indicates that the effects of HSA21 triplication is progenitor-type specific and suggests that the molecular mechanism underlying these defects should be different.

3. DYRK1A

Human *DYRK1A* (Dual-specificity tyrosine-(Y)-phosphorylation Regulated Kinase 1A) maps within the DSCR in HSA21 (Guimera et al., 1996), and it is overexpressed in foetal and adult DS brains (Dowjat et al., 2007; Guimera et al., 1996; Guimera et al., 1999). As it will be discussed later, the phenotypes of mutant mice with one or three copies of *Dyrk1a* have revealed that this kinase plays a role in brain development and that *Dyrk1a* gene dosage imbalance leads to defects in learning and memory (see chapter 3.1 in the Introduction section). Importantly, humans and flies with haploinsufficiency of *DYRK1A* (*minibrain* in *Drosophila melanogaster)* also show microcephaly and behavioural abnormalities, which indicate that DYRK1A has conserved functions across evolution (Courcet et al., 2012; Moller et al., 2008; Tejedor et al., 1995). The above-mentioned observations led to the proposal that trisomy of *DYRK1A* could be at the basis of some of the neurological alterations associated with DS (Dierssen, 2012; Haydar and Reeves, 2012).

3.1 Neural phenotypes in *Dyrk1a* mutant mice

Loss-of-function mutations:

Dyrk1a knockout mice die during gestation around E11.5 precluding the use of this model to study brain development. *Dyrk1a*$^{-/-}$ embryos are smaller than wild-type littermates and present a severe developmental delay (Fotaki et al., 2002). Mice with the *Dyrk1a* targeted mutation in heterozygosis (*Dyrk1a*$^{+/-}$ mice) are viable and also show a general growth delay and body size reduction of around 30% at birth. *Dyrk1a*$^{+/-}$ brains are

microcephalic, but the reduction in brain size is not uniform. The tectum, which is composed by the superior and inferior colliculus, and some ventral regions, such as the thalamus, display a more significant size reduction in these mutants than other anterior structures such as the cerebral cortex and the olfactory bulbs. Cell counts performed in some brain regions revealed an increased cell density in the somatosensory and pyriform cortex of *Dyrk1a*$^{+/-}$ mice. By contrast, these mice present normal cell densities in another laminated structure of the brain, the superior colliculus, which presents severe hypocellularity (Fotaki et al., 2002). Moreover, a detailed analysis of neocortical pyramidal neurons in adult *Dyrk1a*$^{+/+}$ and *Dyrk1a*$^{+/-}$ littermate mice revealed that mutant pyramidal neurons are less branched and with less number of spines per branch than in wild-type animals (Benavides-Piccione et al., 2005). This result indicates that haploinsufficiency of *Dyrk1a* influences the complexity of pyramidal cells and thus their capability to integrate information. In agreement, *Dyrk1a*$^{+/-}$ mice show a reduced execution in a spatial learning task and impaired performance in a hippocampal-dependent memory task (Arque et al., 2008). In addition, *Dyrk1a*$^{+/-}$ mice present an altered motor function (Fotaki et al., 2004), which could be caused by the deficit of *sustancia nigra* dopaminergic neurons reported in these mice (Martinez de Lagran et al., 2004; Barallobre et al., 2014).

Gain-of-function mutations:

Different DYRK1A overexpression mouse models have been generated in the last decades. These models contain an extra copy of the *DYRK1A* gene alone (Tg*Dyrk1a*; BACTg*DYRK1A*

and mBACTg*Dyrk1a*) or together with 4 additional HSA21 genes (TgYAC152f7).

The **TgYAC152f7 mouse** contains in a YAC a HSA21 segment that includes *DSCR5*, *TTC3*, *DSCR9*, *DSCR3* and *DYRK1A* (Smith et al., 1997). These mice present neurodevelopmental delay, motor abnormalities and deficits in learning and memory (Smith et al., 1997; Chabert et al., 2004). Importantly, a transgenic mouse that contains a deleted YAC, and has only *DYRK1A* in trisomy show learning and memory defects that are similar to those in TgYAC152f7 mice (Smith et al., 1997), suggesting that these defects are caused by the overexpression of DYRK1A. Brain morphological alterations have also been observed in TgYAC152f7 mice. Magnetic resonance imaging showed a general increase in brain volume, which is more pronounced in the thalamus-hypothalamus area (Sebrie et al., 2008). The administration of Epigallocatechin gallate (EGCG), an inhibitor of DYRK1A activity (Bain et al., 2003) to pregnant females restores brain size and long-term memory impairments in TgYAC152f7 mutant mice (Guedj et al., 2009), indicating that in fact, *DYRK1A* is the gene in YAC152f7 that is causing these alterations.

The **Tg*Dyrk1a* mouse** expresses the full-length cDNA of rat *Dyrk1A* under the control of an inducible and heterologous promoter, the sheep metallothionein-Ia (sMt-Ia) promoter (Altafaj et al., 2001). Contrary to the TgYAC152f7 mouse, this transgenic mouse do not present gross anatomical brain alterations. However, neurobehavioral analysis showed severe impairment in the performance of spatial learning and memory tasks, delayed motor acquisition, alterations in the organization of locomotor

behaviour and hyperactivity (Martinez de Lagran et al., 2004), which agree with some reported clinical observations in DS individuals. The motor phenotypic alterations in Tg*Dyrk1A* mice can be rescue by stereotaxic injection into the striatum of an adeno-associated vector driving the expression of a short-hairpin RNA to silence *Dyrk1a* (Ortiz-Abalia et al., 2008). This indicates that motor alterations in this model are caused by DYRK1A overexpression and that they can be reverted in the adulthood reducing the levels of DYRK1A. Alterations in the expression of NMDA receptor subunits and in NMDA-induced calcium responses have also been observed in Tg*Dyrk1A* cerebellar neurons (Altafaj et al., 2008), suggesting a role for DYRK1A in the modulation of excitatory transmission in the brain. Moreover, a recent study showed that like in the trisomic DS models Ts65Dn and TsCje1 (Clark et al., 2006) (Ishihara et al., 2010), Tg*Dyrk1a* mice display impaired adult neurogenesis in the hippocampus due to reduced cell proliferation and cell cycle exit rates (Pons-Espinal et al., 2013). In addition, in this study the authors observed reduced survival of newly born cells in Tg*Dyrk1a* mice. Treatment with the DYRK1A inhibitor EGCG reverted hippocampal neurogenic alterations and hippocampal-dependent learning and memory impairments in Tg*Dyrk1a* mice (Pons-Espinal et al., 2013).

Two different mouse models with an extra copy of DYRK1A have been generated by using a bacterial artificial chromosome (BAC): the **BACTg*DYRK1A*** mouse, which contains an extra copy of the human *DYRK1A* gene (Ahn et al., 2006), and the **mBACTg*Dyrk1a* mouse**, which contain an extra copy of the mouse *Dyrk1a* gene (Guedj et al., 2012). Both BAC models show

memory and learning impairments similar to those described in the DS trisomic models, but only the mBACTg*Dyrk1a* mouse show motor abnormalities (Ahn et al., 2006; Souchet et al., 2014). These mice show increased brain weight. In addition, BACTg*DYRK1A* and mBACTg*Dyrk1a* mice show alterations in LTP in the hippocampus and the prefrontal cortex, respectively (Ahn et al., 2006; Thomazeau et al., 2014), indicating that synaptic plasticity and the excitatory/inhibitory balance may be disturbed in these models (Luscher et al., 2000). Although no detailed histological analysis of the cerebral cortex have been done in these mutants, western blot analysis of adult brain protein extracts show alterations in the levels of glutamatergic and GABAergic proteins in mBACTg*Dyrk1a* mice, suggesting that like in the DS trisomic model Ts65Dn (Souchet et al., 2014; Chakrabarti et al., 2010; Perez-Cremades et al., 2010), there is an excess of GABAergic inhibition in this transgenic *Dyrk1a* model (Souchet et al., 2014).

It is important to highlight that these BAC models present important advantages with respect to the Tg*Dyrk1a* mouse: first, they have only one copy of the *DYRK1A* transgene integrated into the genome compared to the 2 to 20 copies integrated in the different Tg*Dyrk1A* mouse lines; and second, the transgene in the BAC lines is driven by its own regulatory sequences, and therefore its temporal and spatial expression should be similar to the endogenous gene. Given that mouse and human DYRK1A proteins have 99% homology and that different species may have different gene regulatory elements in their promoters, the **mBACTg*Dyrk1a* mouse** represents the best available model to study the effect of DYRK1A overexpression in DS.

3.2 Structure and regulation of the kinase activity

DYRK1A is a protein kinase that belongs to a family of proteins known as DYRK, which is present in all eukaryotes and shows a high degree of conservation across evolution (Aranda et al., 2011). All DYRK members have been associated to functions related to cell homeostasis and differentiation. There are five DYRK members in mammals: DYRK1A, DYRK1B, DYRK2, DYRK3 and DYRK4. Phylogenetic analysis revealed that *DYRK* genes arose from gene duplication events during late periods of metazoan evolution. Based on this analysis, DYRK proteins are classified in two subfamilies: class I and class II. DYRK1A and DYRK1B belong to class I and DYRK2, DYRK3 and DYRK4 to class II. The conservation between these proteins is restricted to the kinase domain and to a sequence upstream this domain, the DH-box motif that is characteristic of the subfamily and seems to be important for maintaining the protein in a catalytically active conformation (Soundararajan et al., 2013). The paralogous DYRK1A and DYRK1B share additional homologies; a nuclear localization signal (NLS) and a PEST motif within the N-terminal and C-terminal regions, respectively (Aranda et al., 2011). These two proteins show different patterns of expression, while DYRK1A is expressed at different levels in all mammalian adult tissues examined (Guimera et al., 1999) DYRK1B shows a more limited expression with the highest expression in skeletal muscle, heart, testes and brain. Importantly, DYRK1B expression is enhanced in lung and colon tumours suggesting a role of this kinase in carcinogenesis (Guimera et al., 1999; Lee et al., 2000).

DYRKs phosphorylate tyrosine (Tyr), serine (Ser) and threonine (Thr) residues. DYRKs autophosphorylate on Tyr residues and all

their exogenous substrates described until now are phosphorylated in Ser or Thr residues (Becker et al., 1998) (Aranda et al., 2011). Autophosphorylation occurs within the activation loop of the catalytic domain on the second Tyr-residue of the motif Tyr-X-Tyr (Becker and Joost, 1999). This phosphorylation is essential for DYRK kinase activity (Himpel et al., 2000) and occurs while the protein is translated (Lochhead et al., 2005). Hence, DYRK kinases are constitutively active. The defined consensus sequence for DYRK1A phosphorylation is RPx(S/T)P, where x corresponds to all amino acids (aa) and S/T are the phosphorylable residues (Himpel et al., 2000). However, despite the definition of this consensus sequence, several substrates have been reported where the phosphorylation site do not match perfectly to the consensus (Aranda et al., 2011).

DYRK1A contains 754-763 aa and has an estimated molecular weight of around 90 kDa. The use of alternative acceptor splicing sites in exon 4 gives rise to 2 protein isoforms that differ in the inclusion/exclusion of 9 aa in the N- terminus of the protein. Experimental evidence suggests the existence of more than 3 DYRK1A protein variants that might be translated from the different transcripts (Aranda et al., 2011). However, no functional differences among these protein isoforms have been reported to date.

In addition to the classical kinase domain (Becker and Joost, 1999) and the DH-box motif, DYRK1A protein contains two NLS domains, one in their amino-terminal region (NLS1) (Alvarez et al., 2003); and a second one (NLS2), which partially overlaps with the predicted nuclear export signal (NES) within the kinase domain (Alvarez et al., 2003). In the carboxy-terminal of DYRK1A

there is a PEST motif, which is commonly associated to protein stability; a polyhistidine domain (His) that localizes the protein to the nuclear compartment of splicing factors or nuclear speckles (Alvarez et al., 2003; Salichs et al., 2009) and that mediates protein-protein interactions, such the one described with the protein Sprouty2 (Aranda et al., 2008); and a region rich in Ser and Thr residues with an unknown function (see Figure I-10).

Figure I-10: DYRK1A protein motifs. Schematic representation of DYRK1A showing the different protein motifs from the N-terminus to the carboxy-terminus domains: NLS, nuclear localization signal; DH, DYRK homology box; KINASE, kinase domain; PEST, motif rich in proline, glutamic acid, serine and threonine; HIS, polyhistidine domain; S/T, motif rich in serine and threonin residues.

Since DYRK1A is a constitutively active and dosage-dependent kinase, its expression needs to be tightly regulated. *DYKR1A* gene is organized in 17 exons and is expressed as several transcripts, which differ in their 5'-ends due to alternative promoter usage and first exon choice (Guimera et al., 1997). DYRK1A has 3 putative promoter regions: pA, pB and pM, which have distinct regulation and expression. pM and pB contain binding sites for activator protein 4 (AP4) that are able to recruit both AP4 and its corepressor parter germinin to repress *DYRK1A* transcription in non-neuronal cells (Kim et al., 2006). In addition, pB responds to E2F1 overexpression, although the responsive element for this transcription factor has not been identified (Maenz et al., 2008). A high-throughput analysis of CREB (cAMP-response element binding protein) dependent gene expression identified a putative CREB-binding site in pA,

however this site needs experimental confirmation (Impey et al., 2004). Moreover, *DYRK1A* transcription in neural cells is upregulated by the transcription factor REST (RE1 silencing transcription factor) (Lu et al., 2011) and by the Alzheimer senile plaques component beta-amyloid protein in adult mice and humans (Kimura et al., 2007). Moreover, DYRK1A protein shows circadian oscillation in the mouse liver (Kurabayashi et al., 2010), although the mechanism of this regulation remains unknown. Additionally, recent studies have shown that DYRK1A expression is regulated in different cell contexts by the miRNA let-7b, miR-199b and miR-1246 (Buratti et al., 2010; da Costa Martins et al., 2010; Zhang et al., 2011). It is important to point out that some of the transcriptional/posttranscriptional effects described above could be part of regulatory loops. One example is the negative feedback loop between REST, which induces the expression of DYRK1A (Lu et al., 2011), and DYRK1A, which represses *REST* transcription (Canzonetta et al., 2008) and protein stability (Lu et al., 2011). Another example of a feedback loop has been reported in the context of cardiac hypertrophy: hypertrophic stimulus via activation of Calcineurin/NFATc signalling induces the expression of the miR-199b, which directly target DYRK1A, a well known negative regulator of the this pathway (Arron et al., 2006; Gwack et al., 2006), and thus increases the nuclear factor of activated T-cells (NFAT)c activity (da Costa Martins et al., 2010).

DYRK1A kinase activity is regulated through the interaction with regulatory proteins. For example, the autophosphorylation of DYRK1A on Ser520 allows DYRK1A association with 14-3-3b, which induces a conformational change that enhances its

catalytic activity (Alvarez et al., 2007). In contrast, the binding of SPRED1/2 (Sprouty-related protein with EVH1 domain) with the kinase domain of DYRK1A inhibits its catalytic activity (Li et al., 2010).

Given that DYRK1A has nuclear and cytoplasmatic substrates (see Chapter 3.4 in the Introduction section), the regulation of DYRK1A subcellular localization represents another way to control DYRK1A activity linked to substrate accessibility. Studies performed in human, mouse and chick samples have shown that DYRK1A in the CNS localizes in the cytoplasm and the nucleus of different cell types (Hammerle et al., 2003; Marti et al., 2003; Wegiel et al., 2004; Laguna et al., 2008). Moreover, regulation of the nuclear-cytosolic distribution of DYRK1A is suggested by the transient nuclear translocation that is observed *in vivo* in the chick during Purkinje cell differentiation (Hammerle et al., 2002). In line with these observations, biochemical fractionation experiments indicate that DYRK1A in the adult rat (Murakami et al., 2009), mouse (Marti et al., 2003) (Aranda et al., 2008) (Kaczmarski et al., 2014) and human (Kaczmarski et al., 2014) brains is distributed in cytosolic and nuclear fractions. Within the cytosolic fraction, DYRK1A is distributed in a pool associated with the synaptic plasma membrane and a pool associated with the vesicle-containing fractions (Aranda et al., 2008; Murakami et al., 2009). In addition, the great majority of cytosolic DYRK1A is associated to the cytoskeleton forming complexes with filamentous actin, neurofilaments, and tubulin (Kaczmarski et al., 2014). In fact, in differentiating neurons DYRK1A is expressed in growing dendritic trees both in primary neuronal cultures (Aranda et al., 2008) and in the embryonic forebrain (Hammerle et al.,

2003). A mass spectrometry analysis identified one phosphorylated residue in the cytosolic DYRK1A and multiple phosphorylated residues in the cytoskeletal DYRK1A, which suggest that intracellular distribution and compartment-specific functions of DYRK1A may depend on its phosphorylation pattern (Kaczmarski et al., 2014).

Within the nucleus, DYRK1A accumulates in nuclear speckles through its His-repeat domain (Alvarez et al., 2003; Salichs et al., 2009), suggesting that it could be involved in transcriptional regulation. *In vivo*, only a small fraction of DYRK1A (around 10%) is detected in the nucleus (Murakami et al., 2009; Marti et al., 2003; Kaczmarski et al., 2014), however when it is exogenously expressed it accumulates within the nucleus in stable cell lines (Alvarez et al., 2003; Guo et al., 2010; Mao et al., 2002), primary hippocampal neurons (Sitz et al., 2004) and in cortical NPCs (Yabut et al., 2010).

3.3 Expression in the brain

DYRK1A is expressed at different levels in all mammalian adult tissues examined showing relative high levels of expression in the heart, lung, skeletal muscle, kidney, testis and brain (Guimera et al., 1999; Okui et al., 1999).

During brain development *Dyrk1a* transcripts are detected at early embryonic stages, particularly in the neural tube and otic vesicle of mouse embryos (Fotaki et al., 2002; Okui et al., 1999). In situ hybridizations of *Dyrk1a* during chick development suggest that DYRK1A expression in neural cells is regulated during development. In fact, *Dyrk1a* transcripts seem to follow a

stage-dependent expression pattern: *Dyrk1a* mRNA expression is transient in pre-neurogenic progenitors; cell-cycle regulated in neurogenic progenitors; down-regulated in post-mitotic neurons as they migrate radially to the CP; and persistent in late differentiating neurons (Hammerle et al., 2008, 2011). Interestingly, mouse and chick *Dyrk1a* mRNAs in neuroepithelial progenitor cells are asymmetrically distributed during the mitosis of these cells before the first neurogenic division, pointing to a possible role for this kinase in the transition from NPC proliferative to neurogenic divisions (Hammerle et al., 2002). It has also been shown that DYRK1A protein in neural stem cells of the adult SVZ can be distributed symmetrically or asymmetrically during mitosis and that normal levels of the protein are needed to sustain epidermal growth factor receptor in the two daughters of symmetrically dividing progenitors, which is important for maintaining the stem cell reservoir in this niche (Ferron et al., 2010).

DYRK1A expression in different CNS structures peaks around birth and decreases during postnatal development. The expression of DYRK1A in the adult brain is internal (Okui et al., 1999; Hammerle et al., 2008) and more restricted to specific regions such as the cortex, the hippocampus, the cerebellum, the olfactory bulb, deep motor nuclei and hypothalamic nuclei (Wegiel et al., 2004; Marti et al., 2003). This pattern of expression indicates that DYRK1A is involved in the physiology of high brain functions.

3.4 Cellular functions

DYRK1A interacts with components of several cell-signalling pathways and proteins involved in different cell processes (see scheme in Figure I-11). As expected for its subcellular localization (see Chapters 3.2 and 3.3 in the Introduction section) the interaction of DYRK1A with its substrates can occur at both cytosolic and nuclear compartments (Aranda et al., 2011; Tejedor and Hammerle, 2011). Moreover, DYRK1A interaction can involve different mechanisms that go beyond the phosphorylation of substrates. For example, DYRK1A binds to the endocytic proteins clathrin heavy chain and endophilin 1 but do not phosphorylates them (Murakami et al., 2009).

The phenotypes of *Dyrk1a* loss- and gain-of-function mouse models and the results obtained in other experimental models indicate that DYRK1A controls key neurodevelopmental and aging processes (Tejedor and Hammerle, 2011; Wegiel et al., 2011). For the purpose of this thesis I summarize only the evidences related to the role of DYRK1A in neurodevelopment.

DYRK1A interacts with proteins that have a role in cell cycle regulation and neuronal survival. In fact, there is evidence that DYRK1A attenuates cell cycle progression in neural progenitors and that positively regulates cell survival at least in the retina and in the mesencephalon inhibiting caspase-9 apoptotic activity (Laguna et al., 2008, 2013; Barallobre et al., 2014). The evidences related to DYRK1A and cell cycle regulation are summarized in next Chapter.

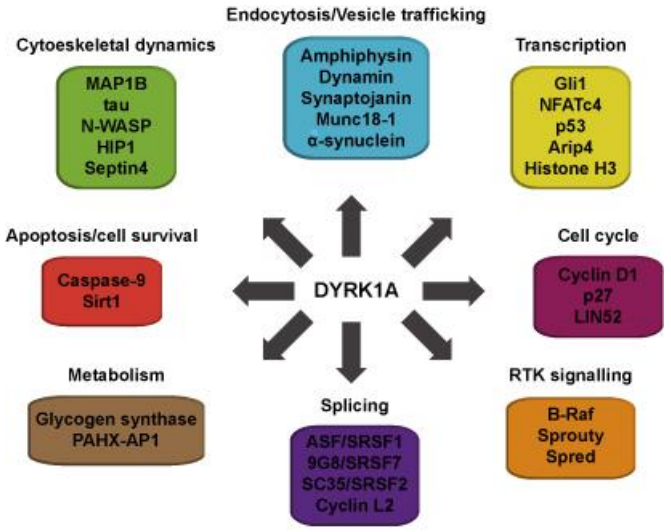

Figure I-11: Substrates and functions of DYRK1A. Substrates of DYKR1A are depicted in boxes accordingly to the type of cell process, indicated above each box, they are involved.

DYRK1A interacts with components of key developmental signalling pathways such as FGF, Shh and Notch (see Figure I-11). DYRK1A phosphorylates the FGF signalling inhibitor Sprouty2 in mammalian cell lines, leading to increase FGF signalling (Aranda et al., 2008). Regarding Shh signalling, it was reported that DYRK1A phosphorylates the Shh downstream effector Gli1 and increases its transcriptional activity in fibroblast cells (Mao et al., 2002). DYRK1A negatively regulates Notch signalling, *via* the phosphorylation of the Notch intracellular domain and reduction of its transcriptional activity (Fernandez-Martinez et al., 2009). DYRK1A regulation of these pathways strongly supports the involvement of DYRK1A in early neurodevelopmental processes such as neural progenitors expansion, maintenance and differentiation.

Moreover there is evidence that DYRK1A regulate other processes of neuronal differentiation, such as neuritogenesis and synaptogenesis. DYRK1A reduction or overexpression leads to decreased dendritic complexity *in vivo* and in cultured cells (Martinez de Lagran et al., 2012; Gockler et al., 2009; Scales et al., 2009; Benavides-Piccione et al., 2005). This effect of DYRK1A has been associated to phosphorylation of microtubule-associated protein 1B (MAP1B), which alters microtubule dynamics (Scales et al., 2009). In addition, the reported negative action of DYRK1A on the Calcineurin/NFATc signalling pathway, through phosphorylation of NFAT and induction of its nuclear export (Arron et al., 2006; Gwack et al., 2006), can also contribute to the impaired neuritogenesis observed in *Dyrk1a* mutant mice. In fact, one of the main functions of the Calcineurin/NFAT signalling pathway in neurons is to induce neurite outgrowth upon neurotrophins and netrins stimulation (Graef et al., 2003). On the other hand, DYRK1A alters synaptogenesis through the phosphorylation of the GTPase binding domain of the neural Wiskott-Aldrich syndrome protein (N-WASP), which inhibits actin polymerization (Park et al., 2012). In accordance, ectopic DYRK1A overexpression in cultured hippocampal neurons causes a reduction in dendritic spine formation (Park et al., 2012), and cultured neurons from Tg*Dyrk1A* mice displayed a reduction in spine density, synapse formation, and dendritic filopodia length as well as an abnormal spine morphology (Martinez de Lagran et al., 2012). All these alterations, together with the fact that some DYRK1A interactors are involved in endocytosis and vesicle trafficking (see Figure I-11) indicate that DYRK1A may have synaptic functions in adult brains.

3.5 Role in corticogenesis

At the beginning of this thesis the effect of DYRK1A overexpression in the development of the cerebral cortex was unexplored. However, in the last years two groups have addressed this question electroporating a DYRK1A expression construct into the mouse embryo at mid-corticogenesis (Yabut et al., 2010; Hammerle et al., 2011). In both studies the authors show that the overexpression of DYRK1A induces cell cycle exit in dorsal cortical progenitors. Similar results were obtained by electroporating the same DYRK1A construct into the chick spinal cord (Hammerle et al., 2011).

Despite both studies led to the same conclusion regarding the role of DYRK1A in cell cycle progression they show substantial differences in the implications of this alteration. In the first study, the increased cell cycle exit was accompanied by an increased number of IPs and newborn neurons. Based on this, the authors concluded that DYRK1A overexpression leads to premature neuronal differentiation (Yabut et al., 2010). The second study also showed that DYRK1A overexpression induces cell cycle exit but in this case instead of promoting differentiation the overexpression of DYRK1A abrogates the differentiation of the progenitors. Based on this, the authors claimed that the levels of DYRK1A protein have to be decreased in newborn cells in order to differentiate into neurons (Hammerle et al., 2011). Another difference between these two studies is that they proposed different molecular mechanisms to explain the effect of DYRK1A on cell cycle arrest. In the first one and based on results obtained coelectroporating Cyclin D1 and DYRK1A, the authors proposed that cell cycle arrest in DYRK1A electroporated progenitors

results from an effect of DYRK1A on Cyclin D1 nuclear export and degradation (Yabut et al., 2010). In the second one, and based on the expression of $P27^{KIP1}$ and the Notch downstream target *Hes5* in DYRK1A electroporated cells, the authors suggested that the effect of DYRK1A on cell cycle exit is mediated by the induction of the expression of $p27^{KIP1}$ gene and the inhibition of Notch signalling (Hammerle et al., 2011).

A third study indicated that DYRK1A promotes cell cycle arrest in neuronal progenitors through another mechanism that involves DYRK1A phosphorylation of p53 and the up-regulation of p53 target genes such $p21^{CIP1}$ in rat and human NPCs (Park et al., 2010). The authors of this work also showed that the levels of both phosphorylated p53 and $p21^{CIP1}$ protein were increased in the brain of DS foetuses and of BACTg*DYRK1A* embryos. Importantly, cortical progenitors in BACTg*DYRK1A* embryos show decreased BrdU incorporation, suggesting decreased proliferation (Park et al., 2010).

These studies show that DYRK1A plays a role in neural progenitor cell cycle regulation. In this line, it has been reported that DYRK1A promotes quiescence and senescence in mammalian cells by phosphorylating the subunit of the DREAM complex Lin52, which induces the assembly of the complex and the repression of cell cycle-dependent genes (Litovchick et al., 2011). It is worthy to note that, as already mentioned, neurogenesis in the dorsal telencephalon of Ts65Dn embryos is decreased (Chakrabarti et al., 2007), which is the opposite to the effect induced by forced overexpression of DYRK1A in dorsal apical progenitors during mid-corticogenesis (Yabut et al., 2010). However, it has been recently shown that a modest

overexpression of DYRK1A in mouse embryos during early-corticogenesis also achieved by *in utero* electroporation of a DYRK1A expression construct delays neuron production, but only when DYRK1A is co-expressed with the HSA21 gene *RCAN1* (Kurabayashi and Sanada 2013), initially named *DSCR1* (Fuentes et al., 1995). Given the functional interaction of DYRK1A and RCAN1 on NFATc signalling (Arron et al., 2006) and that NFATc activity in the Ts1Cje DS mouse model is decreased, the authors of this work proposed that the early defect of cortical neuron production in DS is due to the cooperative action of DYRK1A and RCAN1 on the activity of NFATc transcription factors. Interestingly, they show that the overexpression of higher levels of DYRK1A in cortical progenitors produced the same phenotype previously described (Kurabayashi and Sanada 2013); increased cell cycle exit and increased neuron production (Yabut et al., 2010). This final observation implies that the levels of DYRK1A overexpression influence downstream pathways differently.

Despite of the lack of consensus about the effect of DYRK1A overexpression on cortical neurogenesis and the mechanism by which DYRK1A could regulate cell cycle in cortical progenitors, the before mentioned studies point to *DYRK1A* as one of the HSA21 gene that could contribute to the neuronal deficit observed in the cerebral cortex of DS individuals. Whether this is or not the case needs to be confirmed in a suitable *in vivo* trisomic model of the disorder.

HYPOTHESIS AND OBJETIVES

The cerebral cortex is the key structure for highest functions in mammals. Hypocellularity in this structure is a characteristic feature in Down syndrome (DS) and arises during prenatal development. Similarly, the trisomic model of the syndrome, the Ts65Dn mouse, shows an attenuation of cortical neurogenesis and a deficit of glutamatergic neurons in the neocortex of postnatal animals. At the beginning of this Doctoral Thesis, the knowledge about the pathogenic mechanisms underlying the deficit of cortical neurons in DS was limited and the trisomic genes responsible of the phenotype were unknown.

Our hypothesis was that triplication of the human chromosome 21 (HSA21) gene *DYRK1A* may contribute to attenuate cortical neurogenesis in DS. The following evidences support this hypothesis: First, *DYRK1A* gene lies on the critical region for DS in HSA21; second, *DYRK1A* is expressed in the developing cortex since the beginning of neurogenesis and it is overexpressed in DS foetal brains; third, *DYRK1A* is a dosage-sensitive gene; forth, the gene product of *DYRK1A* is a protein kinase and some of its substrates have relevant functions in cortical development; and fifth, the brain of *Dyrk1a* haploinsufficieny mice present increased cell densities in the neocortex.

The **main objective** of this Thesis was to assess the impact of having 3 functional copies of *DYRK1A* in the development of the cerebral cortex with the ultimate goal of provide evidence about the contribution of this gene in the formation of the cortical circuitry in DS. To this end, we have used mutant mice with 3 copies (mBACTg*Dyrk1a*) or with 1 copy (*Dyrk1a*$^{+/-}$) of the *Dyrk1a*

gene, and trisomic Ts65Dn mice with *Dyrk1a* in trisomy or disomy.

The **particular objectives** are detailed below; some of them were formulated during the process of this work according to the results obtained and to the data published by other groups.

1) To perform a comparative morphological analysis of the brain in the transgenic mBACTg*Dyrk1a* model and the trisomic Ts65Dn model.

2) To assess the cellularity and the number of excitatory and inhibitory neuron types in the cerebral cortex of adult mBACTg*Dyrk1a* and *Dyrk1a*$^{+/-}$ mice.

3) To analyse the expansion of the neocortical wall in the mBACTg*Dyrk1a* model.

4) To identify the pathogenic mechanism/s underlying the developmental cortical defects in the mBACTg*Dyrk1a* model.

5) To assess the contribution of *Dyrk1a* trisomy in the developmental defects described previously in the Ts65Dn model.

MATERIALS AND METHODS

1. Mouse models

1.1 General description and breeding

In this study we have used three different genetically modified mouse lines. To determine the effects of *Dyrk1a* dosage imbalance on cerebral cortex development we used a *Dyrk1a* loss-of-function model, generated in the laboratory by gene targeting (Fotaki et al., 2002), and a *Dyrk1a* overexpressing model, kindly provided by Dr. Jean Maurice Delabar (Université Paris Diderot, Paris, France). To determine the implication of *Dyrk1a* trisomy in the cortical alterations associated to DS, we used a trisomic model for DS, the Ts65Dn mouse (Davisson et al., 1993).

Knockout *Dyrk1a* (*Dyrk1a*$^{-/-}$) mice die at the first stages of brain development, around E11.5 (Fotaki et al., 2002). For this reason, we used mice heterozygous for the mutation (***Dyrk1a***$^{+/-}$). These mice were maintained in their original genetic background by repeated backcrossing of *Dyrk1a*$^{+/-}$ males to C57BL/6Jx129S2/SvHsd F1 wild-type females (Harlan Laboratories).

The *Dyrk1a* gain-of-function model used in this study, the **mBACTg*Dyrk1a*** mouse, carries an extra copy of the full-length mouse *Dyrk1a* gene under the control of its endogenous regulatory sequences. This mouse was obtained by microinjection of an ES cell line carrying a BAC that contains the entire *Dyrk1a* gene (Guedj et al., 2012) into C57BL/6 blastocysts. Mice were maintained in their original genetic background by

repeated backcrossing of C57BL/6 wild-type females (Charles River) and mBACTg*Dyrk1a* mutant males.

The generation of Ts65Dn mice has been previously described (Davisson et al., 1993). Ts65Dn mice are the best-characterised mouse model for DS and carries a segmental trisomy of MMU16 containing around 100 HSA21 orthologous genes including those in the DSCR. These mice were maintained by crossing Ts65Dn females (Jackson Laboratory) to B6EiC3 wild-type males (Harlan laboratories). To obtain Ts65Dn mice disomic for *Dyrk1a (*Ts-*D1a*$^{++-}$*)* we performed crosses between Ts65Dn females and *Dyrk1a*$^{+/-}$ males.

To collect embryos in a particular gestation day, we set up controlled matings. Two to three females (6 weeks to 4 months of age) were placed in the same cage with a single male and the morning after females were checked for the presence of a copulation vaginal plug. The day on which the vaginal plug was detected was considered as embryonic day 0.5 (E0.5). Postnatal and adult (age 2-month or older) mice were generated by continuous matings and the day of birth was considered as postnatal day 0.5 (P0.5).

During the first two years of this thesis, animals were maintained in the animal facility of the Parc de Recerca Biomèdica de Barcelona (PRBB). After, animals were maintained in the animal facility of the Parc Científic de Barcelona (PCB). In both animal facilities the housing conditions were under a 12 hours light / 12 hours dark schedule in controlled environmental conditions of humidity (60%) and temperature (22 ± 2ºC) with food and water *ad libitum*. All experimental procedures were carried out following protocols approved by the PRBB and the PCB ethic committees.

1.2 Genotyping

Genotyping of embryos and mice was performed by polymerase chain reaction (PCR) analysis using genomic DNA obtained from a tissue sample. DNA was extracted by incubating fresh or frozen tissue in NaOH 50 mM at 95ºC for 60 min. Then, the solution was neutralized by the addition of 1:10 volumes of Tris-HCl 100 mM pH 8. For mice, we incubated 2-3 cm of tail in 300 μl of NaOH solution. Samples were centrifuged in a microcentrifuge at maximum speed for 10 min and 1 μl of the supernatant containing DNA was used for each PCR reaction. Some Ts65Dn mice were genotyped by semi-quantitative PCR. This protocol consists in simultaneously amplify two MM16 genes (*App* and *Mx1*) and a control gene lying on another chromosome (*ApoB*), using specific primer oligonucleotides and Taqman probes. Semi-quantitative PCRs were performed in a 7900HT Fast Real-Time PCR System apparatus (Applied Biosystems). B6EiC3 mice carry the recessive retinal degeneration 1 mutation (*Pde6b*^{rd1}), which in homozygosis leads to blindness (Costa et al., 2010) (Chang et al., 2002). Ts65Dn females used to maintain the colony were screened for this mutation by PCR amplifying the *rd1* locus and digestion of the resulting fragment with the enzyme *DdeI* during 12 hours. Sequences of oligonucleotide primers and probes and PCR conditions used in this work are detailed in Tables M1 and M2. PCR primers were from Sigma-Aldrich and Taqman probes from Applied Biosystems.

Table M1: Oligonucleotide primers for mouse genotyping by PCR

Usage	Primer	Primer sequence 5'-3'	T/N	bp
Dyrk1a$^{+/-}$	Neo T2(F)	AAGACAATAGCAGGCATGCTGGGGATG	61/28	250/**160**[1]
	Dyrk1a- I5(R)	ACGGCTTATGTTCTTCAACAGGTCAGG		
	Dyrk1a- I4(F)	ACAGTGAGGCTGTTCCTAGTGAAACTG		
mBACTg*D1a*	Bac11-u(F)	CCGGGGATCCTCTAGAGTCG	66/35	200
	Dyrk-r(R)	ACCCCAGCTAACCAACATCCAT		
	Dyrk-l(F)	TGGGCCAAGCAGTTAGGAGTTT	66/35	200
	Bac11-r(R)	CCATGATTACGCCAAGCTATTTAGG		
Ts65Dn	Wt-IMR8545(F)	AAAGTCGCTCTGAGTTGTTAT	55/40	600/**275**[1]
	Wt-IMR8546(R)	GGAGCGGGAGAAATGGATATG		
	Chr17(F)	GTGGCAAGAGACTCAAATTCAAC		
	Chr16(R)	TGGCTTATTATTATCAGGGCATTT		
Rd1	W149(F)	CATCCCACCTGAGCTCACAGAAAG	58/35	298
	W150(R)	GCCTACAACAGAGGAGCTTCTAGC		

[1] The size of the mutant allele is in bold. T: Tº Annealing in ºC; N: number of cycles; bp: base pairs. Genotyping of mBACtgDyrk1a (mBACTgD1a) mice was done with primers Bac11-u(F) and Dyrk-r(R), or with primers Dyrk-l(F) and Bac11-r(R).

Table M2: Oligonucleotide for mouse genotyping by quantitative PCR

Primer/ probe	Sequence 5'-3' (1)	bp
ApoB(F)	CACGTGGGCTCCAGCATT	74
ApoB(R)	TCACCAGTCATTTCTGCCTTTG	
App(F)	TGCTGAAGATGTGGGTTCGA	79
App(R)	GACAATCACGGTTGCTATGACAA	
Mx1(F)	TCTCCGATTAACCAGGCTAGCTAT	75
Mx1(R)	GACATAAGGTTAGCAGCTAAAGGATCA	
ApoB-vic	CCAATGGTCGGGCACTGCTCAA	
App-FAM	CAAAGGCGCCATCATCGGACTCA	
Mx1-FAM	CTTTCCTGGTCGCTGTGCA	

(1) Sequences obtained from The Jackson Laboratory. Annealing temperature was 60ºC and the number of PCR cycles 40. bp. Base pair. Taqman probes are in bold.

2. Histology

2.1 Sample preparation

To obtain embryonic brain sections, pregnant females were sacrificed by cervical dislocation and the embryos removed from the uterus. Embryo heads were dissected and fixed by immersion in 4% (w/v) paraformaldehyde (PFA) in 0.1 M phosphate buffer saline (PBS; pH 7.4) for 24 hours at 4ºC. To obtain postnatal and adult

brain sections, mice were deeply anesthetized with Carbon dioxide (CO_2) and transcardially perfused with 4% PFA at room temperature (RT). Then brains were removed and post-fixed at 4°C in 4% PFA for 24 hours. In both cases fixed samples were rinsed in PBS and processed to obtain either vibratome or cryostat sections.

For cryostat sectioning, brains and embryonic heads were cryoprotected in 30% (w/v) sucrose in PBS at 4ºC for 1 to 2 days. Embryos were embedded in Tissue-Tek O.C.T. (Sakura Finetek) and frozen at -30ºC in isopentane (Panreac), previously cooled with dry ice. Coronal sections (14 μm) were collected serially on Starfrost precoated slides (Knittel Glasser). Postnatal and adult fixed brains were placed on an OCT-base and coronal or sagittal sections (40 μm) were collected in 48-well plates filled with a cryoprotective solution (40% v/v gylcerol – 40% v/v etylenglycol in PBS), which allows long-term storage of the sections at -20ºC. Sections were obtained with a Leica CM3050S cryostat.

For vibratome sectioning, brains were stored in PBS at 4ºC until being embedded in 2% agarose. Embedded brains were cut in 40 – 50 μm coronal sections in a Leica VT1000S vibratome and placed in 48-well plates filled with PBS. These sections were used for Dyrk1a immunostaining.

2.2 Immunostainings and microscopy

Immunohistochemistry (IHC) was done using the avidin-biotin-peroxidase method (Vectastain ABC kit, Vector Laboratories). Briefly, after washing the sections in PBS, endogenous peroxidase

activity was blocked by incubation with 3% H_2O_2 (v/v) and 10% (v/v) methanol in PBS for 30 min at RT. Sections were then permeabilized for 30 to 90 min with 0.2% Triton-X100 in PBS and afterward incubated 60 min at RT in blocking solution (BS: 0.2% Triton-X100 and 10% foetal bovine serum (FBS, Invitrogen) in PBS). Sample incubations with primary antibody were performed overnight (ON) at 4ºC in incubating solution (IS: 0.2% Triton-X100 and 5% FBS in PBS). After washing with 0.2% Triton-X100 in PBS, sections were incubated with the corresponding biotinylated secondary antibody (1:200; Vector Laboratories) in IS for 60 min, washed and incubated with avidin-biotin-peroxidase solution (Vectastain ABC kit, Vector Laboratories) according to manufacturer's indications. Peroxidase activity was visualized with 0.03% diaminobenzidine (Sigma-Aldrich) and 0.003% H_2O_2. Samples were counterstained with Nissl (Cresyl violet 0.5%, pH 3.6) to visualize the nuclei, dehydrated and mounted in Eukitt mounting medium (Sigma-Aldrich).

For immunofluorescence (IF), samples were washed in PBS and permeabilized as described above. For accurate immunostaining with some antibodies (see Table M3) it was necessary to perform an antigen retrieval treatment before permeabilization. This treatment consisted in boiling the sections for 10 min in sodium citrate buffer (2 mM citric acid monohydrate, 8 mM tri-sodium citrate dihydrate, pH 6.0). For 5-bromo-2'-deoxyuridine (BrdU) immunostaining, sections were incubated before permeabilization in 50% formamide diluted in 2X SSC at 64ºC for 10 min followed by an incubation in 2 N HCL at 37ºC for 30 min and finally 10 min in

0.1 M boric acid (pH 8.5) at RT. After 60 min incubation in BS, sections were incubated ON at 4ºC with primary antibodies. After washing, incubation with fluorescent secondary antibodies was performed in IS for 60 min at RT. Secondary antibodies used for IF were: Alexa Fluor 568-conjugated donkey anti-mouse and donkey anti-rabbit; Alexa Fluor 488-conjugated donkey anti-mouse, goat anti-rabbit, donkey anti-rat and donkey anti-goat, (1:1000, Life Technologies); and biotinylated goat anti-mouse IgG or anti-guinea pig IgG (1:200, Vector Laboratories) followed by 60 min incubation with streptavidin conjugated to Alexa Fluor-488 (1:1000, Life Technologies). Cell nuclei were stained with Hoechst (Sigma-Aldrich) and samples were mounted in Vectashield mounting medium.

Primary antibodies used for IHQ and IF are detailed in Table M3. In all cases, specificity of the immunoreaction was verified in parallel samples incubated in BS without primary antibody. No immunoreaction was detected in these samples. Samples from animals of different genotypes were processed in parallel to avoid day-to-day variations in the immunostaining.

Bright field images were viewed with an Olympus BX51 microscope or with a Leica AF7000 motorized wide-field microscope and acquired with a DFC-550 color camera. Immunofluorescence images were viewed under a Zeiss Observer.Z1 microscope and acquired with an AxioCam MRm camera or under a Leica AF7000 motorized wide-field microscope and acquired with Digital CCD camera ORCA-R2. Confocal images were taken in a sequential

Table M3: Primary antibodies used for immunostainings

Antibody	Host	Source (Reference)	Dilution
A-Cas-3*	Rabbit	BD Pharmigen (559565)	1:500
BrdU	Rat	Abd serotec (OBT0030G)	1:75
BrdU	Mouse	Hybrydoma Bank (G3G4)	1:50
CR	Rabbit	Swant (7699/3H)	1:3000
Cyclin D1	Rabbit	Thermo scientifics (RM-9104)	1:100
Ctip2*	Rat	Abcam (ab18465)	1:250
Cuxl*	Goat	Santa cruz Biot. (sc-6327)	1:50
Dyrk1a	Mouse	Abnova (H00001859)	1:250
Ki67*	Rabbit	Abcam (ab15580)	1:100
NeuN	Mouse	Milipore (MAB377)	1:50**
Nkx2.1*	Rabbit	Abcam (ab76013)	1:200
Nkx6.2	G. Pig	Karolinska Institutet	1:1000
PV	Mouse	Sigma-Aldrich (P3088)	1:250**
Pax6*	Mouse	Hybrydoma Bank	1:50
Pax6	Rabbit	Covance (PRB-278P)	1:500
pH3	Rat	Sigma-Aldrich (H 9908)	1:200
RC2	Mouse	Hybrydoma Bank	1:5
SST	Rat	Milipore (MAB354)	1:250
Tbr1*	Rabbit	Abcam (ab31940)	1:200
Tbr2*	Rabbit	Abcam (ab23345)	1:200
TujI	Mouse	Covance (MMS435P)	1:500
TujI	Rabbit	Sigma-Aldrich (T2200)	1:500

* Citrate pretreatment; ** Dilution for IHC; 1:1000 dilution was used for IF. The Nkx6.2 antibody was a gift from Dr. Ericson. A-Cas-3: active-caspase-3; CR: Calretinin; PV: Parvalbumin; SST: Somatostatin.

mode with a Leica TCS SP5 confocal microscope using the Leica Confocal Software (LCS). Images were taken in the Centre de

Regulació Genòmica (CRG, Barcelona) or at the Advanced Fluorescence Microscopy Unit of the Institut de Biologia Molecular de Barcelona (IBMB-CSIC, Barcelona).

2.3 Detection of BrdU and EdU labelled cells

To quantify cell cycle exit rates and neuronal production pregnant females were intraperitoneally injected with one pulse of BrdU (100 mg/kg; Sigma-Aldrich) and sacrificed 24 hours later. Embryos were collected and processed as describe in Section 2.1. For cell cycle exit rates, sections were immunostained for BrdU and Ki67 and total $BrdU^+$ cells and $BrdU^+Ki67^-$ cells were counted. For neuronal production, sections were immunostained for BrdU and Tbr1 and total $BrdU^+$ cells and double ($BrdU^+Tbr1^+$) immunolabelled cells were counted.

To measure cell cycle duration of radial glial progenitors the cumulative EdU-labelling protocol described by Arai et al., (Arai et al., 2011) was followed. Briefly, pregnant females (E11.5) were repeatedly injected with 5-ethynyl-2'-deoxyuridine (EdU) (3.3 mg/kg; Life Technologies) and sacrificed at different time points according to the schedule shown in Figure R25. EdU was detected in brain sections immunolabelled for Tbr2 and Tuj1 using the Click-iT EdU Alexa Fluor 647 kit (Life Technologies). The proportion of EdU^+Tbr2^- nuclei localised in the VZ at the different EdU-exposured times (Labelling Index) were plotted as described previously (Nowakowski, 1989) and used to calculate: the growth fraction, GF; the cell cycle duration, Tc; and the S phase duration, Ts. For

estimating the duration of G2 and M phases, sections were immunostained for pH3 to identify mitotic progenitors. The average G2 duration was considered as the time required for half-maximal appearance of EdU in mitotic progenitors. Duration of M phase corresponds to the proportion of RG progenitors (nucleus in VZ that do not express Tbr2 or Tuj1) that were in mitosis ($pH3^+$ cells) multiply to the total cell cycle duration (Arai 2011). All these values were then used to calculate G1 phase duration.

2.4 Morphometry and cell counts

- Ventricle volume

Volumes of the lateral, third ventral and third dorsal ventricles were estimated on coronal brain sections, from bregma -1.34 mm to -1.58 mm, obtained from 2-month-old mice. The area of the ventricles were measured by using the tool “Area” of the CAST GRID software package (Olympus) adapted to an Olympus BX51 microscope with an interactive computer system consisting of a high-precision motorized microscope stage, a microcator for reading z- positions (Heidenhain MT-12 gauge microcator) and a high resolution video monitor.

The volume was obtained with the following equation:

$$V = t \times (1/ssf) \times \sum areas$$

where V represents the total volume of the region of interest, t the section thickness (40 μm) and ssf (section sampling fraction) the

ratio of the sections sampled with respect to the total number of sections that spanned the region of interest.

- Thickness of the cortex

The thickness of the cerebral cortex was measured in the somatosensory barrel cortex of 2-month-old animals in a minimum of 3 coronal sections (bregma -0.82 mm to bregma -0.94) per animal stained with Nissl. The different cortical layers were discriminated by eye using the differences in cell density between them. This measurement was done using the tool “length” of the CAST GRID software package adapted to the Olympus BX51 microscope previously described.

- Cell counts in adult mice

Cell quantifications were performed in the somatosensory barrel cortex of 2-month-old animals in a minimum of 3 coronal sections (bregma -0.82 mm to bregma -0.94) per animal.

Total cell and neuronal densities were estimated in sections stained with Nissl and immunostained for NeuN by means of stereological techniques, which involve counting cells with dissectors in a sample that constitutes a known fraction of the structure to be analysed (West and Gundersen 1990). The stereological measurements were performed according to Benavides-Piccione et al., (Benavides-Piccione et al., 2005). Briefly, to count neuronal nuclei in sampling probes we counted ten dissectors probes of a determine volume (Vdis), which was determined by fixing the surface and the thickness of the dissector, using a 40X objective.

The numerical density of Nissl and NeuN staining cells was estimated by dividing the total count in the uniformly sampled dissectors by the total number of dissectors multiplied by the volume of the dissector (Vdis). Dissectors whose upper right corner was not within the sampled area were not included in the total number of dissectors. Nuclei touching either of two predetermined adjacent sides of the rectangular dissector frame were not included in the count. The coefficient of error (CE = SEM/mean) was calculated according to Gundersen and Jensen (Gundersen and Jensen, 1987) to evaluate the precision of the estimates, sampling was optimised to maintain this coefficient below the observed biological variability (CE <10%). These measurements were done using the Olympus BX51 microscope previously described with the interactive computer system and the CAST GRID software package.

Interneurons expressing the somatostatin, the calretinin or the parvalbumin cell marker were counted in images of immunostained coronal brain sections acquired with the DFC-550 color camera for HIS or with the Digital CCD camera ORCA-R2 for IF, associated to Leica AF7000 motorized wide-field microscope with the 20X objective. Immunopositive cells were quantified in a wide column of 600 µm of the somatosensory barrel cortex in a minimum of three sections per animal.

- Cell counts in embryos and postnatal animals

Cell counts in brain embryo sections were done on confocal images obtained from the region of interest in a minimum of 3 images per

animal. Images were taken with a 20X objective at intervals of 1µm and confocal projections obtained using the "z-projection" tool of the Image-J software for image processing (developed and maintained by the National Institutes of Health, Bethesda, MD, Maryland, USA). Labelled cells in the dorsal pallium were counted in a 100 µm width column of the lateral cortical wall, with the exception of cleaved-caspase3$^+$ cells, pH3$^+$ cells and EdU-labelled cells that were counted in 400 µm, 600 µm and 250 µm width columns, respectively. In the ventral pallium, Nkx6.2$^+$ progenitors were counted in all the Nkx6.2$^+$ area and numbers were expressed as the proportion of total number of cells (Hoescht-labelled nuclei). Nx2.1$^+$ progenitors were counted in rectangles of 200 µm x 50 µm localised at the dorsal, the medial and the caudal regions of the MGE. Cell cycle exit rates were estimated as explained in section 2.3 by counting cells in squares of 100 µm^2 in the same dorsal, medial and caudal MGE regions.

Cell counts in postnatal animals were done on images obtained from the region of interest in a minimum of 4 images per animal. Images were acquired using the Leica AF7000 motorized wide-field microscope. Labelled cells were counted in a 350 µm width column of the somatosensory cortex. All counts and morphometric quantifications were done under blind conditions.

2.5 Immunolabelling quantifications

Relative cytoplasmatic and nuclear Cyclin D1 protein levels were estimated in confocal images of brain sections stained for Cyclin D1

and the nuclei labelled with Hoechst. First, images were converted to binary images by applying a threshold level on them using the Image-J software. Cytoplasmatic Cyclin D1 was assigned to the Cyclin D1 signal that did not overlap with the Hoechst signal and was obtained by subtracting the Hoechst binary image to the Cyclin D1 binary image. Nuclear Cyclin D1 corresponded to the Cyclin D1 signal that overlapped with the Hoechst signal and was obtained by subtracting the cytoplasmatic Cyclin D1 binary image to the total Cyclin D1 binary image (see Figure M1). Labelling intensities of total, nuclear and cytoplasmatic Cyclin D1 were measured in a rectangle of 250 µm x 50 µm in a minimum of three brain sections per embryo using the integrated density option of the Image-J software.

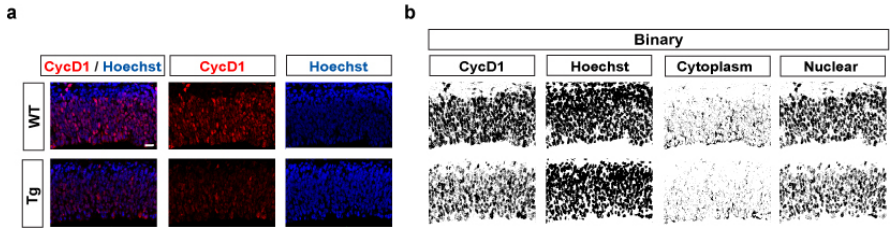

Figure M1. Quantifications of Cyclin D1 levels in confocal images of coronal brain sections. (**a**) Representative images from E11.5 wild-type (WT) and Tg*Dyrk1a* (Tg) embryos showing Cyclin D1 (CycD1) immunostaining (red) and the nuclei visualized with Hoechst (blue). (**b**) Binary images were generated from images like the ones shown in **a** using the ImageJ software. "Cytoplasm" image was obtained by subtracting the binary "Hoechst" image from the binary "CycD1" image, and "Nuclear" image by subtracting the "Cytoplasm" image from the binary "CycD1" image as indicated in the Methods section. Bar = 20 µm.

3. Flow cytometry

3.1. Isolation of cells

To obtain brain progenitors the telencephalon of E10.5 and E11.5 embryos was dissected and incubated for 20 min at 37ºC in 50 µl of DMEM (Life Technologies) containing 1 mM N-acetil cystein (Sigma-Aldrich), 7 U/ml papain (Worthington), 12 mg/ml DNAse (Life Technologies) and 5 mM HEPES (Life Technologies). Papain was inactivated by adding 500 µl of dissociating media (DM; DMEM containing 5mM HEPES) and tissue pieces and cells were collected by centrifugation at 200g for 5 min. Cells were dissociated in 100 µl of DM by gentle trituration (30 up-and-down passages using a p200 tip). After adding 400 µl of DM, dissociated cells were passed trough a filter (BD falcon; cell strainer of 12 mm x 75 mm).

3.2 Cell cycle profiles

Cells (≈ 1 x 10^5) isolated from single embryos were fixed in 70% ethanol diluted in PBS containing 5 mM EDTA at 4ºC ON. After genotyping, cells were pooled according to their genotypes (minimum of 2 embryos per pool) and incubated for 24 hours at 4ºC with 15 µg/ml propidium iodide (Life technologies) diluted in PBS containing 5 mM EDTA, 0.3 mg/ml RNAse A (Sigma-Aldrich) and 38 mM Sodium citrate (Sigma-Aldrich). DNA content profiles (propidium iodide signal) of single cell suspensions were obtained using the Epics XL cytometer from the Cytometer Unit of Centres Científics i Tecnològics (CCiT) of the Universitat de Barcelona.

4. RNA manipulation

4.1 RNA extraction

Embryonic telencephalon or ganglionic eminences were dissected out and immediately frozen in dry ice. Samples were homogenized by mechanically trituration and the RNA extracted using the RNeasy Mini kit (Quiagen) following manufacturer's instructions. The eluted RNA was treated with DNAse (Ambion) for 30 min at 37ºC to eliminated DNA contamination. RNA was quantified using a NanoDrop (Agilent) and its quality was assessed by RNA visualization in a 0.8% agarose gel, before storage at -80ºC.

4.2 RT-qPCR

cDNAs were synthesized from 1μg of total RNA using Superscript II retrotranscriptase (Life Technologies) and random examers (Life Technologies). RT-qPCR was carried out with the Lightcycler 480 platform (Roche), using SYBR Green I Master Kit (Roche). cDNAs were diluted 1:10 and the reagents were mixed following manufacturer's instructions. PCR conditions used were the following: one cycle: 95°C 5 min; 40 cycles: 95°C 10 sec, 60°C 10 sec, 72°C 10 sec; one cycle: 95°C 5 sec, and a final cycle: 65°C 1 min. Primers for RT-qPCR, are listed in Table M4 and were designed using the "Primer3" free tool (http://frodo.wi.mit.edu/cgi-bin/primer3/primer3) to obtain amplicons of 80 to 250 bp, and optimal annealing temperatures between 59 and 61ºC for each primer pair. Data were analyzed on the basis of the crossing

temperature (ct) values obtained, according to the Pfaffl Method (Pfaffl 2001) using *Peptidyl-prolyl isomerase a (Ppia)* as reference gene for data normalization.

Table M4: Oligonucleotide primers for RT-qPCR

Gene		Primer sequence 5'-3'	bp
Calb1	F	CCACCTGCAGTCATCTCTGA	116
	R	GTCCCTGGATCAAGTTCTGC	
CyclinD1	F	CACAACGCACTTTCTTTCCA	88
	R	TGACTCCAGAAGGGCTTCAA	
Delta1	F	CGGCTCTTCCCCTTGTTCTAA	126
	R	GGGGAGGAGGCACAGTCATC	
Dyrk1a	F	ATCCAGCAACTGCTCCTCTG	140
	R	CCGCTCCTTCTTATGACTGG	
Gli1	F	ACGCCTTGAAAACCTCAAGA	189
	R	GGATCTGTGTAGCGCTTGGT	
Gli2	F	TACCTCAACCCTGTGGATGC	148
	R	CTACCAGCGAGTTGGGAGAG	
Gli3	F	ATTCCCGTAGCAGCTCTTCA	137
	R	TTGCTGTCGGCTTAGGATCT	
Hes1	F	CGGCATTCCAAGCTAGAGA	159
	R	GCGGGTCACCTCGTTC	
Hes5	F	ATGCTCAGTCCCAAGGAGAA	202
	R	TAGTCCTGGTGCAGGCTCTT	
Hes6	F	TGCAGGCCAAGCTAGAGAAC	202
	R	TCAGCTGAGACAGTGGCATC	
Lhx6	F	AACAGGACAGTCAGCCCAAG	181
	R	GGCAGTTTTGAAACCACACC	
NeuroD1	F	CTCGGACTTTCTTGCCTGAG	201
	R	TTTCAAAGAAGGGCTCCAGA	

Notch1	F	CGCAAGCACCCAATCAAG	136
	R	TGTCGATCTCCAGGTAGACAATG	
p21	F	TTGTCGCTGTCTTGCACTCT	103
	R	AATCTGTCAGGCTGGTCTGC	
p27	F	TTGGGTCTCAGGCAAACTCT	131
	R	TCTGTTCTGTTGGCCCTTTT	
Ppia	F	ATGGCAAGACCAGCAAGAAG	143
	R	TTACAGGACATTGCGAGCAG	
Ptch1	F	GGCAAGTTTTTGGTTGTGGGTC	157
	R	CCTCTTCTCCTATCTTCTGACGGG	
Rcan 1-1	F	CCGTAGGGTGACTCTG	243
	R	GCTCTTAAAATACTGGAAGGT	
Rcan 1-2	F	GCGAGTCGTTCGTTAAG	185
	R	ATACTGGAAGGTGGTGT	
Shh	F	TCACAAGAAACTCCGAACGA	140
	R	AGAGATGGCCAAGGCATTTA	

5. Protein manipulation

5.1 Sample preparation

Embryonic telencephalon or ganglionic eminences were dissected out and immediately frozen in dry ice. Protein extracts from frozen tissues were prepared by resuspending the tissue in 10 volumes of SDS-buffer (25 mM Tris-HCl pH7.4, 1 mM EDTA, 1% (w/v) SDS, 10 mM sodium pyrophosphate, 20 mM beta-glycerol phosphate, 2 mM sodium orthovanadate, 2 mM phenylmethylsulphonyl fluoride and protease inhibitors (Roche) and mechanically homogenized them using first a scalpel and after a micropipette. Then, samples were

sonicated with 4 pulses of 30 sec each in a Bioruptor (Diagenode), boiled for 15 min at 98ºC and centrifuged for 10 min at 800g at RT. Protein concentration was determined using a colorimetric assay (BCA Protein Assay Kit, Pierce) according to the manufacturer's indications.

5.2. Western Blotting

Protein extracts (30 to 80 µg) were mixed with 6X Laemmli buffer (0.5 M Tris-HCl pH6.8, 12% (w/v) SDS, 60% (v/v) glycerol, 0.6 M dithiothreitol, 0.06% bromophenol blue), heated for 5 min at 98ºC and resolved on SDS-PAGE gels of different acrylamide percentages depending on the molecular weight of the protein at 125 V in 1X running buffer (25 mM Tris-base, 200 mM glycine, 0,1% (w/v) SDS). Proteins were transferred onto a nitrocellulose membrane (Hybond-ECL, Amersham Biosciences) at 400 mA for 60 min at 4ºC in 1X transfer buffer (25 mM Tris-HCl pH8.3, 200 mM glycine, 20% (v/v) methanol). Correct protein transfer was checked by staining with Ponceau (Sigma-Aldrich). Transferred membranes were blocked for 60 min at RT in 5 - 10% Bovine Serum Albumin (BSA) (w/v) in TBS-T (10 mM Tris-HCl pH7.5, 100 mM NaCl, and 0.1% Tween-20), and then incubated ON at 4ºC with the corresponding primary antibody diluted in 5% BSA in TBS-T. The antibodies and dilutions used for Western blotting are in Table M5. After four washes of 10 min with TBS-T, membranes were incubated for 60 min at RT with the fluorescent secondary antibodies goat anti-mouse IgG IRDye-800CW and/or goat anti-

rabbit IgG IRDye-680CW. Infrared fluorescence was visualized using the LI-COR Odyssey IR Imaging System V3.0 (LI-COR Biosciences) and protein levels were quantified using the Odissey software version 3.0. Alternatively, the binding of some antibodies was visualized using chemiluminiscence. In this case, membranes were incubated with rabbit anti-mouse or goat anti-rabbit IgGs conjugated to horseradish peroxidase (1:2000; Dako) diluted in 5% BSA in TBS-T for one hour. Proteins were detected by enhanced chemiluminiscence with ECL or ECL plus Western blotting detection reagents (Amersham Life Sciences) using X-ray Films (AGFA) and the hyperprocessor model AM4 (Amersham Pharmacia Biotech). Quantifications were done using the Image-J software. In both cases protein values were normalised for the levels of α-tubulin, actin or vinculin proteins.

Table M5: Primary antibodies used for Western blotting

Antibody	Host	Source (Reference)	Dilution
Actin	Rabbit	Sigma-Aldrich (A2066)	1:5000
α-tubulin	Mouse	Sigma-Aldrich (T6199)	1:10000
Ciclin D1	Rabbit	Thermo Sci. (RM-9104)	1:2000
DYRK1A	Mouse	Abnova (H00001859)	1:500
p21	Mouse	Santa Cruz (sc-6246)	1:200
p27	Mouse	BD Trans. Lab. (610241)	1:500
RCAN1	Rabbit	Laboratory (1)	1:1000
Ret.	Rabbit	BD Pharmigen (554136)	1:500
Vinculin	Mouse	Sigma-Aldrich V9131	1:10000

(1) Porta et al., Eur J Neurosci. 2007; Ret: Retinoblastoma.

6. Statistical Analysis

Data are presented as the mean ± S.E.M. To calculate the statistical significance of cell cycle parameters in Figure R25 data were analysed by the two-way ANOVA. Otherwise, data were analyzed by the two-tailed Student's t-test. A minimum of three embryos or mice of the same genotype were analysed in each experiment. Differences were considered significant at p-values <0.05: *p<0.05, **p<0.001 and ***p<0.0001.

1. Effects of *Dyrk1a* gene-dosage variation in brain growth

DYRK1A loss of function leads to microcephaly in humans (Courcet et al., 2012), mouse (Fotaki et al., 2002; Guedj et al., 2012) and flies (Tejedor et al., 1995). *Dyrk1a*$^{+/-}$ mice show a 30% reduction in brain size. Importantly, size reductions are very evident in particular structures such as the mesencephalic tectum or the hypothalamus, while the size of the olfactory bulbs and the thickness of the cerebral cortex are almost normal (Fotaki et al., 2002).

To assess the dose-dependent role of DYRK1A in mammalian brain growth, we performed a histological analysis in the mBACTg*Dyrk1a* mouse model and compared brain size and gross morphological alterations in this model with those in the *Dyrk1a*$^{+/-}$ haploinsufficient model. The mBACTg*Dyrk1a* model carries one extra copy of the entire *Dyrk1a* mouse gene including its regulatory sequences. As expected for the genetic complement, the brain of this transgenic mouse has a 1.5 fold increase in Dyrk1a protein levels compared to their wild-type littermates (Guedj et al., 2012). The macroscopic analysis of sagittal (Figure R-1) and coronal (Figure R-2a) sections of adult (age 2-month-old) mBACTg*Dyrk1a* mice and their wild-types littermates indicate that transgenic brains do not have gross citoarchitectural alterations. All brain structures were present and no gross alterations in lamination were observed. However, mBACTg*Dyrk1a* mice showed alterations in brain size and shape.

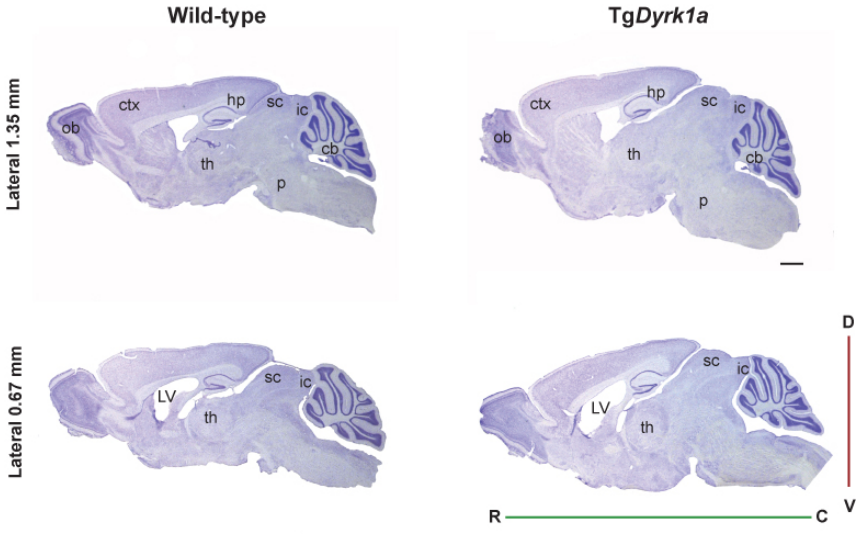

Figure R-1: mBACTg*Dyrk1a* mice have brachycephalic brains. Representative Nissl-stained sagittal brain sections at two different medio-lateral levels of 2-month-old wild-type and mBACTg*Dyrk1a* (Tg*Dyrk1a*) mice. Green and red bars correspond to the rostro-caudal and the dorso-ventral axis respectively. cb: cerebellum; ctx: cortex; hp: hippocampus; ic: inferior colliculus; LV: lateral ventricle; ob: olfactory bulb; p: pons; sc: superior colliculus; th: thalamus. Scale bar: 1 mm.

In agreement with the increased brain weight described in Guedj et al., 2012, the size of mBACTg*Dyrk1a* brains was slightly increased (Fig R-1 and R-2a). In addition, these animals showed brachycephaly (decreased rostro-caudal length compared to the dorso-ventral length) (Figures R-1 and R-2a). Similar to *Dyrk1a*$^{+/-}$ mice (Fotaki et al., 2002), some brain structures in mBACTg*Dyrk1a* mice were more affected than others. For example, the thickness of the cerebral cortex was quite normal in mBACTg*Dyrk1a* mice (Figures R-1 and R-2a) and in *Dyrk1a*$^{+/-}$ mice (Figure R-2b). In contrast, the size of the

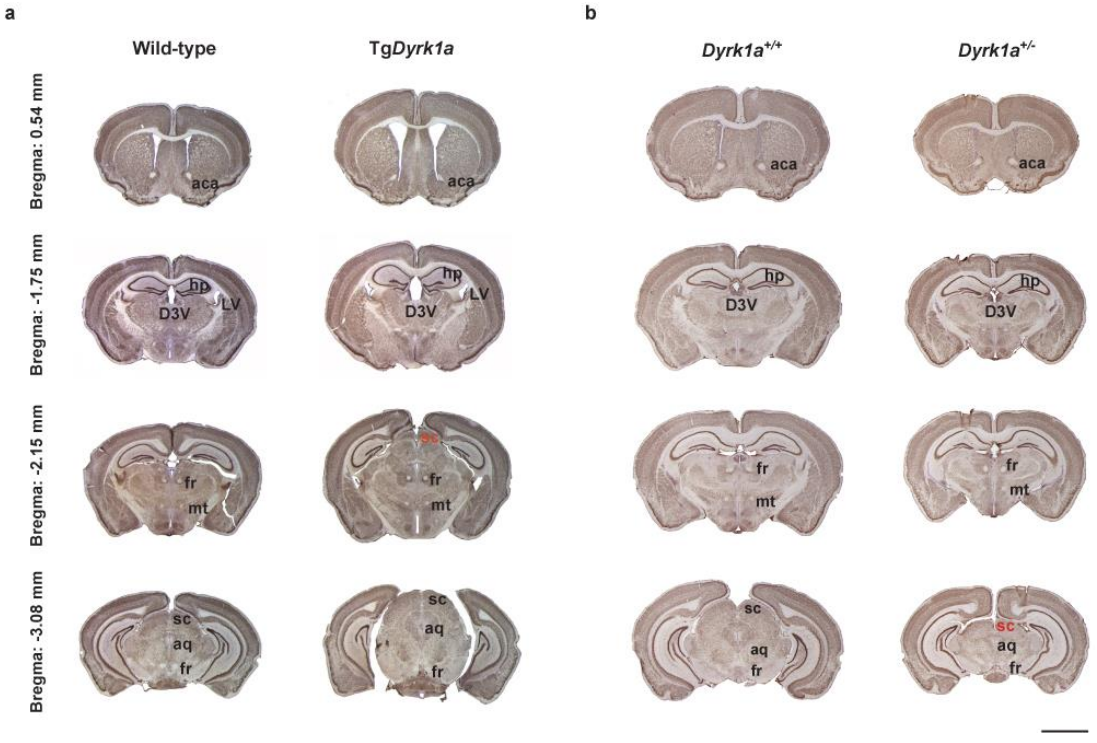

Figure R-2: *Dyrk1a* mutant brains show size alterations that are region specific. Representative coronal brain sections at different rostro-caudal levels of 2-months old wild-type and mBACTg*Dyrk1a* (Tg*Dyrk1a*) **(a)** and wild-type (*Dyrk1a*$^{+/+}$) and *Dyrk1a*$^{+/-}$ **(b)** mice immunolabelled for NeuN and co-stained with Nissl. Note that the size of the superior colliculus (sc) is significantly altered in both *Dyrk1a* mutants. ac: anterior commissure; aq: cerebral aqueduct; D3V: dorsal third ventricle; hp: hippocampus; LV: lateral ventricle; mt: mamilothalamic tract; sc: superior colliculus; 4V: fourth ventricle. Scale bar: 2 mm

superior colliculus, a structure that is substantially decreased in *Dyrk1a*$^{+/-}$ mice (Figure R-2b, bregma -3.08 mm), was significantly increased in mBACTg*Dyrk1a* animals. Indeed, the superior colliculus was observed in more rostral sections in these animals than in the wild-types (Figure R-2a, bregma -2.15 mm). Another visible alteration in both *Dyrk1a* mutant models was the shape of the hippocampus that was more rounded in mBACTg*Dyrk1a* mice (Figure R-2a, bregma -1.75 mm) and more elongated in *Dyrk1a*$^{+/-}$ mice (Figure R-2b, bregma -2.15 mm) than in their respective control littermates.

To evaluate to what extend *Dyrk1a* trisomy could be involved in DS morphological brain alterations we performed the same macroscopic analysis in Ts65Dn mice and their wild-type littermates (Figure R-3). As has been previously described (Aldridge et al., 2007; Richtsmeier et al., 2002) and in contrast to what we observed in the mBACTg*Dyrk1a* mouse, the overall brain volume in the trisomic Ts65Dn model was normal (Figure R-3). However, Ts65Dn mice also present brachycephaly (Figure R-3). Importantly, the superior colliculus in these animals was also larger than in the wild-types (Figure R-3, bregma -2.15 mm) and, like in the mBACTg*Dyrk1a* model, the hippocampus also had a more rounded shape (Figure R-3, bregma -1.75 mm).

In addition, the brain of Ts65Dn mice showed an enlargement of the ventricles (Figure R-3, bregma -1.75 mm), phenotype that has been also observed in the DS mouse model Ts1Cje (Ishihara et al., 2010) and in DS individuals (Pearlson GD et al., 1998).

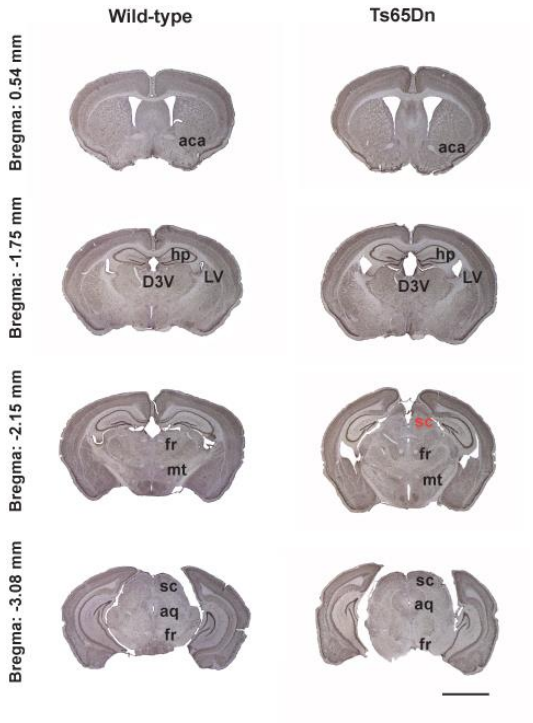

Figure R-3: Morphological brain alterations in Ts65Dn mice. Representative coronal brain sections at different rostro-caudal levels of 2-month-old wild-type and Ts65Dn mice immunolabelled for NeuN and co-stained with Nissl. Note that the superior colliculus in the Ts65Dn model is observed at more rostral sections than in the wild-types and that the hippocampus has a more rounded shape. ac: anterior commisure; aq: cerebral aqueduct; D3V: dorsal third ventricle; fr: fasciculus retroflexus; hp: hippocampus; LV: lateral ventricle; mt: mamilothalamic tract; sc: superior colliculus; 4V: fourth ventricle. Scale bar: 2 mm.

Importantly, the ventricles in mBACTg*Dyrk1a* mice seemed larger than normal (Figure R-2a). To confirm this, we estimated the volume of the lateral ventricles and the dorsal and ventral third ventricles in coronal sections of mBACTg*Dyrk1a* and wild-type littermate adult mice (bregma -1.75 mm) using the Cavalieri method. As at this rostro-caudal level the volume of the brain is increased in transgenic animals (Figure R-4a, b), we measured the volume of the ventricles and expressed them relative to the

volume of the brain section. The lateral and the dorsal third ventricles were relatively bigger in mBACTg*Dyrk1a* mice than in wild-type mice (Figure R-4c).

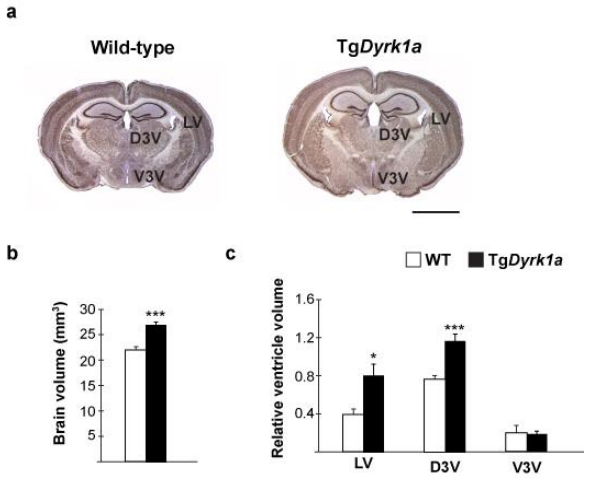

Figure R-4: mBACTg*Dyrk1a* mice show hydrocephaly. (a) Representative coronal brain sections of 2-month-old mBACTg*Dyrk1a* (Tg*Dyrk1a*) and wild-type mice immunolabelled for NeuN and co-stained with Nissl. D3V: dorsal third ventricle; LV: lateral ventricle; V3V: ventral third ventricle. **(b)** Histogram showing the brain volume of transgenic and wild-types mice at the rostro-caudal level were ventricle measurements were done. **(c)** Histogram showing the volume of the three ventricles with respect to the brain volume. All measurements were done in brain sections from bregma -1.34 to bregma -1.58. Histogram values are the mean ± S.E.M. *P<0.05, ***P<0.001 (n = 7). Scale bar: 2 mm.

Altogether these observations show that the overall size of the brain depends on *Dyrk1a* gene copy number and that the effect of DYRK1A in brain growth is region specific. Moreover, the fact that some morphological alterations in the Ts65Dn mouse were also observed in the mBACTg*Dyrk1a* mouse indicates that trisomy of *DYRK1A* may contribute to shape the brain in DS.

2. Effects of *Dyrk1a* gene-dosage variation in cortical lamination and cellularity

As it is mentioned in the introduction (Chapter 2.5), the cerebral cortex of DS individuals shows hypocellularity and an altered lamination (Ross et al., 1984). Given the importance of the cerebral cortex for cognition it has been proposed that these alterations could significantly contribute to the cognitive impairment associated with the syndrome. To determine whether *DYRK1A* aneuploidy could affects the citoarchitecture of the cortex, we analyzed the lamination and the cellularity of the cerebral cortex in adult mBACTg*Dyrk1a* and *Dyrk1a*$^{+/-}$ mice. First of all we measured the total thickness and the thickness of every cortical layer in the somatosensory barrel cortex (SBC) of coronal sections stained with Nissl. As shown in Figure R-5 the total thickness of the cortex was normal in both *Dyrk1a* mutant mice (Figure R-5a-b, d-e). However, when we measured the thickness of each cortical layer we observed that the thickness of layer V was decreased in *Dyrk1a*$^{+/-}$ mice and increased in mBACTg*Dyrk1a* mice (Figure R-5c, f). We next estimated using stereological methods the cellularity in every cortical layer of the SBC in the same tissue preparations. In agreement with previous work of the laboratory (Fotaki et al., 2002), *Dyrk1a*$^{+/-}$ mice showed increased cellularity in all cortical layers reaching statistical significance in layers V and VI (Figure R-6a).

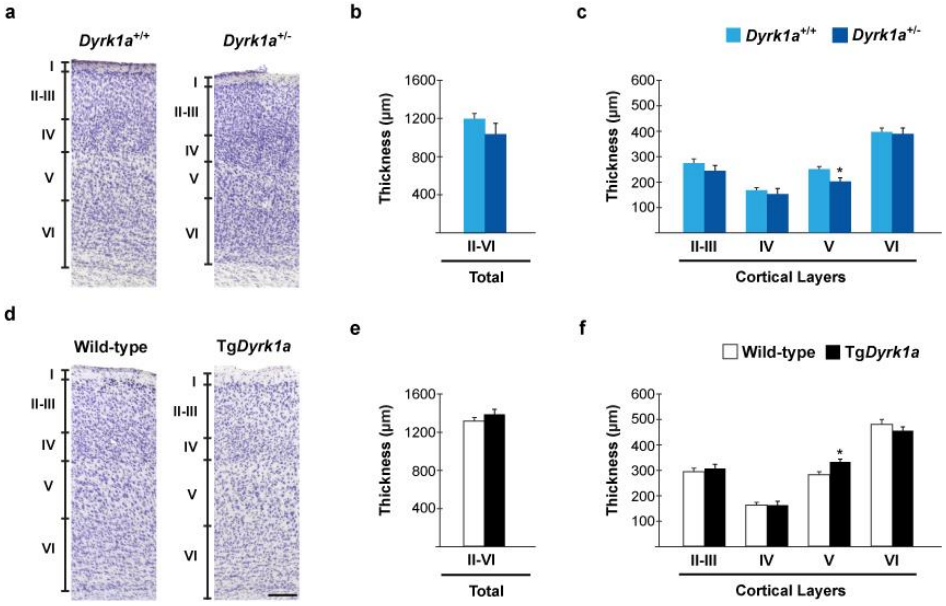

Figure R-5: *Dyrk1a*$^{+/-}$ and mBACTg*Dyrk1a* mice show subtle alterations in cortical lamination. Representative Nissl-stained sections of the somatosensory barrel cortex of 2-month-old *Dyrk1a*$^{+/+}$ and *Dyrk1a*$^{+/-}$ mice **(a)** or wild-type and mBACTg*Dyrk1a* (Tg*Dyrk1a*) mice **(d)**. Histograms comparing the total cortical thickness **(b, e)** and the thickness of each cortical layer **(c, f)** between *Dyrk1a*$^{+/+}$ and *Dyrk1a*$^{+/-}$ mice **(b, e)** or between wild-type and Tg*Dyrk1a* mice **(c, f)**. Histogram values are the mean ± S.E.M. *$P<0.05$ ($n \geq 4$). Scale bar: 200 µm.

Conversely, cell densities were decreased in the SBC of mBACTg*Dyrk1a* mice and, in this case, differences were statistically significant in all layers (Figure R-6b). Therefore, alterations in *Dyrk1a* gene-dosage change the lamination and cellularity of the cerebral cortex and importantly, the phenotype of the mBACTg*Dyrk1a* model resembles that previously described in DS individuals.

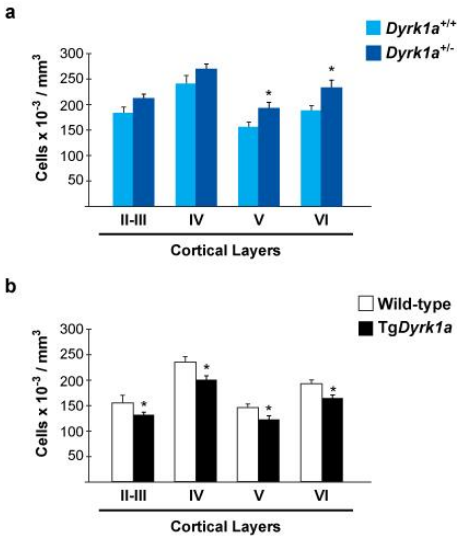

Figure R-6: *Dyrk1a* gene copy number inversely correlates with cortical cellularity. Histograms comparing cell densities in the somatosensory barrel cortex of 2-month-old *Dyrk1a*$^{+/+}$ and *Dyrk1a*$^{+/-}$ mice **(a)** or wild-type and mBACTg*Dyrk1a* (Tg*Dyrk1a*) mice **(b)**. Cells were counted in Nissl-stained coronal sections and values are the mean ± S.E.M. *P<0.05 (n ≥ 4).

Like other regions in the brain, the cerebral cortex is composed by neurons and glial cells (Jones et., 1984). To determine if the observed differences in cellularity are due to variations in one or both cell types, we used stereological methods to estimate neuron and glial cell densities in coronal sections immunostained with the neuronal marker NeuN and co-stained with Nissl. We considered glial cells the nuclei that did not express NeuN.

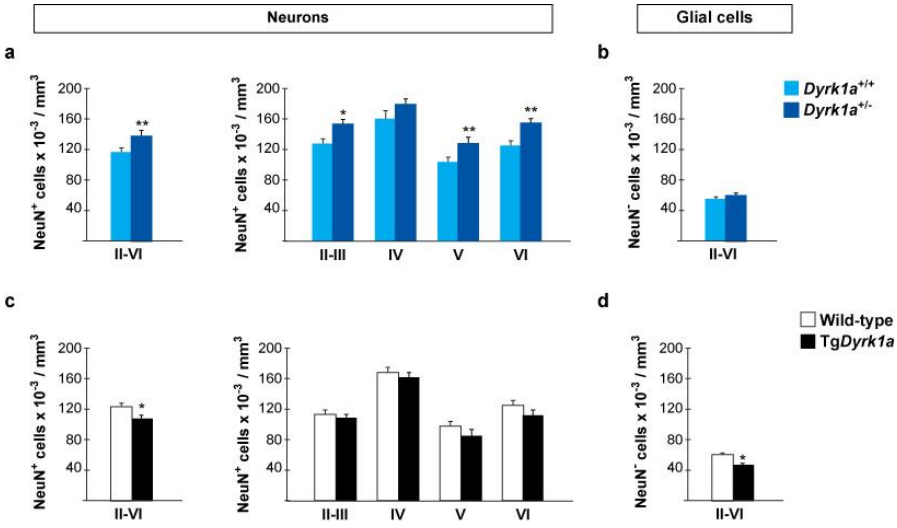

Figure R-7: *Dyrk1a* gene copy number affects cortical neuronal densities but not glial densities. Histograms showing neuronal ($NeuN^+$ cells) densities in the whole cortex (layers II to VI) and in each cortical layer **(a, c)** and total glial ($NeuN^-$ cells) densities in the whole cortex **(b, d)** in 2-month-old *Dyrk1a*$^{+/+}$ and *Dyrk1a*$^{+/-}$ mice **(a, b)** and wild-type and mBACTg*Dyrk1a* (Tg*Dyrk1a*) mice **(c, d)**. Histogram values are the mean ± S.E.M. *P<0.05, **P<0.01 ($n \geq 4$).

Neuronal densities were increased in the cerebral cortex of *Dyrk1a*$^{+/-}$ mice, affecting almost all cortical layers (Figure R-7a). mBACTg*Dyrk1a* mice showed the opposite phenotype, a reduction in total neuronal density, which again was not layer specific (Figure R-7c). Glial cell densities were decreased in the cerebral cortex of mBACTg*Dyrk1a* mice but were normal in *Dyrk1a*$^{+/-}$ mice (Figure R-7b, c). These results show an inverse correlation between the overall brain size and the neuronal cellularity of the cerebral cortex in the gain- and loss-of-function *Dyrk1a* mutants analyzed.

Around 80% of cortical neurons are glutamatergic projection neurons, while the remaining ones are GABAergic interneurons (Parnavelas et., 2000). Both types of neurons are generated

during embryonic development but from different sources of neural progenitors (see Chapter 1.2 in the Introduction section). The abnormal neural densities observed in *Dyrk1a* mutant mice could result from an alteration in one or both types of neurons. The fact that mBACTg*Dyrk1a* mice show normal numbers of cortical GABAergic interneurons (unpublished data of the laboratory) indicate that the decreased neuronal densities observed in this work (Figure R-7c) result from a deficit of glutamatergic neurons that could be originated during development. Importantly, in the Ts65Dn mouse the production of glutamatergic neurons and specific subtypes of GABAergic interneurons is altered leading to an excess of GABAergic inhibition (Chakrabarti et al., 2007; 2010; see Chapter 2.5 in the Introduction section). Specifically, the cerebral cortex of Ts65Dn mice show an excess of PV and SST expressing interneurons, while the number of CR expressing interneurons is normal (Chakrabarti et al., 2010). Despite mBACTg*Dyrk1a* mice have normal numbers of GABAergic interneurons, these published results prompted us to quantify the same interneuron populations in the cerebral cortex of *Dyrk1a* transgenic animals. With this aim, we performed immunostainings for PV, SST and CR in coronal sections of 2-month-old mBACTg*Dyrk1a* and wild-type littermate mice (Figure R-8b-d) and counted the immunopositve cells in external (II-IV) and internal (V-VI) layers of the SBC. Importantly, these three molecular markers cover almost 90% of the interneuron populations in the mouse neocortex (Figures I-2 and R-8a).

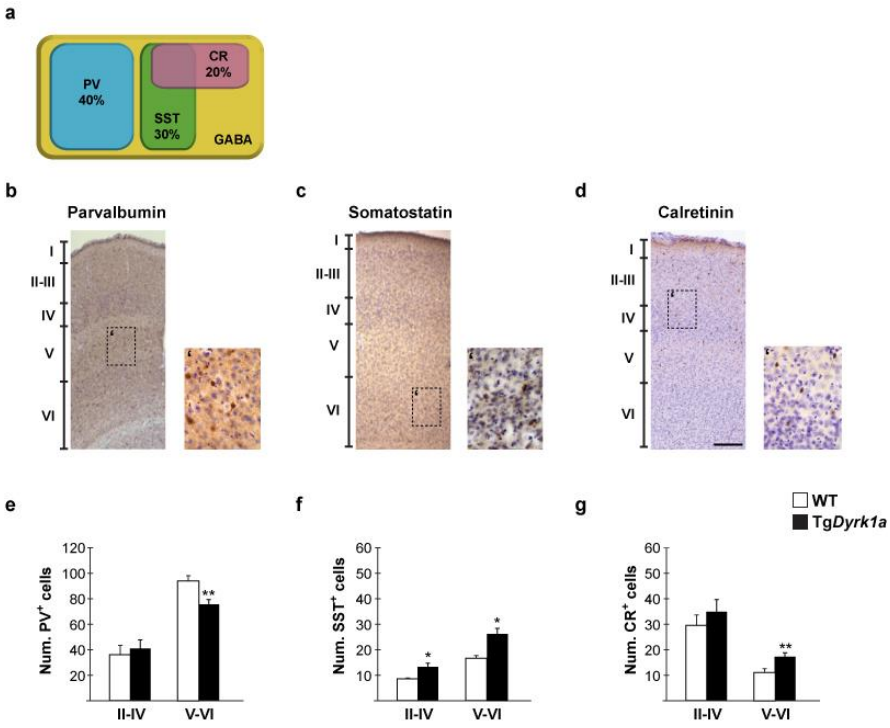

Figure R-8: mBACTg*Dyrk1a* mice show altered numbers of cortical interneuron subtypes. (a) Diagram showing the proportion of GABAergic interneurons expressing parvalbumin (PV) or somatostatin (SST) and/or calretinin (CR). **(b, c, d)** Sections of the somatosensory barrel cortex of 2-month-old wild-type mice immunostained for parvalbumin **(b)**, somatostatin **(c)** or calretinin **(d)**. Rectangles indicate the regions magnified in the images at the right (‘). **(e-g)** Histograms showing the number of PV^+ **(e)**, SST^+ **(f)** and CR^+ **(g)** interneurons in the external (II-IV) and the internal (V-VI) cortical layers of wild-type and mBACTg*Dyrk1a* (Tg*Dyrk1a*) mice. Histogram values are the mean ± S.E.M. *P<0.05, **P<0.01 (n ≥ 3). Scale bar: 200 µm.

Transgenic animals had less PV^+ cells in the internal layers (Figure R-8e), more SST^+ cells in both internal and external layers (Figure R-8f), and more CR^+ cells in the internal layers (Figure R-8g). As it was explained in the introduction (see Chapter 1.2.3) most CR interneurons are generated in the CGE,

however a small population of CR that coexpress SST is generated in the MGE. To determine if an extra copy of *Dyrk1a* could affects neurogenesis in the CGE, we performed a double immunostaining for SST and CR and quantified the number of CR interneurons that do not express SST (white arrows in Figure R-9a). This quantification revealed that the $CR^{+}SST^{-}$ interneuron population is not affected in the cerebral cortex of mBACTg*Dyrk1a* mice (Figure R-9b) and suggest that the development of the CGE is not affected. Most PV and SST cortical interneurons are generated in the MGE, hence the observed phenotypes could arise from an alteration in MGE neurogenesis. To further characterized the alterations observed in SST interneurons we quantified the proportion of these interneurons that coexpress or not CR (orange and blue arrows respectively in Figure R-9a), because they are generated from two different kinds of MGE progenitors (Fogarty et al., 2007; Sousa et al., 2009). Our results showed that both subtypes are increased in mBACTg*Dyrk1a* mice (Figure R-9c) and suggest that the defect in MGE neurogenesis is not restricted to a particular progenitor domain.

In summary, our results suggest that the overexpression of DYRK1A, at levels that mimics DS situation, alters the development of the cortical neuron populations that are affected in the trisomic Ts65Dn model.

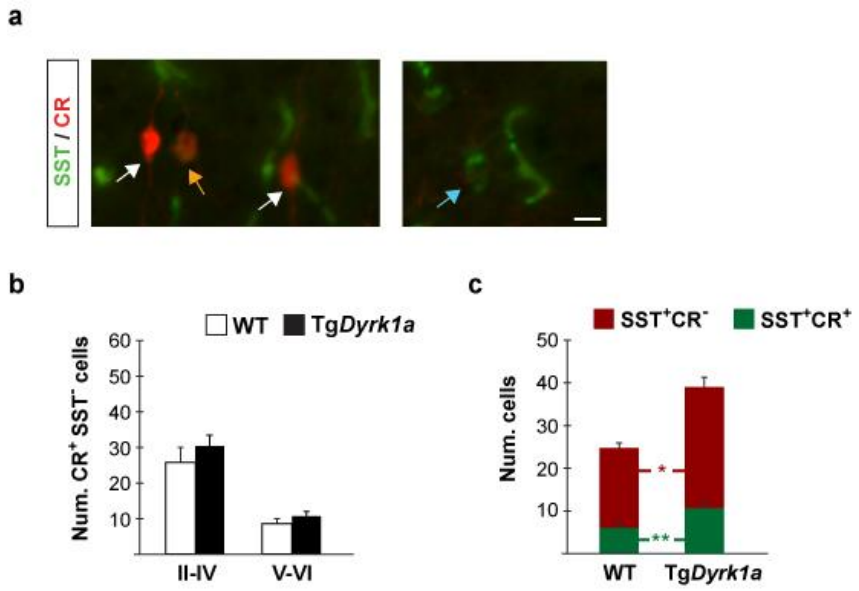

Figure R-9: The cerebral cortex of mBACTg*Dyrk1a* mice show normal numbers of CGE-derived interneurons. (a) Images of the somatosensory barrel cortex of wild-type (WT) mice immunostained for somatostatin (SST) and calretinin (CR) showing interneurons that co-express both markers (orange arrow) and that only express SST (blue arrow) or CR (white arrows). Histograms showing the number of CR^+ SST^- interneurons in the external (II-IV) and the internal (V-VI) cortical layers **(b)** and the numbers of SST-interneurons that express CR (SST^+CR^+ cells, green bars) and that do not express CR (SST^+CR^- cells, red bars) in the whole cortex (layers II to VI) **(c)** in 2-month-old WT and mBACTg*Dyrk1a* (Tg*Dyrk1a*) mice. Histogram values are the mean ± S.E.M. *$P<0.05$, **$P<0.01$ ($n \geq 4$). Scale bar: 10 µm.

3. Dyrk1a expression in the telencephalon during embryonic neurogenesis

Glutamatergic and GABAergic cortical neurons are generated from progenitors localized in the dorsal telencephalon (pallium) and the ventral telencephalon (subpallium) respectively. If DYRK1A is affecting the generation of these two types of neurons it must be expressed in the telencephalic germinal

regions. The expression of mouse DYRK1A in these regions was assessed by immunofluorescence using a commercial DYRK1A specific antibody (Laguna et al., 2008).

It has been previously observed that pre-neurogenic neuroepithelial cells from E9.5 mouse embryos express *Dyrk1a* mRNA (Hammerle et., 2008). Immuofluorescence for DYRK1A at the onset of cortical neurogenesis (E11.5) confirmed the expression of DYRK1A in VZ progenitors of the dorsal pallium (Figure R-10a, b). Moreover, as in other cell types, DYRK1A was localized in the cytoplasm and the nucleus of these progenitors (Arrows in Figure R-10b). At mid-corticogenesis (E13.5) DYRK1A is expressed in the two types of dorsal progenitors, RG progenitors ($Pax6^+$ cells) and IPs ($Tbr2^+$ cells), as well as in neurons ($Tuj1^+$ cells; Figure R-10c, d). In ventral territories, DYRK1A was also expressed in proliferative regions (VZ/SVZ) and in the mantel zone of the MGE, where GABAergic newborn neurons are localized (Figure R-11a, b).

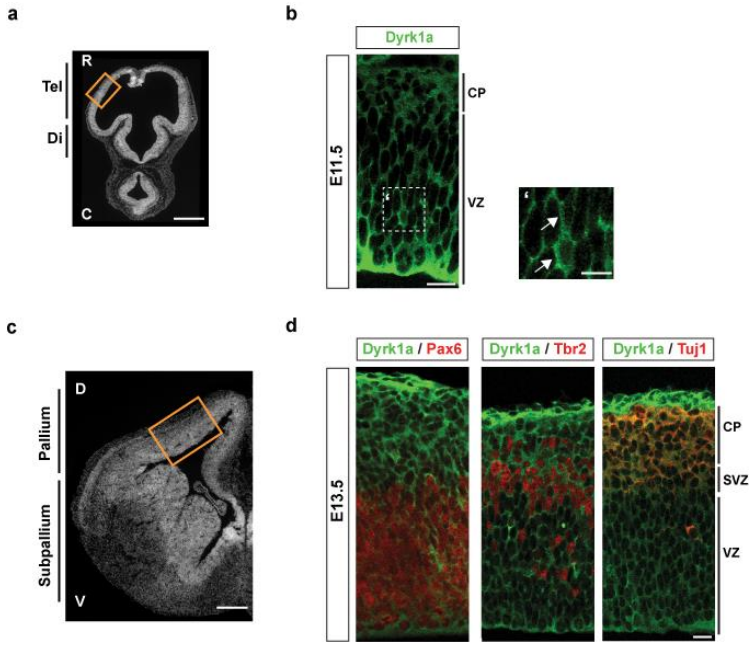

Figure R-10: Dyrk1a is expressed in progenitors and differentiating neurons of the mouse dorsal telencephalon. (a, c) Pictures of coronal brain sections of E11.5 **(a)** and E13.5 **(c)** embryos with nuclei visualized with Hoechst. Rectangles indicate the regions corresponding to images in **b** and **d**. **(b)** Confocal image of a coronal E11.5 brain section showing expression of Dyrk1a in the cytoplasm of radial glial progenitors in the ventricular zone (VZ) and differentiating neurons in the cortical plate (CP). Arrows in the magnified image (') point to progenitors with Dyrk1a immunostaining in their nuclei. **(d)** Confocal images of a coronal E13.5 brain section showing Dyrk1a immunostaining in radial glial progenitors expressing Pax6 (left), in intermediate progenitors expressing Tbr2 (middle), and in postmitotic cells expressing the neuronal marker Tuj1 (right). Di: diencephalon; Tel: telencephalon; SVZ: subventricular zone. Bars = 500 μm (**a, c**), 20 μm (**b**, **d**), 10 μm (magnification in **b**).

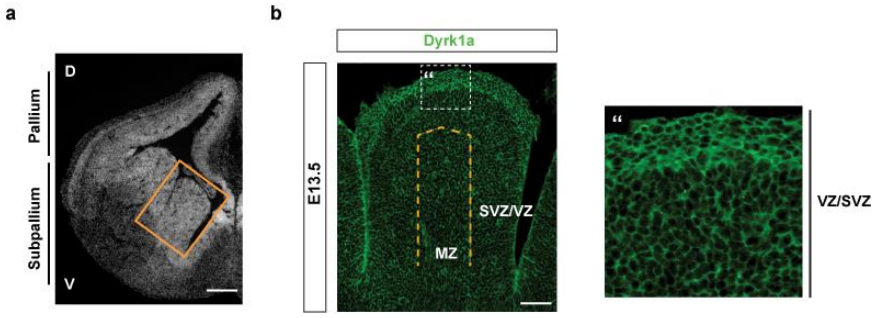

Figure R-11: Dyrk1a is expressed in progenitors and differentiating neurons of the mouse ventral telencephalon. (a) Picture of a coronal brain section of an E13.5 embryo with nuclei visualized with Hoechst. The Rectangle indicates the region in the medial ganglionic eminence corresponding to images in **b**. **(b)** Confocal image showing expression of Dyrk1a in progenitors of the ventricular (VZ) and subventricular (SVZ) zones and in differentiating neurons of the mantel zone (MZ). The white square indicates the region magnified in the right image. Bars = 500 μm (**a**), 100 μm (**b**).

In summary, DYRK1A is expressed both in progenitors and in newborn neurons, of the dorsal and ventral telencephalon. Therefore, it is plausible that one extra copy of *DYRK1A* influences cortical neurogenesis in DS.

4. Effects of *Dyrk1a* trisomy in the development of cortical glutamatergic neurons

As a first approach to determine which process of cortical glutamatergic neurogenesis could be affected by *DYRK1A* trisomy, we performed a general histological examination of the dorsal telencephalon in wild-type and mBACTg*Dyrk1a* embryos at two developmental stages: at the onset of neurogenesis, by E11.5, and during mid-corticogenesis, at E14.5. As shown in Figure R-12a, the general morphology of the brain was

maintained in the transgenic embryos at both stages. The thickness of the proliferative regions (VZ at E11.5, and VZ/SVZ at E14.5), which are the regions adjacent to the dorsal ventricle that do not express the neuronal marker Tuj1, was similar in both genotypes (Figure R-12b). However, in the transgenic embryos the thickness of the CP, which is the region immunolabeled with Tuj1, was decreased at E11.5 but it was normal at E14.5 (Figure R-12c). These results indicate that DYRK1A overexpression does not affect the pool of progenitors in the dorsal telencephalon but it delays the radial expansion of the CP.

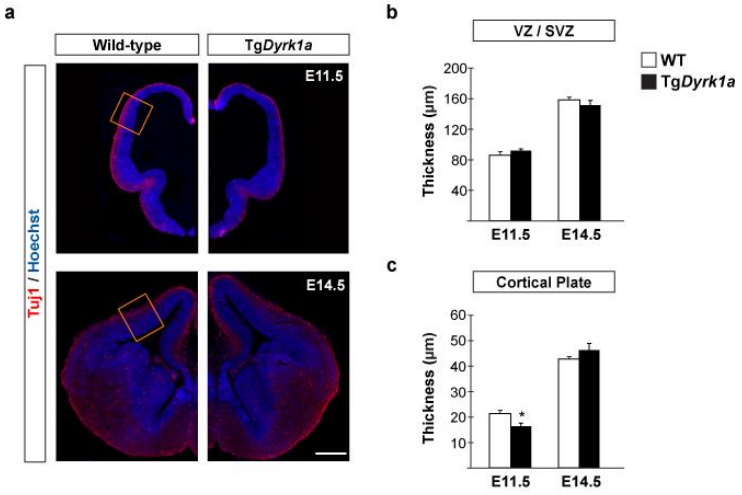

Figure R-12: mBACTg*Dyrk1a* embryos have thinner cortical plates during early neurogenesis. **(a)** Pictures of E11.5 (upper) and E14.5 (lower) wild-type (WT) and mBACTg*Dyrk1a* (Tg*Dyrk1a*) coronal brain sections of embryos immunostained for the neuronal marker Tuj1 and the nuclei labelled with Hoechst. Rectangles indicate the regions where measurements were done. **(b, c)** Histograms showing the thickness of the germinal ventricular and subventricular zones (VZ/SVZ) **(b)** and the cortical plate **(c)** of WT and Tg*Dyrk1a* embryos at the indicated developmental stages. Note that differences between genotypes were significant only in the cortical plate of E11.5 embryos. Histograms values are the mean ± S.E.M. *$P<0.05$, ($n \geq 4$). Scale bar: 500 µm.

4.1 Early neurogenesis

During neurogenesis RG progenitors divide asymmetrically in the VZ producing another RG cell and either one neuron or one IP (Noctor et al., 2004; Attardo et al., 2008; see Chapter 1.2.2 in the Introduction section). We first confirmed that, as expected from the normal thickness of the VZ (Figure R-12a, b), the number of RG progenitors ($Pax6^+$ cells) was not altered in mBACTg*Dyrk1a* embryos at E11.5 (Figure R-13a). Since the main alteration observed in mutant embryos was a thinner CP at the beginning of corticogenesis (Figure R-12a, c), we wonder whether one extra copy of *Dyrk1a* could affect the neurogenic potential of RG progenitors. To assess this, we counted the number of cells expressing the neuronal marker Tbr1 in brain sections of E11.5 wild-type and mBACTg*Dyrk1a* embryos. The number of $Tbr1^+$ neurons was significantly reduced in *Dyrk1a* transgenic embryos (Figure R-13b). This reduction in the number of neurons could be due to increased cell death or to decreased neuronal production. We explored the first possibility by performing an immunostaining for Tuj1 and active caspase-3, which labels apoptotic cells. Since in both genotypes the number of apoptotic cells in the VZ and the CP was similar (Figure R-13c) we excluded a possible implication of cell death in the observed neuronal phenotype. Thus, the deficit of CP differentiating neurons in the transgenic embryos (Figure R-13b) should result from an impaired neuronal production. To confirm this, we injected the S phase marker BrdU into E11.5 pregnant females and 24 hours later we estimated the number of newborn neurons by counting $BrdU^+$ cells and double BrdU and Tbr1 immunopositive cells. The results of these quantifications showed a reduction of around 40% in the

production of RG-derived neurons in mBACTg*Dyrk1a* embryos (Figure R13d).

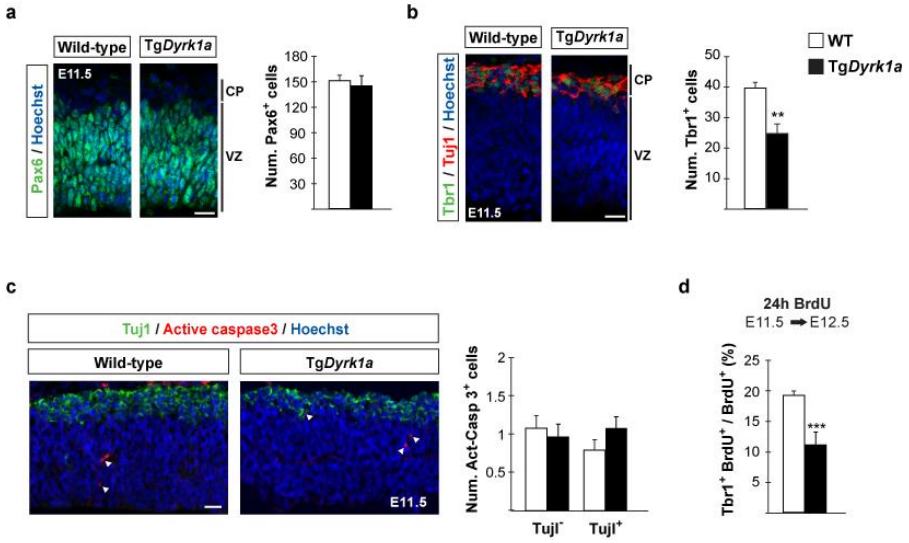

Figure R-13: Impaired early neurogenesis in the dorsal telencephalon of mBACTg*Dyrk1a* embryos. (a, b) Representative confocal images of the dorsal telencephalon of E11.5 wild-type (WT) and mBACTg*Dyrk1a* (Tg*Dyrk1a*) embryos showing Pax6 expression **(a)** or Tbr1 and Tuj1 expression **(b)**, and the total numbers of $Pax6^+$ radial glial progenitors **(a)** or $Tbr1^+$ neurons **(b)**. **(c)** Representative confocal images from coronal brain sections of E11.5 embryos of the indicated genotype showing active caspase-3 and Tuj1 expression and the number of apoptotic progenitors (active $caspase3^+Tuj1^-$ cells) and newborn neurons (active $caspase3^+Tuj1^+$ cells). Arrowheads indicate apoptotic cells. **(d)** Histogram showing neuronal production in the dorsal telencephalon of WT and TgDyrk1a embryos obtained from BrdU-injected females at E11.5 and harvested 24 hours later. Values are the percentage of $BrdU^+$ cells that express the neuronal marker Tbr1. Histogram values are the mean ± S.E.M. $^{**}P<0.01$, $^{***}P<0.001$ (n = 3 in **a, b;** n = 4 in **d**). Bars = 20 μm. VZ: ventricular zone; CP: cortical plate.

We then wondered if the production of cortical RG-derived IPs is altered in *Dyrk1a* transgenic embryos. The transition of a RG progenitor to an IP is associated with the downregulation of Pax6 and the upregulation of Tbr2 (Englund et al., 2005), which is a transcription factor required for IP specification and marks this

progenitor type (Sessa et al., 2008). The Pax6-Tbr2 switch also takes place in RG-derived neurons, but the expression of Tbr2 in these cells is shutdowned as they move from the VZ to the CP and start to express neuronal markers. However, at early development stages some neurons still have detectable levels of Tbr2 (Englund et al., 2005). Therefore, to estimate RG-derived IP production at E11.5, we quantified the number of $Tbr2^+$ cells that did not express the neuronal marker $Tuj1^-$ (arrows in Figure R-14a). As shown in Figure R14a, the number of $Tbr2^+/Tuj1^-$ cells was significantly increased in the dorsal telencephalon of mBACTg*Dyrk1a* embryos. This suggests that the deficit of early-born cortical neurons in the transgenic condition may result from an increased proportion of RG proliferative divisions at the expense of neurogenic divisions (Figure R-14b).

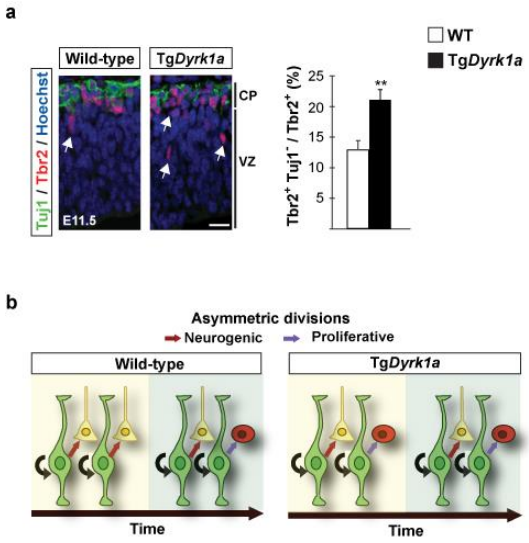

Figure R-14: Increased early production of intermediate progenitors in the dorsal telencephalon of mBACTg*Dyrk1a* embryos. (a) Representative confocal images of the dorsal telencephalon of E11.5 wild-type (WT) and mBACTg*Dyrk1a* (Tg*Dyrk1a*) embryos showing Tbr2 and Tuj1 expression. Histogram shows the percentage of $Tbr2^+$ intermediate progenitors ($Tbr2^+$ $Tuj1^-$ cells indicated

by arrows). Values are the mean ± S.E.M. **P<0.01 (n = 3). Bar = 20 μm. CP: cortical plate; VZ: ventricular zone. **(b)** Scheme summarizing the cell count results in **a** and **Figure R-12**. Radial glial progenitors ($Pax6^+$ cells in green) in the dorsal VZ of both WT and Tg*Dyrk1a* embryos divide asymmetrically producing another Pax6 progenitor (black arrows) and a neuron (yellow cell) or an intermediate progenitor (red cell). In Tg*Dyrk1a* embryos the number of divisions producing intermediate progenitors increases while the number of divisions producing neurons decreases.

Since neuronal densities were increased in adult *Dyrk1a*$^{+/-}$ mice (Figure R-7a), we hypothesized that cortical neurogenesis may also be affected in the *Dyrk1a* haploinsufficient model. To test this hypothesis we performed the same analysis in *Dyrk1a*$^{+/+}$ and *Dyrk1a*$^{+/-}$ embryos. As in the mBACTg*Dyrk1a* model, the number of RG progenitors ($Pax6^+$ cells) was similar in E11.5 *Dyrk1a*$^{+/-}$ and wild-types embryos (Figure R-15a). However, the mutant embryos showed more Tbr1 expressing neurons than the wild-types (Figure R-15b). Two days latter (at E13.5) the germinal SVZ is well formed in both genotypes but the number of IPs ($Tbr2^+$ cells) was reduced in the VZ of *Dyrk1a*$^{+/-}$ embryos (Figure R-15c), indicating that mutant RG progenitors produce fewer IPs than the controls Accordingly, the number of IPs in the SVZ was also decreased in *Dyrk1a*$^{+/-}$ mutants (Figure R-15c). These results suggest that, contrary to what happens in the mBACTg*Dyrk1a* model, RG neurogenic divisions are increased in *Dyrk1a* haploinsufficient embryos (Figure R-15d).

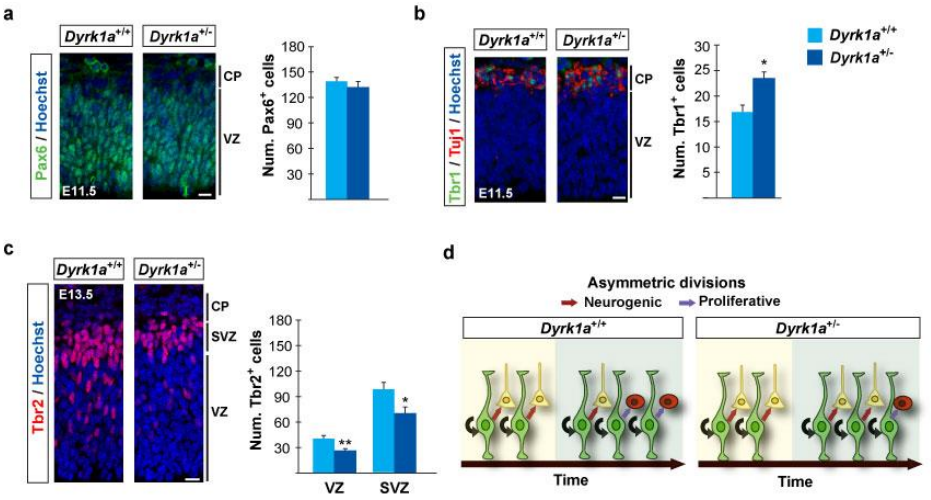

Figure R-15: Increased early neurogenesis and decreased production of intermediate progenitors in the dorsal telencephalon of *Dyrk1a*$^{+/-}$ embryos. (a-c) Representative confocal images of the dorsal telencephalon of E11.5 **(a, b)** and E13.5 **(c)** *Dyrk1a*$^{+/+}$ and *Dyrk1a*$^{+/-}$ embryos showing Pax6 expression **(a)**, Tbr1 and Tuj1 expression **(b)** and Tbr2 expression **(c)**, and the numbers of Pax6^{+} radial glial progenitors in the ventricular zone (VZ) **(a)**, of Tbr1^{+} neurons in the cortical plate (CP) **(b)** and of Tbr2^{+} intermediate progenitors in the VZ and the subventricular zone (SVZ) **(c)** counted in 100 μm-wide fields. (**d**) Scheme summarizing cell count results in **a** to **c**. Radial glial progenitors (Pax6^{+} cells in green) in the VZ of both *Dyrk1a*$^{+/+}$ and *Dyrk1a*$^{+/-}$ embryos divide asymmetrically producing another Pax6 progenitor (black arrows) and a neuron (yellow cell) or an intermediate progenitor (red cell). In *Dyrk1a*$^{+/-}$ mutants the number of divisions producing neurons increases while the number of divisions producing progenitors decreases. Histogram values are the mean ± S.E.M. *P<0.05, **P<0.01 (n ≥ 3 in **a, b**; n = 4 in **c).** Bars = 20 μm.

In summary, our results suggest that a moderate variation in DYRK1A protein levels in RG progenitors biases their type of division, favouring asymmetric proliferative divisions when DYRK1A levels are increased and asymmetric neurogenic divisions when DYRK1A levels are reduced (Figures R-14b and R-15d).

4.2 Mid- and late-neurogenesis

The majority of neurons in the neocortex are generated by indirect neurogenesis from IPs of the SVZ (see Chapter 1.2.2 in the Introduction section and Figure R-16a). Therefore, a small variation in the number of these progenitors is expected to have a significant impact on neuronal cellularity. Since the production of IPs is augmented in E11.5 mBACTg*Dyrk1a* embryos (Figure R-14a), we quantified the number of IPs generated from RG progenitors ($Tbr2^+$ cells in the VZ) and the ones in the SVZ ($Tbr2^+$ cells in the SVZ) in wild-type and mBACTg*Dyrk1a* embryos at different developmental stages (Figure R-16b). During early neurogenesis (E12.5 to E14.5) the number of Tbr2 progenitors in the VZ and SVZ increases in both genotypes (Figure R-16b). However, mBACTg*Dyrk1a* embryos showed more Tbr2 progenitors in both germinal regions until E13.5 (Figure R-16b). In agreement, the number of basal mitosis ($pH3^+$ cells in SVZ) was increased in E13.5 *Dyrk1a* transgenic embryos (Figure R-16c). By contrast, the number of apical divisions ($pH3^+$ cells in VZ) was similar in both genotypes (Figure R-16c), indicating that the number of RG divisions was not altered in *Dyrk1a* transgenic embryos. Accordingly, the numbers of RG progenitors in these embryos were normal (Figure R-16e).

To evaluate how this increased number of IPs affect neuron production in mBACTg*Dyrk1a* embryos, we counted the number of $Tbr1^+$ cells in the dorsal telencephalon of wild-type and mBACTg*Dyrk1a* at E13.5 (Figure R-16d).

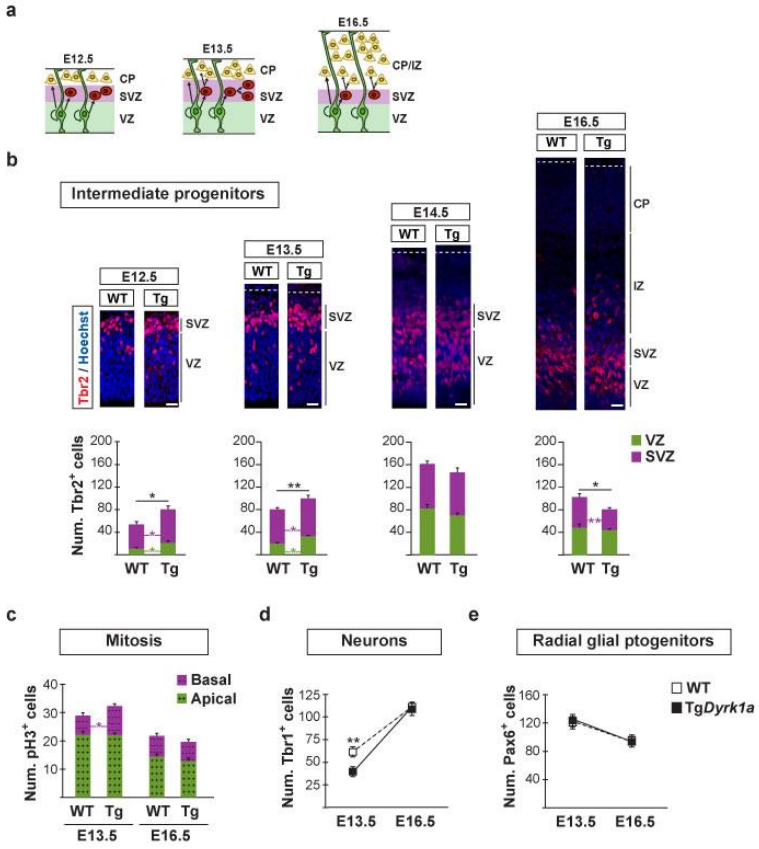

Figure R-16: mBACTg*Dyrk1a* embryos show altered numbers of neurons and intermediate progenitors along corticogenesis. **(a)** Scheme showing the cellularity of the ventricular (VZ) and subventricular (SVZ) germinal layers along the neurogenic phase of neocortical development and the division mode of the two main progenitor types in these layers; radial glial progenitors (in green) and intermediate progenitors (in red). Note that by E16.5, most of the neurons (in yellow) are produced by terminal divisions of intermediate progenitors. **(b)** Representative images of wild-type (WT) and mBACTg*Dyrk1a* (Tg) brain sections of embryos at different stages immunostained for Tbr2 and nuclei labelled with Hoechst, and histograms showing the numbers of $Tbr2^+$ progenitors (intermediate progenitors) in the VZ (green bars) and in the SVZ (purple bars). **(c)** Histogram showing the number of $pH3^+$ cells in the VZ (green bar; apical mitosis) and in the SVZ (purple bar; basal mitosis). **(d, e)** Graphs showing the numbers of $Tbr1^+$ neurons **(d)** and of $Pax6^+$ radial glial progenitors **(e)**. Histogram values are the mean ± S.E.M. *$P<0.05$, **$P<0.01$ ($n \geq 3$). Bars = 20 μm. CP: cortical plate; IZ: intermediate zone.

The number of Tbr1$^+$ neurons in the transgenic embryos was still lower at this developmental stage, but the reduction (15%) was less severe than in E11.5 (40%). This suggests that indirect neurogenesis is higher in transgenic embryos than in the wild-types, partially compensating for the deficit of RG-derived neurons (Figure R-13b, c). To probe this, we labeled cells in S-phase with BrdU at E13.5 and estimated the proportion of these cells that exit the cell cycle 24 hours later by doing double immunostainings for BrdU and Ki67. As shown in Figure R-17a, cell cycle exit rates were similar in both genotypes, confirming that indirect neurogenesis at this stage is compensating for the deficit of RG-derived neurons in the dorsal telencephalon of mBACTg*Dyrk1a* embryos. This result agrees with the fact that the thickness of the CP in E14.5 transgenic embryos is similar than in the wild-types (Figure R-12c). Given that the time of birth determines the fate of neocortical neurons (Figure I-5), we asked whether the advanced production of IPs in mBACTg*Dyrk1a* embryos alters the fate of the neurons that they are producing. To answer this, we performed a birthdate experiment injecting BrdU into pregnant females at E13.5 and analyzed the fate of newborn neurons at postnatal stages by double immunostaining for BrdU and specific layer markers. At E13.5 the production of Ctip2 expressing layer V callosal projection neuron peaks (Molyneaux et al., 2007), accordingly in wild-type embryos almost 50% of the BrdU$^+$ cells expressed high levels of Ctip2 while only 12% of the BrdU$^+$ cells expressed the upper layer marker, Cux1 (Molyneaux et al., 2007) (Figure R-17b). However, mBACTg*Dyrk1a* embryos showed a 5% decrease in the proportion of Ctip2$^+$ neurons and a parallel increase in Cux1$^+$ neurons (Figure R-17b). This result shows that the differentiating

program in the dorsal telencephalon of mBACTg*Dyrk1a* embryos is slightly advanced paralleling the advanced production of IPs.

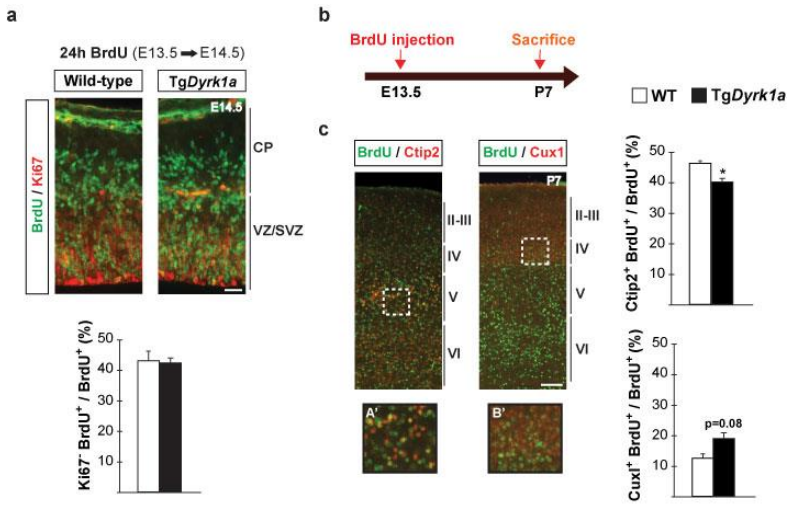

Figure R-17: Telencephalic neurons in mBACTg*Dyrk1a* embryos are produced at normal rates during mid-neurogenesis but they acquire a more advanced fate. (a) Wild-type (WT) and mBACTg*Dyrk1a* (Tg*Dyrk1a*) coronal telencephalic sections immunolabelled for BrdU and Ki67 of embryos obtained from E13.5 BrdU-injected females and harvested 24 hours later. The histogram shows the percentage of $BrdU^+$ cells that do not express the proliferation marker Ki67. **(b)** Schedule of the cell fate experiment in **c**. **(c)** Representative images of the dorsal cortex of P7 WT and Tg*Dyrk1a* coronal sections immunolabelled for BrdU and Ctip2 or for BrdU and Cux1. A' and B' are magnifications of the regions limited by white boxes. Histograms show the proportion of $BrdU^+$ cells that express the layer V marker Ctip2 and the proportion of $BrdU^+$ cells that express the layers II-IV marker Cux1. Values are the mean ± S.E.M. *$P<0.05$ (n = 3). Bars = 20 μm. CP: cortical plate; SVZ: subventricular zone; VZ: ventricular zone.

During the late phase of cortical neurogenesis, by E16.5, the production of IPs from RG progenitors ($Tbr2^+$ cells in the VZ) decreases and IPs terminal divisions in the SVZ increases in wild-type embryos (Kriegstein and and Alvarez-Buylla, 2009) (see Fig-R16a, b). The production of IPs in mBACTg*Dyrk1a* and

wild-type embryos was similar at E14.5 and E16.5 (Figure R16-b). The number of IPs in the SVZ was also normal in mBACTg*Dyrk1a* embryos at E14.5 but decreased at E16.5 (Figure R-16b). This reduction is not due to an increased cell death, since the number of apoptotic cells immunolabeled for active caspase-3 was similar in both genotypes (wild-type: 7.9 ± 1.26 cells; mBACTg*Dyrk1a*: 9.5 ± 1.50 cells). Since the number of mitoses in the SVZ was normal in mBACTg*Dyrk1a* embryos (Figure R-16c), the decreased number of IPs in this layer suggests that terminal divisions are increased in the transgenic embryos, thus producing an advanced exhaustion of the IP pool and a transitory increased in neuronal production. Consequently, at E16.5 the deficit of CP $Tbr1^+$ neurons in the dorsal telencephalon of transgenic embryos was no longer observed (Figure R16-d).

In summary, our results showed that a 1.5-fold increase in DYRK1A protein levels disturbs the number of neocortical neurons that are generated through development by direct and indirect neurogenesis.

4.3 Cellularity of the neocortex at postnatal stages

In order to asses the impact of the observed neurogenic defects in the cellularity of the neocortex, we counted the number of neurons expressing layer-specific markers in wild-type and mBACTg*Dyrk1a* mice at P7, when tangential migration has ended and projection neurons are in their final layer position (Miller et al., 1988). First, we counted the number of neurons in layer VI, which are the first generated neurons and they still

express Tbr1 (Bulfone et al., 1995). According to the neuron deficit observed in mBACTg*Dyrk1a* embryos at E11.5 (Figure R-13b, d), transgenic postnatal animals showed fewer layer VI $Tbr1^+$ neurons than the wild-types (Figure R18-a). Then we counted the number of neurons in layer V, which are generated at mid-corticogenesis, around E13.5 (Molyneaux et al., 2007), and express high levels of Ctip2 (Arlotta et al., 2005). Both genotypes show similar numbers of $Ctip2^+$ neurons (Figure R-18b). This data, together with the decreased production of Ctip2 neurons observed in mBACTg*Dyrk1a* embryos at E13.5 (Figure R-17b), suggest that Ctip2 transgenic neurons are generated earlier in development (Figure R-17d), probably as a result of the advanced production of IPs in mBACTg*Dyrk1a* embryos (Figure R-14a). Finally, we quantified the number of superficial cortical neurons, which are mostly produced by terminal divisions of IPs and express the transcription factor Cux1 (Nieto et al., 2004). The number of $Cux1^+$ neurons in layers II to IV of postnatal mBACTg*Dyrk1a* mice was significantly lower than in wild-types mice (Figure R-18c). This decrease correlated with the earlier exhaustion of IPs observed in the transgenic embryos at E16.5 (Figure R-16b). Nonetheless, $Tbr1^+$, $Ctip2^+$ and $Cux1^+$ neurons in mBACTg*Dyrk1a* postnatal animals have a normal layer distribution (Figure R-18a-c), indicating that overexpression of DYRK1A does not affect radial migration of cortical differentiating neurons. The results presented so far show that a 1.5-fold increase in DYRK1A protein levels diminishes neuron production at the beginning (by E11.5) and at the end (by E16.5) of dorsal cortical neurogenesis. The deficits in early-born neurons and late-born neurons in the mBACTg*Dyrk1a* mouse can be explained, respectively, by the impaired production of RG-derived

neurons and the early exhaustion of the IP pool (see scheme in Figure R-18d).

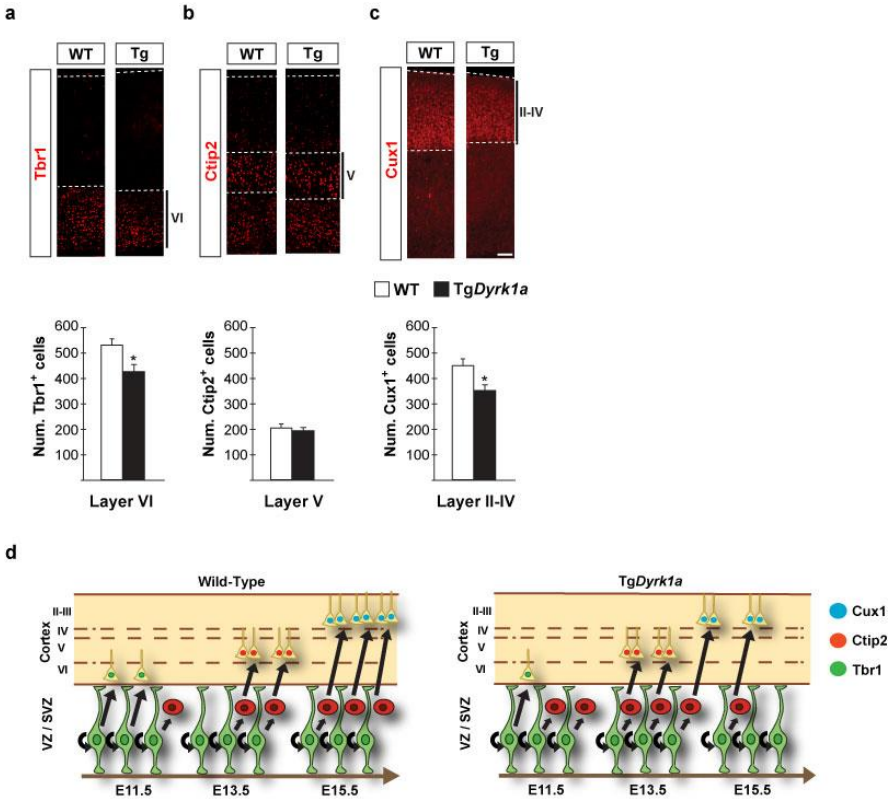

Figure R-18: mBACTg*Dyrk1a* postnatal mice show decreased neuronal cellularity in specific cortical layers. (a-c) Representative coronal sections from P7 wild-type (WT) and mBACTg*Dyrk1a* (Tg) brains immunostained for Tbr1 **(a)**, Ctip2 **(b)** or Cux1 **(c)**, and histograms showing the number of layer VI Tbr1$^+$ neurons **(a)**, layer V Ctip2$^+$ neurons **(b)** and layers II to IV Cux1$^+$ neurons **(c)** counted in 350 μm wide fields. Values are the mean ± S.E.M. *P<0.05 (n = 3). Bars = 20 μm. **(d)** Schemes showing the birth time of Tbr1 neurons, Ctip2 neurons and Cux1 neurons in the dorsal telencephalon of a WT and a Tg embryo and the progenitor type (radial glial (green) or intermediate (red) progenitor) that produces these neurons. The deficits of early-born (Tbr1$^+$) neurons and late born (Cux1$^+$) neurons in transgenic animals result, respectively, from the decreased neuronal production during early neurogenesis and from the premature exhaustion of the intermediate progenitor pool during late neurogenesis.

4.4 Pathogenic molecular mechanisms

Different studies have shown that abnormal overexpression of DYRK1A in cortical progenitors alters neural production. However, the phenotypes observed in these studies and the proposed pathogenic mechanisms are different (see Chapter 3.5 in the Introduction section). In order to identify the molecular mechanism underlying the neuronal deficit observed in mBACTg*Dyrk1a* postnatal mice, we started by evaluating the neurogenic signaling pathways and processes that have been previously shown to be regulated by DYRK1A.

One of these pathways is the NOTCH signaling (Fernandez-Martinez et al., 2009; Hammerle et al., 2011). NOTCH signaling plays a crucial role in CNS development regulating neuronal differentiation (see Chapter in the Introduction section 1.2.2). Forced overexpression of DYRK1A in neuronal cells in culture, in the chick spinal cord and in the mouse dorsal telencephalon attenuates NOTCH signaling promoting neuronal differentiation (Hammerle et al., 2011; Fernandez-Martinez et al., 2009). In contrast we showed here that neurogenesis in the VZ of mBACTg*Dyrk1a* embryos is decreased (Figure R-13b, d), suggesting that a 1.5 fold increase in DYRK1A protein levels is not sufficient to alter NOTCH signaling in RG progenitors. To assess this, we quantified the mRNA levels of NOTCH signaling components in the dorsal telencephalon of wild-type and mBACTg*Dyrk1a* embryos at the onset of neurogenesis. As expected, *Dyrk1a* mRNA levels were 1.5 fold higher in E11.5 transgenic embryos compared to wild-types (Figure R-19). However, the levels of *Notch1*, *Hes1*, *Hes5* and *Delta1* transcripts were similar in both genotypes (Figure R-19),

indicating that NOTCH signaling is not attenuated in *Dyrk1a* transgenic embryos.

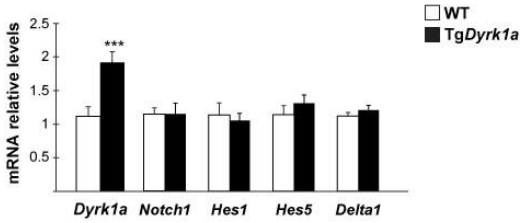

Figure R-19: Notch signalling is not altered in the dorsal telencephalon of mBACTg*Dyrk1a* embryos. Relative expression of *Dyrk1a*, *Notch1*, *Hes1, Hes5* and *Delta1* transcripts determined by RT-qPCR on mRNA obtained from the dorsal telencephalon of E11.5 wild-type (WT) and mBACTg*Dyrk1a* (Tg*Dyrk1a*) embryos. Note that the only statistically significant difference between genotypes was *Dyrk1a* expression. Histogram values are the mean ± S.E.M. ($n \geq 3$). ***$P<0.001$

Another signaling pathway that is regulated by DYRK1A in the developing cerebral cortex is the calcineurin-NFATc signaling pathway. The coelectroporation of DYRK1A and RCAN1 in cortical progenitors at the onset of neurogenesis attenuates NFATc signalling, which leads to decreased neurogenesis and increased progenitor cell cycle re-entry (Kurabayashi and Sanada 2013). As a result, the number of $Tbr1^+$ neurons in the cortical internal layers was decreased and the number of $Cux1^+$ neurons in the external layers was increased in the electroporated embryos (Kurabayashi and Sanada, 2013). However, the electroporation of the same concentration of the DYRK1A-expression plasmid alone did not disturb cortical neurogenesis (Kurabayashi and Sanada, 2013). These results prompted us to measure the relative levels of Rcan1 transcripts and protein isoforms in the dorsal telencephalon of E11.5 wild-type and mBACTg*Dyrk1a* embryos. As shown in Figure R-20,

both wild-type and transgenic embryos showed similar levels of the two main *Rcan1* transcripts, *Rcan1-1* and *Rcan1-4,* and Rcan1 protein isoforms (Davies et al., 2007). The proximal promoter of *Rcan1-4* has several NFATc binding sites and activation of NFATc transcription induces *Rcan1-4* expression in different cell types (Yang et al., 2000). Thus, the fact that *Rcan1-4* transcripts are at normal levels in the transgenic tissue suggests that deregulation of NFATc activity is not what is causing the early delay in cortical neurogenesis in mBACTg*Dyrk1a* embryos.

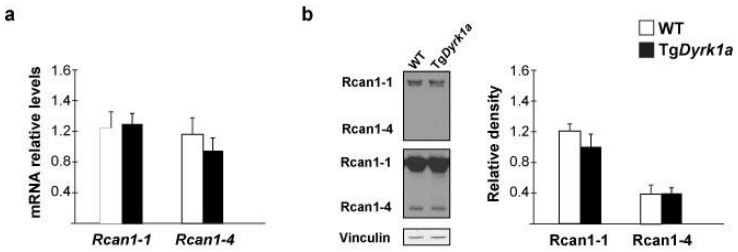

Figure R-20: The mRNA and protein levels of Rcan1 isoforms are not altered in the dorsal telencephalon of mBACTg*Dyrk1a* embryos. (a) Relative expression of *Rcan1-1* and *Rcan1-4* transcripts determined by RT-qPCR on mRNA obtained from the dorsal telencephalon of E11.5 wild-type (WT) and mBACTg*Dyrk1a* (Tg*Dyrk1a*) embryos. **(b)** Representative western blot at two different exposure times of extracts prepared from the dorsal telencephalon of E11.5 embryos and probed with an antibody against Rcan1 that hybridizes with Rcan1-1 and Rcan1-4 isoforms. Histograms show the protein levels in Tg*Dyrk1a* embryos normalized to vinculin levels and expressed relative to the WTs. Histogram values are the mean ± S.E.M. ($n \geq 3$). Differences between genotypes were not statistically significant.

Control of cell cycle progression in cortical progenitors is crucial for the generation of normal numbers of neurons (Dehay and Kennedy, 2007; see Chapter 1.2.2 in the Introduction section). Forced expression of DYRK1A in neural progenitors induces cell

cycle exit by different means: promoting the degradation of the cell cycle activator Cyclin D1 (Yabut et al., 2010) or inducing the expression of the CDK inhibitors *p27*^{KIP1} (Hammerle et al., 2011) and *p21*^{CIP1} (Park et al., 2010). To have evidence about a possible cell cycle alteration in cortical RG mBACTg*Dyrk1a* progenitors, we compared the mRNA and protein levels of these cell cycle regulators in the telencephalon of E11.5 wild-type and mBACTg*Dyrk1a* embryos. As expected, Dyrk1a mRNA and protein levels were increased (1.5-1.7 folds) in the transgenic tissue (Figure R-21). However, mRNA and protein levels of the cell cycle regulators examined were similar in both genotypes with the exception of Cyclin D1 protein levels that were decreased in mBACTg*Dyrk1a* embryos (Figure R-21b).

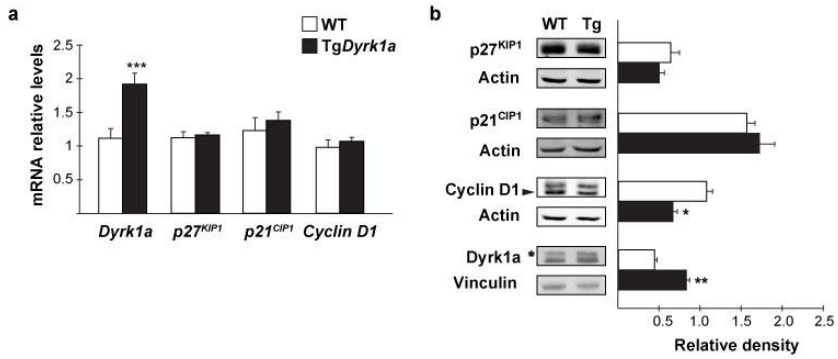

Figure R-21: Cyclin D1 protein levels are decreased in the dorsal telencephalon of mBACTg*Dyrk1a* embryos. **(a)** Relative mRNA expression of *Dyrk1a*, *p27*^{KIP1}, *p21*^{CIP1} and *Cyclin D1* in the dorsal telencephalon of E11.5 wild-type (WT) and mBACTg*Dyrk1a* (Tg*Dyrk1a*) embryos. **(b)** Representative western blots of extracts prepared from the dorsal telencephalon of E11.5 embryos and probed with the indicated antibodies. Histograms show the protein levels in Tg*Dyrk1a* embryos normalized to actin or vinculin levels and expressed relative to the WTs. Arrowhead indicates the band corresponding to the Cyclin D1 isoform that contains Thr286 and asterisk the band corresponding to Dyrk1a. Histogram values are the mean ± S.E.M. *P<0.05, **P<0.01, ***P<0.001 ($n \geq 3$).

We next performed the same analysis in E10.5 whole embryos and observed the same results, normal amounts of *CyclinD1*, *p27*^{KIP1}and *p21*^{CIP1} transcripts but less Cyclin D1 protein levels in transgenic embryos compared to wild-types (Figure R-22a, b). Conversely, E10.5 whole *Dyrk1a*$^{+/-}$ embryos exhibited a 50% reduction of Dyrk1a levels accompanied by an increase in the amount of Cyclin D1 protein (Figure R-22c, d). These results show that the levels of DYRK1A inversely correlate with Cyclin D1 protein levels and suggest that this effect of DYRK1A is not restricted to dorsal brain neural progenitors. The fact that *Cyclin D1* mRNA levels were normal in both *Dyrk1a* mutant mice (Figure R-22a, c) suggests that DYRK1A may regulate Cyclin D1 degradation in neural progenitors *in vivo* as has been shown before in cultured cells by Yabut et al (Yabut et al., 2010).

Phosphorylation on Thr286 in Cyclin D1 promotes Cyclin D1 nuclear export and degradation *via* the ubiquitin-proteosome pathway (Diehl et al., 1997; 1998). Taking into account our previous results and the fact that DYRK1B, which is the closest member of DYRK1A in the DYRK family of proteins (Aranda et al., 2011), phosphorylates Cyclin D1 on Thr286 (Ashford et al., 2014), we hypothesized that DYRK1A phosphorylates Cyclin D1 in RG progenitors thereby regulating its degradation. Indeed, a recent study has demonstrated that this is the case at least in fibroblast skin cells (Chen et al., 2013).

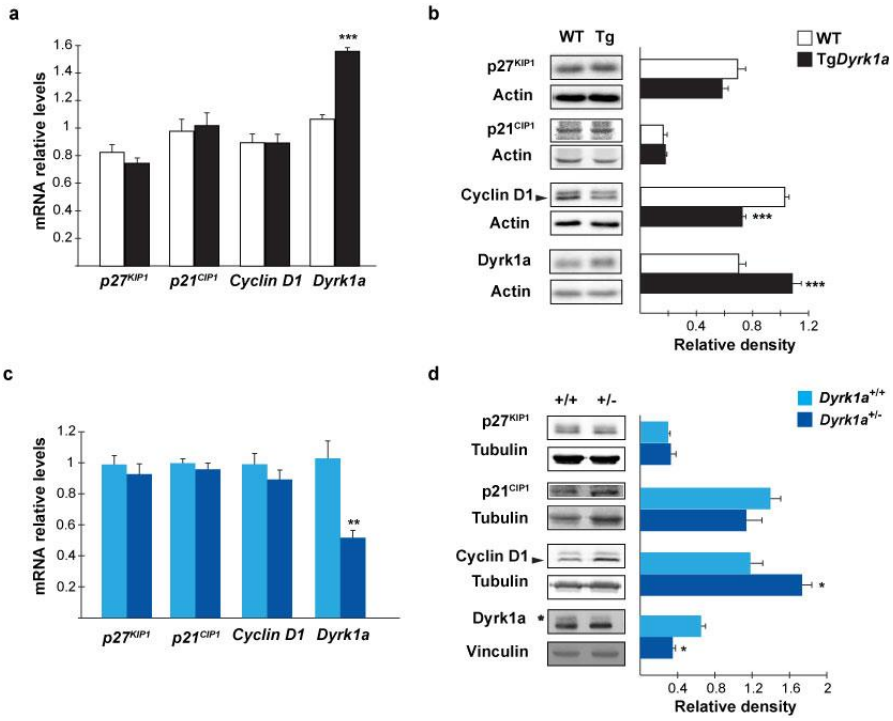

Figure R-22: Cyclin D1 protein levels inversely correlate with *Dyrk1a* gene dosage in whole E10.5 embryos. (a, c) Relative mRNA expression of *p27*^{KIP1}, *p21*^{CIP1}, *Cyclin D1* and *Dyrk1a*, in whole E10.5 wild-type (WT) and mBACTg*Dyrk1a* (Tg*Dyrk1a*) embryos (**a**) or *Dyrk1a*$^{+/+}$ and *Dyrk1a*$^{+/-}$ embryos **(c)**. **(b, d)** Representative western blots of extracts prepared from whole E10.5 embryos and probed with the indicated antibodies. Histograms show the protein levels normalized to actin, tubulin or vinculin levels of WT and Tg*Dyrk1a* embryos (**b**) or *Dyrk1a*$^{+/+}$ and *Dyrk1a*$^{+/-}$ embryos (**d**). Arrowheads in **b** and **d** indicate the band corresponding to the Cyclin D1 isoform that contains Thr286 and asterisk in **d** the band corresponding to Dyrk1a. Histogram values are the mean ± S.E.M. *P<0.05, **P<0.01, ***P<0.001 (n ≥ 3).

Mouse *Cyclin D1* gene, like its human counterpart, expresses two spliced mRNA variants. These two variants encode the canonical Cyclin D1 isoform that contains Thr286 in its carboxy-terminus (Cyclin D1a), and a longer protein isoform with a distinct carboxy-terminus domain that lacks the sequence surrounding Thr286 (Cyclin D1b) (Wu et al., 2009). Despite we were not able to check the phosphorylation state of Cyclin D1 in telencephalic

extracts of *Dyrk1a* mutant embryos due to the inexistence of a phospho-CyclinD1 antibody with mouse specificity, the observation that the Cyclin D1 isoform that was significantly decreased in *Dyrk1a* transgenic embryos (arrowhead in Figure R-21b) corresponds to Cyclin D1a supports the hypothesis that DYRK1A regulates Cyclin D1 protein levels through its phosphorylation in RG progenitors *in vivo*. To provide more evidences on that we performed an immunostaining for Cyclin D1 in coronal sections of E11.5 mBACTg*Dyrk1a* and wild-type embryos (Figure R-23a) and quantified the proportion of nuclear and cytoplasmatic Cyclin D1 in RG progenitors (see Figure M-1 in Materials and methods section). If DYRK1A controls degradation of Cyclin D1 in these progenitors, mBACTg*Dyrk1a* RG progenitors should have decreased levels of nuclear Cyclin D1, which is what we observed in brain sections of mBACTg*Dyrk1a* embryos (Figure R-23a).

One of the main nuclear functions of Cyclin D1 is to promote G1 to S phase transition through association with its partner CDK4/6. This leads to the phosphorylation of the retinoblastoma protein (Rb), which promotes the release of E2F transcription factor from the pRb/E2F complex and the expression of genes necessary for cell cycle progression (Cunningham and Roussel, 2001; Malumbres and Barbacid, 2005). Consistent with the decreased levels of nuclear Cyclin D1 (Figure R-21b), the relative amount of hyperphosphorylated Rb in the telencephalon of E11.5 transgenic embryos was lower than in the wild-types (Figure R-23b), indicating that 1.5 fold increase in DYRK1A protein levels is sufficient to reduce Cyclin D1/CDK activity in telencephalic RG progenitors *in vivo*.

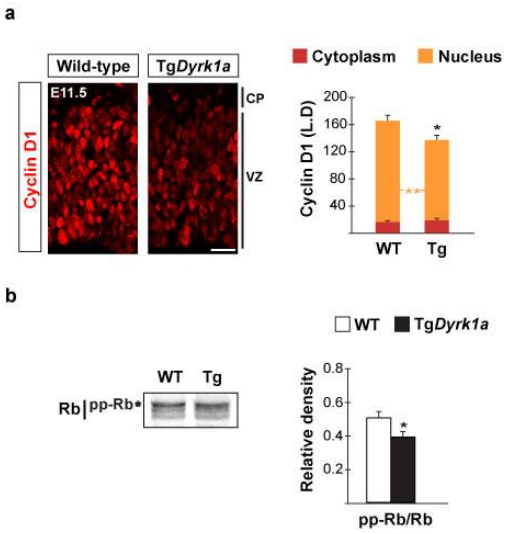

Figure R-23: mBACTg*Dyrk1a* dorsal radial glial progenitors show decreased levels of nuclear Cyclin D1 and hyperphosphorylated Retinoblastoma. **(a)** Representative coronal sections of E11.5 wild-type (WT) and mBACTg*Dyrk1a* (Tg*Dyrk1a*) sections immunostained for Cyclin D1. The histogram shows the calculated labelling densities (L.D) of Cyclin D1 fluorescence signals in the nucleus and cytoplasm of ventricular zone (VZ) radial glial dorsal progenitors. CP: cortical plate. **(b)** Representative western blot and its quantification showing the levels of retinoblastoma (Rb) that is hyperphsophorylated (pp-Rb) in E11.5 WT and mBACTg*Dyrk1a* (Tg) dorsal telencephalic extracts. Histogram values are the mean ± S.E.M. *P<0.05, **P<0.001 ($n \geq 4$). Bars = 20 μm.

Given the importance of Cyclin D1/CDK activity in cell cycle progression, we wonder whether the deficit in Cyclin D1 observed in E11.5 mBACTg*Dyrk1a* RG progenitors affects G1 phase duration. To test this, we first performed flow cytometry cell cycle profiles of progenitors isolated from the telencephalon of wild-type and mBACTg*Dyrk1a* embryos at E10.5 and E11.5 (Figure R-24a). This experiment revealed a moderate increase (4-5%) in the proportion of progenitors in G0/G1 phases in

mBACTg*Dyrk1a* samples (Figure R-24b), which indicated that G1 phase duration could be increased in transgenic progenitors.

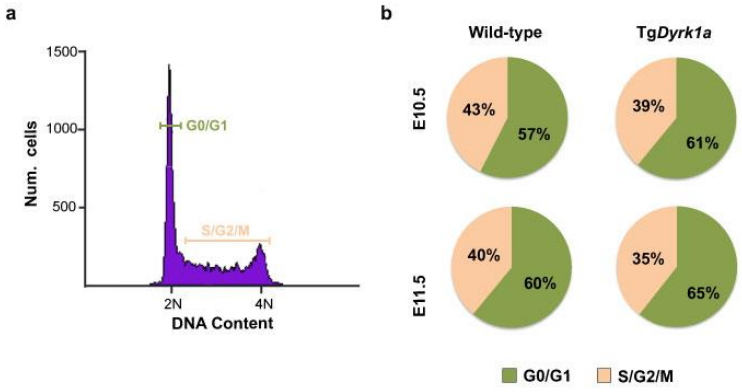

Figure R-24: mBACTg*Dyrk1a* embryos show increased proportion of dorsal telencephalic progenitors in G0/G1 phases. (a) Representative cell cycle profile of propidium iodide stained progenitors obtained from the dorsal telencephalon of wild-type (WT) and mBACTg*Dyrk1a* (Tg*Dyrk1a)* embryos at the onset of cortical neurogenesis (E10.5 – E11.5), and **(b)** the proportion of E10.5 and E11.5 progenitors in G0/G1 (green) and in S/M/G2 (yellow). Percentages are mean values of three independent experiments.

To directly prove this possibility, we estimated the duration of the total cell cycle and the length of the different cell cycle phases in telencephalic RG progenitors of E11.5 wild-type and mBACTg*Dyrk1a* embryos *in vivo*. To do this we used a previous described protocol based on repetitive injections of the S phase marker EdU into pregnant females and subsequently assessment of EdU accumulation in RG progenitors (Takahashi et al., 1993; Arai et al., 2011; see schedule in Figure R-25a). The proportion of RG progenitors (nuclei in the VZ that do not express Tbr2 or Tuj1 (Figure R-25b)) labeled with EdU were counted at the different time points indicated in Figure R-25a and were plotted in

a graph for each genotype (Figure R25-c). As shown in Figure R-25c, the growth fraction (GF) reached the maximum value in both genotypes, which indicates that all progenitors were cycling. However, total cell cycle duration (Tc) and S phase duration (Ts) were increased by 4.8 hours and by 2.8 hours, respectively in transgenic progenitors overexpressing DYRK1A (Figure R-25c, e). Duration of G2 and M phases, which were measured by combining EdU labeling with a staining for the mitotic marker pH3 (Figure R-25d), were similar in both genotypes. (Figure R-25e). Consistent with the flow cytometry results (Figure R-24) the duration of the G1 phase, calculated by subtracting S/G2/M phase durations from the Tc value, was around 2 hours longer in transgenic progenitors than in the wild-types (Figure R-25e). These results showed that mBACTg*Dyrk1a* RG progenitors have longer cell cycles due to an increased duration of the G1 and the S phase.

The results obtained so far show that 1.5 fold increase in DYRK1A protein is sufficient to alter cell cycle parameters of RG progenitors through a mechanisms that involves increased degradation of Cyclin D1 protein. The cell cycle alterations in mBACTg*Dyrk1a* RG progenitors are concomitant with an increased proportion of asymmetric proliferative divisions at the expense of neurogenic divisions. Based on this and on previous studies showing a direct link between G1 phase duration and neuron production (Lange et al., 2009; Pilaz et al., 2009), we proposed that the bias we have observed on the division mode of mBACTg*Dyrk1a* RG progenitors is caused by the enlargement of the cell cycle G1 phase.

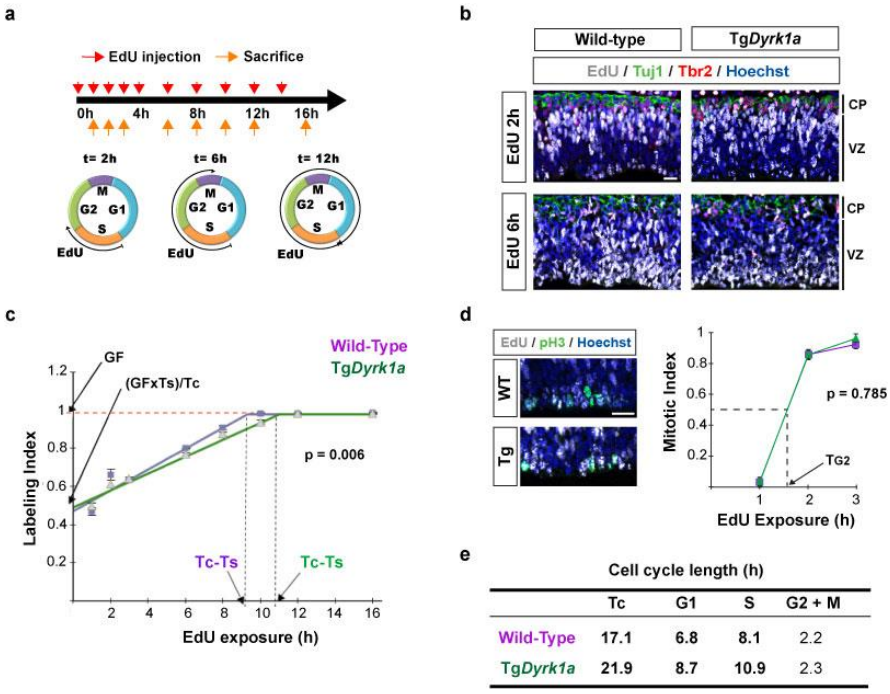

	Tc	G1	S	G2 + M
Wild-Type	17.1	6.8	8.1	2.2
Tg*Dyrk1a*	21.9	8.7	10.9	2.3

Figure R-25: mBACTg*Dyrk1a* dorsal radial glial progenitors have longer cell cycles due to an enlargement of the G1 and S phases. **(a)** Schedule of the cumulative EdU-labelling protocol employed to calculate the cell cycle parameters in E11.5 radial glial progenitors of the dorsal telencephalon. Red and orange arrows indicate the time points at which EdU was injected and the time points at which embryos were harvested, respectively. **(b)** Representative confocal images of brain sections from wild-type (WT) and mBACTg*Dyrk1a* (Tg*Dyrk1a*) embryos exposed to EdU for the indicated time, and stained for EdU, Tuj1 and Tbr2 and the nuclei visualized with Hoechst. CP: cortical plate; VZ: ventricular zone. **(c)** Values are the labelling indexes (proportion of EdU-labelled nuclei) of radial glial progenitors ($Tbr2^-Tuj1^-$ cells in the VZ) in WT and Tg*Dyrk1a* embryos at the indicated time of EdU exposure. GF: growth fraction (dashed orange line); Tc: cell cycle duration; Ts: S-phase duration; Tc-Ts: time at which the labelling index reaches a plateau (dashed black lines). **(d)** Representative images of sections from WT and Tg*Dyrk1a* embryos (2 hours EdU exposure) stained for EdU and pH3 and nuclei visualized with Hoechst, and plot showing the mitotic index (proportion of EdU-labelled cells in mitosis ($pH3^+$) at the indicated times of EdU exposure. T_{G2}: G2-phase duration. **(e)** Table summarizing the cell cycle parameters of WT and Tg*Dyrk1a* radial glial progenitors. p values in the two-way ANOVA test are indicated in **c** and **d**. The slopes of the regression lines in **c** are statistically different (p=0.001). n ≥ 3. Bars = 20 µm.

5. Contribution of *Dyrk1a* trisomy to the cortical defects in the Ts65Dn mouse model

Postmortem studies in DS brains indicates that cortical neurogenesis is altered in this condition (see Chapter 2.5 in the Introduction section). The DS Ts65Dn model shows impaired cortical neurogenesis that results in a long-lasting deficit of projection neurons at postnatal stages (Chakrabarti et al., 2007; 2010; 2010), and a specific lengthening of the cell cycle G1 and S phases in dorsal telencephalic RG progenitors (Chakrabarti et al., 2007). The similarities between this phenotype and the one shown here in mBACTg*Dyrk1a* embryos suggest that the overexpression of Dyrk1a due to triplication of the causes the cell cycle alterations and impaired neurogenesis in the Ts65Dn mouse. To provide evidence on this, we first checked the levels of Cyclin D1 in total telencephalic extracts of E11.5 Ts65Dn embryos, which have 50% more Dyrk1a protein than control euploid extracts (Figure R-26a). The levels of Cyclin D1 in the trisomic samples were significantly lower than in the controls (Figure R-26b). As in the two *Dyrk1a* mutants analyzed in this work, the Cyclin D1 protein isoform that was more affected is the canonical Cyclin D1a that contains the Thr286 (arrowhead in Figure R26-b). This result suggest that increased phosphorylation of this residue by DYRK1A could be the pathogenic mechanism that causes cell cycle defects in the Ts65Dn developing neocortex.

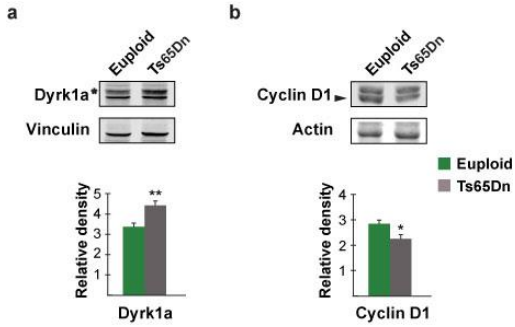

Figure R-26: Dyrk1a and Cyclin D1 protein levels are inversely correlated in Ts65Dn dorsal radial glial progenitors. Representative western blots of extracts prepared from the dorsal telencephalon of E11.5 euploid and trisomic Ts65Dn embryos probed with the indicated antibodies and histograms showing the protein levels of Dyrk1a **(a)** and Cyclin D1 **(b)** in Ts65Dn embryos normalized to vinculin or actin levels. Asterisk indicates the band corresponding to Dyrk1a and arrowhead the band corresponding to the Cyclin D1 isoform that contains Thr286. Histogram values are the mean ± S.E.M. *P<0.05, **P<0.01 (n ≥ 3).

To provide further evidences, we crossed Ts65Dn females with *Dyrk1a*$^{+/-}$ males and quantified the levels of nuclear and cytoplasmatic Cyclin D1 on brain sections obtained from E12.5 embryos of the four genotypes resulting from these crosses (Figure R-27 and R-28).

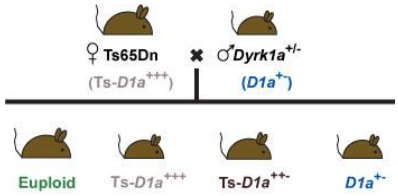

Figure R-27: Strategy to normalize *Dyrk1a* gene dosage in Ts65Dn mice. Scheme of the crosses to generate Ts65Dn mice (Ts-*D1a*$^{+++}$), Ts65Dn mice with 2 functional copies of *Dyrk1a* (Ts-*D1a*$^{++-}$), euploid mice monosomic for *Dyrk1a* (*Dyrk1a*$^{+/-}$) and control (euploid) mice.

Consistent with the western blot data (Figure R-26b), Ts65Dn (Ts-*D1a*$^{+++}$) RG progenitors had decreased levels of Cyclin D1

(Figure R-28). Moreover, like in the mBACTg*Dyrk1a* progenitors, the levels of nuclear Cyclin D1 in dorsal RG progenitors were diminished (compare histograms in Figure R-28 and Figure R-23a). This data indicates that nuclear levels of Cyclin D1 in Ts65Dn apical progenitors are controlled by DYRK1A phosphorylation. Accordingly, nuclear Cyclin D1 levels in RG progenitors of trisomic embryos with normal dosage of *Dyrk1a* (Ts-*D1a*$^{++-}$ embryos) were similar to euploid embryos. As expected, *Dyrk1a*$^{+/-}$ (*D1a*$^{+-}$) embryos showed increased levels of nuclear Cyclin D1 (Figure R-28). These results demonstrate that trisomy of *Dyrk1a* is responsible for the decreased levels of Cyclin D1 in Ts65Dn RG progenitors.

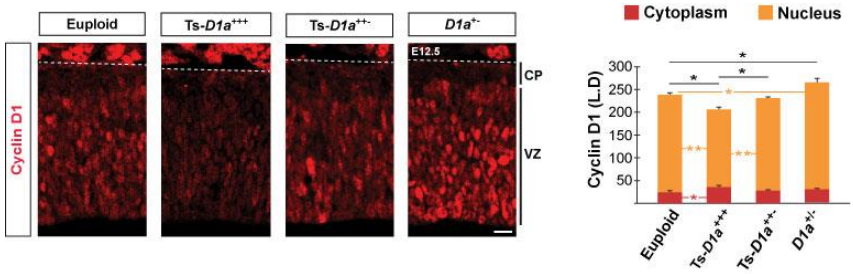

Figure R-28: Trisomy of *Dyrk1a* reduces nuclear Cyclin D1 protein levels in Ts65Dn dorsal radial glial progenitors. Representative brain coronal sections obtained from E12.5 embryos of the indicated genotypes and immunostained for Cyclin D1. Histogram shows the labelling density (L.D) of Cyclin D1 fluorescence signal in the nucleus and the cytoplasm of ventricular zone (VZ) progenitors. Histogram values are the mean ± S.E.M. *P<0.05, **P<0.01 (n ≥ 3). Bars = 20 μm. CP: cortical plate.

If G1 phase lengthening biases the type of RG self-renewing divisions, as we propose for mBACTg*Dyrk1a* progenitors, Ts65Dn RG progenitors should produce less neurons and more IPs. To investigate this possibility we counted the number of

apical progenitors ($Pax6^+$ cells), the number of neurons ($Tbr1^+$ cells) and the percentage of IPs ($Tbr2^+$ cells that do not express the neuronal marker Tuj1) in E12.5 brain sections of the four genotypes resulting from the crosses depicted in Figure R-27. As expected, the numbers of $Pax6^+$ progenitors were similar in euploid and Ts65Dn embryos (Figure R-29a). Moreover, Ts65Dn progenitors produced fewer neurons (Figure R-29b) and more IPs (Figure R-29c) than euploid progenitors. The phenotype in Ts65Dn embryos reported here is consistent with the delayed grow of the neocortical wall and the increased number of $Tbr2^+$ progenitors in the SVZ previously observed in these embryos (Chakrabarti et al., 2007). Importantly, both neuron and IP numbers were normal in Ts65Dn embryos with normal *Dyrk1a* gene-dosage. In accordance with the data shown in Figure R-15, *Dyrk1a*$^{+/-}$ littermate embryos showed normal numbers of $Pax6^+$ progenitors but increased number of neurons and decreased number of $Tbr2^+$ progenitors (Figure R-29a-c).

The decreased early neurogenesis in Ts65Dn embryos leads to a reduction in the number of layer VI $Tbr1^+$ neurons in Ts65Dn postnatal animals (Chakrabarti et al., 2007) (Chakrabarti et al., 2010). Ts65Dn postnatal animals resulting from crosses between trisomic mice and *Dyrk1a*$^{+/-}$ mice (Figure R-27) also have fewer Tbr1 neurons than euploid animals (Figure R-30). Importantly, the normalization of *Dyrk1a* gene-dosage in the trisomic embryos also normalized the number of postnatal layer VI Tbr1 neurons (Figure R-30). As expected, the cellularity of $Tbr1^+$ neurons was increased in postnatal *Dyrk1a*$^{+/-}$ neocortices.

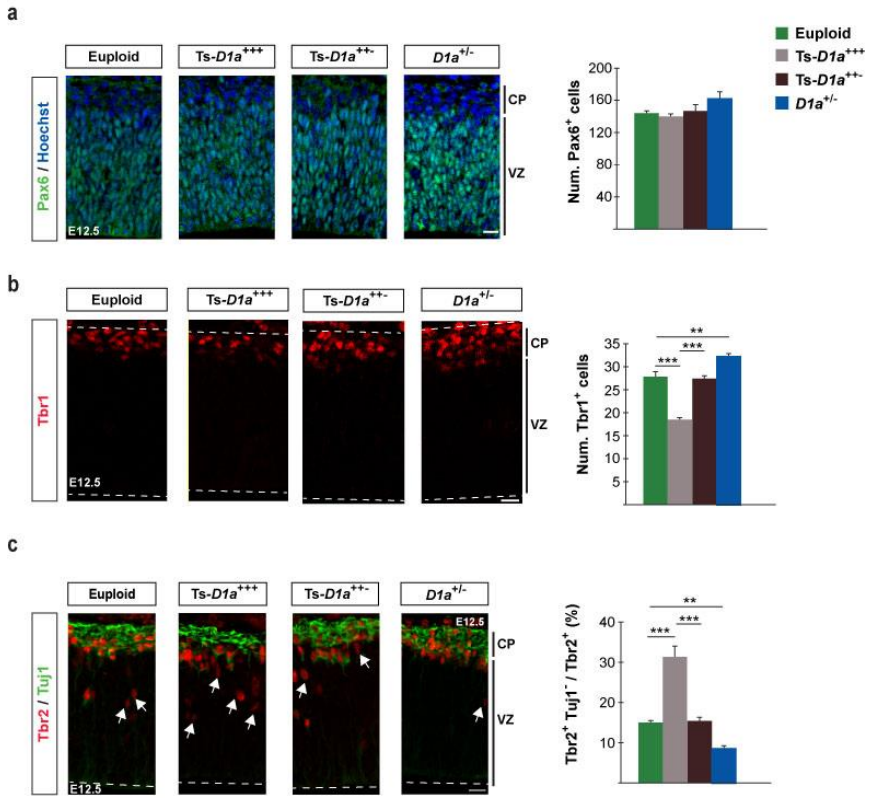

Figure R-29: Trisomy of *Dyrk1a* impairs early neurogenesis in the dorsal telencephalon of Ts65Dn embryos. **(a-c)** Representative brain coronal sections obtained from E12.5 embryos of the indicated genotypes and immunostained for Pax6 **(a)**, Tbr1 **(b),** or Tbr2 and Tuj1 **(c)**. Histograms show the numbers of $Pax6^+$ radial glial progenitors **(a)**, the numbers of $Tbr1^+$ neurons **(b)**, and the percentage of $Tbr2^+$ intermediate progenitors; $Tbr2^+Tuj1^-$ cells (arrows in **c**). Histograms values are the mean ± S.E.M. **P<0.01, ***P<0.001 ($n \geq 3$). Bars = 20 μm. CP: cortical plate; VZ: ventricular zone.

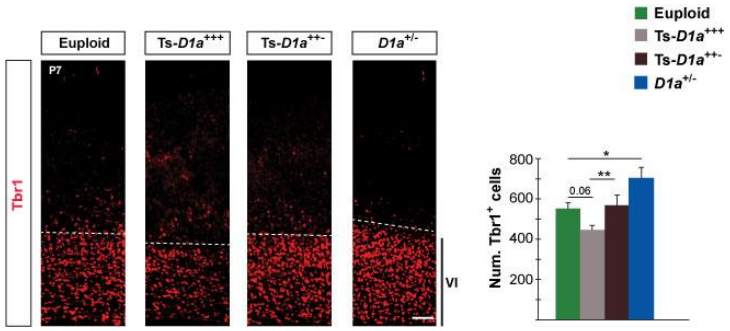

Figure R-30: Trisomy of *Dyrk1a* leads to a deficit of internal layer cortical neurons in Ts65Dn mice. Representative coronal brain sections of P7 animals of the indicated genotypes immunostained for Tbr1 and histogram showing the number of layer VI Tbr1$^+$ neurons. Histogram values are the mean ± S.E.M. *P<0.05, **P<0.01 (n ≥ 3). Bars = 20 μm.

In summary, these data demonstrate that *Dyrk1a* is the triplicated gene that causes the neurogenic defects in the developing cerebral cortex of the DS mouse model Ts65Dn. In addition, these data suggest that DYRK1A-mediated degradation of Cyclin D1 is the likely basis of the altered cell cycle parameters previously observed in RG Ts65Dn progenitors.

6. Effects of *Dyrk1a* trisomy in the development of cortical GABAergic interneurons

The cerebral cortex of adult mBACTg*Dyrk1a* mice showed a misbalanced number of the two main GABAergic interneuron types, PV and SST, which are generated in the embryonic MGE (Figure R-8 and R-9). This indicates that neurogenesis in the MGE could be affected by DYRK1A overexpression. To investigate this possibility, first we measured the area occupied

by the MGE at three different rostro-caudal levels in coronal sections prepared from E13.5 wild-type and mBACTg*Dyrk1a* embryos (Figure R-31a). The area of the MGE was similar in both genotypes (Figure R-31b), indicating that the gross morphology of this structure is maintained in mBACTg*Dyrk1a* embryos.

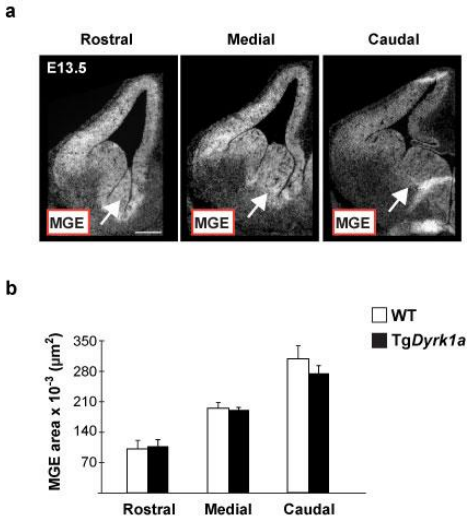

Figure R-31: The size of the medial ganglionic eminence is normal in mBACTg*Dyrk1a* embryos. **(a)** Pictures of E13.5 coronal brain sections at three different rostro-caudal levels with nuclei visualized with Hoechst. Arrows point the medial ganglionic eminence (MGE). **(b)** Histogram shows the area of the MGE at the indicated levels in wild-type (WT) and mBACTg*Dyrk1a* (Tg*Dyrk1a*) embryos. Histogram values are the mean ± S.E.M. Bars = 200 μm.

Next, we estimated the pool size of the two principal types of MGE progenitors in E13.5 coronal sections immunostained for Nkx2.1 and Nkx6.2 (Figure R-32). As has been explained in the introduction (see Chapter 1.2.3), most SST interneurons are generated from Nkx6.2 expressing progenitors localized in the dorsal MGE and from Nkx2.1 expressing progenitors localized in the medial region of the MGE (Wonders et al., 2008). Most PV

interneurons are generated from Nkx2.1 expressing progenitors localized in the medial and the ventral part of the MGE (Wonders et al., 2008; Flames et al., 2007). Therefore, we hypothesized that the increased number of SST^+ interneurons and the reduction of PV^+ interneurons observed in transgenic adult mice (Figure R-8 and R-9) could result from an expansion of the Nkx6.2 progenitor domain to more medial and ventral regions. To investigate this possibility, we measured the area occupied by Nkx6.2 and Nkx2.1 progenitors at different rostro-caudal levels in embryo sections immunostained for Nkx2.1 and Nkx6.2 (Figure R-32). Our results revealed that the area occupied by these two types of progenitors were similar in mBACTg*Dyrk1a* and wild-type embryos (Figure R-32b and e).

To extend this analysis we counted the proportion of Nkx6.2 progenitors within the Nkx6.2-labeled region (Figure R-32a) at different rostro-caudal levels of the MGE, but we did not observed differences between genotypes (Figure R-32c). Then we counted Nkx2.1 progenitors in different dorso-ventral MGE regions (rectangles in Figure R-32d) in sections corresponding to the medial part of the rostro-caudal axis of the brain. The number of Nkx2.1 progenitors was increased in mBACTg*Dyrk1a* embryos, but differences between genotypes were statistically significant only in the medial sampled region (Figure R-32f).

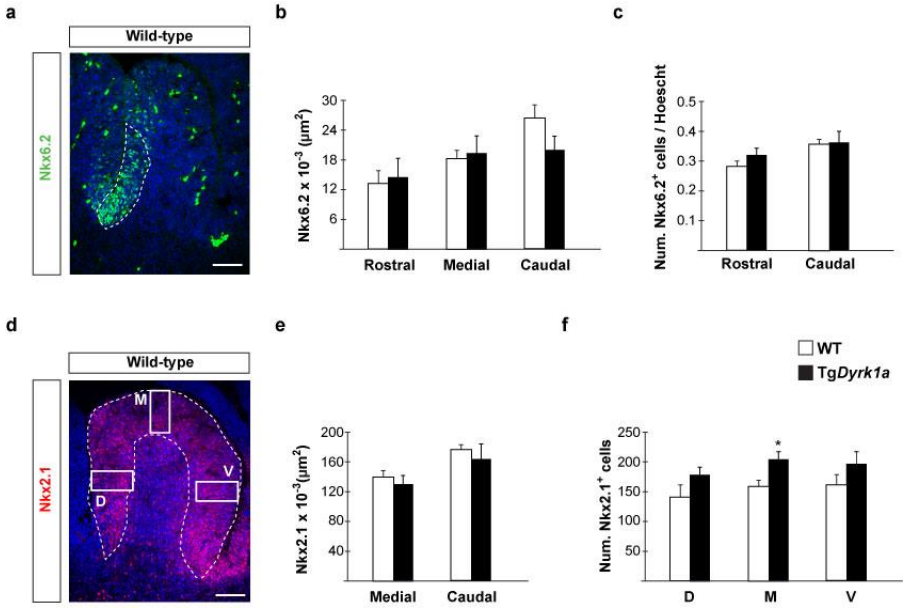

Figure R-32: mBACTg*Dyrk1a* embryos show increased number of Nkx2.1 progenitors in the medial ganglionic eminence. **(a, d)** Representative confocal images of E13.5 coronal brain sections immunostained for the progenitor markers Nkx6.2 **(a)** and Nkx2.1 **(d)**. Dashed lines delineate the domain occupied by these progenitors. **(b, e)** Histograms show the area occupied by Nkx6.2$^+$ **(b)** or Nkx2.1$^+$ **(e)** progenitors at the rostro-caudal levels indicated in wild-type (WT) and mBACTg*Dyrk1a* (Tg*Dyrk1a*) embryos. **(c)** Histogram showing the proportion of Nkx6.2$^+$ progenitors at the indicated rostro-caudal levels in WT and Tg*Dyrk1a* embryos. **(f)** Histogram showing the number of Nkx2.1$^+$ progenitors counted at three dorso-ventral regions of the MGE (rectangles in **d**) in sections from the medial level of WT and Tg*Dyrk1a* embryos. Histogram values are the mean ± S.E.M. *P<0.05 (n ≥ 3). Bars = 100 µm.

Next, we wonder whether the increased number of MGE progenitors in transgenic embryos leads to an increased production of GABAergic interneurons. To investigate this, we first evaluated the mRNA levels of *Lhx6, Calbindin* and *Shh*, which are expressed in newly generated interneurons but not in progenitors of the MGE (Flandin et al., 2011), in ganglionic eminences isolated from E13.5 wild-type and mBACTg*Dyrk1a*

embryos. As shown in Figure R-33, transgenic embryos showed increased levels of *Calbindin* and *Shh* transcripts.

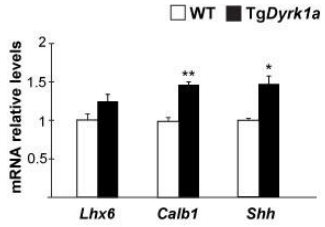

Figure R-33: mBACTg*Dyrk1a* embryos show increased expression of interneuron markers in the ganglionic eminences. Histogram showing the relative expression of *Lhx6, Calbindin (Calb1)* and *Shh* transcripts in the ganglionic eminences of E13.5 wild-type (WT) and mBACTg*Dyrk1a* (Tg*Dyrk1a*) embryos. Histogram values are the mean ± S.E.M. *P<0.05, **P<0.01 (n ≥ 3).

This result suggests that MGE neurogenesis at this developmental stage might be increased in mBACTg*Dyrk1a* embryos. To provide further evidences on this, we labeled cells in S phase with BrdU at E13.5 and estimated the proportion of these cells that exited the cell cycle 24 hours later in different MGE regions (rectangles in Figure R-34) of wild-type and mBACTg*Dyrk1a* embryos. Double immunostainings for BrdU and Ki67 showed that cell cycle exit rates were increased in the transgenic MGEs, but again differences between genotypes reached statistical significance only in medial regions (Figure R-34).

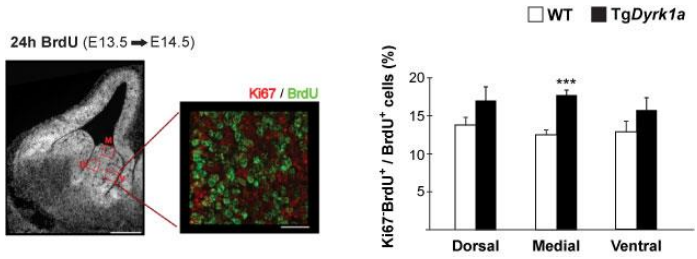

Figure R-34: E13.5 mBACTg*Dyrk1a* embryos show increased cell cycle exit rates in the medial ganglionic eminence. Picture in the left shows a coronal brain section with nuclei visualized with Hoechst of an E14.5 embryo. Red rectangles indicate the three regions: dorsal (D), medial (M), and ventral (V) where cell counts were performed. Picture on the right corresponds to an amplification of the indicated region showing cells immunolabelled for BrdU and Ki67. Histogram shows the percentage of cells that exited the cell cycle from E13.5 to E14.5 in the indicated regions of wild-type (WT) and mBACTg*Dyrk1a* (Tg*Dyrk1a*) embryos. Histogram values are the mean ± S.E.M. ***P<0.001 (n ≥ 3). Scale bars = 200 μm (left) and 20 μm (right).

As already mentioned, the proliferative medial region of the MGE generates SST as well as PV GABAergic interneurons. Taking into account that most SST interneurons are generated before E14.5 while generation of PV interneurons last until birth (see Figure I-9), we asked whether the increased cell cycle exit rate observed between E13.5 and E14.5 in the MGE of transgenic embryos could lead to an early depletion of the progenitor pool, and consequently to a decreased production of PV interneurons. To answer this, we counted Nkx2.1$^+$ progenitors one day later, at E14.5, in different regions of the MGE of wild-type and mBACTg*Dyrk1a* embryos (Figure R-33d). At this stage, there were no differences in the number of Nkx2.1 progenitors between genotypes (Figure R-35a). In both genotypes the number of Nkx2.1 progenitors decreases from E13.5 to E14.5, but this reduction was more pronounced in the transgenic embryos (25% reduction in the wild-type vs 40% reduction in the transgenic;

data in Figure R-32f, R-35a) suggesting that the Nkx2.1 progenitor pool would be exhausted earlier in the mBACTg*Dyrk1a* embryos. This hypothesis is supported by the increased cell cycle exit rate observed in transgenic embryos from E14.5 to E15.5 (Figure R-35b).

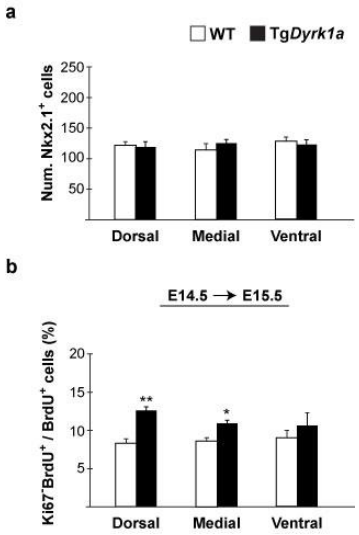

Figure R-35: E14.5 mBACTg*Dyrk1a* embryos show normal number of Nkx2.1$^+$ progenitors but increased cell cycle exit rates in the medial ganglionic eminence. (a, b) Histograms showing the number of Nkx2.1 immunopositive cells in the indicated regions of the MGE in E14.5 wild-type (WT) and mBACTg*Dyrk1a* (Tg*Dyrk1a*) embryos **(a)** and the percentage of cells that exited the cell cycle (BrdU$^+$Ki67$^-$ cells) in the same MGE regions in E15.5 WT and Tg*Dyrk1a* embryos after 24-hours treatment with BrdU **(b)**. Histogram values are the mean ± S.E.M. *P<0.05, **P<0.01 (n ≥ 3).

In fact, if we assume that the reduction in the number of Nkx2.1 progenitors and the cell cycle exit rate mantain the linear progression observed from E13.5 to E14.5, we would expect that at E15.5 the number of Nkx2.1 progenitors will be much more reduced in transgenic embryos. This would lead to a decrease in the production of neurons that at this stage correspond to PV interneurons (Figure R-36), which is consistent with the decreased number of PV interneurons observed in the neocortex of adult mBACTg*Dyrk1a* animals (Figure R-8b).

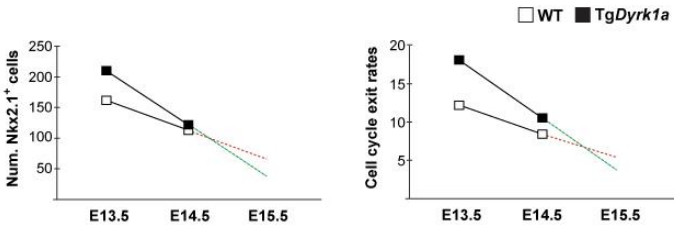

Figure R-36: Summary of numbers of Nkx2.1 progenitors and cell cycle exit rates in the medial ganglionic eminences of wild-type and mBACTg*Dyrk1a* embryos. Graph values correspond to the quantifications performed in the medial MGE region of wild-type (WT) and mBACTg*Dyrk1a* (Tg*Dyrk1a*) embryos and shown in the histograms in Figure R-34 and R-35. Dashed lines indicate the predicted numbers of Nkx2.1 cells and the cell cycle exit rates later in neurogenesis (WT in red; Tg*Dyrk1a* in green). Note that the tendency is that E15.5 transgenic embryos would have less Nkx2 progenitors and less differentiation in the medial MGE than the WTs.

Together, the results presented so far indicate that the increase in SST^+ GABAergic interneurons is probably due to an early expansion of the Nkx2.1 domain in the mBACTg*Dyrk1a* MGE while the decrease in PV^+ population is caused by an advanced depletion of Nkx2.1 progenitors in this domain.

The molecular mechanisms that regulate neurogenesis in the subpallium are not well defined (see Chapter 1.2.3 in the Introduction section). Considering the importance of cell cycle regulation in neurogenesis and the effect of DYRK1A regulating Cyclin D1 turnover in dorsal telencephalic RG progenitors observed here, we asked whether the overexpression of DYRK1A affects Cyclin D1 protein levels in ventral telencephalic progenitors. To answer this, we prepared protein extracts from dorsal telencephalon and ganglionic eminences isolated from mBACTg*Dyrk1a* and wild-type embryo littermates at E13.5, when the neurogenic waves of SST and PV interneurons overlap (Figure I-9) and cell cycle exit rates in the Nkx2.1 MGE domain

are increased in the *Dyrk1a* transgenic embryos (Figure R-36). Cyclin D1 levels in mBACTg*Dyrk1a* dorsal telencephalic (pallium) extracts were lower than in the wild-types (Figure R-37b), similarly to what we previously observed in E11.5 dorsal brain extracts (Figure R-21b). In contrast, Cyclin D1 levels in ventral telencephalic (subpallium) extracts were similar in both genotypes (Figure R-37a).

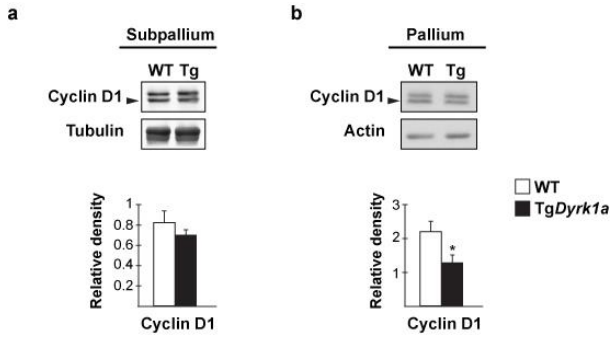

Figure R-37: mBACTg*Dyrk1a* embryos show normal levels of Cyclin D1 protein in the ventral telencephalon. Representative western blots of extracts prepared from the ventral telencephalon (subpallium) **(a)** or the dorsal telencephalon (pallium) **(b)** of E13.5 wild-type (WT) and mBACTg*Dyrk1a* (Tg) embryos probed with the indicated antibodies. Histograms show the protein levels of Cyclin D1 normalized to tubulin or actin levels in the subpallium **(a)** and the pallium **(b)** of embryos from both genotypes. Arrowhead indicates the band corresponding to the Cyclin D1 isoform that contains Thr286. Histogram values are the mean ± S.E.M. *$P<0.05$ ($n \geq 3$).

This result suggests that the effect of DYRK1A on Cyclin D1 turnover is cell-type specific. Nonetheless, it does not exclude the possibility that the overexpression of DYRK1A alters cell cycle parameters in ventral progenitors by a mechanism other than deregulation of Cyclin D1 turnover.

There is evidence that Shh regulates neurogenesis in the MGE (see Chapter 1.2.3 in the Introduction section). Indeed, the

artificial activation of Shh signaling in MGE progenitors leads to increased numbers of SST interneurons and decreased numbers of PV interneurons (Xu et al., 2010). Given that these alterations resemble those observed in mBACTg*Dyrk1a* mice (Figure R-8), and that DYRK1A increases the transcriptional activity of Gli1 (Mao et al., 2002), we hypothesized that Shh signaling could be enhanced in our mutant. To provide evidence on this, we performed RT-PCRs from RNAs isolated from the ganglionic eminences of E13.5 mBACTg*Dyrk1a* and wild-type littermate embryos. As shown in Figure R-38, we did not see differences between genotypes in the expression of the Shh downstream genes *Ptch1, Gli1, Gli2* and *Gli3*. This result indicates that deregulation of Shh signaling is probably not the cause of the altered numbers of SST and PV interneurons in mice overexpressing DYRK1A.

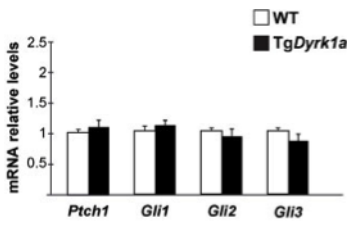

Figure R-38: Shh signalling is not altered in the ganglionic eminence of mBACTg*Dyrk1a* embryos. Histogram showing the relative expression of *Ptch1, Gli1, Gli2* and *Gli3* genes determined by RT-qPCR on mRNA obtained from the ganglionic eminences of E13.5 wild-type (WT) and mBACTg*Dyrk1a* (Tg*Dyrk1a*) embryos. Histogram values are the mean ± S.E.M. ($n \geq 3$).

DISCUSSION

1. Effect of DYRK1A overexpression in the generation of cortical glutamatergic and GABAergic neurons

Glutamatergic and GABAergic neurons in the adult neocortex are generated respectively from progenitors of the dorsal and the ventral telencephalon (Kriegstein and Alvarez-Buylla, 2009; Welagen and Anderson, 2011). In the present work we show that the overexpression of DYRK1A due to trisomy of the *Dyrk1a* gene alters the generation of both glutamatergic and GABAergic neurons in the mouse embryo telencephalon. Quantifications of neuronal production during the early phase of telencephalic neurogenesis showed that neurogenesis in mBACTg*Dyrk1* embryos is decreased in the dorsal telencephalon and increased in the ventral telencephalon. This indicates that the pathogenic effect of DYRK1A overexpression is progenitor-type specific and that the molecular mechanism that underlies the neurogenic defects in dorsal and ventral progenitors should be different.

1.1 Alterations in cell cycle duration and mode of division of dorsal radial glial progenitors

Our results showed that one extra copy of *Dyrk1a* in mouse RG progenitors of the dorsal telencephalon leads to longer cell cycles and to decreased production of RG-derived neurons. Different observations indicate that the overexpression of DYRK1A in RG progenitors favours RG asymmetric proliferative divisions at the expense of asymmetric neurogenic divisions: 1) During the early phase of cortical neurogenesis, when the majority of neocortical

neurons are generated by asymmetric neurogenic divisions of RG progenitors (Kowalczyk et al., 2009), the proportion of IPs ($Tbr2^{+}Tuj1^{-}$ cells) that delaminate from the VZ and migrate to basal positions increases in mBACTg*Dyrk1a* embryos while the number of neurons ($Tbr1^{+}$ cells) decreases (see Figures R-13 and R-14); 2) The number of RG progenitors ($Pax6^{+}$ cells) and the number of apical mitosis in mBACTg*Dyrk1a* embryos are normal along corticogenesis (see Figure R-16); and 3) The SVZ of mBACTg*Dyrk1a* embryos have increased numbers of IPs and mitosis from the onset of neurogenesis to mid-corticogenesis (see Figure R-16).

Our *in vivo* cell cycle measurement of RG progenitors at the beginning of neurogenesis (E11.5) reveals that DYRK1A overexpression leads to a 4.8 hours increase in cell cycle duration due to an enlargement of the G1 and the S phase (see Figure R-25). The increased duration in G1 phase correlates with the increased proportion of RG progenitors in G0/G1 phases observed by flow cytometry in mBACTg*Dyrk1a* embryos (see Figure R-24).

The total cell cycle duration and the G1 phase duration obtained here in wild-type RG progenitors at E11.5 are 2 hours (10%) and 4.8 hours (41%) shorter, respectively, than those previously reported for E14.5 RG progenitors using the same *in vivo* EdU-cumulative protocol (Arai et al., 2011). These differences are in accordance with the progressive lengthening of the cell cycle and the G1 phase along neurogenesis reported previously in the ventricular epithelium of the mouse developing neocortex (Takahashi et al., 1995). Moreover, our results showing defects in G1 length and division mode of RG progenitors observed in

mBACTg*Dyrk1a* embryos are in line with the accepted idea that the time that a RG progenitor spends in G1 determines the fate of their daughter cells (Gotz and Huttner, 2005; Dehay and Kennedy, 2007; Salomoni and Calegari, 2010). Importantly, as corticogenesis advances and G1 phase duration increases, the production of IPs from RG progenitors increases (see Figure R-16). These observations, together with the phenotype observed here in *Dyrk1a* transgenic embryos make us hypothesise that the type of asymmetric division (proliferative vs neurogenic) that a RG progenitor undergoes depends on the duration of the G1 phase, which is controlled in a dosage-dependent manner by DYRK1A (see next Chapter). Although we cannot rule out the possibility that the enlargement of the G1 is secondary to an effect of DYRK1A overexpression on the division mode of RG progenitors, our genetic rescue experiments performed in Ts65Dn embryos (see Chapter 2.1 in the Discussion section) suggest that this is not the case.

The cell cycle defects observed in mBACTg*Dyrk1a* RG progenitors challenge previous findings showing that shortening the G1 cell cycle phase in these progenitors by *in utero* electroporation of Cyclin D1 or CyclinD1/CDK4 constructs favours RG proliferative divisions at the expense of neurogenic divisions (Pilaz et al., 2009; Lange et al., 2009), which is the same we have observed here in transgenic embryos overexpressing DYRK1A. It is possible that forced overexpression of cell cycle regulators deeply disturb cell cycle progression, and hence the progenitor neurogenic program. In fact, the overexpression of CyclinD1/CDK4 not only leads to shorter G1 phase but also to longer S and G2/M phases (Lange

et al., 2009). Moreover, in embryos in which the G1 of apical progenitors has been manipulated by forced overexpression of Cyclin D1/CDK4 there is an expansion of IP proliferative divisions in the SVZ and, as a consequence, the number of external layer neurons is significantly increased (Lange et al., 2009), which is the contrary to what we have observed here in mBACTg*Dyrk1a* mice (see Chapter 1.3 in this section).

A comparative analysis of cell cycle parameters in neurogenic and non-neurogenic mouse cortical progenitors at mid-corticogenesis has shown that the length of the S phase is significantly shorter in progenitors committed to produce neurons than in those undergoing self-expanding divisions (1.8 *vs* 8.3 hours in apical progenitors) (Arai et al., 2011). This observation has been interpreted as a need of self-expanding progenitors to guarantee high fidelity DNA replication and repair (Arai et al., 2011). Tacking into account this study the S phase lengthening observed in this work in mBACTg*Dyrk1a* RG progenitors could be secondary to the altered mode of division of these progenitors due to the action of DYRK1A on G1.

Previous studies have shown that forced overexpression of DYRK1A in proliferating neural cells in culture (Yabut et al., 2010; Hammerle et al., 2011; Soppa et al., 2014) and in progenitors of the dorsal mouse telencephalon achieved by different electroporation techniques (Yabut et al., 2010; Hammerle et al., 2011) promotes neuronal differentiation. In contrast, we have observed that neuron production in the dorsal telencephalon of mBACTg*Dyrk1a* embryos is significantly decreased (see Figure R-13). Given that DYRK1A function is highly sensitive to DYRK1A dosage, these discrepancies could be due to

differences in the levels of DYRK1A overexpression in mBACTg*Dyrk1a* embryos and DYRK1A-eletroporated embryos. In fact, our results show that 1.5 fold increase in DYRK1A leads to a 2 hours enlargement of the G1 duration, thus it is plausible that higher levels of DYRK1A overexpression could have a greater impact on G1 duration and force RG progenitors to exit the cell cycle and differentiate. In agreement with this suggestion, a recent study shows that the electroporation of different amounts of DYRK1A-plasmid in the embryo affects the behaviour of RG progenitors in a DYRK1A dosage-dependent manner (Kurabayashi and Sanada, 2013). We have shown that, similar to other cell types, endogenous DYRK1A in mouse RG progenitors is mostly cytosolic (see Figure R-10). However, DYRK1A expressed by transfected DYRK1A-plasmids tends to accumulate in the nucleus *in vivo* and in cultured neural precursors (Yabut et al., 2010; Hammerle et al., 2011; Soppa et al., 2014). Therefore, differences in the cellular location (nucleus vs cytoplasm) of the overexpressed kinase would affect a different set of DYRK1A substrates (see Chapter 3.2 in the Introduction section), thus explaining the distinct phenotypes of mBACTg*Dyrk1a* embryos and DYRK1A-electroporated embryos (Yabut et al., 2010; Hammerle et al., 2011).

1.2 Pathogenic mechanisms underlying neurogenic alterations in dorsal radial glial progenitors

There is evidence showing that in neural cells DYRK1A regulates the levels of cell cycle regulators acting on G1 phase. Different groups have shown that the overexpression of DYRK1A in cultured cells increases the degradation of Cyclin D1 (Yabut et al.,

2010), the transcription of $p21^{CIP1}$ trough regulation of p53 transcriptional activity (Park et al., 2010), and the stability of $p27^{KIP1}$ protein (Soppa et al., 2014). Moreover, the overexpression of DYRK1A in the chick neural tube induces *p27*^{KIP1} transcription (Hammerle et al., 2011). Thus, altered levels of these cell cycle regulators could be the underlying cause of the longer G1 phases described here in *Dyrk1a* transgenic embryos. However, at the onset of neurogenesis, *Cyclin D1* transcript levels and $p21^{CIP1}$ and $p27^{KIP1}$ transcript and protein levels were normal in the dorsal VZ of mBACTg*Dyrk1a* embryos. In contrast, protein levels of Cyclin D1 were significantly decreased in these transgenic embryos (see Figure R-21). The observation that the levels of Cyclin D1 protein but not of *Cyclin D1* transcripts were decreased in transgenic progenitors is in accordance with previous observations (Yabut et al., 2010) and suggest that DYRK1A promotes Cyclin D1 degradation.

Degradation of Cyclin D1 is regulated by the phosphorylation of the Thr286 residue, which induces Cyclin D1 nuclear export and subsequent degradation of the protein through the ubiquitin-proteasome pathway (Diehl et al., 1997, 1998). Among the two described Cyclin D1 isoforms, the shorter one that contains the phosphorylable Thr286 residue is the one altered in mBACTg*Dyrk1a* RG progenitors (see Figure R-21). This observation together with the decreased levels of nuclear Cyclin D1 observed in mBACTg*Dyrk1a* sections of the dorsal telencephalon (see Figure R-23) strongly suggest that DYRK1A phosphorylates Cyclin D1 and induce its degradation in RG progenitors *in vivo*, as it has been recently shown in cultured

fibroblasts (Chen et al., 2013) and neuroblastoma cells (Soppa et al., 2014).

It is important to mention that DYRK1B, the closest member to DYRK1A in the DYRK family of protein kinases (Becker and Joost, 1999) can also phosphorylate Cyclin D1 on Thr286 (Zou et al., 2004; Ashford et al., 2014). *In situ* hybridizations of *Dyrk1b* in the developing mouse brain at mid-corticogenesis (by E14.5) revealed that *Dyrk1b* is not expressed in the VZ but it is expressed in the SVZ (www.emouseatlas.org). This observation indicates that DYRK1A is the DYRK kinase that control Cyclin D1 nuclear activity in dorsal RG progenitors. However, we cannot rule out the possibility that DYRK1B play a function similar to that described here for DYRK1A in SVZ progenitors or other neural progenitor types.

It has been recently shown that in addition to regulate cell cycle progression nuclear Cyclin D1 can regulate transcription and DNA repair (Pestell, 2013). During early stages of neural system development the repair of DNA double-strand breaks in proliferating cells occurs *via* homologous recombination (Orii et al., 2006). Mutant embryos in which homologous recombination has been abolished show early lethality and impaired neurogenesis due to a massive apoptosis of neural progenitors indicating that this DNA repair mechanism is crucial for CNS development (Orii et al., 2006). Cyclin D1 can promote homologous recombination by recruiting two essential homologous recombination proteins to the DNA breaks: RAD51 and BRCA2 (Jirawatnotai et al., 2011). In this scenario, and given that repair of DNA double-strand breaks occurs during S phase (O'Driscoll and Jeggo, 2008), a limiting amount of nuclear Cyclin

D1 might increase the time that a progenitor spent in this phase. Hence, dysregulation of DYRK1A-mediated degradation of Cyclin D1 may contribute to the S phase lengthening observed in mBACTg*Dyrk1a* dorsal RG progenitors (see Figure R-25).

The decision of a neural progenitor to further divide or differentiate is controlled by external and internal factors, which act mainly during G1 (Gotz and Huttner, 2005; Dehay and Kennedy, 2007; Salomoni and Calegari, 2010). Therefore, external factors promoting asymmetric proliferative divisions would have more time to act in mBACTg*Dyrk1a* RG progenitors than in wild-type progenitors explaining the bias on the division mode of these progenitors. In addition to that, the overexpression of DYRK1A in mBACTg*Dyrk1a* progenitors might also inhibit the action of differentiating external factor or enhance the action of proliferative external factors. One of the main external factors involved in progenitor maintenance is Notch (Kageyama et al., 2009). During RG asymmetric divisions the daughter cell that maintains high Notch activity remains as a progenitor while the one with low Notch activity differentiates into a neuron (Kageyama et al., 2008). DYRK1A represses Notch signalling *via* the phosphorylation of the intracellular domain of Notch, which reduces its transcriptional activity (Fernandez-Martinez et al., 2009). In fact, it has been shown that ectopic overexpression of DYRK1A in the VZ of the mouse embryo telencephalon decreases the expression of the Notch target gene *Hes5,* while a transient knockdown of *Dyrk1a* by siRNA produces the opposite effect (Hammerle et al., 2011). According to these data, overexpression of DYRK1A in this germinal layer should restrain Notch signalling, thus favouring the acquisition of a differentiated

fate. Our results show that neuron production in the VZ of mBACTg*Dyrk1a* embryos is decreased rather than increased. Moreover, *Notch1*, *Delta1*, *Hes1* and *Hes5* expression in the telencephalon of E11.5 mBACTg*Dyrk1a* embryos was similar than in wild-type embryos (see Figure R-19), indicating that Notch signalling is not significantly attenuated in VZ progenitors. On the other hand, it has been demonstrated that Cyclin D1 upregulates the transcription of components of the Notch signalling pathway and downstream targets in the chick spinal cord (Lukaszewicz and Anderson, 2011) and in the mouse retina (Bienvenu et al., 2010). However, the effect of Cyclin D1 in these two CNS regions is different; in the spinal cord Cyclin D1 promotes neurogenesis upregulating the expression of the Hes1 inhibitor Hes6 (Lukaszewicz and Anderson, 2011) while in the retina it promotes precursors maintenance increasing the expression of Notch and Hes5 (Bienvenu et al.; 2010). This indicates that transcriptional activity of Cyclin D1 is cell-type specific. Our results showing normal levels of *Notch*, *Hes1*, *Hes5* and *Hes6* transcripts in the dorsal telencephalon of E11.5 mBACTg*Dyrk1a* embryos (see Figure R-19; and data non shown), suggest that Cyclin D1 is not involved in the transcriptional regulation of these genes in the dorsal telencephalic VZ.

The transcription factor Pax6 represses the expression of *CDK6* in dorsal RG progenitors thereby controlling G1 to S phase progression (Mi et al., 2013). In addition, Pax6 induces the expression of the transcription factor gene *Tbr2* (Faedo et al., 2004), which is essential for the formation and proliferation of IPs (Sessa et al., 2008). Indeed, Pax6 knock-out embryos show

decreased number of IPs and increased number of neurons at early stages of development (Quinn et al., 2007). Thus, Pax6 influences cell cycle progression and the generation of RG-derived IPs. It has been recently shown that Pax6 transcriptional activity in cortical RG progenitors is repressed by the mSWI/SNF component BAF170, which recruits the repressor complex REST (Tuoc et al., 2013). The overexpression of DYRK1A reduces *REST* transcription and the stability of the REST protein in mouse embryonic stem cells and in HEK293 cells (Canzonetta et al., 2008; Lu et al. 2011). If the overexpression of DYRK1A has similar effects on REST in RG progenitors, it is reasonable to think that dysregulation of Pax6 transcriptional activity could contribute to the cell cycle phenotype and the increased production of IPs observed in mBACTg*Dyrk1a* embryos. An hypothesis that should be tested by measuring REST protein levels and the expression of Pax6 target genes in the dorsal telencephalon of mBACTg*Dyrk1a* embryos.

Finally, it is also important to mention that as corticogenesis advances proliferation is also regulated by complex feedback mechanisms. For instances, GABAergic interneurons that are migrating from the subpallium to the CP release GABA and Shh, which induce proliferation of the dorsal progenitors (Wang and Kriegstein, 2009; Komada et al., 2008). Moreover, newborn neurons in the pallium express factors, such as the transcription factor Sip1, that regulates proliferation and differentiation of dorsal progenitors and that influences the fate of the new neurons (Seuntjens et al., 2009). On the other hand, thalamocortical axons, which reach the CP around E14.5 guided by the first cortical neurons generated form the subplate (Kanold

and Luhmann, 2010) release a diffusible factor, probably FGF, that promotes proliferation regulating cell cycle duration (Dehay et al., 2001). Therefore, the deficit of external layer neurons observed in postnatal mBACTg*Dyrk1a* embryos could be secondary to the deficit of early born glutamatergic neurons and the altered fate of MGE GABAergic interneurons (see Chapter 1.4 in this section) observed in this transgenic model.

1.3 Effect on the neurogenic potential of dorsal intermediate progenitors

IPs divides symmetrically in the SVZ to self-expand or to generate two neurons and they are the main neuron source of external cortical layers (Pontious et al., 2008). As already discussed, in mBACTg*Dyrk1a* embryos the production of IPs and the number of mitosis in the SVZ are increased until mid-corticogenesis. However, later on development, the number of these progenitors in the transgenic embryo SVZ decreases to levels that are lower that in the wild-type SVZ (see Figure R-16), and consequently there is a deficit of $Cux1^+$ neurons in the external cortical layers of postnatal mBACTg*Dyrk1a* mice (see Figure R-18). This observation opens the possibility that DYRK1A overexpression in SVZ progenitors favours neurogenic divisions at the expense of self-expanding divisions leading to an earlier exhaustion of these progenitors.

The artificial manipulation of the G1 in the apical progenitors increases the proportion of proliferative divisions in the SVZ leading to increased number of external cortical neurons and increased postnatal cortex surface area (Lange et al., 2009)

(Nonaka-Kinoshita et al., 2013), indicating that G1 phase duration may also influence the division mode of IPs. The information regarding the mechanisms that regulate progression through the cell cycle G1 phase in IPs is limited. Nonetheless, there are indications that Cyclin D2 could be the relevant G1 CyclinD in IPs progenitors: 1) The expression of Cyclin D2, contrary to Cyclin D1, is much higher in the SVZ than in the VZ (Glickstein et al., 2007), and 2) The lack of Cyclin D2 in the mouse embryo induces cell cycle exit of SVZ progenitors (Glickstein et al., 2009). Given the explained correlation between S phase duration and the neurogenic capacity of NPCs (Arai et al., 2011), the observation that IPs from *Cyclin D2* null embryos not only show the expected G1 lengthening but also a shorter S phase indicates that IP terminal divisions should be increased in these mutants.

Similar to Cyclin D1, the phosphorylation of Cyclin D2 on a Thr residue in the C-terminal region of the protein induces its nuclear export and subsequent degradation *via* the ubiquitin- proteasome pathway in primary leukemic and myeloma cells (Kida et al., 2007). This Thr in Cyclin D2 is within a consensus sequence for DYRK1A phosphorylation. Thus, phosphorylation of Cyclin D2 by DYRK1A could be a mean of regulating Cyclin D2 turnover in IPs. In this hypothetical situation, the overexpression of DYRK1A could have an impact on G1 phase duration and, consequently, on the fate of IP daughter cells. Several experiments need to be performed to test this possibility including in *vivo* measurement of Cyclin D2 protein levels in the available *Dyrk1a* mutant mice.

1.4 Proliferative defects in the ventral medial ganglionic eminence

We have observed that in mBACTg*Dyrk1a* embryos the pool of MGE Nkx2.1 progenitors that give rise to SST and PV interneurons is expanded during early neurogenesis (see Figure R-32) and that this expansion correlates with a significant increase in cell cycle exit rates (see Figure R-33 and R-34). We have also observed that cell cycle exit rates in this particular proliferative domain decrease from E13.5 to E14.5 more abruptly in mBACTg*Dyrk1a* embryos than in the wild-types, which could be indicative of a premature exhaustion of the Nkx2.1 progenitor pool in the transgenic condition (see Figure R-36). The generation of SST and PV Nkx2.1-derived interneurons takes place in two partially overlapping waves that peak at two different developmental times; first the neurogenic SST wave and after PV neurogenic wave (Inan et al., 2012; see Figure I-8). Thus, the number of Nkx2.1 progenitors and the cell cycle exit rates in the Nkx2.1 domain observed in mBACTg*Dyrk1a* embryos could underlie the excess of SST interneurons and the deficit of PV interneurons observed in the neocortex of this transgenic model (see Figure R-8).

During the neurogenesis of MGE interneurons, by E13.5, Cyclin D1 protein levels are normal in the ventral telencephalon of mBACTg*Dyrk1a* embryos (see Figure R-37), while in the dorsal telencephalon are lower than in the controls (see Figures R-21 and R-37). This result suggests that DYRK1A-regulation of Cyclin D1 turnover is progenitor-type specific.

Interestingly, both the initial expansion of the progenitor pool and the altered cell cycle-exit rates observed in mBACTg*Dyrk1a* embryos are not uniform along the dorso-ventral axis of the MGE, being the dorsal and medial regions the most affected ones. Given that DYRK1A is expressed uniformly in the MGE (see Figure R-11), it could be possible that DYRK1A regulates a factor that is expressed in a gradient from the dorsal to the ventral part of the MGE. Importantly, the two principal morphogens that regulate proliferation and differentiation in ventral progenitors, Shh and FGF, show a dorso-ventral gradient of activation within in the MGE (Xu et al., 2010; Bansal et al., 2003).

Shh signalling plays different roles within the ventral telencephalon: regulates the initial patterning of this brain region; maintains the fate-determining transcription factor Nkx2.1 during neurogenesis (Xu et al., 2005); and induces proliferation in the MGE (Britto et al., 2002; Machold et al., 2003). During neurogenesis Shh is expressed in the mantle zone of the MGE, where newborn neurons are localised. However, the expression of the Shh downstream targets *Gli1* and *Ptch1* indicates that Shh activity during neurogenesis occurs in the proliferative region of the MGE and that it is high in the dorsal MGE (Xu et al., 2010). Upregulation of Shh signalling in MGE progenitors expands the region of *Gli1* and *Ptch1* expression, which induces the acquisition of a dorsal fate in medial MGE progenitors and, as a consequence, the production of SST interneurons increases and the production of PV interneurons decreases (Xu et al., 2010). Given that DYRK1A positively regulates Shh signalling through phosphorylation of Gli1 (Mao et al., 2002), and that overexpression of DYRK1A and overactivation of Shh signalling

lead to similar phenotypes, it is possible that the defects in proliferation/differentiation of MGE progenitors observed in mBACTg*Dyrk1a* embryos result from an increased activity of the Shh pathway. However, this hypothesis is challenged by the unaltered expression of the main components of the Shh signalling pathway (*Ptch1*, *Gli1*, *Gli2* and *Gli3*) in the ventral telencephalon of mBACTg*Dyrk1a* embryos (see Figure R-38).

Ventral telencephalic neural precursors express three FGF receptors (FGFRs): 1, 2 and 3. FGFR1 and 3 are expressed along the VZ of the MGE in a dorso-ventral gradient, being more expressed in dorsal and medial regions (Bansal et al., 2003). The double deletion of FGFR1 and 2 in MGE progenitors impairs the establishment of the Nkx2.1 progenitor domain and leads to an ectopic ventral expression of the dorsal fate-determining transcription factor Pax6, indicating that this two receptors are crucial for the correct specification of ventral progenitors. In contrast, the double deletion of FGFR1 and 3 in MGE progenitors do not affect the specification of ventral progenitors but it impairs neuronal production by preventing cell cycle exit (Gutin et al., 2006). Therefore, both maintenance and proliferation of Nkx2.1 progenitors in the MGE are dependent on FGF signalling. DYRK1A increases FGF signalling through phosphorylation and inhibition of the FGF signalling antagonist Sprouty2 (Aranda et al., 2008). Expression of *Sprouty2* has been shown by *in situ* hybridization in the VZ of the LGE and the dorsal and medial regions of the MGE in E14.5 mouse embryos (www.genepaint.org). Thus, the alterations observed in the MGE of mBACTg*Dyrk1a* embryos could be a consequence of

increased FGF signalling. It would be interesting to experimentally assess this possibility.

1. 5 Functional consequences

We have shown that DYRK1A overexpression leads to decreased number of cortical neurons in two-month-old mBACTg*Dyrk1a* mice (see Figure R-7). Total numbers of GABAergic interneurons in mBACTg*Dyrk1a* mice are the same than in wild-type mice (unpublished data of the laboratory), which is consistent with our quantifications of the most abundant interneuron subtypes in the cerebral cortex of this model (see Figure R-8). Moreover, the proportion of excitatory neurons is decreased in mBACTg*Dyrk1a* mice, which is in agreement with the impaired neurogenesis observed in this mouse model. Next I summarize how the defects in neuron cellularity observed here in the cerebral cortex of mBACTg*Dyrk1a* mice may contribute to the altered synaptic plasticity and cognitive impairments recently described in this transgenic model (Thomazeau et al., 2014; Souchet et al., 2014).

Recent optogenetic studies have shown that PV and SST interneurons of the hippocampus and the cerebral cortex are very different in the way they control the timing, the rate and the burst of glutamatergic neurons (Royer et al., 2012; Atallah et al. 2012; Wilson et al., 2012; see Figure I-2). For example, PV interneurons, which target the soma or the initial axonal segment of pyramidal neurons, are the main interneuron-type responsible for the theta-rhythms oscillations, which synchronize cortical networks (Wulff et al., 2009), and for the generation of gamma-

rhythms oscillations, which enhance signal transmission in the neocortex, reducing circuit noise and amplifying circuit signals (Sohal et al., 2009). In contrast, SST interneurons, which target pyramidal dendrites, show spontaneous activity that provides a tonic inhibition to cortical excitatory neurons (Gentet et al., 2012). SST interneurons also mediate di-synaptic inhibition between neighbouring pyramidal neurons, receiving facilitating synapses from a pyramidal neuron and forming inhibitory synapses onto dendrites of neighbouring pyramidal neurons. This feedback pathway allows the inhibition of neighbouring pyramidal cells in an activity-dependent manner and it has been proposed as a central mechanism for the regulation of cortical activity (Berger et al., 2009; Silberberg and Markram, 2007). Therefore, although there are not differences in the total number of cortical GABAergic interneurons between mBACTg*Dyrk1a* and wild-type mice, the deficit of PV interneurons and the excess of SST interneurons here observed in the neocortex of young mBACTg*Dyrk1a* animals could have an impact on the excitability, network dynamics and functionality of the cerebral cortex.

In addition, the deficit of glutamatergic neurons observed in *Dyrk1a* transgenic mice might alter the excitatory/inhibitory balance of the cerebral cortex towards an over-inhibition. In agreement with this, mBACTg*Dyrk1a* mice show impaired LTP in the prefrontal cortex and a low performance in a cortical dependent short-term memory task (Thomazeau et al., 2014; Souchet et al., 2014). mBACTg*Dyrk1a* mice also show a imbalance towards an excess of inhibition in excitatory/inhibitory synaptic proteins in the hippocampus and this defect correlates with a low performance in the Morris water test that evaluates

hippocampal-dependent visuo-spatial learning and memory (Souchet et al., 2014). These results indicate that the excitatory/inhibitory imbalance in the mBACTg*Dyrk1a* brain is not restricted to the cerebral cortex.

Cortical glutamatergic neurons send axons to intracortical and subcortical brain areas (Franco and Muller, 2013). Therefore, the neuronal deficit in mBACTg*Dyrk1a* mice could lead to a reduction in cortical afferences and efferences that may disturb the global wiring of the brain.

Finally, it is worthy to say that DYRK1A plays a role in dendritogenesis and in synaptic vesicle endocytosis (Park and Chung, 2013), functions that may also be disturbed in the cerebral cortex of mBACTg*Dyrk1a* mice contributing to the deficits in synaptic plasticity, learning and memory observed in this transgenic model (Thomazeau et al., 2014; Souchet et al., 2014). This possibility will be later discussed in the Chapter 2.2 in this section.

2. Contribution of *DYRK1A* trisomy on the developmental brain alterations associated with Down syndrome

2.1 Development of the cerebral cortex

The cerebral cortex of DS individuals show decreased cellularity and alterations in lamination, defects that arise during prenatal development (see Chapter 2.5 in the Introduction section). The analysis of the development of the cerebral cortex in the trisomic

Ts65Dn model showed that defects in cortical neuron cellularity in this model start early in development and that involved alterations in the neurogenesis of both the pallium and the subpallium (Chakrabarti et al., 2007, 2010). Importantly, this analysis showed that neurogenic defects in the pallium were associated with an increased cell cycle duration of RG progenitors (Chakrabarti et al., 2007). Next, I will comment on the possible contribution of *Dyrk1a* on these phenotypes.

Neurogenic defects in the subpallium of Ts65Dn embryos lead to an excess of GABAergic interneurons in the neocortex of postnatal trisomic mice that results from a specific increase in SST and PV interneurons (Chakrabarti et al., 2010). In contrast, the numbers of GABAergic interneurons in the same cortical region of young mBACTg*Dyrk1a* mice was normal but they had an excess of SST interneurons and a deficit of PV interneurons (see Figure R-8). The different phenotype of these two models indicate that triplication of *Dyrk1a* is not the cause of the interneuron phenotype in the Ts65Dn mouse, although it may contribute to the phenotype. Indeed, *in vivo* genetic rescue experiments have shown that normalization of the dosage of *Olig1/Olig2* genes is sufficient to completely rescue the GABAergic phenotype in Ts65Dn mice (Chakrabarti et al., 2010).

In contrast to the situation in the subpallium, there are striking similarities in the development of the dorsal telencephalon between the Ts65Dn model and the mBACTg*Dyrk1a* model. Both models show a severe deficit of neurons during early neurogenesis and more IPs in the SVZ at mid-corticogenesis. Moreover, both models have RG progenitors with longer cell cycle duration that results from a specific lengthening of the cell

cycle phases G1 and S (Chakrabarti et al., 2007) (see Figures R-13, R-16 and R-25).

Our analysis of early dorsal neurogenesis in Ts65Dn embryos revealed that like in mBACTg*Dyrk1a* embryos, Ts65Dn RG progenitors generate less neurons and more IPs (see Figure R-29). The complete rescue of the phenotype by normalizing the dosage of *Dyrk1a* in Ts65Dn embryos (see Figure R-29) demonstrate that triplication of *Dyrk1a* is sufficient to attenuate RG-derived neurogenesis in the Ts65Dn developing neocortex.

Recently, it has been suggested that defects in cortical neurogenesis associated with DS could be caused by an increased NFATc activity due to the trisomy of *DYRK1A* and *DSCR1* (also known as *RCAN1;* Kurabayashi and Sanada, 2013). In this study it was shown that the overexpression of DYRK1A and DSCR1 in dorsal telencephalic progenitors achieved by *in utero* electroporation of expression plasmids attenuates neuron production, an effect that requires the cooperative action of these two proteins on NFATc activity (Kurabayashi and Sanada, 2013). Upon activation of the calcineurin-NFATc signalling pathway, NFATc transcription factors are dephosphorylated in the cytoplasm by the phosphatase calcineurin inducing their translocation into the nucleus. This pathway is negatively regulated by DYRK1A, which phosphorylates active NFATc (Gwack et al., 2006; Arron et al. 2006) and by RCAN1, which can inhibit calcineurin activity (Park et al., 2009). In fact it has been proposed that in DS there is an increased NFATc activity due to the genetic interaction of *DYRK1A* and *RCAN1* (Arron et al., 2006; de la Luna and Estivill, 2006). However, NFATC activity is not significantly disturbed in mBACTg*Dyrk1a* progenitors since

Rcan1-4 gene expression, which is induced by calcineurin-NFATc signalling (Yang et al., 2000, Davies et al., 2007), is not altered in mBACTg*Dyrk1a* RG progenitors. Therefore trisomy of *Dyrk1a* is sufficient to attenuate early cortical neurogenesis without disturbing calcineurin-NFATc signalling. Tacking into account that Rcan1 levels are normal in the telencephalon of mBACTg*Dyrk1a*, that *Rcan 1* is in the chromosomal region that is triplicated in the Ts65Dn model (Haydar and Reeves, 2012), and our genetic rescue experiment performed in Ts65Dn embryos, we propose that overexpression of DYRK1A attenuates early cortical neurogenesis in DS through a mechanisms that is independent on the action of DYRK1A on NFATc activity. Our results showing that mBACTg*Dyrk1a* RG progenitors have similar cell cycle alterations than those previously reported in the Ts65Dn model, that nuclear Cyclin D1 levels are reduced in the dorsal telencephalon of Ts65Dn embryos (Figure R-26), and that genetic normalization of *Dyrk1a* dosage restores Cyclin D1 levels in the trisomic embryos (see Figures R-28) strongly suggest that cell cycle alterations in Ts65Dn RG progenitors due to the action of DYRK1A on Cyclin D1 degradation are the major cause of the delayed cortical neurogenesis in the DS Ts65Dn model.

2.2 Functionality of the brain

Adult Ts65Dn mice show impaired LTP in the hippocampus and deficits in hippocampal-dependent cognitive tasks, alterations that are caused, at least in part, by an excess of inhibitory currents due to an increased number of GABAergic interneurons and an increased proportion of inhibitory synapses in the hippocampus (Chakrabarti et al., 2010; Belichenko et al., 2009).

Indeed, it has been shown that chronic systemic treatment of Ts65Dn mice with $GABA_A$ antagonists at non-epileptic doses causes a persistent post-drug recovery of both, hippocampal LTP and hippocampal-dependent cognitive tasks (Fernandez et al., 2007). As already mentioned, the cerebral cortex of adult Ts65Dn mice also shows an imbalanced number of excitatory and inhibitory neurons (Chakrabarti et al., 2010), suggesting that there could be an over-inhibition also in this structure. In addition, the Ts65Dn mouse presents other phenotypes that might contribute to an excess of GABAergic inhibition in the cerebral cortex. Cortical pyramidal neurons in this mouse model show small dendritic arborization, decreased number of synapses and dendritic spine abnormalities (Dierssen et al.; 2003). All these observations strongly suggest that excitatory currents in the cerebral cortex may be reduced, not only by the decreased number of cortical glutamatergic neurons but also by a deficient connection of these neurons. A post-mortem Golgi study of cortical pyramidal cells from DS children and adults revealed similar alterations: the morphology of the dendritic arbor is altered and dendrites have less spines (Takashima et al., 1989; Marin-Padilla, 1976). Therefore, alterations in the cerebral cortex circuitry could be on the basis of the cognitive impairment associated with DS.

As it has been previously explained (see Chapter 1.5 in this section), there is evidence that, like in the Ts65Dn mouse, the mBACTg*Dyrk1a* mouse could have an over-inhibition of the cortical circuitry. This defect may result from the combination of the altered cortical glutamatergic and GABAergic neurogenesis described in this work and by a possible detrimental effect of

DYRK1A overexpression in neuritogenesis and synaptogenesis (see Chapter 3.4 in the Introduction section). Indeed, the dendritic arbor of cortical pyramidal neurons is also small in transgenic mice overexpressing *Dyrk1a* under a heterologous promoter (Martinez de Lagran et al., 2012) and in *Dyrk1a*$^{+/-}$ mice (Benavides-Piccione et al., 2005). This *Dyrk1a* transgenic model also presents decreased number of spines, impair neurite growth and decreased number of synapses (Martinez de Lagran et al., 2012). The effect of DYRK1A on the regulation of microtubule dynamics and actin polymerization may be on the basis of these defects (Park et al., 2012; Scales et al., 2009; Martinez de Lagran et al., 2012).

Protein levels of some glutamatergic synaptic markers, such as the vesicular glutamate transporter 1 (vGlut1) and the glutamate receptor subunits NR1 and NR2A, are decreased in the cerebral cortex and the hippocampus of mBACTg*Dyrk1a* mice. Moreover, in both structures, there is an increased expression of GABAergic synaptic proteins, such as the vesicular GABA transporter and the enzyme glutamate decarboxylase (Souchet et al., 2014). These alterations are also observed in the cerebral cortex of the DS mouse models Ts65Dn and Dp(16)1Yey/+ (Souchet et al., 2014), further indicating that the overexpression of DYRK1A in these models contribute to the imbalanced numbers of excitatory/inhibitory synapses.

Altogether, these observations show that triplication of the *DYRK1A* gene could contribute to the formation of the brain synaptic circuitry in DS at the cellular level, altering neurogenesis in the pallium and the subpallium, and at the synaptic level, altering neuritogenesis and spine formation.

2.3 Brain size and morphology

The brain of DS individuals shows brachycephaly, reduced volume and enlarged ventricles, alterations that arise during development (see Chapter 2.4 in the Introduction section). The overall brain size in Ts65Dn and TsCje1 mice is normal (Baxter et al., 2000; Aldridge et al., 2007; Ishihara et al., 2010), but slightly increased in the Ts1Rhr mouse (Olson et al., 2007), which is the one carrying the smaller trisomic region since it only has in trisomy the genes included in the DSCR (see Figure I-10). This indicates that the overexpression of one or more genes within this minimal critical region is causing the brain overgrowth in this model and that common triplicated genes in TsCje1 and Ts65Dn mice outside this region are counteracting this overgrowth. Moreover, the morphometric analysis of the brain in these models suggest the possibility that HSA21 gene/s that are not in trisomy in the Ts65Dn model should be the ones responsible of the brain size reduction in DS. Other possibilities to explain the normal brain size in the Ts65Dn mouse include differences on the functionality of the triplicated genes between humans and mice.

The overall size of the brain is increased in the mBACTg*Dyrk1a* model (see Figure R-2; Guedj et al., 2012). A similar increase in brain size has been previously observed in the TgYAC152F7 mouse model that contains five HSA21 genes in trisomy including *DYRK1A* (Sebrie et al., 2008; Branchi et al., 2004). On the contrary, the brain size of another YAC transgenic mouse, TgYAC141G6, which carries an extra copy of all the genes included in TgYAC152F7 except *DYRK1A*, is normal (Branchi et al., 2004). Importantly, brain size in TgYAC152F7 mice is

normalized upon prenatal treatment with the DYRK1A inhibitor EGCG (Guedj et al., 2009). All these observations strongly suggest that triplication of *DYRK1A* is contributing to the brain size phenotype in the Ts1Rhr mouse model. In addition, the anatomical comparison of the brain in the mBACTg*Dyrk1a* mouse and the *Dyrk1a*$^{+/-}$ mouse (see Figure R-2) shows that DYRK1A regulates brain growth in a dosage dependent manner.

Brain size is determined by the balance between neural proliferation and programmed cell death. During the proliferative phase of brain development neuroepithelial cells undergo self-renewing symmetric divisions to increase the pool of neural progenitors and horizontally expand the ventricle wall (Noctor et al., 2004), which will influence the final size of the brain. Programmed cell death occurs from early stages of embryonic development to postnatal development when synaptogenesis is taking place and is involved in brain morphology and in the refinement of the final number of neurons in the brain (Haydar et al., 1999). Several evidences show that these two processes have a fundamental role in the formation of the cerebral cortex. The increased self-renewal divisions of forebrain neuroepithelial cells induced by a constitutive activation of the Wnt/β-catenin pathway leads to a significant enlargement of the cortical surface that can form cerebral convolutions (Chenn and Walsh, 2002). Caspase-3 and caspase-9 knockout mice present an enlarged cerebral cortex with convolutions due to the lack of apoptotic cell death during embryonic development (Kuida et al., 1996, 1998) In addition to regulate neural proliferation, DYRK1A inhibits caspase-9-mediated apoptosis in differentiating neurons in at least two CNS structures: the retina (Laguna et al., 2008; 2013)

and the ventral mesencephalon (Barallobre et al., 2014). In these two structures neurogenesis in mBACTg*DYRK1A* and *Dyrk1a*$^{+/-}$ embryos is normal but the number of neurons in postnatal mice is increased in *Dyrk1a* transgenic animals and decreased in *Dyrk1a* haploinsufficient animals (Laguna et al., 2008; Barallobre et al., 2014). Contrary, in this work we show that postnatal *Dyrk1a* transgenic animals have less neurons in the neocortex while *Dyrk1a* haploinsufficient animals have more (see Figures R-7). Moreover, the results showing normal numbers of active caspase-3 in the dorsal telencephalon of mBACTg*Dyrk1a* embryos (see Figure R-13) indicate that developmental apoptosis is not altered in this structure.

We have observed that at the beginning of cortical neurogenesis, by E11.5, the length of the telencephalic neuroepithelium is reduced in *Dyrk1a*$^{+/-}$ embryos and increased in mBACTg*Dyrk1a* embryos (data non shown), which is in accordance with the overall brain size defects in the two models. This suggests that horizontal expansion of dorsal neuroepithelial cells is increased in the *Dyrk1a* transgenic model while, as we have already discussed, cortical radial expansion is delayed. Thus, the overexpression of DYRK1A, in addition to promote asymmetric RG-proliferative divisions, it might promote symmetric self-renewing divisions in VZ progenitors.

Despite brain size alterations in DS and in mBACTg*Dyrk1a* mice are opposite, both brains show brachycephaly (see Figures R-1 and R-2) (Pinter et al., 2001), a defect that can be also observed in the DS trisomic mouse models Ts65Dn, Ts1Rhr and TsCje1 mice (Richtsmeier et al., 2002; Aldridge et al., 2007; see Figure R-3). Brachycephaly is characterised by decreased rostro-caudal

length and increased dorso-ventral length and it can be caused by abnormal growth of different brain regions (Moss and Young, 1960). In agreement, with the alterations in brain size and brain cellularity reported here and by others in *Dyrk1a* gain- and loss-of-function mutant mice indicate that the effect of DYRK1A in brain development is region-specific. In these mutants, some brain structures such as the tectum and thalamus show important size alterations (see Figure R-2; Guedj et al., 2012), while alterations in other structures such as the cerebral cortex are more modest (see Figures R-2 and R-5). The similar morphology of the brain in mBACTg*Dyrk1a* and Ts65Dn mice (see Figures R-2 and R-3), strongly suggests that brachycephaly in this DS mouse model could be caused by the region-specific effect of DYRK1A overexpression in brain growth.

The rostro-caudal and the dorso-ventral axis of the brain are established by different morphogens that are secreted from distinct signalling centers and regulate progenitors proliferation and differentiation (Suzuki-Hirano and Shimogori, 2009; Alexandre and Wassef, 2005). One of the principal brain morphogen is FGF8, which has been involved in the patterning of the telencephalon, but also in the patterning of the diencephalon, the midbrain and the hindbrain (Alexandre and Wassef, 2005; Suzuki-Hirano and Shimogori, 2009). It is believed that the ability of FGF8 to pattern the brain relies on the selective expression of transcription factors and other cell-intrinsic factors, which restrict the expression of targets of FGF8 signalling in a region-specific manner (Reim and Brand, 2002). Similarly, programmed cell death can also contribute to abnormal brain morphology since it does not occur homogenously among all brain regions (Urase et

al., 2003; Kuida et al., 1998). Therefore, alterations in programmed cell death and/or in morphogens that regulate brain patterning and progenitor proliferation could lead to abnormal brain morphology, such as brachycephaly.

Premature fusion and ossification of the coronal sutures that joint frontal and parietal bones also can cause brachycephaly (Slater et al., 2008). There is evidence that this process is regulated by FGF signalling: 1) FGF ligands and their receptors are expressed in cranial sutures during embryonic development and regulate foetal bone growth (Kimonis et al., 2007); 2) Gain-of-function mutations in the *FGFR1*, *FGFR2* and *FGFR3* are observed in humans with brachycephaly and other type of craniosynostosis (Kimonis et al., 2007); and 3) Cranial sutures release FGF2 in response to the physical tensions generated by the growing brain, which increases cell membrane permeability and induces its ossification (Moss and Young, 1960; Yu et al., 2001).

Taking into account all these data, and that DYRK1A positively regulates FGF signalling (Aranda et al., 2008) and it is expressed in the mouse cranium during development (unpublished data of the laboratory), it is possible that alterations in FGF-dependent patterning of the brain and/or coronal sutures ossification due to the overexpression of DYRK1A contribute to the brachycephaly observed in mBACTg*Dyrk1a*, Ts65Dn and TsCje1 mice.

2.4 Final considerations about therapeutic interventions

DYRK1A has been proposed as a therapeutic target to ameliorate the cognitive deficit associated with DS (Guedj et al.,

2014) and in fact, treatment with the DYRK1A inhibitor EGCG has been successfully used in DS mouse models and in a pilot study with young DS individuals to improve long-term memory (De la Torre et al., 2014). However, our results indicate that the detrimental effect of DYRK1A overexpression on brain circuitry formation begins early in development and, therefore, therapeutic interventions to correct structural brain defects is DS should start as early as possible. Other important aspects that should be taken into consideration for prenatal therapies in DS targeting DYRK1A are the pathogenic effect of an excess of DYRK1A inhibition (see next Chapter) and the opposite effects that DYRK1A overexpression have on different types of neural precursors (*i.e.*: decrease neurogenesis in the dorsal telencephalon and increased neurogenesis in the ventral). It should also take into consideration the differences between the mBACTg*Dyrk1a* model and the Ts65Dn model (*i.e.*: brain size and total number of cortical GABAergic neurons).

In summary our results suggest that a systemic reduction of DYRK1A kinase activity during gestation is not a good therapy to prevent developmental brain defects in DS and that it will be required to find more specific strategies.

3. DYRK1A monosomies

DYRK1A haploinsufficiency in humans leads to primary microcephaly, cognitive impairments, epilepsy (Courcet et al., 2012) and autism (O'Roak et al., 2012). *Dyrk1a* loss-of-function in mice also leads to microcephaly (Fotaki et al., 2002), cognitive impairments (Arque et al., 2008) and sporadic seizures

(observations from our laboratory), indicating that the pathological mechanisms for these alterations are similar in both species. Cognitive impairment and epilepsy might be caused by an imbalance between excitatory/inhibitory inputs in the cerebral cortex (Marin, 2012), which is one of the relevant epileptogenic regions of the brain (Goldberg and Coulter, 2013). On the other hand, a recent construction of coexpression networks capturing spatial and temporal dimensions of *DYRK1A* and other autism spectrum disorder genes during human brain development led to the conclusion that perturbations in the formation of cortical early neural circuits, mainly those localised in layers V and VI, are likely to increase the risk for autism spectrum disorder (Willsey et al., 2013).

Here we show that early production of RG-derived neurons in the dorsal telencephalon of *Dyrk1a*$^{+/-}$ embryos is significantly increased (see Figures R-15 and R-29), which leads to increased number of glutamatergic neurons in internal cortical layers at postnatal stages (see Figure R-30). In addition, data from the laboratory show that, like in the mBACTg*Dyrk1a* model, young *Dyrk1a*$^{+/-}$ mice show abnormal number of GABAergic interneurons in the cerebral cortex. These defects likely result in an altered excitability of the cerebral cortex that could contribute to the cognitive impairment and other neurological defects associated to heterozygous mutations in the *DYRK1A* gene, such as epilepsy and autistic behaviour.

Despite a more detailed analysis of the development of the cerebral cortex in the *Dyrk1a* haploinsufficient mouse model should be performed, the observations presented in this work related to the levels of Cyclin D1 in cortical RG progenitors and

the neurogenic defects of these progenitors provide some insights into the aetiology of the neurological alterations in humans with haploinsufficient mutations in the *DYRK1A* gene.

CONCLUSIONS

The main conclusion of this Thesis is that the overexpression of DYRK1A contributes to shape the brain circuitry in Down syndrome.

The specific conclusions of the work are:

1) Trisomy of mouse *Dyrk1a* alters the growth of the brain in a region-specific manner.

2) mBACTg*Dyrk1a* and Ts56Dn mice present common morphological brain alterations.

3) The cerebral cortex of mBACTg*Dyrk1a* and *Dyrk1a*$^{+/-}$ mice show alterations in lamination and neuron cell densities. Cell density defects in these mutants inversely correlate with the number of *Dyrk1a* alleles.

4) *Dyrk1a* gene-dosage variation biases the asymmetric division mode of embryonic dorsal telencephalic radial glial progenitors, promoting proliferative divisions when *Dyrk1a* is in trisomy and neurogenic divisions when the gene is in monosomy.

5) Neuron production in the dorsal telencephalon of mBACTg*Dyrk1a* embryos is altered along corticogenesis leading to a deficit of glutamatergic neurons in external and internal layers of the postnatal cerebral cortex.

6) Total cell cycle duration and G1 phase duration are increased in dorsal radial glial progenitors of mBACTg*Dyrk1a* embryos.

7) DYRK1A-mediated degradation of Cyclin D1 is the underlying cause of the G1 phase lengthening in mBACTg*Dyrk1a* and Ts65Dn dorsal radial glial progenitors.

8) Trisomy of *DYRK1A* causes the deficit of neocortical early-born glutamatergic neurons in Ts65Dn mice.

9) Neurogenesis is altered in the medial ganglionic eminence of mBACTg*Dyrk1a* embryos, which leads to abnormal numbers of somatostatin and parvalbumin GABAergic interneurons in the adult neocortex.

BIBLIOGRAPHY

Aaku-Saraste, E., Hellwig, A., and Huttner, W.B. 1996. Loss of occludin and functional tight junctions, but not ZO-1, during neural tube closure--remodeling of the neuroepithelium prior to neurogenesis. *Dev Biol* **180**(2): 664-679.

Ahn, K.J., Jeong, H.K., Choi, H.S., Ryoo, S.R., Kim, Y.J., Goo, J.S., Choi, S.Y., Han, J.S., Ha, I., and Song, W.J. 2006. DYRK1A BAC transgenic mice show altered synaptic plasticity with learning and memory defects. *Neurobiol Dis* **22**(3): 463-472.

Alcantara, S., Frisen, J., del Rio, J.A., Soriano, E., Barbacid, M., and Silos-Santiago, I. 1997. TrkB signaling is required for postnatal survival of CNS neurons and protects hippocampal and motor neurons from axotomy-induced cell death. *J Neurosci* **17**(10): 3623-3633.

Aldridge, K., Reeves, R.H., Olson, L.E., and Richtsmeier, J.T. 2007. Differential effects of trisomy on brain shape and volume in related aneuploid mouse models. *Am J Med Genet A* **143A**(10): 1060-1070.

Alexandre, P. and Wassef, M. 2005. Does the isthmic organizer influence D/V patterning of the midbrain? *Brain Res Brain Res Rev* **49**(2): 127-133.

Ali, F., Hindley, C., McDowell, G., Deibler, R., Jones, A., Kirschner, M., Guillemot, F., and Philpott, A. 2011. Cell cycle-regulated multi-site phosphorylation of Neurogenin 2 coordinates cell cycling with differentiation during neurogenesis. *Development* **138**(19): 4267-4277.

Altafaj, X., Dierssen, M., Baamonde, C., Marti, E., Visa, J., Guimera, J., Oset, M., Gonzalez, J.R., Florez, J., Fillat, C. et al. 2001. Neurodevelopmental delay, motor abnormalities and cognitive deficits in transgenic mice overexpressing Dyrk1A (minibrain), a murine model of Down's syndrome. *Hum Mol Genet* **10**(18): 1915-1923.

Altafaj, X., Ortiz-Abalia, J., Fernandez, M., Potier, M.C., Laffaire, J., Andreu, N., Dierssen, M., Gonzalez-Garcia, C., Cena, V., Marti, E. et al. 2008. Increased NR2A expression and prolonged decay of NMDA-induced calcium transient in cerebellum of TgDyrk1A mice, a mouse model of Down syndrome. *Neurobiol Dis* **32**(3): 377-384.

Alvarez, M., Altafaj, X., Aranda, S., and de la Luna, S. 2007. DYRK1A autophosphorylation on serine residue 520 modulates its kinase activity via 14-3-3 binding. *Mol Biol Cell* **18**(4): 1167-1178.

Alvarez, M., Estivill, X., and de la Luna, S. 2003. DYRK1A accumulates in splicing speckles through a novel targeting

signal and induces speckle disassembly. *J Cell Sci* **116**(Pt 15): 3099-3107.

Anderson, C.T. and Stearns, T. 2009. Centriole age underlies asynchronous primary cilium growth in mammalian cells. *Curr Biol* **19**(17): 1498-1502.

Anthony, T.E., Mason, H.A., Gridley, T., Fishell, G., and Heintz, N. 2005. Brain lipid-binding protein is a direct target of Notch signaling in radial glial cells. *Genes Dev* **19**(9): 1028-1033.

Antonarakis, S.E., Lyle, R., Dermitzakis, E.T., Reymond, A., and Deutsch, S. 2004. Chromosome 21 and down syndrome: from genomics to pathophysiology. *Nat Rev Genet* **5**(10): 725-738.

Arai, Y., Pulvers, J.N., Haffner, C., Schilling, B., Nusslein, I., Calegari, F., and Huttner, W.B. 2011. Neural stem and progenitor cells shorten S-phase on commitment to neuron production. *Nat Commun* **2**: 154.

Aranda, S., Alvarez, M., Turro, S., Laguna, A., and de la Luna, S. 2008. Sprouty2-mediated inhibition of fibroblast growth factor signaling is modulated by the protein kinase DYRK1A. *Mol Cell Biol* **28**(19): 5899-5911.

Aranda, S., Laguna, A., and de la Luna, S. 2011. DYRK family of protein kinases: evolutionary relationships, biochemical properties, and functional roles. *FASEB J* **25**(2): 449-462.

Arlotta, P., Molyneaux, B.J., Chen, J., Inoue, J., Kominami, R., and Macklis, J.D. 2005. Neuronal subtype-specific genes that control corticospinal motor neuron development in vivo. *Neuron* **45**(2): 207-221.

Arque, G., Fotaki, V., Fernandez, D., Martinez de Lagran, M., Arbones, M.L., and Dierssen, M. 2008. Impaired spatial learning strategies and novel object recognition in mice haploinsufficient for the dual specificity tyrosine-regulated kinase-1A (Dyrk1A). *PLoS One* **3**(7): e2575.

Arron, J.R., Winslow, M.M., Polleri, A., Chang, C.P., Wu, H., Gao, X., Neilson, J.R., Chen, L., Heit, J.J., Kim, S.K. et al. 2006. NFAT dysregulation by increased dosage of DSCR1 and DYRK1A on chromosome 21. *Nature* **441**(7093): 595-600.

Ashford, A.L., Oxley, D., Kettle, J., Hudson, K., Guichard, S., Cook, S.J., and Lochhead, P.A. 2014. A novel DYRK1B inhibitor AZ191 demonstrates that DYRK1B acts independently of GSK3beta to phosphorylate cyclin D1 at Thr(286), not Thr(288). *Biochem J* **457**(1): 43-56.

Atallah, B.V., Bruns, W., Carandini, M., and Scanziani, M. 2012. Parvalbumin-expressing interneurons linearly transform cortical responses to visual stimuli. *Neuron* **73**(1): 159-170.

Attardo, A., Calegari, F., Haubensak, W., Wilsch-Brauninger, M., and Huttner, W.B. 2008. Live imaging at the onset of cortical neurogenesis reveals differential appearance of the neuronal phenotype in apical versus basal progenitor progeny. *PLoS One* **3**(6): e2388.

Aylward, E.H., Li, Q., Honeycutt, N.A., Warren, A.C., Pulsifer, M.B., Barta, P.E., Chan, M.D., Smith, P.D., Jerram, M., and Pearlson, G.D. 1999. MRI volumes of the hippocampus and amygdala in adults with Down's syndrome with and without dementia. *Am J Psychiatry* **156**(4): 564-568.

Bain, J., McLauchlan, H., Elliott, M., and Cohen, P. 2003. The specificities of protein kinase inhibitors: an update. *Biochem J* **371**(Pt 1): 199-204.

Bansal, R., Lakhina, V., Remedios, R., and Tole, S. 2003. Expression of FGF receptors 1, 2, 3 in the embryonic and postnatal mouse brain compared with Pdgfralpha, Olig2 and Plp/dm20: implications for oligodendrocyte development. *Dev Neurosci* **25**(2-4): 83-95.

Barallobre, M.J., Perier, C., Bove, J., Laguna, A., Delabar, J.M., Vila, M., and Arbones, M.L. 2014. DYRK1A promotes dopaminergic neuron survival in the developing brain and in a mouse model of Parkinson's disease. *Cell Death Dis* **5**: e1289.

Barnabe-Heider, F., Wasylnka, J.A., Fernandes, K.J., Porsche, C., Sendtner, M., Kaplan, D.R., and Miller, F.D. 2005. Evidence that embryonic neurons regulate the onset of cortical gliogenesis via cardiotrophin-1. *Neuron* **48**(2): 253-265.

Bartolini, G., Ciceri, G., and Marin, O. 2013. Integration of GABAergic interneurons into cortical cell assemblies: lessons from embryos and adults. *Neuron* **79**(5): 849-864.

Batista-Brito, R., Rossignol, E., Hjerling-Leffler, J., Denaxa, M., Wegner, M., Lefebvre, V., Pachnis, V., and Fishell, G. 2009. The cell-intrinsic requirement of Sox6 for cortical interneuron development. *Neuron* **63**(4): 466-481.

Baxter, L.L., Moran, T.H., Richtsmeier, J.T., Troncoso, J., and Reeves, R.H. 2000. Discovery and genetic localization of Down syndrome cerebellar phenotypes using the Ts65Dn mouse. *Hum Mol Genet* **9**(2): 195-202.

Becker, L., Mito, T., Takashima, S., and Onodera, K. 1991. Growth and development of the brain in Down syndrome. *Prog Clin Biol Res* **373**: 133-152.

Becker, W. and Joost, H.G. 1999. Structural and functional characteristics of Dyrk, a novel subfamily of protein kinases with dual specificity. *Prog Nucleic Acid Res Mol Biol* **62**: 1-17.

Becker, W., Weber, Y., Wetzel, K., Eirmbter, K., Tejedor, F.J., and Joost, H.G. 1998. Sequence characteristics, subcellular localization, and substrate specificity of DYRK-related kinases, a novel family of dual specificity protein kinases. *J Biol Chem* **273**(40): 25893-25902.

Belichenko, N.P., Belichenko, P.V., Kleschevnikov, A.M., Salehi, A., Reeves, R.H., and Mobley, W.C. 2009a. The "Down syndrome critical region" is sufficient in the mouse model to confer behavioral, neurophysiological, and synaptic phenotypes characteristic of Down syndrome. *J Neurosci* **29**(18): 5938-5948.

Belichenko, P.V., Kleschevnikov, A.M., Masliah, E., Wu, C., Takimoto-Kimura, R., Salehi, A., and Mobley, W.C. 2009b. Excitatory-inhibitory relationship in the fascia dentata in the Ts65Dn mouse model of Down syndrome. *J Comp Neurol* **512**(4): 453-466.

Belichenko, P.V., Masliah, E., Kleschevnikov, A.M., Villar, A.J., Epstein, C.J., Salehi, A., and Mobley, W.C. 2004. Synaptic structural abnormalities in the Ts65Dn mouse model of Down Syndrome. *J Comp Neurol* **480**(3): 281-298.

Benavides-Piccione, R., Dierssen, M., Ballesteros-Yanez, I., Martinez de Lagran, M., Arbones, M.L., Fotaki, V., DeFelipe, J., and Elston, G.N. 2005. Alterations in the phenotype of neocortical pyramidal cells in the Dyrk1A+/- mouse. *Neurobiol Dis* **20**(1): 115-122.

Bentivoglio, M. and Mazzarello, P. 1999. The history of radial glia. *Brain Res Bull* **49**(5): 305-315.

Berger, J., Berger, S., Tuoc, T.C., D'Amelio, M., Cecconi, F., Gorski, J.A., Jones, K.R., Gruss, P., and Stoykova, A. 2007. Conditional activation of Pax6 in the developing cortex of transgenic mice causes progenitor apoptosis. *Development* **134**(7): 1311-1322.

Berger, T.K., Perin, R., Silberberg, G., and Markram, H. 2009. Frequency-dependent disynaptic inhibition in the pyramidal network: a ubiquitous pathway in the developing rat neocortex. *J Physiol* **587**(Pt 22): 5411-5425.

Betizeau, M., Cortay, V., Patti, D., Pfister, S., Gautier, E., Bellemin-Menard, A., Afanassieff, M., Huissoud, C., Douglas, R.J., Kennedy, H. et al. 2013. Precursor diversity and complexity of lineage relationships in the outer subventricular zone of the primate. *Neuron* **80**(2): 442-457.

Bienvenu, F., Jirawatnotai, S., Elias, J.E., Meyer, C.A., Mizeracka, K., Marson, A., Frampton, G.M., Cole, M.F., Odom, D.T., Odajima, J. et al. 2010. Transcriptional role of

cyclin D1 in development revealed by a genetic-proteomic screen. *Nature* **463**(7279): 374-378.

Blaschke, A.J., Staley, K., and Chun, J. 1996. Widespread programmed cell death in proliferative and postmitotic regions of the fetal cerebral cortex. *Development* **122**(4): 1165-1174.

Bonni, A., Sun, Y., Nadal-Vicens, M., Bhatt, A., Frank, D.A., Rozovsky, I., Stahl, N., Yancopoulos, G.D., and Greenberg, M.E. 1997. Regulation of gliogenesis in the central nervous system by the JAK-STAT signaling pathway. *Science* **278**(5337): 477-483.

Bozzi, Y., Casarosa, S., and Caleo, M. 2012

. Epilepsy as a neurodevelopmental disorder. *Front Psychiatry* **3**: 19.

Branchi, I., Bichler, Z., Minghetti, L., Delabar, J.M., Malchiodi-Albedi, F., Gonzalez, M.C., Chettouh, Z., Nicolini, A., Chabert, C., Smith, D.J. et al. 2004. Transgenic mouse in vivo library of human Down syndrome critical region 1: association between DYRK1A overexpression, brain development abnormalities, and cell cycle protein alteration. *J Neuropathol Exp Neurol* **63**(5): 429-440.

Breunig, J.J., Haydar, T.F., and Rakic, P. 2011. Neural stem cells: historical perspective and future prospects. *Neuron* **70**(4): 614-625.

Britto, J., Tannahill, D., and Keynes, R. 2002. A critical role for sonic hedgehog signaling in the early expansion of the developing brain. *Nat Neurosci* **5**(2): 103-110.

Brown, K.N., Chen, S., Han, Z., Lu, C.H., Tan, X., Zhang, X.J., Ding, L., Lopez-Cruz, A., Saur, D., Anderson, S.A. et al. 2011. Clonal production and organization of inhibitory interneurons in the neocortex. *Science* **334**(6055): 480-486.

Bulfone, A., Smiga, S.M., Shimamura, K., Peterson, A., Puelles, L., and Rubenstein, J.L. 1995. T-brain-1: a homolog of Brachyury whose expression defines molecularly distinct domains within the cerebral cortex. *Neuron* **15**(1): 63-78.

Bultje, R.S., Castaneda-Castellanos, D.R., Jan, L.Y., Jan, Y.N., Kriegstein, A.R., and Shi, S.H. 2009. Mammalian Par3 regulates progenitor cell asymmetric division via notch signaling in the developing neocortex. *Neuron* **63**(2): 189-202.

Buratti, E., De Conti, L., Stuani, C., Romano, M., Baralle, M., and Baralle, F. 2010. Nuclear factor TDP-43 can affect selected microRNA levels. *FEBS J* **277**(10): 2268-2281.

Butt, S.J., Fuccillo, M., Nery, S., Noctor, S., Kriegstein, A., Corbin, J.G., and Fishell, G. 2005. The temporal and spatial

origins of cortical interneurons predict their physiological subtype. *Neuron* **48**(4): 591-604.

Butt, S.J., Sousa, V.H., Fuccillo, M.V., Hjerling-Leffler, J., Miyoshi, G., Kimura, S., and Fishell, G. 2008. The requirement of Nkx2-1 in the temporal specification of cortical interneuron subtypes. *Neuron* **59**(5): 722-732.

Cai, L., Hayes, N.L., Takahashi, T., Caviness, V.S., Jr., and Nowakowski, R.S. 2002. Size distribution of retrovirally marked lineages matches prediction from population measurements of cell cycle behavior. *J Neurosci Res* **69**(6): 731-744.

Cai, Y., Zhang, Q., Wang, C., Zhang, Y., Ma, T., Zhou, X., Tian, M., Rubenstein, J.L., and Yang, Z. 2013. Nuclear receptor COUP-TFII-expressing neocortical interneurons are derived from the medial and lateral/caudal ganglionic eminence and define specific subsets of mature interneurons. *J Comp Neurol* **521**(2): 479-497.

Canzonetta, C., Mulligan, C., Deutsch, S., Ruf, S., O'Doherty, A., Lyle, R., Borel, C., Lin-Marq, N., Delom, F., Groet, J. et al. 2008. DYRK1A-dosage imbalance perturbs NRSF/REST levels, deregulating pluripotency and embryonic stem cell fate in Down syndrome. *Am J Hum Genet* **83**(3): 388-400.

Carmichael, C.L., Majewski, I.J., Alexander, W.S., Metcalf, D., Hilton, D.J., Hewitt, C.A., and Scott, H.S. 2009. Hematopoietic defects in the Ts1Cje mouse model of Down syndrome. *Blood* **113**(9): 1929-1937.

Catapano, L.A., Arnold, M.W., Perez, F.A., and Macklis, J.D. 2001. Specific neurotrophic factors support the survival of cortical projection neurons at distinct stages of development. *J Neurosci* **21**(22): 8863-8872.

Caviness, V.S., Jr., Goto, T., Tarui, T., Takahashi, T., Bhide, P.G., and Nowakowski, R.S. 2003. Cell output, cell cycle duration and neuronal specification: a model of integrated mechanisms of the neocortical proliferative process. *Cereb Cortex* **13**(6): 592-598.

Chabert, C., Jamon, M., Cherfouh, A., Duquenne, V., Smith, D.J., Rubin, E., and Roubertoux, P.L. 2004. Functional analysis of genes implicated in Down syndrome: 1. Cognitive abilities in mice transpolygenic for Down Syndrome Chromosomal Region-1 (DCR-1). *Behav Genet* **34**(6): 559-569.

Chakrabarti, L., Best, T.K., Cramer, N.P., Carney, R.S., Isaac, J.T., Galdzicki, Z., and Haydar, T.F. 2010. Olig1 and Olig2 triplication causes developmental brain defects in Down syndrome. *Nat Neurosci* **13**(8): 927-934.

Chakrabarti, L., Galdzicki, Z., and Haydar, T.F. 2007. Defects in embryonic neurogenesis and initial synapse formation in the forebrain of the Ts65Dn mouse model of Down syndrome. *J Neurosci* **27**(43): 11483-11495.

Chang, B., Hawes, N.L., Hurd, R.E., Davisson, M.T., Nusinowitz, S., and Heckenlively, J.R. 2002. Retinal degeneration mutants in the mouse. *Vision Res* **42**(4): 517-525.

Chapman, R.S. and Hesketh, L.J. 2000. Behavioral phenotype of individuals with Down syndrome. *Ment Retard Dev Disabil Res Rev* **6**(2): 84-95.

Chen, B., Schaevitz, L.R., and McConnell, S.K. 2005. Fezl regulates the differentiation and axon targeting of layer 5 subcortical projection neurons in cerebral cortex. *Proc Natl Acad Sci U S A* **102**(47): 17184-17189.

Chen, J.Y., Lin, J.R., Tsai, F.C., and Meyer, T. 2013. Dosage of Dyrk1a shifts cells within a p21-cyclin D1 signaling map to control the decision to enter the cell cycle. *Molecular cell* **52**(1): 87-100.

Cheng, A., Haydar, T.F., Yarowsky, P.J., and Krueger, B.K. 2004. Concurrent generation of subplate and cortical plate neurons in developing trisomy 16 mouse cortex. *Dev Neurosci* **26**(2-4): 255-265.

Chenn, A. and McConnell, S.K. 1995. Cleavage orientation and the asymmetric inheritance of Notch1 immunoreactivity in mammalian neurogenesis. *Cell* **82**(4): 631-641.

Chenn, A. and Walsh, C.A. 2002. Regulation of cerebral cortical size by control of cell cycle exit in neural precursors. *Science* **297**(5580): 365-369.

Chenn, A. and Walsh, C.A. 2003. Increased neuronal production, enlarged forebrains and cytoarchitectural distortions in beta-catenin overexpressing transgenic mice. *Cereb Cortex* **13**(6): 599-606.

Choi, B.H. and Lapham, L.W. 1978. Radial glia in the human fetal cerebrum: a combined Golgi, immunofluorescent and electron microscopic study. *Brain Res* **148**(2): 295-311.

Ciceri, G., Dehorter, N., Sols, I., Huang, Z.J., Maravall, M., and Marin, O. 2013. Lineage-specific laminar organization of cortical GABAergic interneurons. *Nat Neurosci* **16**(9): 1199-1210.

Clark, S., Schwalbe, J., Stasko, M.R., Yarowsky, P.J., and Costa, A.C. 2006. Fluoxetine rescues deficient neurogenesis in hippocampus of the Ts65Dn mouse model for Down syndrome. *Exp Neurol* **200**(1): 256-261.

Clevers, H. 2006. Wnt/beta-catenin signaling in development and disease. *Cell* **127**(3): 469-480.

Close, J., Xu, H., De Marco Garcia, N., Batista-Brito, R., Rossignol, E., Rudy, B., and Fishell, G. 2012. Satb1 is an activity-modulated transcription factor required for the terminal differentiation and connectivity of medial ganglionic eminence-derived cortical interneurons. *J Neurosci* **32**(49): 17690-17705.

Costa, A.C., Stasko, M.R., Schmidt, C., and Davisson, M.T. 2010. Behavioral validation of the Ts65Dn mouse model for Down syndrome of a genetic background free of the retinal degeneration mutation Pde6b(rd1). *Behav Brain Res* **206**(1): 52-62.

Costa, A.C., Walsh, K., and Davisson, M.T. 1999. Motor dysfunction in a mouse model for Down syndrome. *Physiol Behav* **68**(1-2): 211-220.

Courcet, J.B., Faivre, L., Malzac, P., Masurel-Paulet, A., Lopez, E., Callier, P., Lambert, L., Lemesle, M., Thevenon, J., Gigot, N. et al. 2012. The DYRK1A gene is a cause of syndromic intellectual disability with severe microcephaly and epilepsy. *J Med Genet* **49**(12): 731-736.

Cunningham, J.J. and Roussel, M.F. 2001. Cyclin-dependent kinase inhibitors in the development of the central nervous system. *Cell Growth Differ* **12**(8): 387-396.

da Costa Martins, P.A., Salic, K., Gladka, M.M., Armand, A.S., Leptidis, S., el Azzouzi, H., Hansen, A., Coenen-de Roo, C.J., Bierhuizen, M.F., van der Nagel, R. et al. 2010. MicroRNA-199b targets the nuclear kinase Dyrk1a in an auto-amplification loop promoting calcineurin/NFAT signalling. *Nat Cell Biol* **12**(12): 1220-1227.

Dave, R.K., Ellis, T., Toumpas, M.C., Robson, J.P., Julian, E., Adolphe, C., Bartlett, P.F., Cooper, H.M., Reynolds, B.A., and Wainwright, B.J. 2011. Sonic hedgehog and notch signaling can cooperate to regulate neurogenic divisions of neocortical progenitors. *PLoS One* **6**(2): e14680.

Davies, K.J., Ermak, G., Rothermel, B.A., Pritchard, M., Heitman, J., Ahnn, J., Henrique-Silva, F., Crawford, D., Canaider, S., Strippoli, P. et al. 2007. Renaming the DSCR1/Adapt78 gene family as RCAN: regulators of calcineurin. *FASEB J* **21**(12): 3023-3028.

Davisson, M.T., Schmidt, C., and Akeson, E.C. 1990. Segmental trisomy of murine chromosome 16: a new model system for studying Down syndrome. *Prog Clin Biol Res* **360**: 263-280.

Davisson, M.T., Schmidt, C., Reeves, R.H., Irving, N.G., Akeson, E.C., Harris, B.S., and Bronson, R.T. 1993. Segmental trisomy as a mouse model for Down syndrome. *Prog Clin Biol Res* **384**: 117-133.

Dawson, M.R., Polito, A., Levine, J.M., and Reynolds, R. 2003. NG2-expressing glial progenitor cells: an abundant and widespread population of cycling cells in the adult rat CNS. *Mol Cell Neurosci* **24**(2): 476-488.

de la Luna, S. and Estivill, X. 2006. Cooperation to amplify gene-dosage-imbalance effects. *Trends in molecular medicine* **12**(10): 451-454.

De la Torre, R., De Sola, S., Pons, M., Duchon, A., de Lagran, M.M., Farre, M., Fito, M., Benejam, B., Langohr, K., Rodriguez, J. et al. 2014. Epigallocatechin-3-gallate, a DYRK1A inhibitor, rescues cognitive deficits in Down syndrome mouse models and in humans. *Mol Nutr Food Res* **58**(2): 278-288.

DeFelipe, J., Lopez-Cruz, P.L., Benavides-Piccione, R., Bielza, C., Larranaga, P., Anderson, S., Burkhalter, A., Cauli, B., Fairen, A., Feldmeyer, D. et al. 2013. New insights into the classification and nomenclature of cortical GABAergic interneurons. *Nat Rev Neurosci* **14**(3): 202-216.

Dehay, C. and Kennedy, H. 2007. Cell-cycle control and cortical development. *Nat Rev Neurosci* **8**(6): 438-450.

Dehay, C., Savatier, P., Cortay, V., and Kennedy, H. 2001. Cell-cycle kinetics of neocortical precursors are influenced by embryonic thalamic axons. *J Neurosci* **21**(1): 201-214.

Delabar, J.M., Theophile, D., Rahmani, Z., Chettouh, Z., Blouin, J.L., Prieur, M., Noel, B., and Sinet, P.M. 1993. Molecular mapping of twenty-four features of Down syndrome on chromosome 21. *Eur J Hum Genet* **1**(2): 114-124.

Denaxa, M., Kalaitzidou, M., Garefalaki, A., Achimastou, A., Lasrado, R., Maes, T., and Pachnis, V. 2012. Maturation-promoting activity of SATB1 in MGE-derived cortical interneurons. *Cell Rep* **2**(5): 1351-1362.

Deneen, B., Ho, R., Lukaszewicz, A., Hochstim, C.J., Gronostajski, R.M., and Anderson, D.J. 2006. The transcription factor NFIA controls the onset of gliogenesis in the developing spinal cord. *Neuron* **52**(6): 953-968.

Depaepe, V., Suarez-Gonzalez, N., Dufour, A., Passante, L., Gorski, J.A., Jones, K.R., Ledent, C., and Vanderhaeghen, P. 2005. Ephrin signalling controls brain size by regulating apoptosis of neural progenitors. *Nature* **435**(7046): 1244-1250.

Diehl, J.A., Cheng, M., Roussel, M.F., and Sherr, C.J. 1998. Glycogen synthase kinase-3beta regulates cyclin D1 proteolysis and subcellular localization. *Genes Dev* **12**(22): 3499-3511.

Diehl, J.A., Zindy, F., and Sherr, C.J. 1997. Inhibition of cyclin D1 phosphorylation on threonine-286 prevents its rapid degradation via the ubiquitin-proteasome pathway. *Genes Dev* **11**(8): 957-972.

Dierssen, M. 2012. Down syndrome: the brain in trisomic mode. *Nature reviews Neuroscience* **13**(12): 844-858.

Dierssen, M., Benavides-Piccione, R., Martinez-Cue, C., Estivill, X., Florez, J., Elston, G.N., and DeFelipe, J. 2003. Alterations of neocortical pyramidal cell phenotype in the Ts65Dn mouse model of Down syndrome: effects of environmental enrichment. *Cereb Cortex* **13**(7): 758-764.

Dowjat, W.K., Adayev, T., Kuchna, I., Nowicki, K., Palminiello, S., Hwang, Y.W., and Wegiel, J. 2007. Trisomy-driven overexpression of DYRK1A kinase in the brain of subjects with Down syndrome. *Neurosci Lett* **413**(1): 77-81.

Du, T., Xu, Q., Ocbina, P.J., and Anderson, S.A. 2008. NKX2.1 specifies cortical interneuron fate by activating Lhx6. *Development* **135**(8): 1559-1567.

Echelard, Y., Epstein, D.J., St-Jacques, B., Shen, L., Mohler, J., McMahon, J.A., and McMahon, A.P. 1993. Sonic hedgehog, a member of a family of putative signaling molecules, is implicated in the regulation of CNS polarity. *Cell* **75**(7): 1417-1430.

Elton, T.S., Sansom, S.E., and Martin, M.M. 2010. Trisomy-21 gene dosage over-expression of miRNAs results in the haploinsufficiency of specific target proteins. *RNA Biol* **7**(5): 540-547.

Englund, C., Fink, A., Lau, C., Pham, D., Daza, R.A., Bulfone, A., Kowalczyk, T., and Hevner, R.F. 2005. Pax6, Tbr2, and Tbr1 are expressed sequentially by radial glia, intermediate progenitor cells, and postmitotic neurons in developing neocortex. *J Neurosci* **25**(1): 247-251.

Epstein, C.J. 2002. 2001 William Allan Award Address. From Down syndrome to the "human" in "human genetics". *Am J Hum Genet* **70**(2): 300-313.

Epstein, C.J., Berger, C.N., Carlson, E.J., Chan, P.H., and Huang, T.T. 1990. Models for Down syndrome: chromosome 21-specific genes in mice. *Prog Clin Biol Res* **360**: 215-232.

Faedo, A., Quinn, J.C., Stoney, P., Long, J.E., Dye, C., Zollo, M., Rubenstein, J.L., Price, D.J., and Bulfone, A. 2004.

Identification and characterization of a novel transcript down-regulated in Dlx1/Dlx2 and up-regulated in Pax6 mutant telencephalon. *Dev Dyn* **231**(3): 614-620.

Ferencz, C., Neill, C.A., Boughman, J.A., Rubin, J.D., Brenner, J.I., and Perry, L.W. 1989. Congenital cardiovascular malformations associated with chromosome abnormalities: an epidemiologic study. *J Pediatr* **114**(1): 79-86.

Fernandez, F., Morishita, W., Zuniga, E., Nguyen, J., Blank, M., Malenka, R.C., and Garner, C.C. 2007. Pharmacotherapy for cognitive impairment in a mouse model of Down syndrome. *Nat Neurosci* **10**(4): 411-413.

Fernandez-Martinez, J., Vela, E.M., Tora-Ponsioen, M., Ocana, O.H., Nieto, M.A., and Galceran, J. 2009. Attenuation of Notch signalling by the Down-syndrome-associated kinase DYRK1A. *J Cell Sci* **122**(Pt 10): 1574-1583.

Ferrer, I., Soriano, E., del Rio, J.A., Alcantara, S., and Auladell, C. 1992. Cell death and removal in the cerebral cortex during development. *Prog Neurobiol* **39**(1): 1-43.

Ferron, S.R., Pozo, N., Laguna, A., Aranda, S., Porlan, E., Moreno, M., Fillat, C., de la Luna, S., Sanchez, P., Arbones, M.L. et al. 2010. Regulated segregation of kinase Dyrk1A during asymmetric neural stem cell division is critical for EGFR-mediated biased signaling. *Cell Stem Cell* **7**(3): 367-379.

Fietz, S.A., Kelava, I., Vogt, J., Wilsch-Brauninger, M., Stenzel, D., Fish, J.L., Corbeil, D., Riehn, A., Distler, W., Nitsch, R. et al. 2010. OSVZ progenitors of human and ferret neocortex are epithelial-like and expand by integrin signaling. *Nat Neurosci* **13**(6): 690-699.

Fish, J.L., Kosodo, Y., Enard, W., Paabo, S., and Huttner, W.B. 2006. Aspm specifically maintains symmetric proliferative divisions of neuroepithelial cells. *Proc Natl Acad Sci U S A* **103**(27): 10438-10443.

Flames, N., Long, J.E., Garratt, A.N., Fischer, T.M., Gassmann, M., Birchmeier, C., Lai, C., Rubenstein, J.L., and Marin, O. 2004. Short- and long-range attraction of cortical GABAergic interneurons by neuregulin-1. *Neuron* **44**(2): 251-261.

Flames, N., Pla, R., Gelman, D.M., Rubenstein, J.L., Puelles, L., and Marin, O. 2007. Delineation of multiple subpallial progenitor domains by the combinatorial expression of transcriptional codes. *J Neurosci* **27**(36): 9682-9695.

Flandin, P., Zhao, Y., Vogt, D., Jeong, J., Long, J., Potter, G., Westphal, H., and Rubenstein, J.L. 2011. Lhx6 and Lhx8 coordinately induce neuronal expression of Shh that controls

the generation of interneuron progenitors. *Neuron* **70**(5): 939-950.

Fogarty, M., Grist, M., Gelman, D., Marin, O., Pachnis, V., and Kessaris, N. 2007. Spatial genetic patterning of the embryonic neuroepithelium generates GABAergic interneuron diversity in the adult cortex. *J Neurosci* **27**(41): 10935-10946.

Fotaki, V., Dierssen, M., Alcantara, S., Martinez, S., Marti, E., Casas, C., Visa, J., Soriano, E., Estivill, X., and Arbones, M.L. 2002. Dyrk1A haploinsufficiency affects viability and causes developmental delay and abnormal brain morphology in mice. *Mol Cell Biol* **22**(18): 6636-6647.

Fotaki, V., Martinez De Lagran, M., Estivill, X., Arbones, M., and Dierssen, M. 2004. Haploinsufficiency of Dyrk1A in mice leads to specific alterations in the development and regulation of motor activity. *Behav Neurosci* **118**(4): 815-821.

Fragkouli, A., van Wijk, N.V., Lopes, R., Kessaris, N., and Pachnis, V. 2009. LIM homeodomain transcription factor-dependent specification of bipotential MGE progenitors into cholinergic and GABAergic striatal interneurons. *Development* **136**(22): 3841-3851.

Franco, S.J. and Muller, U. 2013. Shaping our minds: stem and progenitor cell diversity in the mammalian neocortex. *Neuron* **77**(1): 19-34.

Frantz, G.D., Weimann, J.M., Levin, M.E., and McConnell, S.K. 1994. Otx1 and Otx2 define layers and regions in developing cerebral cortex and cerebellum. *J Neurosci* **14**(10): 5725-5740.

Frostad, W.A., Cleall, J.F., and Melosky, L.C. 1971. Craniofacial complex in the trisomy 21 syndrome (Down's syndrome). *Arch Oral Biol* **16**(7): 707-722.

Fuccillo, M., Rallu, M., McMahon, A.P., and Fishell, G. 2004. Temporal requirement for hedgehog signaling in ventral telencephalic patterning. *Development* **131**(20): 5031-5040.

Fuentes, J.J., Pritchard, M.A., Planas, A.M., Bosch, A., Ferrer, I., and Estivill, X. 1995. A new human gene from the Down syndrome critical region encodes a proline-rich protein highly expressed in fetal brain and heart. *Hum Mol Genet* **4**(10): 1935-1944.

Gaiano, N., Nye, J.S., and Fishell, G. 2000. Radial glial identity is promoted by Notch1 signaling in the murine forebrain. *Neuron* **26**(2): 395-404.

Galante, M., Jani, H., Vanes, L., Daniel, H., Fisher, E.M., Tybulewicz, V.L., Bliss, T.V., and Morice, E. 2009. Impairments in motor coordination without major changes in

cerebellar plasticity in the Tc1 mouse model of Down syndrome. *Hum Mol Genet* **18**(8): 1449-1463.

Gardiner, K., Fortna, A., Bechtel, L., and Davisson, M.T. 2003. Mouse models of Down syndrome: how useful can they be? Comparison of the gene content of human chromosome 21 with orthologous mouse genomic regions. *Gene* **318**: 137-147.

Ge, W., Martinowich, K., Wu, X., He, F., Miyamoto, A., Fan, G., Weinmaster, G., and Sun, Y.E. 2002. Notch signaling promotes astrogliogenesis via direct CSL-mediated glial gene activation. *J Neurosci Res* **69**(6): 848-860.

Ge, W.P., Miyawaki, A., Gage, F.H., Jan, Y.N., and Jan, L.Y. 2012. Local generation of glia is a major astrocyte source in postnatal cortex. *Nature* **484**(7394): 376-380.

Gearhart, J.D., Singer, H.S., Moran, T.H., Tiemeyer, M., Oster-Granite, M.L., and Coyle, J.T. 1986. Mouse chimeras composed of trisomy 16 and normal (2N) cells: preliminary studies. *Brain Res Bull* **16**(6): 815-824.

Gelman, D., Griveau, A., Dehorter, N., Teissier, A., Varela, C., Pla, R., Pierani, A., and Marin, O. 2011. A wide diversity of cortical GABAergic interneurons derives from the embryonic preoptic area. *J Neurosci* **31**(46): 16570-16580.

Gelman, D.M. and Marin, O. 2010. Generation of interneuron diversity in the mouse cerebral cortex. *Eur J Neurosci* **31**(12): 2136-2141.

Gelman, D.M., Martini, F.J., Nobrega-Pereira, S., Pierani, A., Kessaris, N., and Marin, O. 2009. The embryonic preoptic area is a novel source of cortical GABAergic interneurons. *J Neurosci* **29**(29): 9380-9389.

Gentet, L.J., Kremer, Y., Taniguchi, H., Huang, Z.J., Staiger, J.F., and Petersen, C.C. 2012. Unique functional properties of somatostatin-expressing GABAergic neurons in mouse barrel cortex. *Nat Neurosci* **15**(4): 607-612.

Glickstein, S.B., Alexander, S., and Ross, M.E. 2007. Differences in cyclin D2 and D1 protein expression distinguish forebrain progenitor subsets. *Cereb Cortex* **17**(3): 632-642.

Glickstein, S.B., Monaghan, J.A., Koeller, H.B., Jones, T.K., and Ross, M.E. 2009. Cyclin D2 is critical for intermediate progenitor cell proliferation in the embryonic cortex. *J Neurosci* **29**(30): 9614-9624.

Gockler, N., Jofre, G., Papadopoulos, C., Soppa, U., Tejedor, F.J., and Becker, W. 2009. Harmine specifically inhibits protein kinase DYRK1A and interferes with neurite formation. *FEBS J* **276**(21): 6324-6337.

Goldberg, E.M. and Coulter, D.A. 2013. Mechanisms of epileptogenesis: a convergence on neural circuit dysfunction. *Nat Rev Neurosci* **14**(5): 337-349.

Golden, J.A. and Hyman, B.T. 1994. Development of the superior temporal neocortex is anomalous in trisomy 21. *J Neuropathol Exp Neurol* **53**(5): 513-520.

Gotz, M., Hartfuss, E., and Malatesta, P. 2002. Radial glial cells as neuronal precursors: a new perspective on the correlation of morphology and lineage restriction in the developing cerebral cortex of mice. *Brain Res Bull* **57**(6): 777-788.

Gotz, M. and Huttner, W.B. 2005. The cell biology of neurogenesis. *Nat Rev Mol Cell Biol* **6**(10): 777-788.

Graef, I.A., Wang, F., Charron, F., Chen, L., Neilson, J., Tessier-Lavigne, M., and Crabtree, G.R. 2003. Neurotrophins and netrins require calcineurin/NFAT signaling to stimulate outgrowth of embryonic axons. *Cell* **113**(5): 657-670.

Greig, L.C., Woodworth, M.B., Galazo, M.J., Padmanabhan, H., and Macklis, J.D. 2013. Molecular logic of neocortical projection neuron specification, development and diversity. *Nat Rev Neurosci* **14**(11): 755-769.

Gropp, A., Kolbus, U., and Giers, D. 1975. Systematic approach to the study of trisomy in the mouse. II. *Cytogenet Cell Genet* **14**(1): 42-62.

Gross, R.E., Mehler, M.F., Mabie, P.C., Zang, Z., Santschi, L., and Kessler, J.A. 1996. Bone morphogenetic proteins promote astroglial lineage commitment by mammalian subventricular zone progenitor cells. *Neuron* **17**(4): 595-606.

Guedj, F., Bianchi, D.W., and Delabar, J.M. 2014. Prenatal treatment of Down syndrome: a reality? *Curr Opin Obstet Gynecol* **26**(2): 92-103.

Guedj, F., Pereira, P.L., Najas, S., Barallobre, M.J., Chabert, C., Souchet, B., Sebrie, C., Verney, C., Herault, Y., Arbones, M. et al. 2012. DYRK1A: a master regulatory protein controlling brain growth. *Neurobiol Dis* **46**(1): 190-203.

Guedj, F., Sebrie, C., Rivals, I., Ledru, A., Paly, E., Bizot, J.C., Smith, D., Rubin, E., Gillet, B., Arbones, M. et al. 2009. Green tea polyphenols rescue of brain defects induced by overexpression of DYRK1A. *PLoS One* **4**(2): e4606.

Guihard-Costa, A.M., Khung, S., Delbecque, K., Menez, F., and Delezoide, A.L. 2006. Biometry of face and brain in fetuses with trisomy 21. *Pediatr Res* **59**(1): 33-38.

Guimera, J., Casas, C., Estivill, X., and Pritchard, M. 1999. Human minibrain homologue (MNBH/DYRK1): characterization, alternative splicing, differential tissue

expression, and overexpression in Down syndrome. *Genomics* **57**(3): 407-418.

Guimera, J., Casas, C., Pucharcos, C., Solans, A., Domenech, A., Planas, A.M., Ashley, J., Lovett, M., Estivill, X., and Pritchard, M.A. 1996. A human homologue of Drosophila minibrain (MNB) is expressed in the neuronal regions affected in Down syndrome and maps to the critical region. *Hum Mol Genet* **5**(9): 1305-1310.

Guimera, J., Pucharcos, C., Domenech, A., Casas, C., Solans, A., Gallardo, T., Ashley, J., Lovett, M., Estivill, X., and Pritchard, M. 1997. Cosmid contig and transcriptional map of three regions of human chromosome 21q22: identification of 37 novel transcripts by direct selection. *Genomics* **45**(1): 59-67.

Gulacsi, A. and Anderson, S.A. 2006. Shh maintains Nkx2.1 in the MGE by a Gli3-independent mechanism. *Cereb Cortex* **16 Suppl 1**: i89-95.

Gulacsi, A.A. and Anderson, S.A. 2008. Beta-catenin-mediated Wnt signaling regulates neurogenesis in the ventral telencephalon. *Nat Neurosci* **11**(12): 1383-1391.

Gundersen, H.J. and Jensen, E.B. 1987. The efficiency of systematic sampling in stereology and its prediction. *J Microsc* **147**(Pt 3): 229-263.

Guo, X., Williams, J.G., Schug, T.T., and Li, X. 2010. DYRK1A and DYRK3 promote cell survival through phosphorylation and activation of SIRT1. *J Biol Chem* **285**(17): 13223-13232.

Gutin, G., Fernandes, M., Palazzolo, L., Paek, H., Yu, K., Ornitz, D.M., McConnell, S.K., and Hebert, J.M. 2006. FGF signalling generates ventral telencephalic cells independently of SHH. *Development* **133**(15): 2937-2946.

Gwack, Y., Sharma, S., Nardone, J., Tanasa, B., Iuga, A., Srikanth, S., Okamura, H., Bolton, D., Feske, S., Hogan, P.G. et al. 2006. A genome-wide Drosophila RNAi screen identifies DYRK-family kinases as regulators of NFAT. *Nature* **441**(7093): 646-650.

Hammerle, B., Carnicero, A., Elizalde, C., Ceron, J., Martinez, S., and Tejedor, F.J. 2003. Expression patterns and subcellular localization of the Down syndrome candidate protein MNB/DYRK1A suggest a role in late neuronal differentiation. *Eur J Neurosci* **17**(11): 2277-2286.

Hammerle, B., Elizalde, C., and Tejedor, F.J. 2008. The spatio-temporal and subcellular expression of the candidate Down syndrome gene Mnb/Dyrk1A in the developing mouse brain

suggests distinct sequential roles in neuronal development. *Eur J Neurosci* **27**(5): 1061-1074.

Hammerle, B., Ulin, E., Guimera, J., Becker, W., Guillemot, F., and Tejedor, F.J. 2011. Transient expression of Mnb/Dyrk1a couples cell cycle exit and differentiation of neuronal precursors by inducing p27KIP1 expression and suppressing NOTCH signaling. *Development* **138**(12): 2543-2554.

Hammerle, B., Vera-Samper, E., Speicher, S., Arencibia, R., Martinez, S., and Tejedor, F.J. 2002. Mnb/Dyrk1A is transiently expressed and asymmetrically segregated in neural progenitor cells at the transition to neurogenic divisions. *Dev Biol* **246**(2): 259-273.

Hansen, D.V., Lui, J.H., Parker, P.R., and Kriegstein, A.R. 2010. Neurogenic radial glia in the outer subventricular zone of human neocortex. *Nature* **464**(7288): 554-561.

Harrison-Uy, S.J., Siegenthaler, J.A., Faedo, A., Rubenstein, J.L., and Pleasure, S.J. 2013. CoupTFI interacts with retinoic acid signaling during cortical development. *PLoS One* **8**(3): e58219.

Hatakeyama, J., Bessho, Y., Katoh, K., Ookawara, S., Fujioka, M., Guillemot, F., and Kageyama, R. 2004. Hes genes regulate size, shape and histogenesis of the nervous system by control of the timing of neural stem cell differentiation. *Development* **131**(22): 5539-5550.

Haubensak, W., Attardo, A., Denk, W., and Huttner, W.B. 2004. Neurons arise in the basal neuroepithelium of the early mammalian telencephalon: a major site of neurogenesis. *Proc Natl Acad Sci U S A* **101**(9): 3196-3201.

Haydar, T.F., Ang, E., Jr., and Rakic, P. 2003. Mitotic spindle rotation and mode of cell division in the developing telencephalon. *Proc Natl Acad Sci U S A* **100**(5): 2890-2895.

Haydar, T.F., Blue, M.E., Molliver, M.E., Krueger, B.K., and Yarowsky, P.J. 1996. Consequences of trisomy 16 for mouse brain development: corticogenesis in a model of Down syndrome. *J Neurosci* **16**(19): 6175-6182.

Haydar, T.F., Kuan, C.Y., Flavell, R.A., and Rakic, P. 1999. The role of cell death in regulating the size and shape of the mammalian forebrain. *Cereb Cortex* **9**(6): 621-626.

Haydar, T.F., Nowakowski, R.S., Yarowsky, P.J., and Krueger, B.K. 2000. Role of founder cell deficit and delayed neuronogenesis in microencephaly of the trisomy 16 mouse. *J Neurosci* **20**(11): 4156-4164.

Haydar, T.F. and Reeves, R.H. 2012. Trisomy 21 and early brain development. *Trends Neurosci* **35**(2): 81-91.

He, F., Ge, W., Martinowich, K., Becker-Catania, S., Coskun, V., Zhu, W., Wu, H., Castro, D., Guillemot, F., Fan, G. et al. 2005. A positive autoregulatory loop of Jak-STAT signaling controls the onset of astrogliogenesis. *Nat Neurosci* **8**(5): 616-625.

Hernandez, S., Gilabert-Juan, J., Blasco-Ibanez, J.M., Crespo, C., Nacher, J., and Varea, E. 2012. Altered expression of neuropeptides in the primary somatosensory cortex of the Down syndrome model Ts65Dn. *Neuropeptides* **46**(1): 29-37.

Hernandez-Miranda, L.R., Cariboni, A., Faux, C., Ruhrberg, C., Cho, J.H., Cloutier, J.F., Eickholt, B.J., Parnavelas, J.G., and Andrews, W.D. 2011. Robo1 regulates semaphorin signaling to guide the migration of cortical interneurons through the ventral forebrain. *J Neurosci* **31**(16): 6174-6187.

Hevner, R.F., Daza, R.A., Englund, C., Kohtz, J., and Fink, A. 2004. Postnatal shifts of interneuron position in the neocortex of normal and reeler mice: evidence for inward radial migration. *Neuroscience* **124**(3): 605-618.

Hibaoui, Y., Grad, I., Letourneau, A., Sailani, M.R., Dahoun, S., Santoni, F.A., Gimelli, S., Guipponi, M., Pelte, M.F., Bena, F. et al. 2013. Modelling and rescuing neurodevelopmental defect of Down syndrome using induced pluripotent stem cells from monozygotic twins discordant for trisomy 21. *EMBO Mol Med* **6**(2): 259-277.

Himpel, S., Tegge, W., Frank, R., Leder, S., Joost, H.G., and Becker, W. 2000. Specificity determinants of substrate recognition by the protein kinase DYRK1A. *J Biol Chem* **275**(4): 2431-2438.

Hindley, C., Ali, F., McDowell, G., Cheng, K., Jones, A., Guillemot, F., and Philpott, A. 2012. Post-translational modification of Ngn2 differentially affects transcription of distinct targets to regulate the balance between progenitor maintenance and differentiation. *Development* **139**(10): 1718-1723.

Hirabayashi, Y., Suzki, N., Tsuboi, M., Endo, T.A., Toyoda, T., Shinga, J., Koseki, H., Vidal, M., and Gotoh, Y. 2009. Polycomb limits the neurogenic competence of neural precursor cells to promote astrogenic fate transition. *Neuron* **63**(5): 600-613.

Hirata, H., Yoshiura, S., Ohtsuka, T., Bessho, Y., Harada, T., Yoshikawa, K., and Kageyama, R. 2002. Oscillatory expression of the bHLH factor Hes1 regulated by a negative feedback loop. *Science* **298**(5594): 840-843.

Ikonomidou, C., Bittigau, P., Koch, C., Genz, K., Hoerster, F., Felderhoff-Mueser, U., Tenkova, T., Dikranian, K., and Olney,

J.W. 2001. Neurotransmitters and apoptosis in the developing brain. *Biochem Pharmacol* **62**(4): 401-405.

Ikonomidou, C., Bosch, F., Miksa, M., Bittigau, P., Vockler, J., Dikranian, K., Tenkova, T.I., Stefovska, V., Turski, L., and Olney, J.W. 1999. Blockade of NMDA receptors and apoptotic neurodegeneration in the developing brain. *Science* **283**(5398): 70-74.

Impey, S., McCorkle, S.R., Cha-Molstad, H., Dwyer, J.M., Yochum, G.S., Boss, J.M., McWeeney, S., Dunn, J.J., Mandel, G., and Goodman, R.H. 2004. Defining the CREB regulon: a genome-wide analysis of transcription factor regulatory regions. *Cell* **119**(7): 1041-1054.

Inan, M., Welagen, J., and Anderson, S.A. 2012. Spatial and temporal bias in the mitotic origins of somatostatin- and parvalbumin-expressing interneuron subgroups and the chandelier subtype in the medial ganglionic eminence. *Cereb Cortex* **22**(4): 820-827.

Ingram, W.J., McCue, K.I., Tran, T.H., Hallahan, A.R., and Wainwright, B.J. 2008. Sonic Hedgehog regulates Hes1 through a novel mechanism that is independent of canonical Notch pathway signalling. *Oncogene* **27**(10): 1489-1500.

Insausti, A.M., Megias, M., Crespo, D., Cruz-Orive, L.M., Dierssen, M., Vallina, I.F., Insausti, R., and Florez, J. 1998. Hippocampal volume and neuronal number in Ts65Dn mice: a murine model of Down syndrome. *Neurosci Lett* **253**(3): 175-178.

Isaacson JS, S.M. 2011. How inhibition shapes cortical activity. *Neuron* **20**(72): 231-243.

Ishihara, K., Amano, K., Takaki, E., Shimohata, A., Sago, H., Epstein, C.J., and Yamakawa, K. 2010. Enlarged brain ventricles and impaired neurogenesis in the Ts1Cje and Ts2Cje mouse models of Down syndrome. *Cerebral cortex* **20**(5): 1131-1143.

Jeong, Y., El-Jaick, K., Roessler, E., Muenke, M., and Epstein, D.J. 2006. A functional screen for sonic hedgehog regulatory elements across a 1 Mb interval identifies long-range ventral forebrain enhancers. *Development* **133**(4): 761-772.

Jirawatnotai, S., Hu, Y., Michowski, W., Elias, J.E., Becks, L., Bienvenu, F., Zagozdzon, A., Goswami, T., Wang, Y.E., Clark, A.B. et al. 2011. A function for cyclin D1 in DNA repair uncovered by protein interactome analyses in human cancers. *Nature* **474**(7350): 230-234.

Jones, P.a. 1984. *Classification of cortical neurons*. Plenum Press, New York.

Kaczmarski, W., Barua, M., Mazur-Kolecka, B., Frackowiak, J., Dowjat, W., Mehta, P., Bolton, D., Hwang, Y.W., Rabe, A., Albertini, G. et al. 2014. Intracellular distribution of differentially phosphorylated dual-specificity tyrosine phosphorylation-regulated kinase 1A (DYRK1A). *J Neurosci Res* **92**(2): 162-173.

Kageyama, R., Ohtsuka, T., and Kobayashi, T. 2007. The Hes gene family: repressors and oscillators that orchestrate embryogenesis. *Development* **134**(7): 1243-1251.

Kageyama, R., Ohtsuka, T., Shimojo, H., and Imayoshi, I. 2008. Dynamic Notch signaling in neural progenitor cells and a revised view of lateral inhibition. *Nat Neurosci* **11**(11): 1247-1251.

Kageyama, R., Ohtsuka, T., Shimojo, H., and Imayoshi, I. 2009. Dynamic regulation of Notch signaling in neural progenitor cells. *Curr Opin Cell Biol* **21**(6): 733-740.

Kamakura, S., Oishi, K., Yoshimatsu, T., Nakafuku, M., Masuyama, N., and Gotoh, Y. 2004. Hes binding to STAT3 mediates crosstalk between Notch and JAK-STAT signalling. *Nat Cell Biol* **6**(6): 547-554.

Kanatani, S., Yozu, M., Tabata, H., and Nakajima, K. 2008. COUP-TFII is preferentially expressed in the caudal ganglionic eminence and is involved in the caudal migratory stream. *J Neurosci* **28**(50): 13582-13591.

Kanold, P.O. and Luhmann, H.J. 2010. The subplate and early cortical circuits. *Annu Rev Neurosci* **33**: 23-48.

Kato, H., Taniguchi, Y., Kurooka, H., Minoguchi, S., Sakai, T., Nomura-Okazaki, S., Tamura, K., and Honjo, T. 1997. Involvement of RBP-J in biological functions of mouse Notch1 and its derivatives. *Development* **124**(20): 4133-4141.

Kawaguchi, D., Yoshimatsu, T., Hozumi, K., and Gotoh, Y. 2008. Selection of differentiating cells by different levels of delta-like 1 among neural precursor cells in the developing mouse telencephalon. *Development* **135**(23): 3849-3858.

Kessaris, N., Fogarty, M., Iannarelli, P., Grist, M., Wegner, M., and Richardson, W.D. 2006. Competing waves of oligodendrocytes in the forebrain and postnatal elimination of an embryonic lineage. *Nat Neurosci* **9**(2): 173-179.

Kessaris, N., Magno, L., Rubin, A.N., and Oliveira, M.G. 2014. Genetic programs controlling cortical interneuron fate. *Curr Opin Neurobiol* **26C**: 79-87.

Kida, A., Kakihana, K., Kotani, S., Kurosu, T., and Miura, O. 2007. Glycogen synthase kinase-3beta and p38 phosphorylate cyclin D2 on Thr280 to trigger its

ubiquitin/proteasome-dependent degradation in hematopoietic cells. *Oncogene* **26**(46): 6630-6640.

Kim, M.Y., Jeong, B.C., Lee, J.H., Kee, H.J., Kook, H., Kim, N.S., Kim, Y.H., Kim, J.K., Ahn, K.Y., and Kim, K.K. 2006. A repressor complex, AP4 transcription factor and geminin, negatively regulates expression of target genes in nonneuronal cells. *Proc Natl Acad Sci U S A* **103**(35): 13074-13079.

Kimonis, V., Gold, J.A., Hoffman, T.L., Panchal, J., and Boyadjiev, S.A. 2007. Genetics of craniosynostosis. *Semin Pediatr Neurol* **14**(3): 150-161.

Kimura, R., Kamino, K., Yamamoto, M., Nuripa, A., Kida, T., Kazui, H., Hashimoto, R., Tanaka, T., Kudo, T., Yamagata, H. et al. 2007. The DYRK1A gene, encoded in chromosome 21 Down syndrome critical region, bridges between beta-amyloid production and tau phosphorylation in Alzheimer disease. *Hum Mol Genet* **16**(1): 15-23.

Kirsammer, G., Jilani, S., Liu, H., Davis, E., Gurbuxani, S., Le Beau, M.M., and Crispino, J.D. 2008. Highly penetrant myeloproliferative disease in the Ts65Dn mouse model of Down syndrome. *Blood* **111**(2): 767-775.

Kleschevnikov, A.M., Belichenko, P.V., Villar, A.J., Epstein, C.J., Malenka, R.C., and Mobley, W.C. 2004. Hippocampal long-term potentiation suppressed by increased inhibition in the Ts65Dn mouse, a genetic model of Down syndrome. *J Neurosci* **24**(37): 8153-8160.

Komada, M. 2012. Sonic hedgehog signaling coordinates the proliferation and differentiation of neural stem/progenitor cells by regulating cell cycle kinetics during development of the neocortex. *Congenit Anom (Kyoto)* **52**(2): 72-77.

Komada, M., Saitsu, H., Kinboshi, M., Miura, T., Shiota, K., and Ishibashi, M. 2008. Hedgehog signaling is involved in development of the neocortex. *Development* **135**(16): 2717-2727.

Konno, D., Shioi, G., Shitamukai, A., Mori, A., Kiyonari, H., Miyata, T., and Matsuzaki, F. 2008. Neuroepithelial progenitors undergo LGN-dependent planar divisions to maintain self-renewability during mammalian neurogenesis. *Nat Cell Biol* **10**(1): 93-101.

Kowalczyk, T., Pontious, A., Englund, C., Daza, R.A., Bedogni, F., Hodge, R., Attardo, A., Bell, C., Huttner, W.B., and Hevner, R.F. 2009. Intermediate neuronal progenitors (basal progenitors) produce pyramidal-projection neurons for all layers of cerebral cortex. *Cerebral cortex* **19**(10): 2439-2450.

Kriegstein, A. and Alvarez-Buylla, A. 2009. The glial nature of embryonic and adult neural stem cells. *Annu Rev Neurosci* **32**: 149-184.

Kuida, K., Haydar, T.F., Kuan, C.Y., Gu, Y., Taya, C., Karasuyama, H., Su, M.S., Rakic, P., and Flavell, R.A. 1998. Reduced apoptosis and cytochrome c-mediated caspase activation in mice lacking caspase 9. *Cell* **94**(3): 325-337.

Kuida, K., Zheng, T.S., Na, S., Kuan, C., Yang, D., Karasuyama, H., Rakic, P., and Flavell, R.A. 1996. Decreased apoptosis in the brain and premature lethality in CPP32-deficient mice. *Nature* **384**(6607): 368-372.

Kurabayashi, N., Hirota, T., Sakai, M., Sanada, K., and Fukada, Y. 2010. DYRK1A and glycogen synthase kinase 3beta, a dual-kinase mechanism directing proteasomal degradation of CRY2 for circadian timekeeping. *Mol Cell Biol* **30**(7): 1757-1768.

Kurabayashi, N. and Sanada, K. 2013. Increased dosage of DYRK1A and DSCR1 delays neuronal differentiation in neocortical progenitor cells. *Genes & development* **27**(24): 2708-2721.

Kurt, M.A., Davies, D.C., Kidd, M., Dierssen, M., and Florez, J. 2000. Synaptic deficit in the temporal cortex of partial trisomy 16 (Ts65Dn) mice. *Brain Res* **858**(1): 191-197.

Lacomme, M., Liaubet, L., Pituello, F., and Bel-Vialar, S. 2012. NEUROG2 drives cell cycle exit of neuronal precursors by specifically repressing a subset of cyclins acting at the G1 and S phases of the cell cycle. *Mol Cell Biol* **32**(13): 2596-2607.

Laguna, A., Aranda, S., Barallobre, M.J., Barhoum, R., Fernandez, E., Fotaki, V., Delabar, J.M., de la Luna, S., de la Villa, P., and Arbones, M.L. 2008. The protein kinase DYRK1A regulates caspase-9-mediated apoptosis during retina development. *Dev Cell* **15**(6): 841-853.

Laguna, A., Barallobre, M.J., Marchena, M.A., Mateus, C., Ramirez, E., Martinez-Cue, C., Delabar, J.M., Castelo-Branco, M., de la Villa, P., and Arbones, M.L. 2013. Triplication of DYRK1A causes retinal structural and functional alterations in Down syndrome. *Hum Mol Genet* **22**(14): 2775-2784.

Lancaster, M.A. and Knoblich, J.A. 2012. Spindle orientation in mammalian cerebral cortical development. *Curr Opin Neurobiol* **22**(5): 737-746.

Lange, C., Huttner, W.B., and Calegari, F. 2009. Cdk4/cyclinD1 overexpression in neural stem cells shortens G1, delays neurogenesis, and promotes the generation and expansion of basal progenitors. *Cell Stem Cell* **5**(3): 320-331.

Larsen, K.B., Laursen, H., Graem, N., Samuelsen, G.B., Bogdanovic, N., and Pakkenberg, B. 2008. Reduced cell number in the neocortical part of the human fetal brain in Down syndrome. *Ann Anat* **190**(5): 421-427.

Lee, J.E. 1997. Basic helix-loop-helix genes in neural development. *Curr Opin Neurobiol* **7**(1): 13-20.

Lee, K., Deng, X., and Friedman, E. 2000. Mirk protein kinase is a mitogen-activated protein kinase substrate that mediates survival of colon cancer cells. *Cancer Res* **60**(13): 3631-3637.

Letourneau, A., Santoni, F.A., Bonilla, X., Sailani, M.R., Gonzalez, D., Kind, J., Chevalier, C., Thurman, R., Sandstrom, R.S., Hibaoui, Y. et al. 2014. Domains of genome-wide gene expression dysregulation in Down's syndrome. *Nature* **508**(7496): 345-350.

Levy, J. 1991. The gastrointestinal tract in Down syndrome. *Prog Clin Biol Res* **373**: 245-256.

Li, D., Jackson, R.A., Yusoff, P., and Guy, G.R. 2010. Direct association of Sprouty-related protein with an EVH1 domain (SPRED) 1 or SPRED2 with DYRK1A modifies substrate/kinase interactions. *J Biol Chem* **285**(46): 35374-35385.

Li, Z., Yu, T., Morishima, M., Pao, A., LaDuca, J., Conroy, J., Nowak, N., Matsui, S., Shiraishi, I., and Yu, Y.E. 2007. Duplication of the entire 22.9 Mb human chromosome 21 syntenic region on mouse chromosome 16 causes cardiovascular and gastrointestinal abnormalities. *Hum Mol Genet* **16**(11): 1359-1366.

Liodis, P., Denaxa, M., Grigoriou, M., Akufo-Addo, C., Yanagawa, Y., and Pachnis, V. 2007. Lhx6 activity is required for the normal migration and specification of cortical interneuron subtypes. *J Neurosci* **27**(12): 3078-3089.

Litovchick, L., Florens, L.A., Swanson, S.K., Washburn, M.P., and DeCaprio, J.A. 2011. DYRK1A protein kinase promotes quiescence and senescence through DREAM complex assembly. *Genes Dev* **25**(8): 801-813.

Liu, C., Belichenko, P.V., Zhang, L., Fu, D., Kleschevnikov, A.M., Baldini, A., Antonarakis, S.E., Mobley, W.C., and Yu, Y.E. 2011. Mouse models for Down syndrome-associated developmental cognitive disabilities. *Dev Neurosci* **33**(5): 404-413.

Lochhead, P.A., Sibbet, G., Morrice, N., and Cleghon, V. 2005. Activation-loop autophosphorylation is mediated by a novel transitional intermediate form of DYRKs. *Cell* **121**(6): 925-936.

Lodato, S., Rouaux, C., Quast, K.B., Jantrachotechatchawan, C., Studer, M., Hensch, T.K., and Arlotta, P. 2011. Excitatory projection neuron subtypes control the distribution of local inhibitory interneurons in the cerebral cortex. *Neuron* **69**(4): 763-779.

Logan, C.Y. and Nusse, R. 2004. The Wnt signaling pathway in development and disease. *Annu Rev Cell Dev Biol* **20**: 781-810.

Louvi, A. and Grove, E.A. 2011. Cilia in the CNS: the quiet organelle claims center stage. *Neuron* **69**(6): 1046-1060.

Lu, M., Zheng, L., Han, B., Wang, L., Wang, P., Liu, H., and Sun, X. 2011. REST regulates DYRK1A transcription in a negative feedback loop. *J Biol Chem* **286**(12): 10755-10763.

Lui, J.H., Hansen, D.V., and Kriegstein, A.R. 2011. Development and evolution of the human neocortex. *Cell* **146**(1): 18-36.

Lukaszewicz, A., Savatier, P., Cortay, V., Giroud, P., Huissoud, C., Berland, M., Kennedy, H., and Dehay, C. 2005. G1 phase regulation, area-specific cell cycle control, and cytoarchitectonics in the primate cortex. *Neuron* **47**(3): 353-364.

Lukaszewicz, A.I. and Anderson, D.J. 2011. Cyclin D1 promotes neurogenesis in the developing spinal cord in a cell cycle-independent manner. *Proc Natl Acad Sci U S A* **108**(28): 11632-11637.

Luscher, C., Nicoll, R.A., Malenka, R.C., and Muller, D. 2000. Synaptic plasticity and dynamic modulation of the postsynaptic membrane. *Nat Neurosci* **3**(6): 545-550.

Machold, R., Hayashi, S., Rutlin, M., Muzumdar, M.D., Nery, S., Corbin, J.G., Gritli-Linde, A., Dellovade, T., Porter, J.A., Rubin, L.L. et al. 2003. Sonic hedgehog is required for progenitor cell maintenance in telencephalic stem cell niches. *Neuron* **39**(6): 937-950.

Maenz, B., Hekerman, P., Vela, E.M., Galceran, J., and Becker, W. 2008. Characterization of the human DYRK1A promoter and its regulation by the transcription factor E2F1. *BMC Mol Biol* **9**: 30.

Malumbres, M. and Barbacid, M. 2005. Mammalian cyclin-dependent kinases. *Trends Biochem Sci* **30**(11): 630-641.

Mann, D.M., Yates, P.O., Marcyniuk, B., and Ravindra, C.R. 1985. Pathological evidence for neurotransmitter deficits in Down's syndrome of middle age. *J Ment Defic Res* **29 (Pt 2)**: 125-135.

Mao, J., Maye, P., Kogerman, P., Tejedor, F.J., Toftgard, R., Xie, W., Wu, G., and Wu, D. 2002. Regulation of Gli1

transcriptional activity in the nucleus by Dyrk1. *J Biol Chem* **277**(38): 35156-35161.

Marin, O. 2012. Interneuron dysfunction in psychiatric disorders. *Nat Rev Neurosci* **13**(2): 107-120.

Marin,O. 2013. Cellular and molecular mechanisms controlling the migration of neocortical interneurons. *Eur J Neurosci* **38**(1): 2019-2029.

Marin, O., Yaron, A., Bagri, A., Tessier-Lavigne, M., and Rubenstein, J.L. 2001. Sorting of striatal and cortical interneurons regulated by semaphorin-neuropilin interactions. *Science* **293**(5531): 872-875.

Marin-Padilla, M. 1976. Pyramidal cell abnormalities in the motor cortex of a child with Down's syndrome. A Golgi study. *J Comp Neurol* **167**(1): 63-81.

Marin-Padilla, M.1978. Dual origin of the mammalian neocortex and evolution of the cortical plate. *Anat Embryol (Berl)* **152**(2): 109-126.

Markram, H., Toledo-Rodriguez, M., Wang, Y., Gupta, A., Silberberg, G., and Wu, C. 2004. Interneurons of the neocortical inhibitory system. *Nat Rev Neurosci* **5**(10): 793-807.

Marti, E., Altafaj, X., Dierssen, M., de la Luna, S., Fotaki, V., Alvarez, M., Perez-Riba, M., Ferrer, I., and Estivill, X. 2003. Dyrk1A expression pattern supports specific roles of this kinase in the adult central nervous system. *Brain Res* **964**(2): 250-263.

Martinez de Lagran, M., Altafaj, X., Gallego, X., Marti, E., Estivill, X., Sahun, I., Fillat, C., and Dierssen, M. 2004. Motor phenotypic alterations in TgDyrk1a transgenic mice implicate DYRK1A in Down syndrome motor dysfunction. *Neurobiol Dis* **15**(1): 132-142.

Martinez de Lagran, M., Benavides-Piccione, R., Ballesteros-Yanez, I., Calvo, M., Morales, M., Fillat, C., Defelipe, J., Ramakers, G.J., and Dierssen, M. 2012. Dyrk1A influences neuronal morphogenesis through regulation of cytoskeletal dynamics in mammalian cortical neurons. *Cereb Cortex* **22**(12): 2867-2877.

McConnell, M.J., MacMillan, H.R., and Chun, J. 2009. Mathematical modeling supports substantial mouse neural progenitor cell death. *Neural Dev* **4**: 28.

McKinsey, G.L., Lindtner, S., Trzcinski, B., Visel, A., Pennacchio, L.A., Huylebroeck, D., Higashi, Y., and Rubenstein, J.L. 2013. Dlx1&2-dependent expression of Zfhx1b (Sip1, Zeb2)

regulates the fate switch between cortical and striatal interneurons. *Neuron* **77**(1): 83-98.

Mi, D., Carr, C.B., Georgala, P.A., Huang, Y.T., Manuel, M.N., Jeanes, E., Niisato, E., Sansom, S.N., Livesey, F.J., Theil, T. et al. 2013. Pax6 exerts regional control of cortical progenitor proliferation via direct repression of Cdk6 and hypophosphorylation of pRb. *Neuron* **78**(2): 269-284.

Miller, M.W. 1988. *Development of projection and local circuit neurons in neocortex. in Development and maturation of cerebral cortex* Plenum Press, New York.

Miller, M.W. 1995. Relationship of the time of origin and death of neurons in rat somatosensory cortex: barrel versus septal cortex and projection versus local circuit neurons. *J Comp Neurol* **355**(1): 6-14.

Mito, T. and Becker, L.E. 1993. Developmental changes of S-100 protein and glial fibrillary acidic protein in the brain in Down syndrome. *Exp Neurol* **120**(2): 170-176.

Miyabara, S., Gropp, A., and Winking, H. 1982. Trisomy 16 in the mouse fetus associated with generalized edema and cardiovascular and urinary tract anomalies. *Teratology* **25**(3): 369-380.

Miyata, T., Kawaguchi, A., Saito, K., Kawano, M., Muto, T., and Ogawa, M. 2004. Asymmetric production of surface-dividing and non-surface-dividing cortical progenitor cells. *Development* **131**(13): 3133-3145.

Miyoshi, G., Butt, S.J., Takebayashi, H., and Fishell, G. 2007. Physiologically distinct temporal cohorts of cortical interneurons arise from telencephalic Olig2-expressing precursors. *J Neurosci* **27**(29): 7786-7798.

Miyoshi, G., Hjerling-Leffler, J., Karayannis, T., Sousa, V.H., Butt, S.J., Battiste, J., Johnson, J.E., Machold, R.P., and Fishell, G. 2010. Genetic fate mapping reveals that the caudal ganglionic eminence produces a large and diverse population of superficial cortical interneurons. *J Neurosci* **30**(5): 1582-1594.

Moldrich, R.X., Dauphinot, L., Laffaire, J., Vitalis, T., Herault, Y., Beart, P.M., Rossier, J., Vivien, D., Gehrig, C., Antonarakis, S.E. et al. 2009. Proliferation deficits and gene expression dysregulation in Down's syndrome (Ts1Cje) neural progenitor cells cultured from neurospheres. *J Neurosci Res* **87**(14): 3143-3152.

Moller, R.S., Kubart, S., Hoeltzenbein, M., Heye, B., Vogel, I., Hansen, C.P., Menzel, C., Ullmann, R., Tommerup, N., Ropers, H.H. et al. 2008. Truncation of the Down syndrome

candidate gene DYRK1A in two unrelated patients with microcephaly. *Am J Hum Genet* **82**(5): 1165-1170.

Molyneaux, B.J., Arlotta, P., Menezes, J.R., and Macklis, J.D. 2007. Neuronal subtype specification in the cerebral cortex. *Nat Rev Neurosci* **8**(6): 427-437.

Morin, X. and Bellaiche, Y. 2011. Mitotic spindle orientation in asymmetric and symmetric cell divisions during animal development. *Dev Cell* **21**(1): 102-119.

Moss, M.L. and Young, R.W. 1960. A functional approach to craniology. *Am J Phys Anthropol* **18**: 281-292.

Mountcastle, V.B. 1997. The columnar organization of the neocortex. *Brain* **120 (Pt 4)**: 701-722.

Mukhopadhyay, A., McGuire, T., Peng, C.Y., and Kessler, J.A. 2009. Differential effects of BMP signaling on parvalbumin and somatostatin interneuron differentiation. *Development* **136**(15): 2633-2642.

Munji, R.N., Choe, Y., Li, G., Siegenthaler, J.A., and Pleasure, S.J. 2011. Wnt signaling regulates neuronal differentiation of cortical intermediate progenitors. *J Neurosci* **31**(5): 1676-1687.

Murakami, N., Bolton, D., and Hwang, Y.W. 2009. Dyrk1A binds to multiple endocytic proteins required for formation of clathrin-coated vesicles. *Biochemistry* **48**(39): 9297-9305.

Mural, R.J. Adams, M.D. Myers, E.W. Smith, H.O. Miklos, G.L. Wides, R. Halpern, A. Li, P.W. Sutton, G.G. Nadeau, J. et al. 2002. A comparison of whole-genome shotgun-derived mouse chromosome 16 and the human genome. *Science* **296**(5573): 1661-1671.

Nakashima, K. and Taga, T. 2002. Mechanisms underlying cytokine-mediated cell-fate regulation in the nervous system. *Mol Neurobiol* **25**(3): 233-244.

Nakashima, K., Yanagisawa, M., Arakawa, H., and Taga, T. 1999. Astrocyte differentiation mediated by LIF in cooperation with BMP2. *FEBS Lett* **457**(1): 43-46.

Namihira, M., Kohyama, J., Semi, K., Sanosaka, T., Deneen, B., Taga, T., and Nakashima, K. 2009. Committed neuronal precursors confer astrocytic potential on residual neural precursor cells. *Dev Cell* **16**(2): 245-255.

Namihira, M., Nakashima, K., and Taga, T. 2004. Developmental stage dependent regulation of DNA methylation and chromatin modification in a immature astrocyte specific gene promoter. *FEBS Lett* **572**(1-3): 184-188.

Nery, S., Wichterle, H., and Fishell, G. 2001. Sonic hedgehog contributes to oligodendrocyte specification in the mammalian forebrain. *Development* **128**(4): 527-540.

Nguyen, L., Besson, A., Heng, J.I., Schuurmans, C., Teboul, L., Parras, C., Philpott, A., Roberts, J.M., and Guillemot, F. 2006. p27kip1 independently promotes neuronal differentiation and migration in the cerebral cortex. *Genes Dev* **20**(11): 1511-1524.

Nieto, M., Monuki, E.S., Tang, H., Imitola, J., Haubst, N., Khoury, S.J., Cunningham, J., Gotz, M., and Walsh, C.A. 2004. Expression of Cux-1 and Cux-2 in the subventricular zone and upper layers II-IV of the cerebral cortex. *J Comp Neurol* **479**(2): 168-180.

Nigg, E.A. and Stearns, T. 2011. The centrosome cycle: Centriole biogenesis, duplication and inherent asymmetries. *Nat Cell Biol* **13**(10): 1154-1160.

Nobrega-Pereira, S., Kessaris, N., Du, T., Kimura, S., Anderson, S.A., and Marin, O. 2008. Postmitotic Nkx2-1 controls the migration of telencephalic interneurons by direct repression of guidance receptors. *Neuron* **59**(5): 733-745.

Nobrega-Pereira, S. and Marin, O. 2009. Transcriptional control of neuronal migration in the developing mouse brain. *Cereb Cortex* **19 Suppl 1**: i107-113.

Noctor, S.C., Martinez-Cerdeno, V., Ivic, L., and Kriegstein, A.R. 2004. Cortical neurons arise in symmetric and asymmetric division zones and migrate through specific phases. *Nat Neurosci* **7**(2): 136-144.

Nonaka-Kinoshita, M., Reillo, I., Artegiani, B., Martinez-Martinez, M.A., Nelson, M., Borrell, V., and Calegari, F. 2013. Regulation of cerebral cortex size and folding by expansion of basal progenitors. *EMBO J* **32**(13): 1817-1828.

O'Doherty, A., Ruf, S., Mulligan, C., Hildreth, V., Errington, M.L., Cooke, S., Sesay, A., Modino, S., Vanes, L., Hernandez, D. et al. 2005. An aneuploid mouse strain carrying human chromosome 21 with Down syndrome phenotypes. *Science* **309**(5743): 2033-2037.

O'Driscoll, M. and Jeggo, P.A. 2008. The role of the DNA damage response pathways in brain development and microcephaly: insight from human disorders. *DNA Repair (Amst)* **7**(7): 1039-1050.

O'Roak, B.J., Vives, L., Fu, W., Egertson, J.D., Stanaway, I.B., Phelps, I.G., Carvill, G., Kumar, A., Lee, C., Ankenman, K. et al. 2012. Multiplex targeted sequencing identifies recurrently

mutated genes in autism spectrum disorders. *Science* **338**(6114): 1619-1622.

Ochiai, W., Nakatani, S., Takahara, T., Kainuma, M., Masaoka, M., Minobe, S., Namihira, M., Nakashima, K., Sakakibara, A., Ogawa, M. et al. 2009. Periventricular notch activation and asymmetric Ngn2 and Tbr2 expression in pair-generated neocortical daughter cells. *Mol Cell Neurosci* **40**(2): 225-233.

Okui, M., Ide, T., Morita, K., Funakoshi, E., Ito, F., Ogita, K., Yoneda, Y., Kudoh, J., and Shimizu, N. 1999. High-level expression of the Mnb/Dyrk1A gene in brain and heart during rat early development. *Genomics* **62**(2): 165-171.

Olson, L.E., Richtsmeier, J.T., Leszl, J., and Reeves, R.H. 2004a. A chromosome 21 critical region does not cause specific Down syndrome phenotypes. *Science* **306**(5696): 687-690.

Olson, L.E., Roper, R.J., Baxter, L.L., Carlson, E.J., Epstein, C.J., and Reeves, R.H. 2004b. Down syndrome mouse models Ts65Dn, Ts1Cje, and Ms1Cje/Ts65Dn exhibit variable severity of cerebellar phenotypes. *Dev Dyn* **230**(3): 581-589.

Olson, L.E., Roper, R.J., Sengstaken, C.L., Peterson, E.A., Aquino, V., Galdzicki, Z., Siarey, R., Pletnikov, M., Moran, T.H., and Reeves, R.H. 2007. Trisomy for the Down syndrome 'critical region' is necessary but not sufficient for brain phenotypes of trisomic mice. *Hum Mol Genet* **16**(7): 774-782.

Orii, K.E., Lee, Y., Kondo, N., and McKinnon, P.J. 2006. Selective utilization of nonhomologous end-joining and homologous recombination DNA repair pathways during nervous system development. *Proc Natl Acad Sci U S A* **103**(26): 10017-10022.

Ortiz-Abalia, J., Sahun, I., Altafaj, X., Andreu, N., Estivill, X., Dierssen, M., and Fillat, C. 2008. Targeting Dyrk1A with AAVshRNA attenuates motor alterations in TgDyrk1A, a mouse model of Down syndrome. *Am J Hum Genet* **83**(4): 479-488.

Paridaen, J.T., Wilsch-Brauninger, M., and Huttner, W.B. 2013. Asymmetric inheritance of centrosome-associated primary cilium membrane directs ciliogenesis after cell division. *Cell* **155**(2): 333-344.

Park, J. and Chung, K.C. 2013. New Perspectives of Dyrk1A Role in Neurogenesis and Neuropathologic Features of Down Syndrome. *Exp Neurobiol* **22**(4): 244-248.

Park, J., Oh, Y., and Chung, K.C. 2009. Two key genes closely implicated with the neuropathological characteristics in Down syndrome: DYRK1A and RCAN1. *BMB Rep* **42**(1): 6-15.

Park, J., Oh, Y., Yoo, L., Jung, M.S., Song, W.J., Lee, S.H., Seo, H., and Chung, K.C. 2010. Dyrk1A phosphorylates p53 and inhibits proliferation of embryonic neuronal cells. *J Biol Chem* **285**(41): 31895-31906.

Park, J., Sung, J.Y., Song, W.J., Chang, S., and Chung, K.C. 2012. Dyrk1A negatively regulates the actin cytoskeleton through threonine phosphorylation of N-WASP. *J Cell Sci* **125**(Pt 1): 67-80.

Parnavelas, J.G. 2000. The origin and migration of cortical neurones: new vistas. *Trends Neurosci* **23**(3): 126-131.

Patterson, D. and Costa, A.C. 2005. Down syndrome and genetics - a case of linked histories. *Nat Rev Genet* **6**(2): 137-147.

Pearlson GD, B.S., Aylward EH, Warren AC, Grygorcewicz M, Frangou S, Barta PE, Pulsifer MB. 1998. MRI brain changes in subjects with Down syndrome with and without dementia. *Dev Med Child Neurol* **40**(5): 326.

Perez-Cremades, D., Hernandez, S., Blasco-Ibanez, J.M., Crespo, C., Nacher, J., and Varea, E. 2010. Alteration of inhibitory circuits in the somatosensory cortex of Ts65Dn mice, a model for Down's syndrome. *J Neural Transm* **117**(4): 445-455.

Pestell, R.G. 2013. New roles of cyclin D1. *Am J Pathol* **183**(1): 3-9.

Peyre, E. and Morin, X. 2012. An oblique view on the role of spindle orientation in vertebrate neurogenesis. *Dev Growth Differ* **54**(3): 287-305.

Pfaffl, M.W. 2001. A new mathematical model for relative quantification in real-time RT-PCR. *Nucleic Acids Res* **29**(9): e45.

Pilaz, L.J., Patti, D., Marcy, G., Ollier, E., Pfister, S., Douglas, R.J., Betizeau, M., Gautier, E., Cortay, V., Doerflinger, N. et al. 2009. Forced G1-phase reduction alters mode of division, neuron number, and laminar phenotype in the cerebral cortex. *Proceedings of the National Academy of Sciences of the United States of America* **106**(51): 21924-21929.

Pinter, J.D., Brown, W.E., Eliez, S., Schmitt, J.E., Capone, G.T., and Reiss, A.L. 2001a. Amygdala and hippocampal volumes in children with Down syndrome: a high-resolution MRI study. *Neurology* **56**(7): 972-974.

Pinter, J.D., Eliez, S., Schmitt, J.E., Capone, G.T., and Reiss, A.L. 2001b. Neuroanatomy of Down's syndrome: a high-resolution MRI study. *The American journal of psychiatry* **158**(10): 1659-1665.

Pinto, L., Drechsel, D., Schmid, M.T., Ninkovic, J., Irmler, M., Brill, M.S., Restani, L., Gianfranceschi, L., Cerri, C., Weber, S.N. et al. 2009. AP2gamma regulates basal progenitor fate in a region- and layer-specific manner in the developing cortex. *Nat Neurosci* **12**(10): 1229-1237.

Pla, R., Borrell, V., Flames, N., and Marin, O. 2006. Layer acquisition by cortical GABAergic interneurons is independent of Reelin signaling. *J Neurosci* **26**(26): 6924-6934.

Pletcher, M.T., Wiltshire, T., Cabin, D.E., Villanueva, M., and Reeves, R.H. 2001. Use of comparative physical and sequence mapping to annotate mouse chromosome 16 and human chromosome 21. *Genomics* **74**(1): 45-54.

Pogue, A.I., Cui, J.G., Li, Y.Y., Zhao, Y., Culicchia, F., and Lukiw, W.J. 2010. Micro RNA-125b (miRNA-125b) function in astrogliosis and glial cell proliferation. *Neurosci Lett* **476**(1): 18-22.

Pohl, D., Bittigau, P., Ishimaru, M.J., Stadthaus, D., Hubner, C., Olney, J.W., Turski, L., and Ikonomidou, C. 1999. N-Methyl-D-aspartate antagonists and apoptotic cell death triggered by head trauma in developing rat brain. *Proc Natl Acad Sci U S A* **96**(5): 2508-2513.

Polleux, F., Whitford, K.L., Dijkhuizen, P.A., Vitalis, T., and Ghosh, A. 2002. Control of cortical interneuron migration by neurotrophins and PI3-kinase signaling. *Development* **129**(13): 3147-3160.

Pons-Espinal, M., Martinez de Lagran, M., and Dierssen, M. 2013. Environmental enrichment rescues DYRK1A activity and hippocampal adult neurogenesis in TgDyrk1A. *Neurobiol Dis* **60**: 18-31.

Pontious, A., Kowalczyk, T., Englund, C., and Hevner, R.F. 2008. Role of intermediate progenitor cells in cerebral cortex development. *Dev Neurosci* **30**(1-3): 24-32.

Postiglione, M.P., Juschke, C., Xie, Y., Haas, G.A., Charalambous, C., and Knoblich, J.A. 2011. Mouse inscuteable induces apical-basal spindle orientation to facilitate intermediate progenitor generation in the developing neocortex. *Neuron* **72**(2): 269-284.

Pritchard, M.A. and Kola, I. 1999. The "gene dosage effect" hypothesis versus the "amplified developmental instability" hypothesis in Down syndrome. *J Neural Transm Suppl* **57**: 293-303.

Pulvers, J.N. and Huttner, W.B. 2009. Brca1 is required for embryonic development of the mouse cerebral cortex to

normal size by preventing apoptosis of early neural progenitors. *Development* **136**(11): 1859-1868.

Quinn, J.C., Molinek, M., Martynoga, B.S., Zaki, P.A., Faedo, A., Bulfone, A., Hevner, R.F., West, J.D., and Price, D.J. 2007. Pax6 controls cerebral cortical cell number by regulating exit from the cell cycle and specifies cortical cell identity by a cell autonomous mechanism. *Dev Biol* **302**(1): 50-65.

Raballo, R., Rhee, J., Lyn-Cook, R., Leckman, J.F., Schwartz, M.L., and Vaccarino, F.M. 2000. Basic fibroblast growth factor (Fgf2) is necessary for cell proliferation and neurogenesis in the developing cerebral cortex. *J Neurosci* **20**(13): 5012-5023.

Rachidi, M. and Lopes, C. 2007. Mental retardation in Down syndrome: from gene dosage imbalance to molecular and cellular mechanisms. *Neurosci Res* **59**(4): 349-369.

Rahmani, Z., Blouin, J.L., Creau-Goldberg, N., Watkins, P.C., Mattei, J.F., Poissonnier, M., Prieur, M., Chettouh, Z., Nicole, A., Aurias, A. et al. 1990. Down syndrome critical region around D21S55 on proximal 21q22.3. *Am J Med Genet Suppl* **7**: 98-103.

Rakic, P. 1978. Neuronal migration and contact guidance in the primate telencephalon. *Postgrad Med J* **54 Suppl 1**: 25-40.

Rakic, P. 1995. A small step for the cell, a giant leap for mankind: a hypothesis of neocortical expansion during evolution. *Trends Neurosci* **18**(9): 383-388.

Rash, B.G., Lim, H.D., Breunig, J.J., and Vaccarino, F.M. 2011. FGF signaling expands embryonic cortical surface area by regulating Notch-dependent neurogenesis. *J Neurosci* **31**(43): 15604-15617.

Reim, G. and Brand, M. 2002. Spiel-ohne-grenzen/pou2 mediates regional competence to respond to Fgf8 during zebrafish early neural development. *Development* **129**(4): 917-933.

Reynolds, L.E., Watson, A.R., Baker, M., Jones, T.A., D'Amico, G., Robinson, S.D., Joffre, C., Garrido-Urbani, S., Rodriguez-Manzaneque, J.C., Martino-Echarri, E. et al. 2010. Tumour angiogenesis is reduced in the Tc1 mouse model of Down's syndrome. *Nature* **465**(7299): 813-817.

Richardson, W.D., Kessaris, N., and Pringle, N. 2006. Oligodendrocyte wars. *Nat Rev Neurosci* **7**(1): 11-18.

Richtsmeier, J.T., Zumwalt, A., Carlson, E.J., Epstein, C.J., and Reeves, R.H. 2002. Craniofacial phenotypes in segmentally trisomic mouse models for Down syndrome. *Am J Med Genet* **107**(4): 317-324.

Rivers, L.E., Young, K.M., Rizzi, M., Jamen, F., Psachoulia, K., Wade, A., Kessaris, N., and Richardson, W.D. 2008. PDGFRA/NG2 glia generate myelinating oligodendrocytes and piriform projection neurons in adult mice. *Nat Neurosci* **11**(12): 1392-1401.

Ronan, A., Fagan, K., Christie, L., Conroy, J., Nowak, N.J., and Turner, G. 2007. Familial 4.3 Mb duplication of 21q22 sheds new light on the Down syndrome critical region. *J Med Genet* **44**(7): 448-451.

Ross, M.H., Galaburda, A.M., and Kemper, T.L. 1984. Down's syndrome: is there a decreased population of neurons? *Neurology* **34**(7): 909-916.

Royer, S., Zemelman, B.V., Losonczy, A., Kim, J., Chance, F., Magee, J.C., and Buzsaki, G. 2012. Control of timing, rate and bursts of hippocampal place cells by dendritic and somatic inhibition. *Nat Neurosci* **15**(5): 769-775.

Rudolph, J., Zimmer, G., Steinecke, A., Barchmann, S., and Bolz, J. 2010. Ephrins guide migrating cortical interneurons in the basal telencephalon. *Cell Adh Migr* **4**(3): 400-408.

Sabbagh, M.N., Fleisher, A., Chen, K., Rogers, J., Berk, C., Reiman, E., Pontecorvo, M., Mintun, M., Skovronsky, D., Jacobson, S.A. et al. 2011. Positron emission tomography and neuropathologic estimates of fibrillar amyloid-beta in a patient with Down syndrome and Alzheimer disease. *Arch Neurol* **68**(11): 1461-1466.

Sago, H., Carlson, E.J., Smith, D.J., Kilbridge, J., Rubin, E.M., Mobley, W.C., Epstein, C.J., and Huang, T.T. 1998. Ts1Cje, a partial trisomy 16 mouse model for Down syndrome, exhibits learning and behavioral abnormalities. *Proc Natl Acad Sci U S A* **95**(11): 6256-6261.

Sago, H., Carlson, E.J., Smith, D.J., Rubin, E.M., Crnic, L.S., Huang, T.T., and Epstein, C.J. 2000. Genetic dissection of region associated with behavioral abnormalities in mouse models for Down syndrome. *Pediatr Res* **48**(5): 606-613.

Sahara, S. and O'Leary, D.D. 2009. Fgf10 regulates transition period of cortical stem cell differentiation to radial glia controlling generation of neurons and basal progenitors. *Neuron* **63**(1): 48-62.

Salehi, A., Faizi, M., Belichenko, P.V., and Mobley, W.C. 2007. Using mouse models to explore genotype-phenotype relationship in Down syndrome. *Ment Retard Dev Disabil Res Rev* **13**(3): 207-214.

Salichs, E., Ledda, A., Mularoni, L., Alba, M.M., and de la Luna, S. 2009. Genome-wide analysis of histidine repeats reveals

their role in the localization of human proteins to the nuclear speckles compartment. *PLoS Genet* **5**(3): e1000397.

Salomoni, P. and Calegari, F. 2010. Cell cycle control of mammalian neural stem cells: putting a speed limit on G1. *Trends Cell Biol* **20**(5): 233-243.

Scales, T.M., Lin, S., Kraus, M., Goold, R.G., and Gordon-Weeks, P.R. 2009. Nonprimed and DYRK1A-primed GSK3 beta-phosphorylation sites on MAP1B regulate microtubule dynamics in growing axons. *J Cell Sci* **122**(Pt 14): 2424-2435.

Schmechel, D.E. and Rakic, P. 1979. A Golgi study of radial glial cells in developing monkey telencephalon: morphogenesis and transformation into astrocytes. *Anat Embryol (Berl)* **156**(2): 115-152.

Schmidt-Sidor, B., Wisniewski, K.E., Shepard, T.H., and Sersen, E.A. 1990. Brain growth in Down syndrome subjects 15 to 22 weeks of gestational age and birth to 60 months. *Clin Neuropathol* **9**(4): 181-190.

Sebrie, C., Chabert, C., Ledru, A., Guedj, F., Po, C., Smith, D.J., Rubin, E., Rivals, I., Beloeil, J.C., Gillet, B. et al. 2008. Increased dosage of DYRK1A and brain volumetric alterations in a YAC model of partial trisomy 21. *Anat Rec (Hoboken)* **291**(3): 254-262.

Seifert, G., Schilling, K., and Steinhauser, C. 2006. Astrocyte dysfunction in neurological disorders: a molecular perspective. *Nat Rev Neurosci* **7**(3): 194-206.

Seo, S., Lim, J.W., Yellajoshyula, D., Chang, L.W., and Kroll, K.L. 2007. Neurogenin and NeuroD direct transcriptional targets and their regulatory enhancers. *EMBO J* **26**(24): 5093-5108.

Seregaza, Z., Roubertoux, P.L., Jamon, M., and Soumireu-Mourat, B. 2006. Mouse models of cognitive disorders in trisomy 21: a review. *Behav Genet* **36**(3): 387-404.

Sessa, A., Mao, C.A., Hadjantonakis, A.K., Klein, W.H., and Broccoli, V. 2008. Tbr2 directs conversion of radial glia into basal precursors and guides neuronal amplification by indirect neurogenesis in the developing neocortex. *Neuron* **60**(1): 56-69.

Seuntjens, E., Nityanandam, A., Miquelajauregui, A., Debruyn, J., Stryjewska, A., Goebbels, S., Nave, K.A., Huylebroeck, D., and Tarabykin, V. 2009. Sip1 regulates sequential fate decisions by feedback signaling from postmitotic neurons to progenitors. *Nat Neurosci* **12**(11): 1373-1380.

Shimojo, H., Ohtsuka, T., and Kageyama, R. 2008. Oscillations in notch signaling regulate maintenance of neural progenitors. *Neuron* **58**(1): 52-64.

Shitamukai, A., Konno, D., and Matsuzaki, F. 2011. Oblique radial glial divisions in the developing mouse neocortex induce self-renewing progenitors outside the germinal zone that resemble primate outer subventricular zone progenitors. *J Neurosci* **31**(10): 3683-3695.

Shukkur, E.A., Shimohata, A., Akagi, T., Yu, W., Yamaguchi, M., Murayama, M., Chui, D., Takeuchi, T., Amano, K., Subramhanya, K.H. et al. 2006. Mitochondrial dysfunction and tau hyperphosphorylation in Ts1Cje, a mouse model for Down syndrome. *Hum Mol Genet* **15**(18): 2752-2762.

Siarey, R.J., Carlson, E.J., Epstein, C.J., Balbo, A., Rapoport, S.I., and Galdzicki, Z. 1999. Increased synaptic depression in the Ts65Dn mouse, a model for mental retardation in Down syndrome. *Neuropharmacology* **38**(12): 1917-1920.

Siegenthaler, J.A., Ashique, A.M., Zarbalis, K., Patterson, K.P., Hecht, J.H., Kane, M.A., Folias, A.E., Choe, Y., May, S.R., Kume, T. et al. 2009. Retinoic acid from the meninges regulates cortical neuron generation. *Cell* **139**(3): 597-609.

Siegenthaler, J.A. and Miller, M.W. 2005. Transforming growth factor beta 1 promotes cell cycle exit through the cyclin-dependent kinase inhibitor p21 in the developing cerebral cortex. *J Neurosci* **25**(38): 8627-8636.

Silberberg, G. and Markram, H. 2007. Disynaptic inhibition between neocortical pyramidal cells mediated by Martinotti cells. *Neuron* **53**(5): 735-746.

Siller, K.H. and Doe, C.Q. 2009. Spindle orientation during asymmetric cell division. *Nat Cell Biol* **11**(4): 365-374.

Sitz, J.H., Tigges, M., Baumgartel, K., Khaspekov, L.G., and Lutz, B. 2004. Dyrk1A potentiates steroid hormone-induced transcription via the chromatin remodeling factor Arip4. *Mol Cell Biol* **24**(13): 5821-5834.

Slater, B.J., Lenton, K.A., Kwan, M.D., Gupta, D.M., Wan, D.C., and Longaker, M.T. 2008. Cranial sutures: a brief review. *Plast Reconstr Surg* **121**(4): 170e-178e.

Smart, I.H. 1976. A pilot study of cell production by the ganglionic eminences of the developing mouse brain. *J Anat* **121**(Pt 1): 71-84.

Smart, I.H., Dehay, C., Giroud, P., Berland, M., and Kennedy, H. 2002. Unique morphological features of the proliferative zones and postmitotic compartments of the neural epithelium giving rise to striate and extrastriate cortex in the monkey. *Cereb Cortex* **12**(1): 37-53.

Smith, D.J., Stevens, M.E., Sudanagunta, S.P., Bronson, R.T., Makhinson, M., Watabe, A.M., O'Dell, T.J., Fung, J., Weier,

H.U., Cheng, J.F. et al. 1997. Functional screening of 2 Mb of human chromosome 21q22.2 in transgenic mice implicates minibrain in learning defects associated with Down syndrome. *Nat Genet* **16**(1): 28-36.

Smith, D.J., Zhu, Y., Zhang, J., Cheng, J.F., and Rubin, E.M. 1995. Construction of a panel of transgenic mice containing a contiguous 2-Mb set of YAC/P1 clones from human chromosome 21q22.2. *Genomics* **27**(3): 425-434.

Sohal, V.S., Zhang, F., Yizhar, O., and Deisseroth, K. 2009. Parvalbumin neurons and gamma rhythms enhance cortical circuit performance. *Nature* **459**(7247): 698-702.

Soppa, U., Schumacher, J., Florencio Ortiz, V., Pasqualon, T., Tejedor, F.J., and Becker, W. 2014. The Down syndrome-related protein kinase DYRK1A phosphorylates p27(Kip1) and Cyclin D1 and induces cell cycle exit and neuronal differentiation. *Cell Cycle* **13**(13): 2084-2100.

Souchet, B., Guedj, F., Sahun, I., Duchon, A., Daubigney, F., Badel, A., Yanagawa, Y., Barallobre, M.J., Dierssen, M., Yu, E. et al. 2014. Excitation/inhibition balance and learning are modified by Dyrk1a gene dosage. *Neurobiol Dis*.

Soundararajan, M., Roos, A.K., Savitsky, P., Filippakopoulos, P., Kettenbach, A.N., Olsen, J.V., Gerber, S.A., Eswaran, J., Knapp, S., and Elkins, J.M. 2013. Structures of Down syndrome kinases, DYRKs, reveal mechanisms of kinase activation and substrate recognition. *Structure* **21**(6): 986-996.

Sousa, V.H. and Fishell, G. 2010. Sonic hedgehog functions through dynamic changes in temporal competence in the developing forebrain. *Curr Opin Genet Dev* **20**(4): 391-399.

Sousa, V.H., Miyoshi, G., Hjerling-Leffler, J., Karayannis, T., and Fishell, G. 2009. Characterization of Nkx6-2-derived neocortical interneuron lineages. *Cereb Cortex* **19 Suppl 1**: i1-10.

Southwell, D.G., Paredes, M.F., Galvao, R.P., Jones, D.L., Froemke, R.C., Sebe, J.Y., Alfaro-Cervello, C., Tang, Y., Garcia-Verdugo, J.M., Rubenstein, J.L. et al. 2012. Intrinsically determined cell death of developing cortical interneurons. *Nature* **491**(7422): 109-113.

Stahl, R., Walcher, T., De Juan Romero, C., Pilz, G.A., Cappello, S., Irmler, M., Sanz-Aquela, J.M., Beckers, J., Blum, R., Borrell, V. et al. 2013. Trnp1 regulates expansion and folding of the mammalian cerebral cortex by control of radial glial fate. *Cell* **153**(3): 535-549.

Stancik, E.K., Navarro-Quiroga, I., Sellke, R., and Haydar, T.F. 2010. Heterogeneity in ventricular zone neural precursors

contributes to neuronal fate diversity in the postnatal neocortex. *J Neurosci* **30**(20): 7028-7036.

Stempfle, N., Huten, Y., Fredouille, C., Brisse, H., and Nessmann, C. 1999. Skeletal abnormalities in fetuses with Down's syndrome: a radiographic post-mortem study. *Pediatr Radiol* **29**(9): 682-688.

Sturgeon, X. and Gardiner, K.J. 2011. Transcript catalogs of human chromosome 21 and orthologous chimpanzee and mouse regions. *Mamm Genome* **22**(5-6): 261-271.

Sultan, K.T., Brown, K.N., and Shi, S.H. 2013. Production and organization of neocortical interneurons. *Front Cell Neurosci* **7**: 221.

Sun, Y., Nadal-Vicens, M., Misono, S., Lin, M.Z., Zubiaga, A., Hua, X., Fan, G., and Greenberg, M.E. 2001. Neurogenin promotes neurogenesis and inhibits glial differentiation by independent mechanisms. *Cell* **104**(3): 365-376.

Sussel, L., Marin, O., Kimura, S., and Rubenstein, J.L. 1999. Loss of Nkx2.1 homeobox gene function results in a ventral to dorsal molecular respecification within the basal telencephalon: evidence for a transformation of the pallidum into the striatum. *Development* **126**(15): 3359-3370.

Suzuki-Hirano, A. and Shimogori, T. 2009. The role of Fgf8 in telencephalic and diencephalic patterning. *Semin Cell Dev Biol* **20**(6): 719-725.

Takahashi, T., Nowakowski, R.S., and Caviness, V.S., Jr. 1993. Cell cycle parameters and patterns of nuclear movement in the neocortical proliferative zone of the fetal mouse. *J Neurosci* **13**(2): 820-833.

Takahashi, T., Nowakowski, R.S., and Caviness, V.S., Jr. 1995. The cell cycle of the pseudostratified ventricular epithelium of the embryonic murine cerebral wall. *The Journal of neuroscience : the official journal of the Society for Neuroscience* **15**(9): 6046-6057.

Takashima, S., Ieshima, A., Nakamura, H., and Becker, L.E. 1989. Dendrites, dementia and the Down syndrome. *Brain Dev* **11**(2): 131-133.

Takizawa, T., Nakashima, K., Namihira, M., Ochiai, W., Uemura, A., Yanagisawa, M., Fujita, N., Nakao, M., and Taga, T. 2001. DNA methylation is a critical cell-intrinsic determinant of astrocyte differentiation in the fetal brain. *Dev Cell* **1**(6): 749-758.

Taniguchi, H., Lu, J., and Huang, Z.J. 2013. The spatial and temporal origin of chandelier cells in mouse neocortex. *Science* **339**(6115): 70-74.

Taverna, E. and Huttner, W.B. 2010. Neural progenitor nuclei IN motion. *Neuron* **67**(6): 906-914.

Tejedor, F., Zhu, X.R., Kaltenbach, E., Ackermann, A., Baumann, A., Canal, I., Heisenberg, M., Fischbach, K.F., and Pongs, O. 1995. minibrain: a new protein kinase family involved in postembryonic neurogenesis in Drosophila. *Neuron* **14**(2): 287-301.

Tejedor, F.J. and Hammerle, B. 2011. MNB/DYRK1A as a multiple regulator of neuronal development. *FEBS J* **278**(2): 223-235.

Temple, S. 2001. The development of neural stem cells. *Nature* **414**(6859): 112-117.

Thomaidou, D., Mione, M.C., Cavanagh, J.F., and Parnavelas, J.G. 1997. Apoptosis and its relation to the cell cycle in the developing cerebral cortex. *J Neurosci* **17**(3): 1075-1085.

Thomazeau, A., Lassalle, O., Iafrati, J., Souchet, B., Guedj, F., Janel, N., Chavis, P., Delabar, J., and Manzoni, O.J. 2014. Prefrontal deficits in a murine model overexpressing the down syndrome candidate gene dyrk1a. *J Neurosci* **34**(4): 1138-1147.

Trazzi, S., Mitrugno, V.M., Valli, E., Fuchs, C., Rizzi, S., Guidi, S., Perini, G., Bartesaghi, R., and Ciani, E. 2011. APP-dependent up-regulation of Ptch1 underlies proliferation impairment of neural precursors in Down syndrome. *Hum Mol Genet* **20**(8): 1560-1573.

Tsunekawa, Y., Britto, J.M., Takahashi, M., Polleux, F., Tan, S.S., and Osumi, N. 2012. Cyclin D2 in the basal process of neural progenitors is linked to non-equivalent cell fates. *EMBO J* **31**(8): 1879-1892.

Tuoc, T.C., Boretius, S., Sansom, S.N., Pitulescu, M.E., Frahm, J., Livesey, F.J., and Stoykova, A. 2013. Chromatin regulation by BAF170 controls cerebral cortical size and thickness. *Dev Cell* **25**(3): 256-269.

Tyler, W.A. and Haydar, T.F. 2013. Multiplex genetic fate mapping reveals a novel route of neocortical neurogenesis, which is altered in the Ts65Dn mouse model of Down syndrome. *J Neurosci* **33**(12): 5106-5119.

Urase, K., Kouroku, Y., Fujita, E., and Momoi, T. 2003. Region of caspase-3 activation and programmed cell death in the early development of the mouse forebrain. *Brain Res Dev Brain Res* **145**(2): 241-248.

Vaccarino, F.M., Schwartz, M.L., Raballo, R., Nilsen, J., Rhee, J., Zhou, M., Doetschman, T., Coffin, J.D., Wyland, J.J., and Hung, Y.T. 1999. Changes in cerebral cortex size are

governed by fibroblast growth factor during embryogenesis. *Nat Neurosci* **2**(3): 246-253.

Valcanis, H. and Tan, S.S. 2003. Layer specification of transplanted interneurons in developing mouse neocortex. *J Neurosci* **23**(12): 5113-5122.

van den Berghe, V., Stappers, E., Vandesande, B., Dimidschstein, J., Kroes, R., Francis, A., Conidi, A., Lesage, F., Dries, R., Cazzola, S. et al. 2013. Directed migration of cortical interneurons depends on the cell-autonomous action of Sip1. *Neuron* **77**(1): 70-82.

Vilardell, M., Rasche, A., Thormann, A., Maschke-Dutz, E., Perez-Jurado, L.A., Lehrach, H., and Herwig, R. 2011. Meta-analysis of heterogeneous Down Syndrome data reveals consistent genome-wide dosage effects related to neurological processes. *BMC Genomics* **12**: 229.

Volvert, M.L., Rogister, F., Moonen, G., Malgrange, B., and Nguyen, L. 2012. MicroRNAs tune cerebral cortical neurogenesis. *Cell Death Differ* **19**(10): 1573-1581.

Wall, D.S., Mears, A.J., McNeill, B., Mazerolle, C., Thurig, S., Wang, Y., Kageyama, R., and Wallace, V.A. 2009. Progenitor cell proliferation in the retina is dependent on Notch-independent Sonic hedgehog/Hes1 activity. *J Cell Biol* **184**(1): 101-112.

Wang, D.D. and Kriegstein, A.R. 2009. Defining the role of GABA in cortical development. *J Physiol* **587**(Pt 9): 1873-1879.

Wang, X., Tsai, J.W., Imai, J.H., Lian, W.N., Vallee, R.B., and Shi, S.H. 2009. Asymmetric centrosome inheritance maintains neural progenitors in the neocortex. *Nature* **461**(7266): 947-955.

Wang, X., Tsai, J.W., LaMonica, B., and Kriegstein, A.R. 2011. A new subtype of progenitor cell in the mouse embryonic neocortex. *Nat Neurosci* **14**(5): 555-561.

Wechsler, J., Greene, M., McDevitt, M.A., Anastasi, J., Karp, J.E., Le Beau, M.M., and Crispino, J.D. 2002. Acquired mutations in GATA1 in the megakaryoblastic leukemia of Down syndrome. *Nat Genet* **32**(1): 148-152.

Wegiel, J., Gong, C.X., and Hwang, Y.W. 2011. The role of DYRK1A in neurodegenerative diseases. *FEBS J* **278**(2): 236-245.

Wegiel, J., Kuchna, I., Nowicki, K., Frackowiak, J., Dowjat, K., Silverman, W.P., Reisberg, B., DeLeon, M., Wisniewski, T., Adayev, T. et al. 2004. Cell type- and brain structure-specific patterns of distribution of minibrain kinase in human brain. *Brain Res* **1010**(1-2): 69-80.

Welagen, J. and Anderson, S. 2011. Origins of neocortical interneurons in mice. *Dev Neurobiol* **71**(1): 10-17.

West, M.J. and Gundersen, H.J. 1990. Unbiased stereological estimation of the number of neurons in the human hippocampus. *J Comp Neurol* **296**(1): 1-22.

Williams, A.D., Mjaatvedt, C.H., and Moore, C.S. 2008. Characterization of the cardiac phenotype in neonatal Ts65Dn mice. *Dev Dyn* **237**(2): 426-435.

Willsey, A.J., Sanders, S.J., Li, M., Dong, S., Tebbenkamp, A.T., Muhle, R.A., Reilly, S.K., Lin, L., Fertuzinhos, S., Miller, J.A. et al. 2013. Coexpression networks implicate human midfetal deep cortical projection neurons in the pathogenesis of autism. *Cell* **155**(5): 997-1007.

Wilson, N.R., Runyan, C.A., Wang, F.L., and Sur, M. 2012. Division and subtraction by distinct cortical inhibitory networks in vivo. *Nature* **488**(7411): 343-348.

Winter, T.C., Ostrovsky, A.A., Komarniski, C.A., and Uhrich, S.B. 2000. Cerebellar and frontal lobe hypoplasia in fetuses with trisomy 21: usefulness as combined US markers. *Radiology* **214**(2): 533-538.

Wisniewski, K.E. 1990. Down syndrome children often have brain with maturation delay, retardation of growth, and cortical dysgenesis. *American journal of medical genetics Supplement* **7**: 274-281.

Wisniewski, K.E., Wisniewski, H.M., and Wen, G.Y. 1985. Occurrence of neuropathological changes and dementia of Alzheimer's disease in Down's syndrome. *Ann Neurol* **17**(3): 278-282.

Wonders, C.P. and Anderson, S.A. 2006. The origin and specification of cortical interneurons. *Nat Rev Neurosci* **7**(9): 687-696.

Wonders, C.P., Taylor, L., Welagen, J., Mbata, I.C., Xiang, J.Z., and Anderson, S.A. 2008. A spatial bias for the origins of interneuron subgroups within the medial ganglionic eminence. *Dev Biol* **314**(1): 127-136.

Woodhead, G.J., Mutch, C.A., Olson, E.C., and Chenn, A. 2006. Cell-autonomous beta-catenin signaling regulates cortical precursor proliferation. *J Neurosci* **26**(48): 12620-12630.

Wu, J., Wu, S.H., Bollig, A., Thakur, A., and Liao, D.J. 2009. Identification of the cyclin D1b mRNA variant in mouse. *Mol Biol Rep* **36**(5): 953-957.

Wulff, P., Ponomarenko, A.A., Bartos, M., Korotkova, T.M., Fuchs, E.C., Bahner, F., Both, M., Tort, A.B., Kopell, N.J., Wisden, W. et al. 2009. Hippocampal theta rhythm and its

coupling with gamma oscillations require fast inhibition onto parvalbumin-positive interneurons. *Proc Natl Acad Sci U S A* **106**(9): 3561-3566.

Xu, Q., Cobos, I., De La Cruz, E., Rubenstein, J.L., and Anderson, S.A. 2004. Origins of cortical interneuron subtypes. *J Neurosci* **24**(11): 2612-2622.

Xu, Q., Guo, L., Moore, H., Waclaw, R.R., Campbell, K., and Anderson, S.A. 2010. Sonic hedgehog signaling confers ventral telencephalic progenitors with distinct cortical interneuron fates. *Neuron* **65**(3): 328-340.

Xu, Q., Tam, M., and Anderson, S.A. 2008. Fate mapping Nkx2.1-lineage cells in the mouse telencephalon. *J Comp Neurol* **506**(1): 16-29.

Xu, Q., Wonders, C.P., and Anderson, S.A. 2005. Sonic hedgehog maintains the identity of cortical interneuron progenitors in the ventral telencephalon. *Development* **132**(22): 4987-4998.

Yabut, O., Domogauer, J., and D'Arcangelo, G. 2010. Dyrk1A overexpression inhibits proliferation and induces premature neuronal differentiation of neural progenitor cells. *J Neurosci* **30**(11): 4004-4014.

Yang, J., Rothermel, B., Vega, R.B., Frey, N., McKinsey, T.A., Olson, E.N., Bassel-Duby, R., and Williams, R.S. 2000. Independent signals control expression of the calcineurin inhibitory proteins MCIP1 and MCIP2 in striated muscles. *Circ Res* **87**(12): E61-68.

Yang, Q., Rasmussen, S.A., and Friedman, J.M. 2002. Mortality associated with Down's syndrome in the USA from 1983 to 1997: a population-based study. *Lancet* **359**(9311): 1019-1025.

Yang, X., Klein, R., Tian, X., Cheng, H.T., Kopan, R., and Shen, J. 2004. Notch activation induces apoptosis in neural progenitor cells through a p53-dependent pathway. *Dev Biol* **269**(1): 81-94.

Yau, H.J., Wang, H.F., Lai, C., and Liu, F.C. 2003. Neural development of the neuregulin receptor ErbB4 in the cerebral cortex and the hippocampus: preferential expression by interneurons tangentially migrating from the ganglionic eminences. *Cereb Cortex* **13**(3): 252-264.

Yingling, J., Youn, Y.H., Darling, D., Toyo-Oka, K., Pramparo, T., Hirotsune, S., and Wynshaw-Boris, A. 2008. Neuroepithelial stem cell proliferation requires LIS1 for precise spindle orientation and symmetric division. *Cell* **132**(3): 474-486.

Yozu, M., Tabata, H., and Nakajima, K. 2005. The caudal migratory stream: a novel migratory stream of interneurons derived from the caudal ganglionic eminence in the developing mouse forebrain. *J Neurosci* **25**(31): 7268-7277.

Yu, J.C., Lucas, J.H., Fryberg, K., and Borke, J.L. 2001. Extrinsic tension results in FGF-2 release, membrane permeability change, and intracellular Ca++ increase in immature cranial sutures. *J Craniofac Surg* **12**(4): 391-398.

Yu, T., Li, Z., Jia, Z., Clapcote, S.J., Liu, C., Li, S., Asrar, S., Pao, A., Chen, R., Fan, N. et al. 2010. A mouse model of Down syndrome trisomic for all human chromosome 21 syntenic regions. *Hum Mol Genet* **19**(14): 2780-2791.

Zdaniuk, G., Wierzba-Bobrowicz, T., Szpak, G.M., and Stepien, T. 2011. Astroglia disturbances during development of the central nervous system in fetuses with Down's syndrome. *Folia Neuropathol* **49**(2): 109-114.

Zecevic, N., Chen, Y., and Filipovic, R. 2005. Contributions of cortical subventricular zone to the development of the human cerebral cortex. *J Comp Neurol* **491**(2): 109-122.

Zetterberg, A., Larsson, O., and Wiman, K.G. 1995. What is the restriction point? *Curr Opin Cell Biol* **7**(6): 835-842.

Zhang, Y., Liao, J.M., Zeng, S.X., and Lu, H. 2011. p53 downregulates Down syndrome-associated DYRK1A through miR-1246. *EMBO Rep* **12**(8): 811-817.

Zhao, Y., Flandin, P., Long, J.E., Cuesta, M.D., Westphal, H., and Rubenstein, J.L. 2008. Distinct molecular pathways for development of telencephalic interneuron subtypes revealed through analysis of Lhx6 mutants. *J Comp Neurol* **510**(1): 79-99.

Zhong, W. and Chia, W. 2008. Neurogenesis and asymmetric cell division. *Curr Opin Neurobiol* **18**(1): 4-11.

Zimmer, C., Tiveron, M.C., Bodmer, R., and Cremer, H. 2004. Dynamics of Cux2 expression suggests that an early pool of SVZ precursors is fated to become upper cortical layer neurons. *Cereb Cortex* **14**(12): 1408-1420.

Zimmer, G., Rudolph, J., Landmann, J., Gerstmann, K., Steinecke, A., Gampe, C., and Bolz, J. 2011. Bidirectional ephrinB3/EphA4 signaling mediates the segregation of medial ganglionic eminence- and preoptic area-derived interneurons in the deep and superficial migratory stream. *J Neurosci* **31**(50): 18364-18380.

Zou, Y., Ewton, D.Z., Deng, X., Mercer, S.E., and Friedman, E. 2004. Mirk/dyrk1B kinase destabilizes cyclin D1 by

phosphorylation at threonine 288. *J Biol Chem* **279**(26): 27790-27798.

ANNEX

Guedj F, Pereira PL, Najas S, Barallobre MJ, Chabert C, Souchet B, Sebrie C, Verney C, Herault Y, Arbones M, Delabar JM. DYRK1A: a master regulatory protein controlling brain growth. Neurobiol Dis. 2012 Apr;46(1):190-203. doi: 10.1016/j.nbd.2012.01.007